Sustainable C-H Functionalisation by Improved Catalyst Design

Heron, Callum

Award date:
2020

Awarding institution:
University of Bath

Sustainable C–H Functionalisation by Improved Catalyst Design

Callum John Heron

A thesis submitted for the degree of Doctor of Philosophy

University of Bath

Centre for Sustainable Chemical Technologies

Department of Chemistry

January 2020

Supervisors:

Prof. Christopher G. Frost (Chemistry)

Dr Emma Emanuelsson-Patterson (Chemical Engineering)

Dr Antonine Buchard (Chemistry)

Copyright

"*The difficulty lies not so much in developing new ideas as in escaping from old ones*."

John Maynard Keynes

Contents

ACKNOWLEDGEMENTS ..... **IX**

ABSTRACT ..... **X**

PUBLICATIONS ..... **XI**

ABBREVIATIONS ..... **XII**

INTRODUCTION **1**

1.1 – Catalysis and Sustainability 1

1.2– Methodologies to Achieve C–H Functionalisation 3

1.3 – Directing Groups in C–H Functionalisation 10

1.4 – Overview of Ruthenium Catalysed *ortho* Functionalisation Reactions 12

1.4.1 – C–C bond Forming Reactions *12*

1.4.2 – C–X Bond Forming Reactions *15*

1.5 – Overview of *meta* C–H Functionalisation Reactions 17

1.5.1 – Sterically Controlled Direct meta C–H functionalisation *18*

1.5.2 – Directing Group Controlled meta C–H Functionalisation *21*

1.5.3 – Traceless Directing Group meta C–H functionalisation *24*

1.5.4 – Electrostatic Controlled meta C–H Functionalisation *28*

1.5.5 – σ Activation Enabled meta C–H Functionalisation *32*

1.6 – Overview of *para* C–H Functionalisation Reactions 48

1.6.1 – Template Assisted para C–H Functionalisation *48*

1.6.2 – Sterically Induced para C–H Functionalisation *52*

1.6.3 – Electronic Induced para C–H Functionalisation *54*

1.7 – Aims and Objectives 62

BIBLIOGRAPHY **63**

CHAPTER 2 – A-HALO CARBONYLS FOR *META* SELECTIVE PRIMARY C–H ALKYLATIONS **72**

2.1 – Synthesis of Starting Materials 78

2.2 – Optimisation of Reaction Using a Nickel Co-Catalyst 80

2.3 – Role of [Ni] and Reoptimisation of Conditions 83

2.4 – Scope and Limitations 86

2.5 – Mechanistic Considerations 90

2.6 – Conclusions and Future Work 99

Bibliography 101

CHAPTER 3 – RUTHENIUM CATALYSED REMOTE C4-SELECTIVE C-H FUNCTIONALISATION OF CARBAZOLES 104

3.1 – Synthesis of Starting Materials 107
3.2 – Reaction Optimisation 112
3.3 – Scope and Limitations 119
3.4 – Mechanistic considerations 123
3.5 – Conclusions and future work 126
Bibliography 128

CHAPTER 4 – STUDIES INTO NEW COUPLING PARTNERS AND SUBSTRATES 131

4.1 – Synthesis of Substrates for Studying the Proposed Reaction Design 134
4.2 – Reaction Optimisation 135
4.3 – Mechanistic Considerations 142
4.4 – Conclusions and Future Work 144

BIBLIOGRAPHY 146

5 - EXPERIMENTAL 147

5.1 – General 147
5.2 – Synthesis of 2-Aryl Pyridine Derivatives 149
*5.2.1 – General Procedure **A** 149*
*5.2.2 – Synthesis of 2-(4-nitrophenyl)pyridine, **1b** 149*
*5.2.3 - Synthesis of 2-(4-methoxypenyl) pyridine, **1c** 150*
*5.2.4 – Synthesis of 2-(4-(trifluoromethyl)phenyl) pyridine, **1d** 151*
*5.2.5 – Synthesis of Ethyl 4-(pyridin-2-yl) benzoate, **1e** 151*
*5.2.6 – Synthesis of 2-([1,1'-biphenyl]-4-yl) pyridine, **1f** 152*
*5.2.7 – Synthesis of 2-(4-(trifluoromethoxy) phenyl) pyridine, **1g** 153*
*5.2.8 – Synthesis of 2-(4fluorophenyl) pyridine, **1h** 154*
*5.2.9 – Synthesis of 2-(4-chlorophenyl) pyridine, **1i** 154*
*5.2.10 – Synthesis of 2-(4-bromophenyl) pyridine, **1j** 155*
*5.2.11 – Synthesis of 2-(4-(methylthio)phenyl) pyridine, **1k** 156*
5.3 – Optimisation for the *meta* alkylation of primary substrates 157
5.4 – Scope of Ruthenium Catalysed *meta* C-H Alkylation of Primary Substrates 160
*5.4.1 – General Procedure **A** for the Formation of ethyl 2-(3-(pyridin-2-yl) phenyl) acetates 160*
*5.4.2 – General procedure **B** for the formation of ethyl 2-(3-(pyridine-2-yl) phenyl) acetates 161*

5.4.3 – Synthesis of ethyl 2-(3-(pyridin-2-yl)phenyl)acetate, ***1.1*** *161*
5.4.4 - Synthesis of ethyl 2-3-(1H-pyrazol-1-yl)phenyl)acetate, ***1.2*** *162*
5.4.5 – Synthesis of ethyl 2-(3-(pyrimidin-2-yl)phenyl)acetate, ***1.3*** *163*
5.4.6 – Synthesis of ethyl 2-(3-(5-fluoropyridin-2-yl)phenyl)acetate, ***1.4*** *164*
5.4.7 – Synthesis of ethyl 2-(3-(5-ethylpyrimidin-2-yl)phenyl)acetate, ***1.5*** *165*
5.4.8 – Synthesis of ethyl 2-(3-(4-methylpyrimidin-2-yl)phenyl)acetate, ***1.6*** *166*
5.4.9 – Synthesis of ethyl 2-(3-(4-methylpyridin-2-yl)phenyl)acetate, ***1.7*** *167*
5.4.10 – Synthesis of ethyl 2-(2-methoxy-5-(4-methylpyridin-2-yl)phenyl)acetate, ***1.8*** *168*
5.4.11 – Synthesis of ethyl 2-(2-methoxy-5-(pyridin-2-yl)phenyl)acetate, ***1.11*** *169*
5.4.12 – Synthesis of ethyl 2-(2-(methylthio)-5-(pyridin-2-yl)phenyl)acetate, ***1.12*** *170*
5.4.13 – Synthesis of ethyl 2-(5-(pyridin-2-yl)-2-(trifluoromethyl)phenyl)acetate, ***1.13*** *171*
5.4.14 – Synthesis of ethyl 2-(5-((pyridin-2-yl)-2-(trifluoromethoxy)phenyl)acetate, ***1.14*** *172*
5.4.15 – Synthesis of ethyl 2-(2-ethoxy-2-oxoethyl)-4-(pyridin-2-yl)benzoate, ***1.15*** *173*
5.4.16 – Synthesis of ethyl 2-(4-(pyridin-2-yl)-[1,1'-biphenyl]-2-yl)acetate, ***1.16*** *174*
5.4.17 – Synthesis of ethyl 2-(2-fluoro-5-(pyridin-2-yl)phenyl)acetate, ***1.17*** *175*
5.4.18 – Synthesis of ethyl 2-(2-chloro-5-(pyridin-2-yl)phenyl)acetate, ***1.18*** *176*
5.4.19 – Synthesis of ethyl 2-(2-bromo-5-(pyridin-2-yl)phenyl)acetate, ***1.19*** *177*
5.4.20 – Synthesis of ethyl 2-(2-methoxy-5-(pyrimidin-2-yl)phenyl)acetate, ***1.22*** *178*
5.5 – MECHANISTIC EXPERIMENTS FOR THE *META* ALKYLATION WITH PRIMARY SUBSTRATES 180
5.5.1 – Radical Inhibitor experiments *180*
5.5.2 – Testing Phosphonium salt as active coupling species in situ *181*
5.5.3 – Mercury drop test *181*
5.6 – SYNTHESIS OF CARBAZOLE AND TRYPTAMINE SUBSTRATES FOR TESTING 182
5.6.1 – Synthesis of N-(2-(1H-indol-3-yl)ethyl)pyrimidin-2-amine, ***2a*** *182*
5.6.2 – Synthesis of N-(2-(1H-indol-3-yl)ethyl)-5-chloropyrimidin-2-amine, ***2b*** *183*
5.6.3 – Synthesis of 2-(1H-indol-3-yl)-N-(pyridin-2-ylmethyl)ethan-1-ammonium chloride, ***2c*** *184*
5.6.4 – Synthesis of 3-((2-(1H-indol-3-yl)ethyl)amino)propanenitrile, ***2d*** *185*
5.6.5 – Synthesis of 9-(pyrimidin-2-yl)-9H-carbazole, ***2e*** *186*
5.6.6 – Synthesis of 9-(pyridin-2-yl)-9H-carbazole, ***2f*** *187*
5.7 – OPTIMISATION FOR THE C-4 ALKYLATION OF 9-(PYRIMIDIN-2-YL)-9*H*-CARABAZOLES 188
5.8 - SCOPE OF RUTHENIUM CATALYSED C-4 C-H ALKYLATION OF CARBAZOLE SUBSTRATES 189
5.8.1 – General Procedure ***C*** *for the synthesis of methyl 2-methyl-2-(9-(pyrimidin-2-yl)-9H-carbazol-4-yl)alkylate substrates* *189*
5.8.2 – Synthesis of ethyl 2-methyl-2-(9-(pyrimidin-2-yl)-9H-carbazol-4-yl)propanoate, ***2.1*** *190*
5.8.3 – Synthesis of methyl 2-methyl-2-(9-(pyrimidin-2-yl)-9H-carbozol-4-yl)propanoate, ***2.2*** *191*

5.8.4 – Synthesis of tert-butyl 2-methyl-2-(9-(pyrimidin-2-yl)-9H-carbazol-4-yl)propanoate, ***2.3*** *.. 192*
5.8.5 – Synthesis of benzyl 2-methyl-2-(9-pyrimidin-2-yl)-9H-carbazol-4-yl)propanoate, ***2.4*** *..... 193*
5.8.6 – Synthesis of cyclohexyl 2-methyl-2-(9-(pyrimidin-2-yl)-9H-carbazol-4-yl)propanoate, ***2.5*** *. 194*
5.8.7 – Synthesis of methyl 1-(9-(pyrimidin-2-yl)-9H-carbazol-4-yl)cyclohexane-1-carboxylate, ***2.6*** *..... 195*
5.8.8 – Synthesis of (perfluorophenyl) methyl 2-methyl-2-(9-(pyrimidin-2-yl)-9H-carbazol-4-yl) propanoate, ***2.9*** *..... 196*
5.8.9 – Synthesis of methyl 2-(6-bromo-9-(pyrimidin-2-yl)-9H-carbazol-4-yl)-2-methylpropanoate, ***2.10*** *..... 197*
5.8.10 – Synthesis of methyl 2-(6-chloro-9-(pyrimidin-2-yl)-9H-carbazol-4-yl)-2-methylpropanoate, ***2.11*** *..... 198*
5.8.11 – Synthesis of methyl 2-methyl-2-(3,6,8-trichloro-9-(pyrimidin-2-yl)-9H-carbazol-4-yl) propanoate, ***2.12*** *..... 199*
5.9 - MECHANISTIC EXPERIMENTS FOR THE C-4 ALKYLATION OF 9-(PYRIMIDIN-2-YL)-9*H*-CARABAZOLES 201
5.9.1 – Deuterium Labelling Experiment 201
5.9.2 – TEMPO Experiments 201
5.9.3 – Mercury Drop Test 202
5.10 – *PARA*-FUNCTIONALISATION OF ANILINE DERIVATIVES 203
5.10.1 – Optimisation for the para carboxylation of 5-chloro-N-phenylpyrimidin-2-amine 203
5.10.2 – Synthesis of 5-chloro-N-phenylpyrimidin-2-amine, ***3a*** *..... 204*
5.10.3 – Synthesis of methyl 4-((5-chloropyrimidin-2-yl)amino)benzoate, ***3.1*** *..... 205*
5.11 – SYNTHESIS OF RUTHENIUM COMPLEXES 207
5.11.1 – Synthesis of [Ru(CO_2Mes)$_2$ η^6-(p-cymene)] (Mes = 2,4,6-trimethylbenzene) 207
5.11.2 – Synthesis of [Ru(CO_2Me)Cl η^6-(p-cymene)] 208
5.11.3 – Synthesis of [Ru(CO_2Me)$_2$ η^6-(p-cymene)] 209
5.11.2 – Synthesis of [Ru(CO_2Ad)$_2$ η^6-(p-cymene)] (Ad = Adamantane) 210
5.11.5 – Synthesis of (rac)-[RuCl(p-cymene)(C_6H_4-2-C_5H_4N-κ-C,N)] 211
5.12 – SYNTHESIS OF OTHER REAGENTS 213
5.12.1 – Synthesis of (2-ethoxy-2-oxoethyl)triphenylphosphonium bromide 213
5.12.2 – Synthesis of potassium phenyltrifluoroborate 213
5.12.3 – Synthesis of N-phenylpyridin-2-amine, ***3b*** *..... 214*
5.12.4 – Synthesis of potassium 2,4,6-trimethylbenzoate (MesCO_2K) 215
5.12.5 – Synthesis of pivaloyl-L-valine (Piv-Val-OH) 216

BIBLIOGRAPHY 217

Acknowledgements

I would like to thank Prof. Christopher Frost for firstly allowing me to undertake my PhD work within his group and for all the support, help and encouragement he has provided to me over my PhD. I would also like to thank Dr Antonine Buchard (Chemistry) and Dr Emma Emanuelsson-Patterson (Chemical Engineering) for useful discussions and help as my co-supervisors over my studies. I'd also like to thank the CSCT for the funding of my PhD project as well as extra-curricular activities that have allowed me to diversify my skillset greatly.

I would also like to thank the Frost group past and present, who provided countless useful discussions, advice and ideas over my time here. In particular I'd like to thank Dr Barrie J. Marsh and Dr Jamie A. Leitch for their help with the writing of this thesis in particular for errors and reality checks; as well as Andy, Sinéad, Sam and last but most certainly not least Dr Sean Goggins for his support and practical advice in the lab, as well as carrying of the chemistry football team. I'd also like to thank the various MChem students I supervised, for trying to carry out my half-witted ideas.

I would also like to thank John Lowe and Catherine Lyall (NMR) for their invaluable help in various aspects of the NMR equipment. I would also like to thank Prof. Frank Maarken for his loaning of electrochemistry equipment and Amelia Langley for helping me use said equipment and interpret the results gained from its use.

Last but by no means least, I'd like to thank my parents: Anne and John and sister Catriona for their support as well as my best friends: Matt, Kirsty, Craig, and the GB2014 squad for their support and ears for countless moans and rants. I also would like to give a special thanks to Caroline, without her love, support and rants at me, I'd have struggled to write my thesis and actually push through to finish all my work!

Abstract

C–H functionalisation in a regioselective manner remains a great challenge in the field of catalysis. There exists a number of novel and unique methodologies to differentiate sterically and electronically similar C–H bonds. One key method to achieve such functionalisations is by use of Lewis basic directing groups, to direct a metal centre to insert into the desired C–H bond which can then be reacted in a desired manner of functionalisation under a set of reaction conditions.

Chapter 2 reports the development of a methodology for the regioselective *meta* C–H primary alkylation of 2-phenylpyridine substrates using α-halo ester coupling partners, and some insights into the reasons for the observed regioselectivity and proposed catalytic cycle.

Chapter 3 reports the application of ruthenium catalysed σ-activation to the remote C–H functionalisation of carbazoles at the C4 position using tertiary α-bromoester coupling partners.

Chapter 4 reports the discovery of a new *para* selective carboxylation of aniline derivatives utilising a tetrabromomethane coupling partner using iron catalysis.

Publications

"α-Halo carbonyls enable *meta* selective primary, secondary and tertiary C–H alkylations by ruthenium catalysis." A.J. Paterson, **C.J. Heron**, C.L. McMullin, M.F. Mahon, N.J. Press and C.G. Frost, *Org. Biomol. Chem.*, 2017, **15**, 5993–6000.

"Ruthenium Catalysed Remote C4-Selective C–H Functionalization of Carbazoles *via* σ-Activation." J.A. Leitch, **C.J. Heron**, J. McKnight, G. Kociok-Köhn, Y. Bhonoah and C.G. Frost, *Chem. Commun.*, 2017, **53**, 13039–13042.

Abbreviations

Ad – Adamantyl

AMLA – Ambiphilic Metal-Ligand Activation

Ar – Aryl

Ar_F – Polyfluorinated Aryl

BHT – 2,6-di(*tert*-butyl)-4-methyl phenol

Bu – Butyl

CMD – Concerted Metalation Deprotonation

CV – Cyclic Voltammetry

Cy – Cyclohexyl

DCM – Dichloromethane

DFT – Density Functional Theory

DG – Directing Group

DMSO – Dimethylsulfoxide

dppe – 1,2-bis(diphenylphosphino)ethane

dppf – 1,2-bis(diphenylphosphino)ferrocene

EDG – Electron Donating group

Equiv – Equivalent

EWG – Electron Withdrawing Group

Et – Ethyl

HFIP – (1,1,1,3,3,3-hexafluoro)propan-2-ol

HOMO – Highest Occupied Molecular Orbital

HRMS – High Resolution Mass Spectrometry

i – ipso

IES – Internal Electrophilic Substitution

IR – Infra-Red

Int – Intermediate

IY – Isolated Yield

KIE – Kinetic Isotope Effect

L_n – Unspecified Ligand Set

LUMO – Lowest Unoccupied Molecular Orbital

M – Metal

m – meta

Me – Methyl

Mes –1,4,6-trimethylbenzene

MS – Molecular Sieves

N-Ac-*L*-Iso – *N*-acylated isoleucine

NBO – Natural Bond Order

NBS – *N*-bromosuccinimide

NFSI – *N*-fluorobenzenesulfonimide

NHC – *N*-Heterocyclic Carbene

NIS – *N*-iodosuccinimide

NMR – Nuclear Magnetic Resonance

o – ortho

OLED – Organic Light Emitting Diode

p – para

Phen – 1,10-phenanthroline

Phth – Phthalimide

Piv –2,2-dimethylpropanoyl

Piv-Val-OH – *N*-pivalated valine

p-TSA – *para*-toluenesulfonic acid

Py – Pyridine

RDS – Rate Determining Step

S_EAr –Electrophilic Aromatic Substitution

SET – Single Electron Transfer

S_NAr – Nucleophilic Aromatic Substitution

SOMO – Singly Occupied Molecular Orbital

TEMPO –(2,2,6,6-tetramethylpiperidin-1-yl)oxidanyl

TLC – Thin Layer Chromatography

TM – Transition Metal

TS – Transition State

Val – Valine

Introduction

1.1 – Catalysis and Sustainability

The construction of new C–C or C–X (X = heteroatom) bonds, is a key requirement in the development of synthetic organic methodologies, for the synthesis of new and unexplored molecular architectures. These substrates can possess desirable properties in the fields of pharmacology, biology, materials chemistry and supramolecular chemistry.

Within this context, cross-coupling reaction methodologies , primarily utilising palladium (Pd) complexes have come to the forefront of the field.[1–3] This domination has been driven by the fact that the Pd pre-catalysts used in such methods are, typically air and moisture stable. They also have relatively simple experimental set ups and work ups allowing for even greater convenience. Primarily though, Pd-catalysed cross-couplings benefit from the enormous scope of reagents and potential transformations possible, with demonstratable reliable efficiency. The use of this chemistry has been utilised on milligram to kilogram and even tonne scale processes by the pharmaceutical and fine chemical industries, becoming the go-to method for the formation of C–C and C–X bonds at the present day (*e.g.* Buchwald-Hartwig couplings for N–C bond formation or Suzuki couplings for C–C bond formations).[4–6]

Current pressures on terrestrial resources, means that ever more focus is being placed upon sustainable process, for the manufacture of materials and products. In a chemistry setting, this sustainability focus means that a process should adhere as closely as possible to the 12 rules of green chemistry.[7] The use of Pd, relates to three of these rules, through: the more efficient catalysis, improved atom economy and the use of safer chemicals.[8] Notwithstanding the substantial advancements in Pd catalysed cross-coupling methodology, certain drawbacks have persisted, as Pd has a relatively low crustal abundance, specific ligands/additives are often required to permit reactivity, and finally its toxicity to humans and animals in the environment.[8] In a bid to overcome some of these limitations, the use of other transition metals, both noble (Rh, Ir, Pt) and abundant

(Cu, Ni, Fe) have been investigated, as well as alternative methodological strategies to achieve these transformations.[9,10]

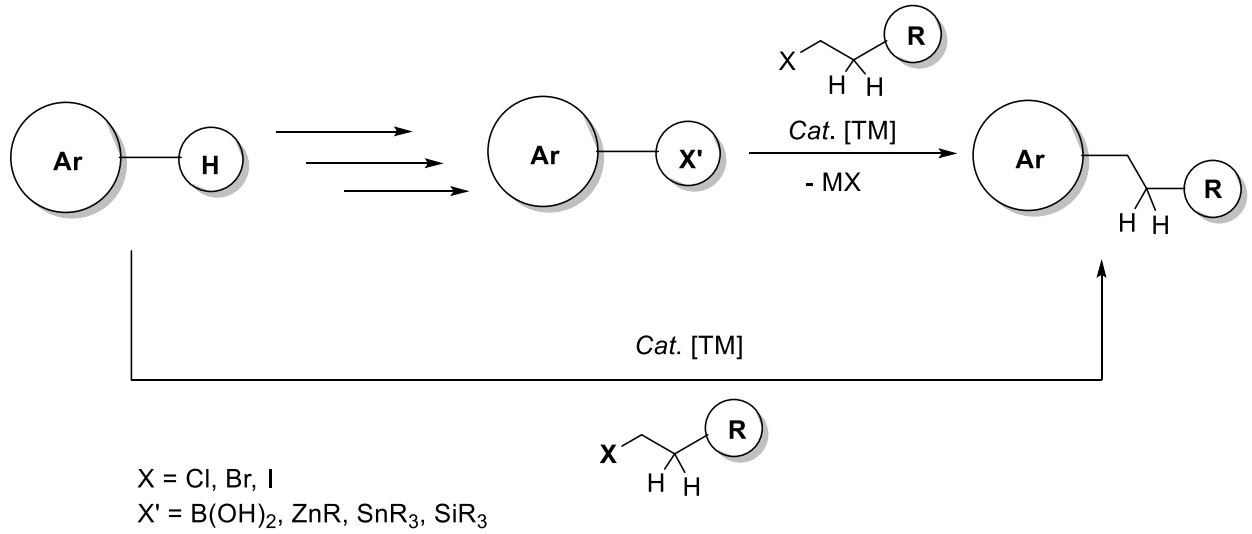

Figure 1: The difference in synthetic pathways required to achieve the same transformation between: a cross-coupling (top path) or C–H functionalisation (bottom path) methodology.

C–H functionalisation is one methodology, which can overcome some of the aforementioned disadvantages associated with classic cross coupling methodologies, as illustrated in Figure **1**. Traditional cross-coupling methods require potentially multi-step pre-functionalisation of the substrates, prior to coupling. This facet reduces the atom efficiency of synthesising a desired molecule of interest, leading to more waste and purification steps.[11] The benefits of C–H functionalisation over cross-coupling methodologies stem from the removal of one (or more) of the pre-functionalisation steps of the substrate molecules. This allows more streamlined synthetic procedures, reduction in time necessitated to access a target molecule, and potential variation to move away from highly pressured metal catalysts and ligand types.[12]

In the research presented here, we have focused upon ruthenium (Ru) catalysis to achieve the C–H functionalisation reactions that are of interest to us, notably, through the use of Ru(II) complexes. Like many Pd complexes utilised in cross-coupling reactions, Ru(II) complexes are also air and moisture stable; many of which are also commercially available. Another advantage is the substantially lower cost of Ru, compared to the other noble metals like Pd, Ir and Rh ($1788/ozt, $1480/ozt, $6000/ozt respectively, compared

with $250/ozt for Ru) (26/11/19 (NYSE)). Although all have similar crustal abundancies, the use of Pd in the automotive industry, Ir in the bulk chemical industry and Rh in the aerospace industry; means they are highly pressured resources. Comparatively Ru has relatively few commercial applications, leading to the lower described commodity price. Hence it is more sustainable, in an economic context and environmental context, as it is a less highly pressured resource.

In the context of selective and sustainable C–H functionalisation methodologies, the following literature review will begin by first studying mechanistic aspects of how reactivity specific to this project occurs. Furthermore, how C–H functionalisation methods can be utilised for the catalytic functionalisation of aromatic and heteroaromatic systems - with a specific focus on the regioselectivity will be discussed.

1.2– Methodologies to Achieve C–H Functionalisation

In the context of C–H functionalisation the strategies developed to overcome some of the challenges associated with these transformations can be classed as either "innate" or "chelate assisted". These challenges arise primarily from the high bond dissociation energy (BDE) of a typical C–H bond and the difficulties in differentiating between electronically and/or sterically similar C–H bonds in a molecule, the latter of which the innate reactivity of a typical C–H bond is dependent upon.[13,14] Many early examples of C–H functionalisation reactions utilise this innate reactivity of the substrates to achieve the desired transformation. Some examples of this include: electrophilic aromatic substitutions (S_EAr) on simple aromatics and heteroaromatics, free radical additions, and deprotonation of acidic C–H bonds.

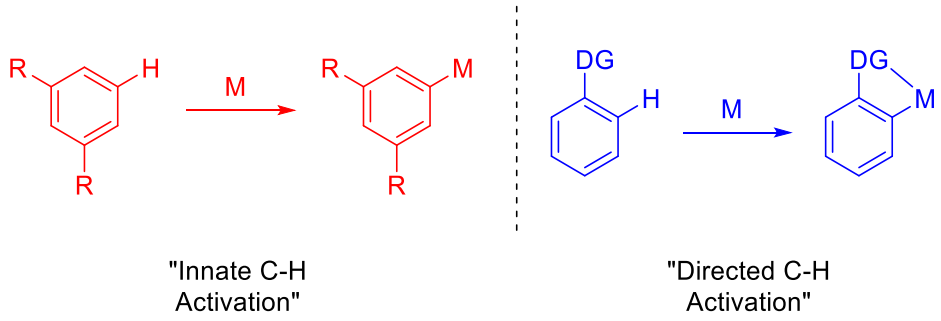

Scheme 1: Innate C–H activation *vs* Directed C–H activation.

More modern attempts to utilise this innate reactivity of C–H bonds has utilised transition metal (TM) catalysts that can directly insert into these C–H bonds, as shown in Scheme **1**. These carefully designed methodologies rely upon the desired C–H bond for the reaction being favoured by either being the least sterically encumbered, electronically rich or electronically poor, as depicted in Scheme **1**, with many reviews on this reactivity having been published to date.[15–17] Namely the methods that can be used to achieve these C–H activation events occur by: Electrophilic addition, oxidative addition, σ-bond metathesis or concerted metalation deprotonation (CMD).

Electrophilic addition generally involves the use of late- or post-transition metals (such as Al, Zn, Au, *etc.*), usually in a strongly polar reaction medium or anhydrous strong acid.[18] In this reaction type, the reactive species [M^{x+2}] proceeds through the presumed intermediate: [$L_nM^{x+2}(R)(X)$]. The use of this reaction type typically leads to functionalised alkanes; however, the intermediates are often very difficult to detect spectroscopically. Examples of this can be seen for the Au(III) catalysed oxidative coupling of aryl silanes with arenes, or the Pd(II) catalysed oxidative coupling of arylboronic acids with arenes.[19,20]

σ-Bond metathesis generally occurs with TMs containing the d^0 electronic configurations, as well as lanthanides and actinides, with a few examples of group 4 and 5 metals also known.[21] The reaction is in equilibrium, although does not typically result in the interconversion of alkyl groups with each other as depicted in Scheme **2**. There are some examples however, of interconversion between dihydrogen and metal alkyls with alkanes and metal hydrides are known.[22,23]

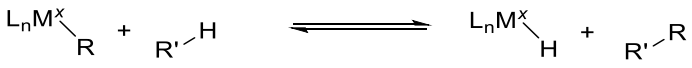

Scheme 2: Formation of a new C–C bond by *σ*-bond metathesis.

Oxidative addition of a TM species into a C–H bond, occurs generally when using low-valent, electron rich complexes of noble, platinum group metals, proceeding by a +2 net change in oxidation state of the metal. In this reaction type, as shown in Scheme **3** the reactive species [L_nM^x] is coordinatively unsaturated and hence almost always unstable. This dictates that it is formed *in situ* either by thermal or photolytic decomposition of a suitable precursor. An example of this can be seen in the photodecomposition of (η^5-C_5H_5)(PMe_3)$Ir^{III}H_2$.[24,25]

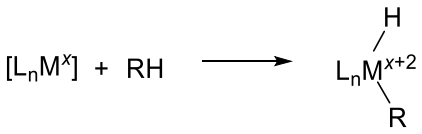

Scheme 3: Example of a C–H activation by oxidative addition.[24,25]

The final mentioned process, by which a TM catalyst can insert into a C–H bond, as mentioned previously is by a process known as concerted metalation deprotonation or CMD. CMD has received great interest in contemporary catalytic development, and work by Fagnou *et al.* and concurrently by McGregor *et al*. to elucidate this process and how the use of the metal catalyst and a suitable (carboxylate) ligand could allow the insertion of the metal into a C–H bond.[26,27] Alternative names for this process have been termed: internal electrophilic substitution (IES) or ambiphilic metal-ligand activation (AMLA).[28,29]

Despite these modern advances, the earliest proposal of a CMD-type mechanism was made by Winstein and Traylor, back in 1955 for the acetolysis of diphenylmercury in acetic acid, the proposed mechanism of which is shown in Scheme **4**.[30] This reaction is the reverse process to CMD, commonly referred to as protodemetallation.

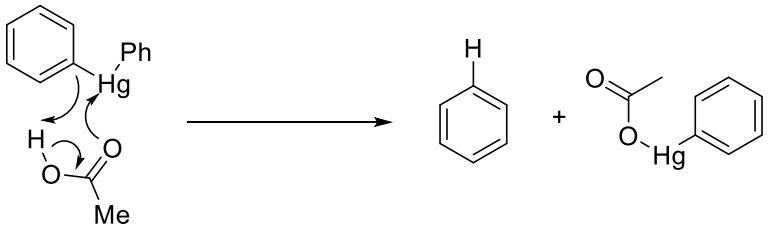

Scheme 4: Representation of the proposed mechanism for the acetolysis of diphenylmercury(II).[30]

Kinetic analysis of this protodemetallation reaction, suggested that the mercurial salt and the arene combined in a reversible fashion to form an intermediate, which then subsequently undergoes an irreversible proton transfer.[31] From this kinetic analysis, it was found from the primary KIE values (*c.a.* 6.0 – 7.0) that the proton transfer step was the rate limiting step.

This report for the protodemetallation process, then led to the first observation of the forward process, CMD in 1980 by Roberts and co-workers, detailing kinetic studies into the mercuration of arenes by $Hg(O_2CCF_3)_2$.[31] Previous studies of this process found the proton transfer step of the reaction to also be rate limiting, by the discovery of a large kinetic isotope effect (KIE) of $k_H/k_D \approx 6$.[32] Previous mechanistic explanations of this reaction had favoured a S_EAr -type process, with discrete σ-complexes.[33–35] Roberts and co-workers proposed the following transition state for the rate determining step (RDS) for the mercuration of arenes, shown in Scheme **5**, which follows very closely to the original mechanism proposed by Winstein and Traylor.[30,31]

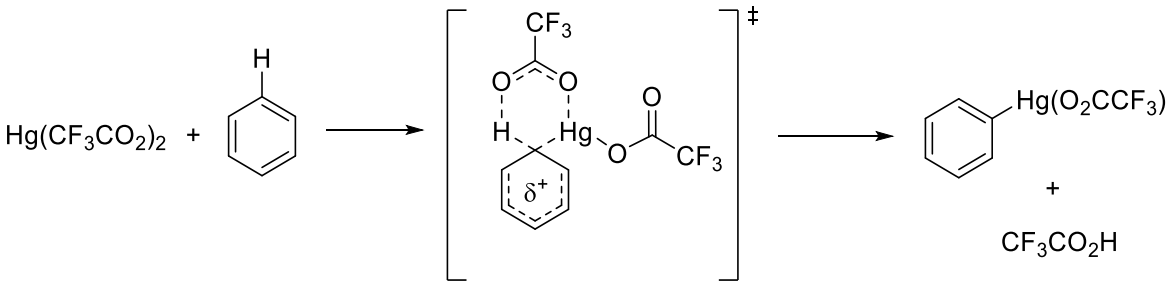

Scheme 5: Reagents and proposed transition state for the base-assisted mercuration of benzene.[31]

Further investigative work by Olah and co-workers, indicated the presence of a weakly bounded intermediate by NMR studies, rapidly exchanging between a σ-complex and an η^2 π-complex, as shown in the transition state (TS) in Scheme **5**.[35] From this data and

kinetic data collected by Roberts and co-workers,[31] it was concluded that the C–H bond cleavage and the C–Hg bond formation both occurred concurrently. Despite these in-depth studies the authors could not completely rule out an S_EAr type mechanism.[31]

When discussing "chelation assisted" or "directing group" methodologies, these transformations use pre-existing functional groups on the molecule to direct a TM catalyst towards a desired C–H bond for functionalisation as seen in Scheme **1**. This method overcomes the intrinsic issues with having multiple C–H bonds in a molecule, by lowering the energetic pathway of the desired reaction, through entropy reduction, placing the TM catalyst proximal to the desired C–H bond. Of these methodologies, there are two methods by which the TM catalyst can insert into a desired C–H bond, namely: oxidative addition and concerted metalation deprotonation (CMD).

The use of Lewis basic directing groups to control the use of such reactivity was first reported in the 1960s, *via* the use of Pd complexes.[36,37] This work by Cope *et al*. found that the choice of Pd catalyst was essential to achieve the desired reactivity, with $[Pd(OAc)_2]$ found to be the most optimal, with the choice of the acetate ligand also playing a key role. It must be noted that the choice of carboxylate ligand used in C–H functionalisation reactions is essential to the system reactivity, by variation of the energetic pathway(s) that lead to the desired product.[38–40]

Further mechanistic investigations demonstrate that the non-innocent acetate ligand first plays the role of aiding solvolysis of the reaction intermediates, with its larger effective volume compared to chloride. Secondly, the ability of an acetate group to fluxionate between a monodentate or bidentate ligation mode, allows the electrophilicity of the Pd complex to be favourably enhanced and can also act as an intermolecular base to deprotonate a substrate, in turn forging the C–Pd bond, *via* a process akin to CMD discussed previously.[39]

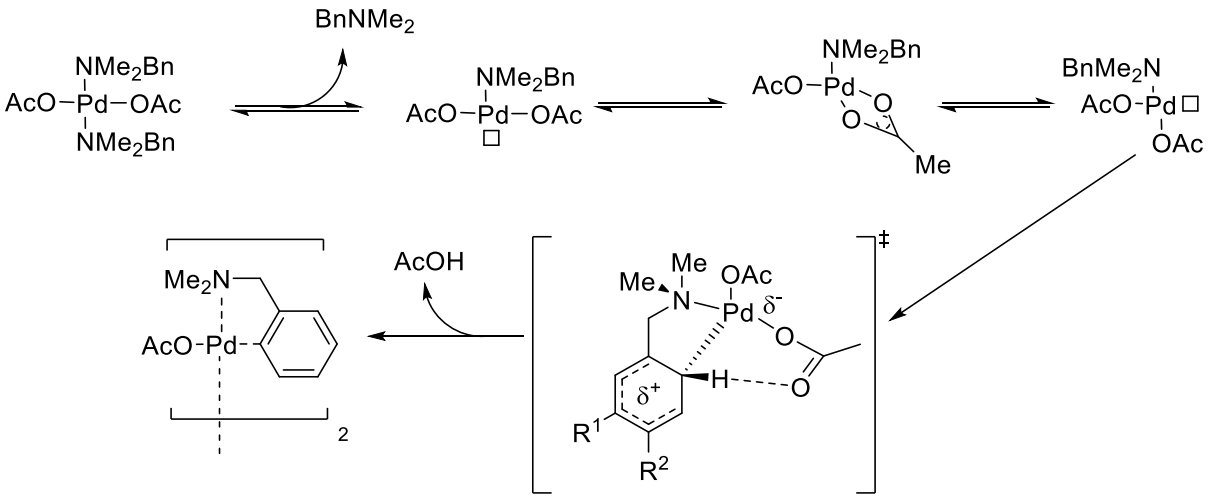

Scheme 6: Mechanism for the cyclometallation of dimethylbenzylamine (DMBA) with $[Pd(OAc)_2]$.[41]

Scheme **6** shows the mechanistic explanation by Ryabov *et al*. for the cyclometallation of *N*,*N*-dimethylbenzylamine (DMBA) with $[Pd(OAc)_2]$.[41] This mechanism was consistent with the observed negative slope of the Hammett plot they found ($\rho = -1.6$), inferring that there is a build-up of negative charge in the transition state of this reaction step, which indicates the simultaneous removal of the proton and formation of the Pd–C bond. This also fits the KIE (k_H/k_D) value of 2.2 and the negative calculated entropy of activation ($\Delta S^{\ddagger} = -60$ kcal K^{-1} mol^{-1}) for the $Pd(OAc)_2$[DMBA-H] complex.[41]

In 2005, Davies, Donald and McGregor reported an in-depth computational analysis which showed that the most thermodynamically accessible route proceeds *via* an agostic interaction between the acetate ligand and proton. This leads to a drop in pK_a of the C–H bond, allowing for nearly barrierless proton transfer to the acetate. This is then followed by an acetate-assisted six-membered cyclic transition state as described in Scheme **7**.[27,29]

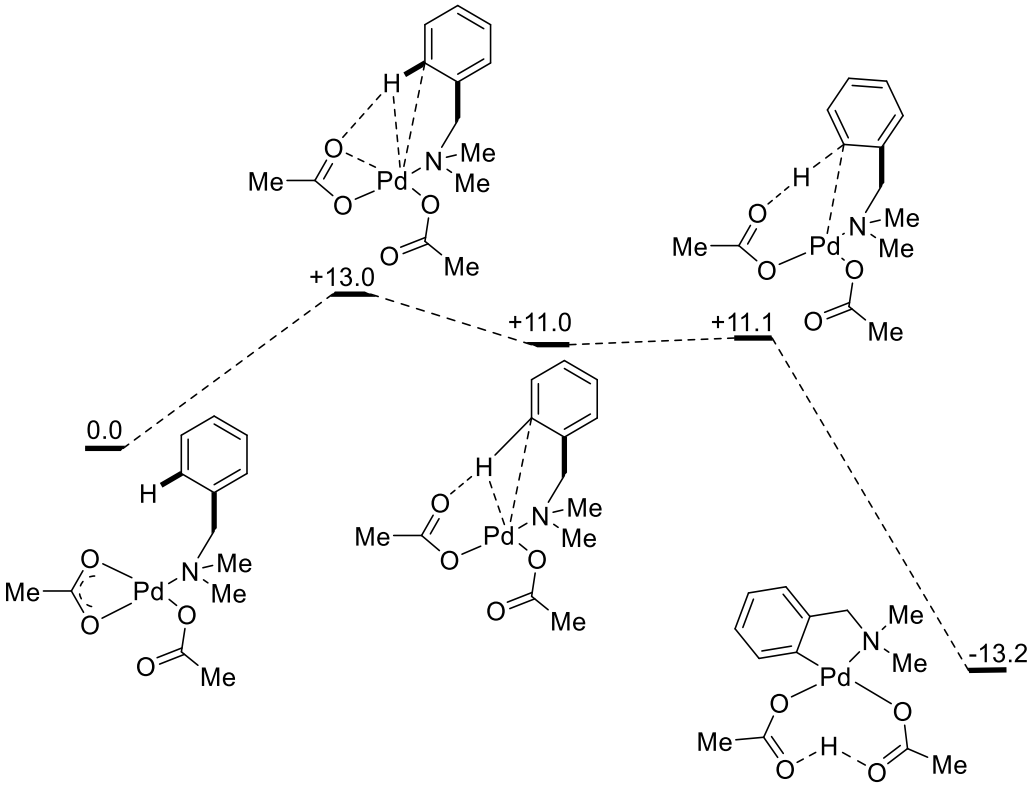

Scheme 7: Computed reaction profile of DMBA-H with Pd(OAc)2. Values in kcal mol^{-1}.[27]

The first reports of utilising Ru(II) salts in a reaction, that involves a step involving a CMD type process was developed in 2008, by Dixneuf *et al.*[42] This study reported the diarylation of 2-phenylpyridine, as shown under the conditions in Scheme **8**. This work reported that the pyridine group acts as a "directing group" to direct the Ru-NHC catalyst towards the *ortho* C–H bond, *via* the intermediate in brackets in Scheme **8**. The computational modelling indicated that a molecule of base, coordinated to the Ru acts as an internal base to make the removal of the *ortho* C–H bond very low in energy, even when using a weak base this mechanism was found to be strongly favoured.[42] This work was found to utilise similar transitions states (TS) and bond lengths of molecules for other reactions, involving similar internal deprotonation events, leading to the conclusion that a CMD process was in operation.[43,44]

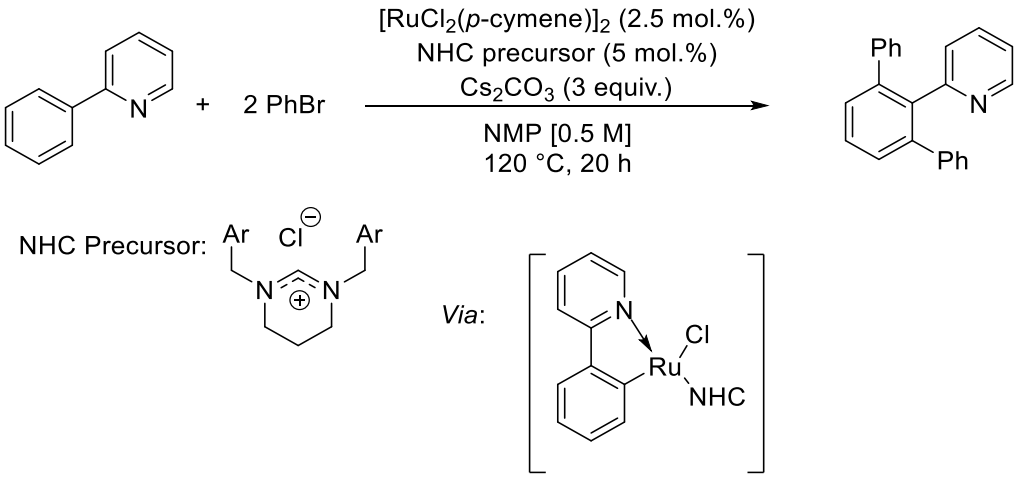

Scheme 8: Reaction conditions and proposed intermediate for the diarylation of 2-phenylpyridine.[42]

1.3 – Directing Groups in C–H Functionalisation

The use of directing groups that strongly coordinate a TM centre, most generally N-based directing groups, has facilitated the rapid expansion of a variety of directing groups. These are generally Lewis basic heteroaromatic groups, such as: pyrazoles, pyrimidine, triazoles, tetrazoles, oxazoline, and then acyclic derivatives, like ketimines for example. The structures of some of these directing groups are shown in Scheme **9**.[45]

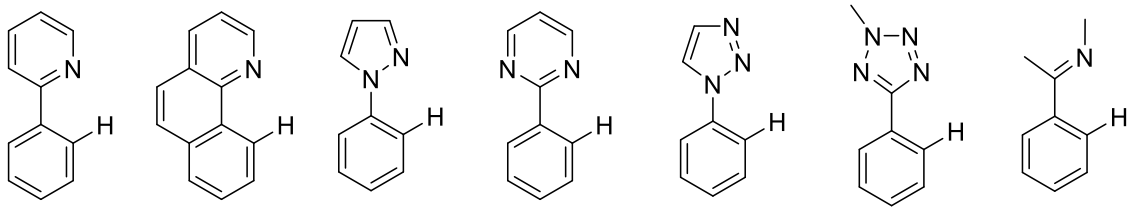

Scheme 9: Examples of strongly coordinating directing groups.

Through extensive study, a toolbox of C–C and C–X bond forming reactions have been developed, a summary of which are shown in Scheme **10**. These transformations were initially achieved through the use of noble, platinum groups metals, such as: Pd,[46] Rh,[47] and Ru.[48] However, more recently there have been reports of these transformations, achieved through first row TMs, such as: Co,[49] Mn,[50] and Fe.[51]

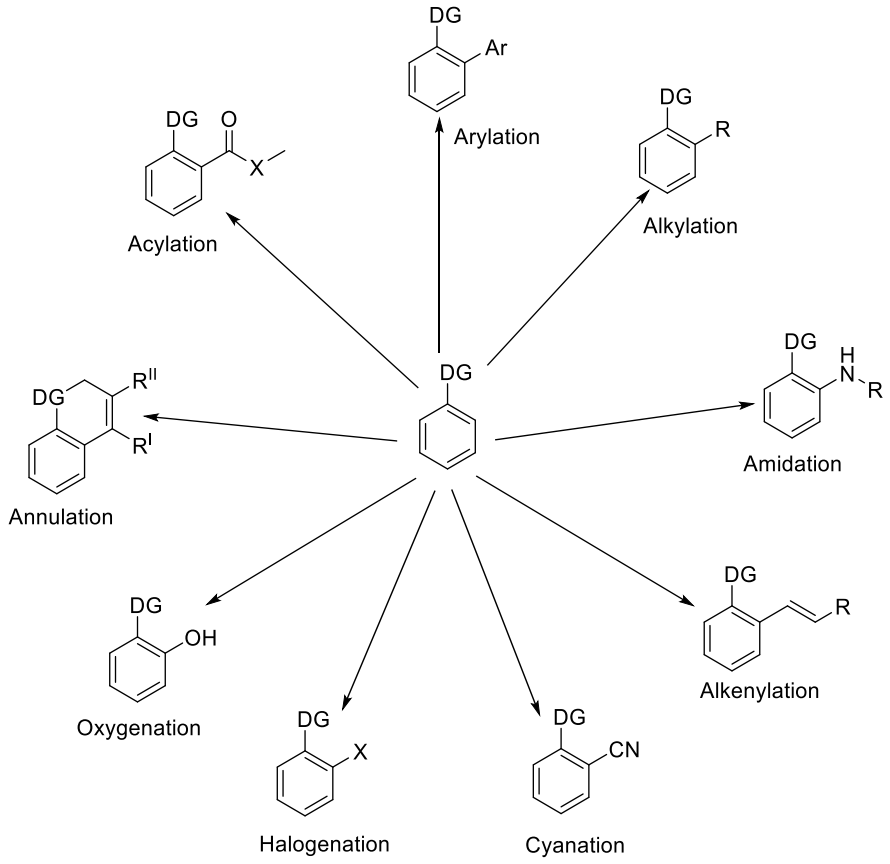

Scheme 10: C–H functionalisation transformations reported, through the use of "strong" directing groups.

Despite the plethora of advances using so-called strongly coordinating directing groups, one drawback of relying upon such directing groups is that they are generally not ubiquitous in organic molecules. To overcome this limitation the use of “weakly” coordinating directing groups (generally achieve coordination through a carbonyl (C=O) group), these are much more commonly encountered functional group motifs, examples of which include: carboxylic acids, aldehydes, esters, anilides and carbamates. The structures of some of these directing groups are shown in Scheme **11**.

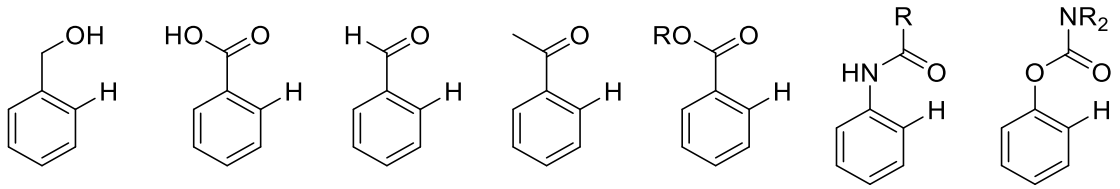

Scheme 11: Examples of weakly coordinating directing groups.

The weaker coordination of the metal in these reactions makes cyclometallation events more energetically challenging, resulting in (to date) a less substantial toolkit of transformations are available to these substrates, when compared to the corresponding strong directing group substrates. These substrates almost exclusively reply upon the use of noble metals, such as: Pd,[52] and Ru.[53]

Directed or chelation assisted C–H activation has enabled the true scope of C–H functionalisation reactions to be realised. A huge majority of these examples result in a large scope of *ortho* selective C–H functionalisation transformations to be realised. However, in order to broaden this scope to include *meta* and *para* C–H functionalisation reactions, different techniques are necessitated. The next section will begin to discuss examples of such *ortho* C–H functionalisations (with specific focus on Ru catalysis), and the techniques subsequently developed to allow for *meta* and *para* C–H functionalisations to be realised.

1.4 – Overview of Ruthenium Catalysed *ortho* Functionalisation Reactions

1.4.1 – C–C bond Forming Reactions

The formation of C–C bonds, in the synthesis of small, unfunctionalised molecules; are amongst the most prevalently used reactions used in the pharmaceutical and fine chemical industries at the present time. Numerous *ortho* C–H to C–C transformations have been demonstrated, utilising Ru(II) catalysis.

The first such report of a such a Ru(II) catalysed transformation was made in 2002 by Inoue *et al*.[54] for the *ortho* selective arylation of an aromatic ketimine, under the conditions shown in Scheme **12**.

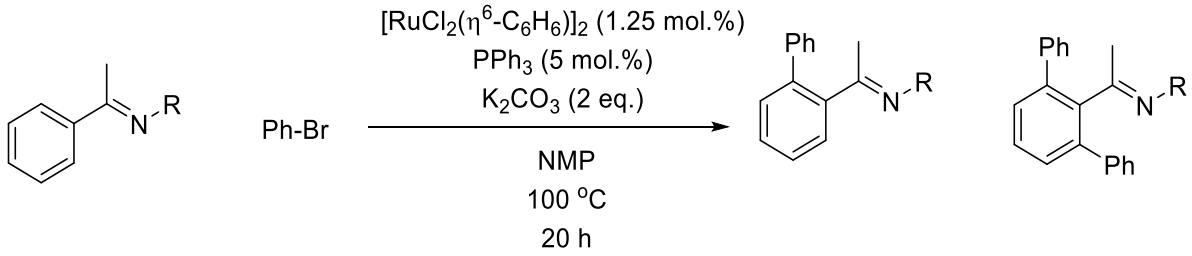

Scheme 12: *ortho* C–H Arylation of a ketimine.[54]

This reaction uses the strongly coordinating ketimine directing group to allow the Ru to insert into the *ortho* C–H bond of the ketimine. This cyclometalated species then reacts with the aryl bromide in an oxidative addition/reductive elimination type process to arylate the *ortho* position and re-enter the catalytic cycle. The addition of 2 equivalents of a phosphine ligand per Ru atom, was found to aid this step of the reaction. For aryl bromides, this addition of phosphines was found to be more effective, and interestingly for using aryl chlorides, phosphine oxide ligands were found to be optimal.[55] The scope of this reaction has since been expanded to include a wide variety of directing groups.[48]

Direct *ortho* C–H alkylations have also been reported, using alkyl halides as coupling partners by Ackermann *et al*.[56] Similarly as before, the Ru inserts into the *ortho* C–H bond *via* a CMD type mechanism, and an analogous oxidative addition/reductive elimination process occur to yield the *ortho* alkylated product. Several directing groups were also utilised, such as: oxazolines, pyridines, imines and pyrazoles, along with a variety of alkyl halides, under the conditions shown in Scheme **13**.[56]

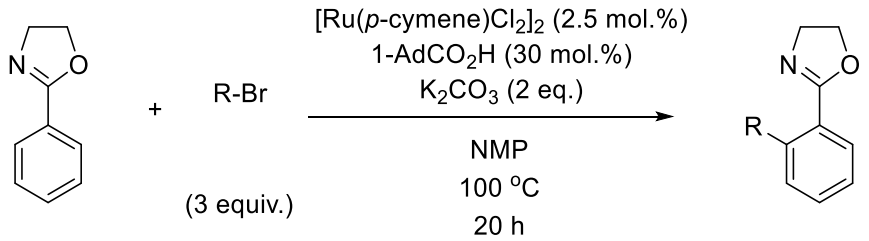

Scheme 13: *ortho* C–H alkylation of a oxazoline.[56]

This reaction was proposed to proceed *via* the mechanistic cycle shown in Scheme **14**.[57] The *ortho* arylation, as depicted in Scheme **12** proceeds by a similar mechanism. However, this reaction has been limited to the use of primary alkyl halides, until a recent

report disclosed by Larrosa *et al*. showed that secondary alkyl halides can also be coupled by using a cyclometallated Ru complex, under relatively mild conditions.[58]

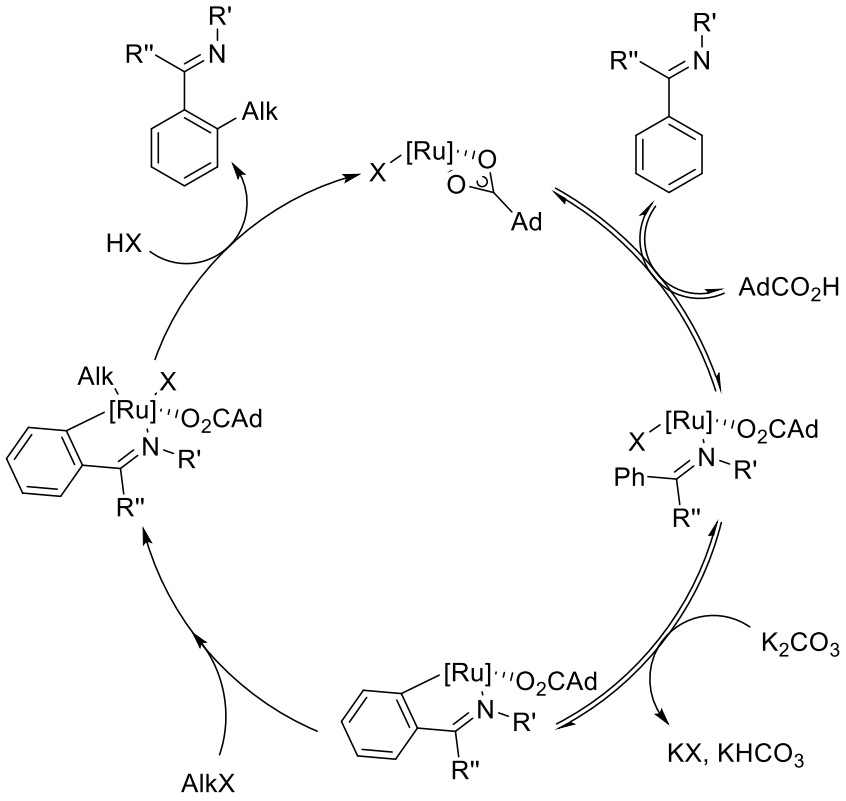

Scheme 14: Proposed mechanism for the *ortho* C–H alkylation of an aromatic ketimine.[57]

Further C–H activation alternatives to traditional S_EAr-type mechanisms have been developed. These transformations obviate the need for stoichiometric amounts of Lewis acids and often proceed with complementary regioselectivity (through chelation assistance proximity, rather than traditional S_EAr electronics). These include acylations, aminocarbonylations and alkoxycarbonylations, which utilise: acid chloride, carbamoyl chloride or chloroformate coupling partners respectively.[59–61]

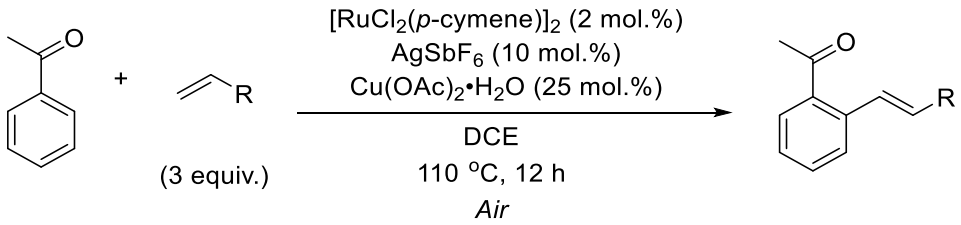

Scheme 15: Ru(II) catalysed *ortho* C–H alkenylations.[62]

Heck-type alkenylations have also been reported by Jeganmohan *et al*. using Ru(II) catalysis, under the conditions shown in Scheme **15**.[62] This proceeds by a normal CMD insertion of the Ru into the *ortho* C–H bond, followed by coordination of the alkene to the Ru, and inserts into the alkene by migratory insertion. β-Hydride elimination then rapidly proceeds, to release the Ru as Ru(0), necessitating the addition of an external oxidant to the reaction to allow for the system to be catalytic. This transformation has been reported for a variety of directing groups, such as: pyridines, pyrazoles, carboxylic acids and amides.[63]

The analogous reaction, for the alkynylations has also been reported, allowing for the direct synthesis of heterocycles, with alkyne coupling partners.[64] This methodology has been reported for the efficient synthesis of: isoquinolines, napthylpyridines, phenyl pyrimidines, phenyl hydrazines, pyridines, isoquinolones, isocoumarins and indoles.[64]

1.4.2 – C–X Bond Forming Reactions

The formation of C–C bond formation reactions cannot be understated in modern synthetic chemistry development. However, the selective and efficient construction of C–X bonds is also of great importance. Recent advances in this area have focused upon utilising chelation assistance to couple the desired functional group or atom. One such example of this can be seen in the direct *ortho* C-H amidation of aromatic substrates, using sulfonyl azides as coupling partners, under the conditions shown in Scheme **16**.[65] This has been achieved on a variety of directing groups such as: amides, ketones, pyridines, pyrazoles and pyrimidines.[65]

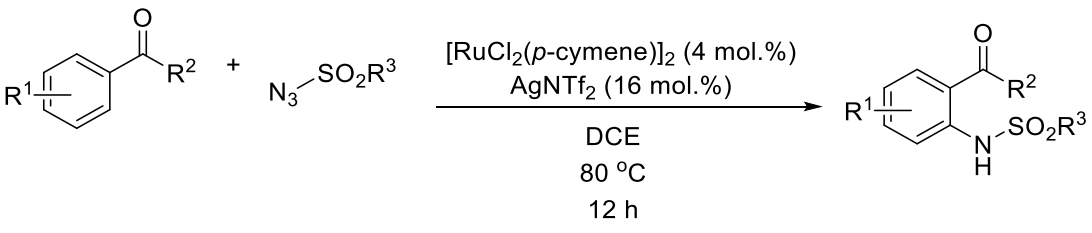

Scheme 16: Direct C–H amidation of aromatic ketones using sulfonyl azide coupling partners.[65]

The direct C–H oxygenation of bonds is also of great interest, as the undirected synthesis of phenols from the corresponding arene, generally requires very harsh

conditions and high temperatures.[66] The use of Ru(II) allows this oxygenation to be achieved under substantially milder conditions, as reported by Ackermann and co-workers in 2012, under the conditions shown in Scheme **17**.[67] This transformation has been reported on a variety of substrates, such as: ketones,[67] esters, Weinreb amides, carbamides and anilides.[65]

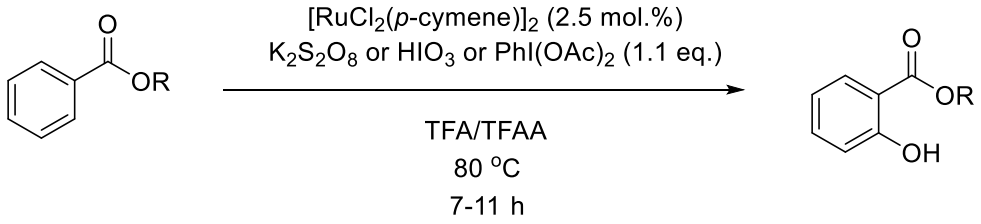

Scheme 17: Directed *ortho* C–H hydroxylation of aromatic esters.[67]

The *ortho*-oxygenations, thiolations and selenations of benzamide substrates have been reported, under Rh catalysis conditions by Yu *et al.*[68] under oxidative conditions; following a similar mechanistic pathway to the aforementioned examples previously mentioned in this section. *ortho*-Aroylation reactions using Cu(II) catalysis are also known, under oxidative conditions.[69]

ortho-Halogenation reactions have been described by Ackermann *et al*., utilising simple *N*-bromosuccinimide (NBS) or *N*-iodosuccinimide (NIS) reagents in a highly selective manner, on benzamide substrates.[70] This transformation differs from the previous Ru mentioned so far, in that it requires a Ru(0) precatalyst, and that a single electron transfer occurs at some point in the mechanistic cycle, as addition of 2,2,6,6-tetramethylpiperidin-1-yl)oxidanyl (TEMPO) results in termination of reaction.[70]

The formation of C–B bonds is of particular use in synthesis, as such molecules can be further utilised in Pd cross-coupling reactions. Such a bond formation has been reported in 2017 by Ackermann and co-workers, utilising commonly encountered boron sources (*e.g.* B_2Pin_2 or B_2Cat_2) under mild conditions, under the conditions shown in Scheme **18**.[71]

This borylation methodology has been extended by Reek *et al.* using Ir catalysis, by creating a hydrogen bonding template to direct the Ir towards the *ortho* C–H bond preferentially over the *meta* or *para* protons.[72]

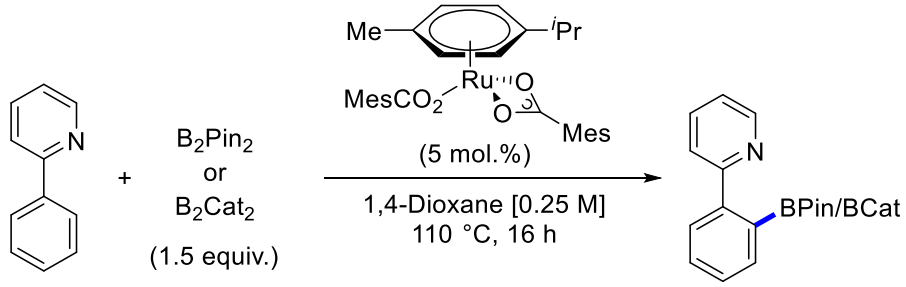

Scheme 18: Ru(II) catalysed *ortho* borylation of 2-phenylpyridines.[71]

A final example, reported by Tobita *et al.* involves the use of an unusual directing group in the form of an alkynyl entity, as shown in Scheme **19**.[73] This work found that an initial *trans*-hydrogenation step occurred first, followed by an *ortho* silylation. The ligand was found to play an essential role in this transformation, by stabilisation of the Ru species.[73]

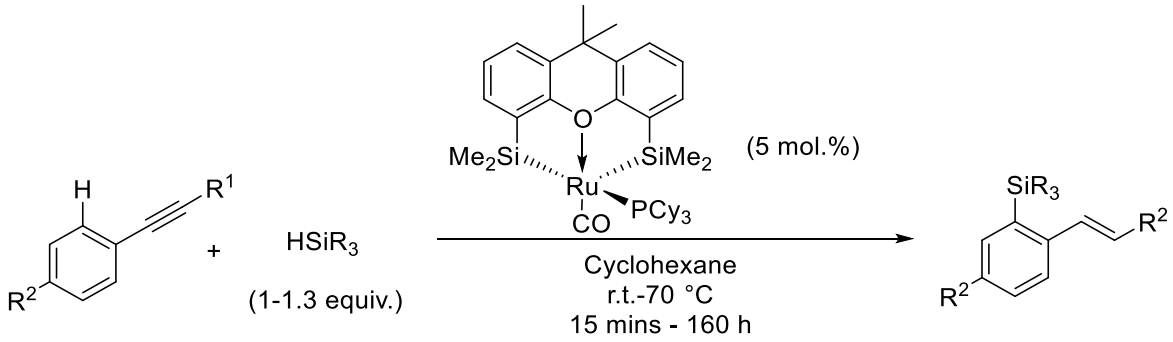

Scheme 19:Ru catalysed *ortho* silylation and *trans*-hydrogenation of aryl alkynes.[73]

1.5 – Overview of *meta* C–H Functionalisation Reactions

The ability to regioselectively functionalise specific C–H bonds is of high importance to contemporary synthetic development. The examples discussed in the previous section, discussed the formation of cyclometalated intermediates which then undergo a reaction with a suitable coupling partner to furnish the desired *ortho* substituted product.

The ability to regioselectively access *meta* functionalised benzene structures is also of great importance.[47] The above methods relied upon proximity-based directing groups to impart selectivity, therefore accessing more remote positions requires the development of more elaborate techniques. For these reasons, often overcoming formation of unwanted regioisomers and low reactivity of the C–H bonds can be a great challenge. This next section will look to understand the methodologies that have succeeded in unlocking *meta* C–H functionalisation.

1.5.1 – Sterically Controlled Direct *meta* C–H functionalisation

The first reported regioselective example of *meta* C–H functionalisation was, to the best of our knowledge, reported by Smith *et al*. for the *meta* borylation of 1,3-disubstituted arenes.[74] This transformation utilises direct C–H activation, as described previously in Scheme **1**, in this case instead exploiting the steric and electronic bias of the substrate.

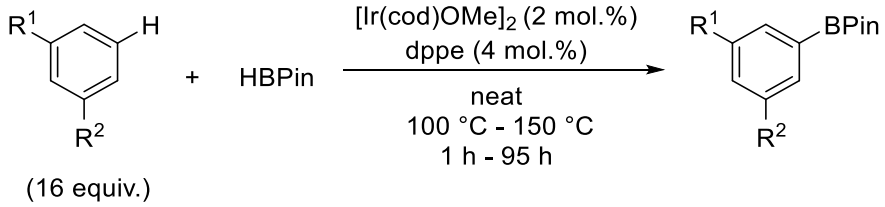

Scheme 20: Ir catalysed *meta* borylation of 1,3-disubstituted arenes.[74]

In this report a vast excess of the arene is used as a reaction medium, and where the arene is a solid, cyclohexane was used as the solvent, under the conditions shown in Scheme **20**. Despite the elegant advance, this transformation uses a fairly high loading of Ir and is limited to only 1,3-disubstituted arene substrates, limiting its widespread applicability. Recent work by Chirik *et al*. demonstrated that this limitation of high catalytic loading can be overcame, through utilising a Co-based catalyst, achieving similar yields and selectivites.[75] Hartwig and co-workers have applied the *meta* selective C–H borylation strategy to subsequent Pd catalysed alkylation and allylation chemistries to allow for a wide range of structurally diverse molecules.[76]

Use of a directed C–H activation methodology has been achieved more recently, to enable *meta* borylations, as described by Nakao *et al*. through use of a bifunctional Ir-

Lewis acid catalyst which forms a H-bonding network to direct the Ir to the *meta* C–H bond, under the reaction conditions shown in Scheme **21**.[77] This is allowed by the coordination of the amide nitrogen atom to the Al, this then brings the Ir proximal to the *meta* C–H bond, allowing for a regioselective outcome of >99:0:0 (*m*:*o*:*p*).

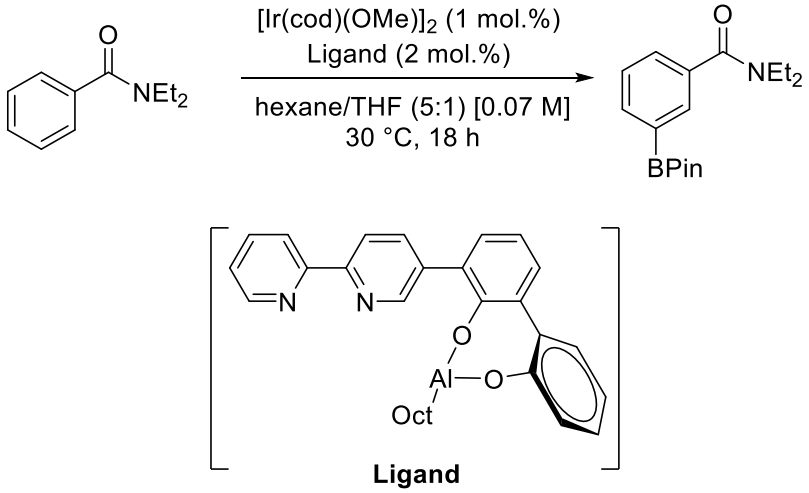

Scheme 21: Reaction conditions for the *meta* borylation of arenes, using a bifunctional Lewis acid-Ir catalyst.[77]

In 2009, Yu *et al*. reported the exploitation of the electronic bias of electron deficient arenes, to achieve a *meta* alkenylation, utilising a specific sterically encumbered pyridine ligand, under the conditions shown in Scheme **22**.[78] Despite the shown preference for the *meta* isomer, the competing *para* isomer was also observed in the majority of examples. A similar methodology has been explored computationally and experimentally by Wu and Zeng, utilising a different ligand subset (mono-*N*-protected amino acids).[79] Sanford and co-workers have also reported the acetoxylation of electronically biased arenes, where the discrepancy between the *meta*/*para* isomers is more prevalent.[80]

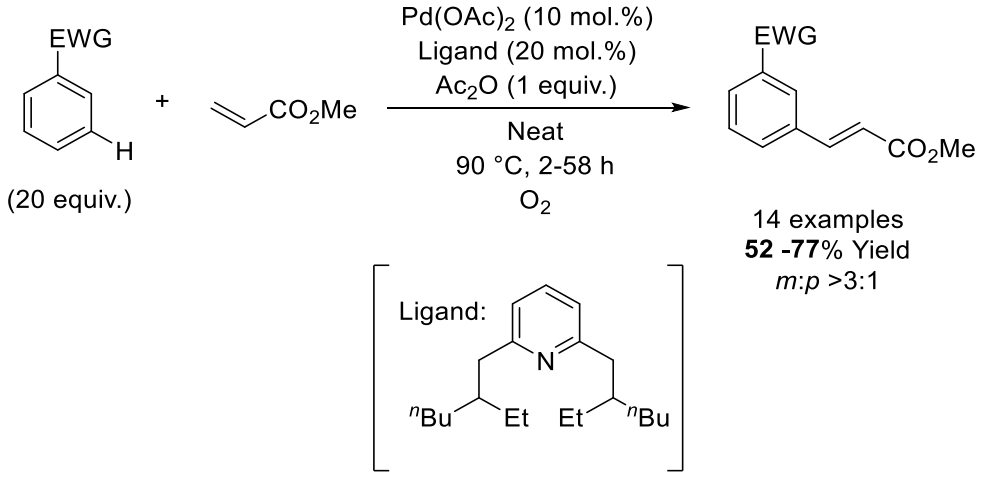

Scheme 22: Pd catalysed *meta* C–H alkenylation of electronically biased arenes.[78]

The reactions discussed in this section so far, all require a vast excess of the arene substrate in the reaction, commonly using them as a solvent. Ritter and co-workers have described the C–H imidation of electronically biased arenes, utilising dual Pd/Ag catalysis, with the arene as a limiting reagent, under the conditions shown in Scheme **23**.[81]

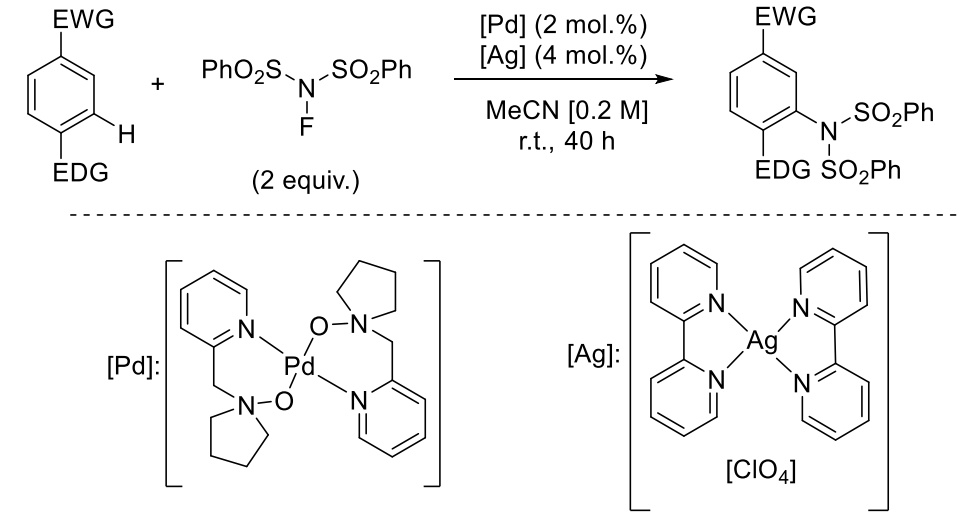

Scheme 23: Pd/Ag catalysed *meta* C–H imidation of electronically biased arenes.[81]

This work was shown to proceed only when a mixture of electron withdrawing (EWG) *meta* directing and electron donating groups (EDG) *ortho*/*para* directing groups were present to direct towards the *meta* C–H bond. This was shown to proceed through a radical mechanism, whereby the Ag salt engages in a single electron transfer (SET) process, which then subsequently reacts with the Pd catalyst.[81]

1.5.2 – Directing Group Controlled *meta* C–H Functionalisation

Moving from direct C–H activation, as controlled by a substrates steric and electronic biases, the use of directed C–H functionalisation is by far the most commonly encountered method of achieving *meta* C–H functionalisation. The first use of directing group mediated *meta* C–H functionalisation was reported by Gaunt *et al*., who demonstrated the *meta* arylation of aromatic acetamides using an electrophilic Cu catalyst as shown in Scheme **24**.[82]

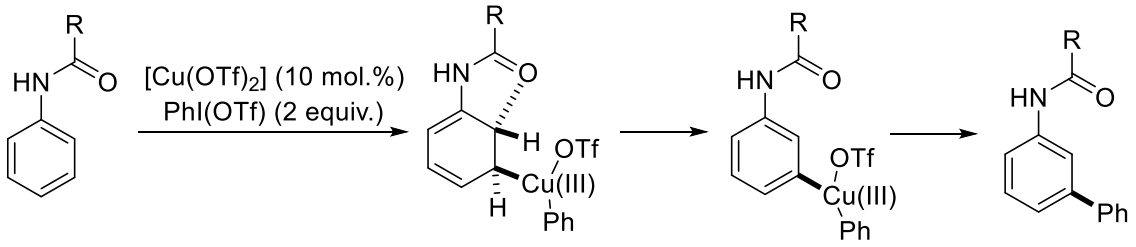

Scheme 24:Reaction conditions and proposed mechanistic explanation for the *meta* C–H arylation of acetamides.[82]

This reaction has also been shown to be applicable for α-aryl carbonyl compounds utilising a Cu catalyst.[83] Studies on the mentioned reaction using α-aryl carbonyl compounds have been shown to work at higher temperatures in the absence of a metal catalyst. It was concluded that the Cu catalyst and hypervalent iodine species interact to form the active catalyst to facilitate the transformation.[82,83]

Another example of this directing group methodology was pioneered by Yu and co-workers, where a "U-shaped" directing group is utilised to facilitate *meta* alkenylation of arenes.[84,85] The presence of the bulky ^{t}Bu groups, as shown in the substrate molecule in Scheme **25**, suggested to fix the geometry of the molecule, such that the nitrile directing group is proximal to the *meta* C-H bond, shown in the molecule. This approach is normally made difficult by the required rigid, cyclic transition state (TS) that becomes energetically unfavourable when the ring size is greater than seven, due to the entropic cost.[85] The method developed by Yu *et al.* solves this problem by using a weakly coordinating nitrile group, which alleviates the generated ring-strain of the 12-membered palladacycle. A CMD process is then proposed by the authors, allowing the insertion of

the Pd into the C-H bond, followed by a classical Heck-type mechanism, with the Ag salt oxidising the Pd(0) generated back to Pd(II).

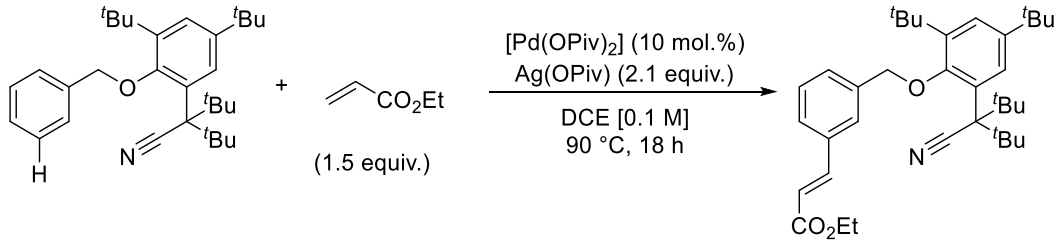

Scheme 25: Pd(II) catalysed *meta* C–H alkenylation of toluene derivatives, using "U-shaped" template.[84]

The use of aryl boronic acids/esters as coupling partners, under slightly modified reaction conditions has also be reported by Yu *et al*.[84] A drawback of this methodology is the requirement of a bulky ligand to be attached to the substrate molecule, *thus* requiring two additional steps to install and remove the directing group. One iteration of this work by Tan *et al*. makes the installation and removal steps simpler by using a silyl ether (Figure **2**) linker to attach the directing group, which can then be removed simply by reacting with TsOH.[86]

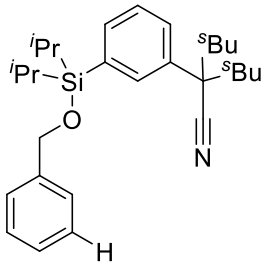

Figure 2: Si-based *meta* directing template developed by Tan *et al*.[86]

From this point onwards, there has been a tremendous volume of reports from Yu and Maiti and co-workers, amongst many others. A summary of these templates and the transformations available to them, are shown in Scheme **26**. Firstly, Maiti and co-workers reported the *meta* alkenylation phenylacetic acid derivatives (Scheme **26a**).[87] Li and co-workers then showed that an *in situ* created phthalimide (from phenylethylamides derivatives) enabled *meta* selective alkenylation chemistry (Scheme **26b**).[88] Yu then reported that his U-shaped template was also amenable to the *meta*-alkenylation of phenylacetic acid derivatives (Scheme **26c**).[89] Maiti and co-workers demonstrated that

sulfonates could be used as linkers for this methodology and were shown to be able to undergo a Julia reaction give the di-vinylated benzene (Scheme **26d**).[90] Yu and co-workers then reported that the use of a pyridine template enabled *meta*-alkenylation and iodination of benzyl alcohol derivatives. This was an important step as can potentially unlock other chemistry that pyridyl directing groups can carry out in Pd catalysis (Scheme **26e**).[91] Li showed that amide linked templates could be used in *meta*-alkenylation reactions (Scheme **26f**).[92] Maiti and co-workers demonstrated that their sulfonate template from before was also amenable to *meta*-hydroxylation methodology (Scheme **26g**)[93] and that increasing the linker size maintained reactivity in remote functionalisation (Scheme **26h**).[94]

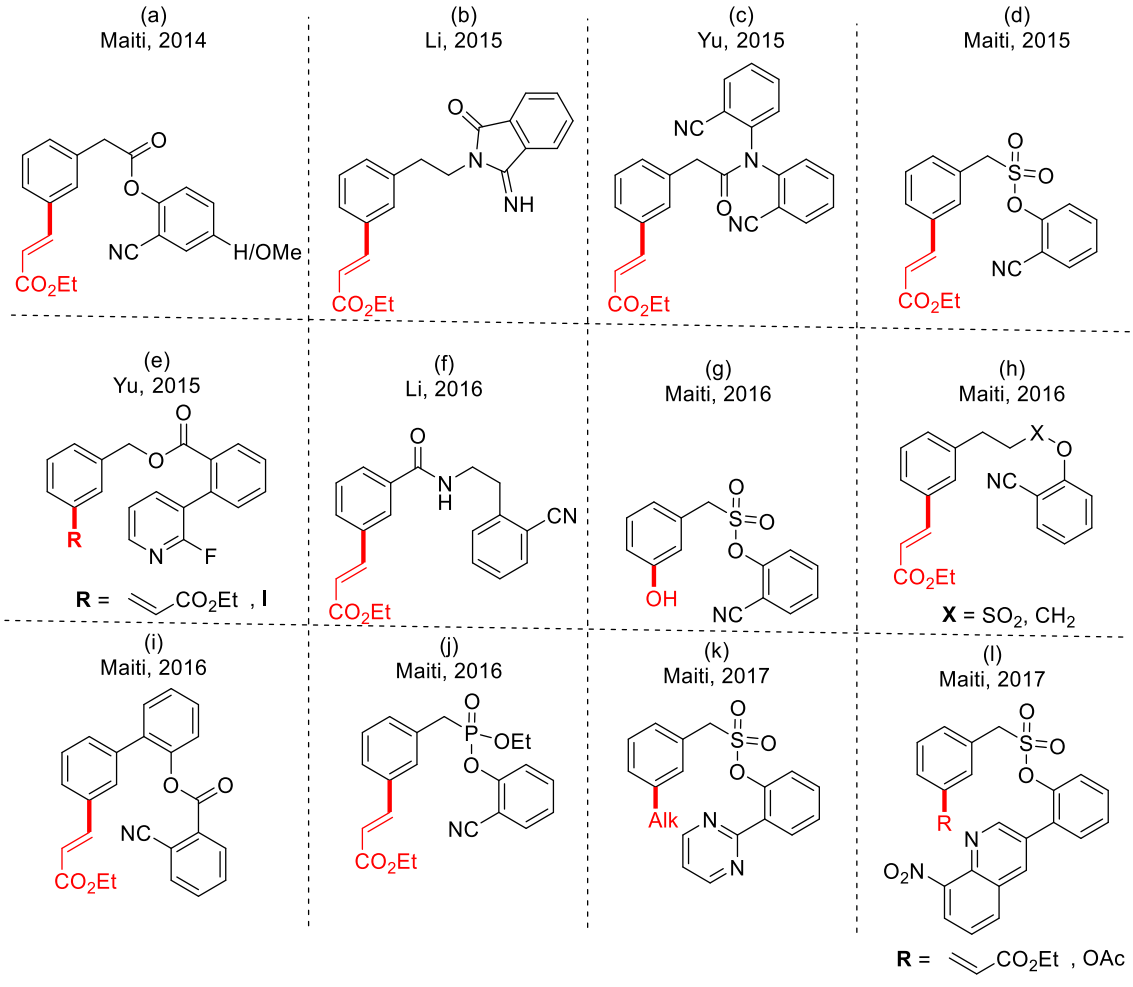

Scheme 26: Summary of templates and transformations used in template-assisted remote meta-functionalisation.

The same group then demonstrated that a biaryl system (Scheme **26i**),[95] and phosphonate linkers (Scheme **26j**),[96] were tolerated in catalysis. They also demonstrated that sulfonates furnished with pyrimidine (Scheme **26k**),[97] and nitroquinoline (Scheme **26l**),[98] granted access to *meta* functionalised arenes.

More recent work by Maiti *et al*. has expanded the scope of this methodology to include the Pd catalysed selective *meta* alkylation, alkynylation, allylation, cyanation of aromatic amide derivatives.[99] Recent work by the same group also recently disclosed the selective *meta* allylation of a broad variety of substrates using a pyrimidine-derived template DG.[100] This work allows for the access of terminal allyl groups to be selectively coupled at the *meta* position on the substrates reported.

Recent work disclosed by Falck *et al*. reported the Fe catalysed *meta* amination of aromatic picolinates, under very mild conditions.[101] This methodology utilises a very cheap and commonly found $FeCl_3$ catalyst, with no complicated or expensive ligands required to enable reactivity. However, the substrate requires EWG groups in order to allow for reactivity. The presence of the Fe catalyst was shown to be vital for the reactivity of the system, under the conditions are shown in Scheme **27**.

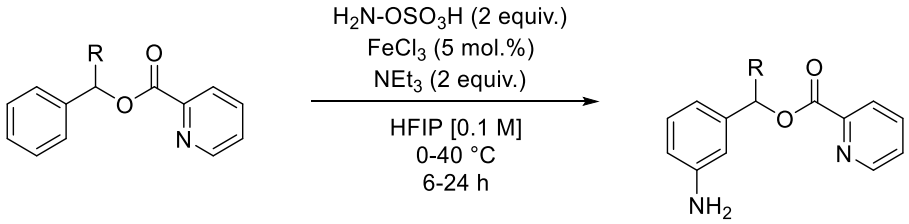

Scheme 27: Fe catalysed *meta* amination of picolinates.[101]

1.5.3 – Traceless Directing Group *meta* C–H functionalisation

The use of a traceless directing group methodology to achieve *meta* functionalisation of aromatic substrates can be broken down as two subsequent *ortho* functionalisations. This concept was first demonstrated by Larrosa *et al*. to synthesise *meta* substituted benzoic arenes and phenols.[102,103] This reaction is performed in one-pot, simplifying the procedure, and making it attractive to users due to the limitation of purification steps to an absolute minimum, particularly as the directing group cleavage

results in the energetically favourable release of CO_2. Scheme **28** shows the developed reaction conditions for the traceless *meta* arylation of phenols. Steps i. and ii. involves the *in-situ* formation of a potassium phenolate and subsequent *ortho* carboxylation of this species, followed by a Pd catalysed *ortho* arylation at 130 °C, and *in situ* decarboxylation leading to the desired product in good yields. Larrosa reported that the reaction is selective for the mono-arylated product exclusively, with no *ortho* or *para* products detected, nor the *O*-alkylated product.[102]

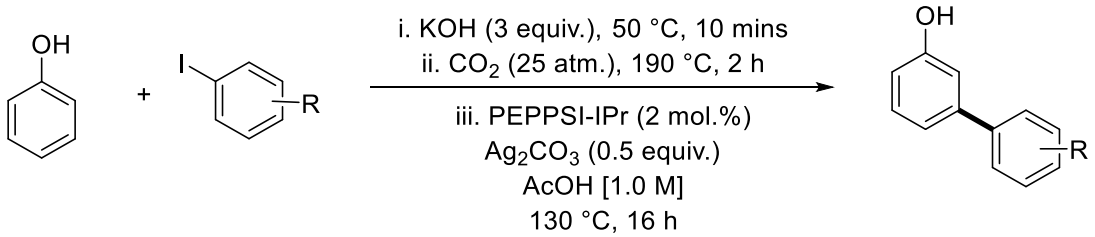

Scheme 28: Reaction conditions for the *meta* arylation of phenolic substrates by a traceless directing group methodology.[102]

This traceless directing group has also been extended to heterocyclic coupling partners such as thiophene- and furan-based molecules, with the most acidic proton in the heterocycle determining the regioselectivity on the heterocycle.[104] However, this methodology requires that a blocking group be in place at the position adjacent to the carboxylic acid directing group to prevent the formation of the disubstituted product.

A variation on this traceless directing group methodology was published by Yu *et al*. in which a norbornene is utilised as a transient ligand to facilitate the *meta* alkylation of various aromatic substrates, containing an amide-based directing group under the reaction conditions shown in Scheme **29**.[105] A quinolone-based ligand is required to minimise competing side reactions, thought to proceed *via* by reductive elimination on various catalytic intermediates as shown in Scheme **30**.

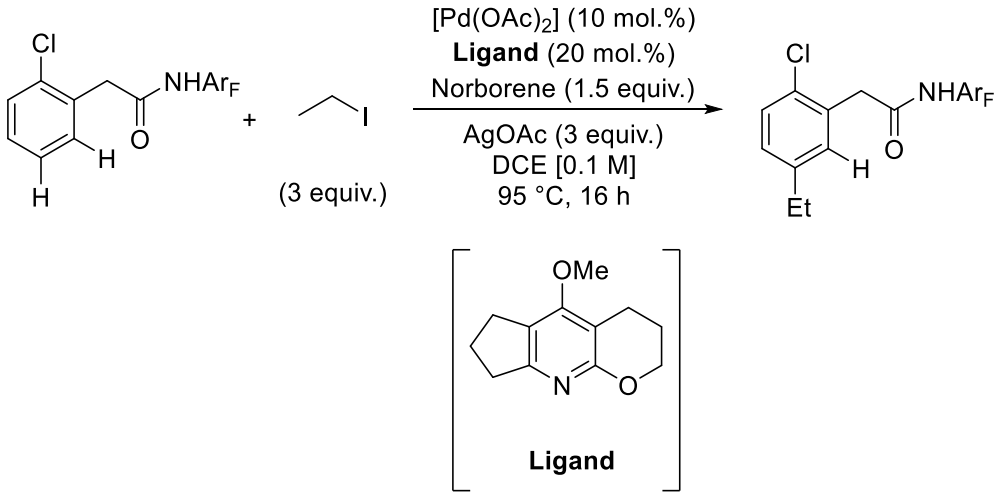

Scheme 29: Reaction conditions for the *meta* alkylation of phenyl acetic amides using a transient directing group.[105]

This transformation utilises the Catellani reaction.[106] Were it was discovered that norbornenes react with aryl halides to perform bi- or tri-functionalisation of the arene, terminating with a C–H functionalisation of an *ortho* proton to the C–X bond. Yu *et al.* exploiting this mechanistic understanding to use norbornene as a transient or traceless directing group.

The norbornene acts as a co-catalytic type terminating reagent to help prevent unwanted *ortho* functionalisation and di-functionalisation. The subsequent use of aryl halides as coupling partners and phenylacetamides with functionalisation at the α-position relative to the carbonyl, have also been shown with the use of a modified norbornene.[107]

The proposed mechanism as shown in Scheme **30** begins by the CMD insertion of the Pd into the *ortho* C-H bond, directed by the acetamide group (**I**). From this point a molecule of norbornene inserts into the C–Pd bond (**I** to **II**), forming a new intermediate where the Pd is now proximal to the *meta* C–H proton. This intermediate then undergoes a second intramolecular CMD insertion to form the 5-membered palladacycle (**II** to **III**), this is the proposed intermediate which can lead to by-product formation (**III**).[105,107,108]

Oxidative addition (**III** to **IV**) and then reductive elimination of the alkyl halide (**IV** to **V**) onto the palladacycle produces the *meta* substituted, norbornene inserted Pd intermediate (**V**). The expulsion of the norbornene from **V**, followed by protodemetallation of the *meta*

alkenylated product (**VI**), releases the product and regenerates the Pd(II) catalyst to re-enter the cycle.[107]

The use of transient mediators to selectively alkylate the *meta* position of an aromatic ring presents a novel combination of several smaller reactions into one process to selectively functionalise the *meta* position of a suitable arene ring. However, one drawback associated with this methodology, is it is limited to the use of primary alkyl halides. In comparison this methodology provides a nice complementary technique to the standard Friedel-Crafts alkylation methodology, which is limited to tertiary and some secondary alkyl halides (*i.e.* carbocation stabilising groups), with the added benefit of good regioselective control and superior atom economy.[109]

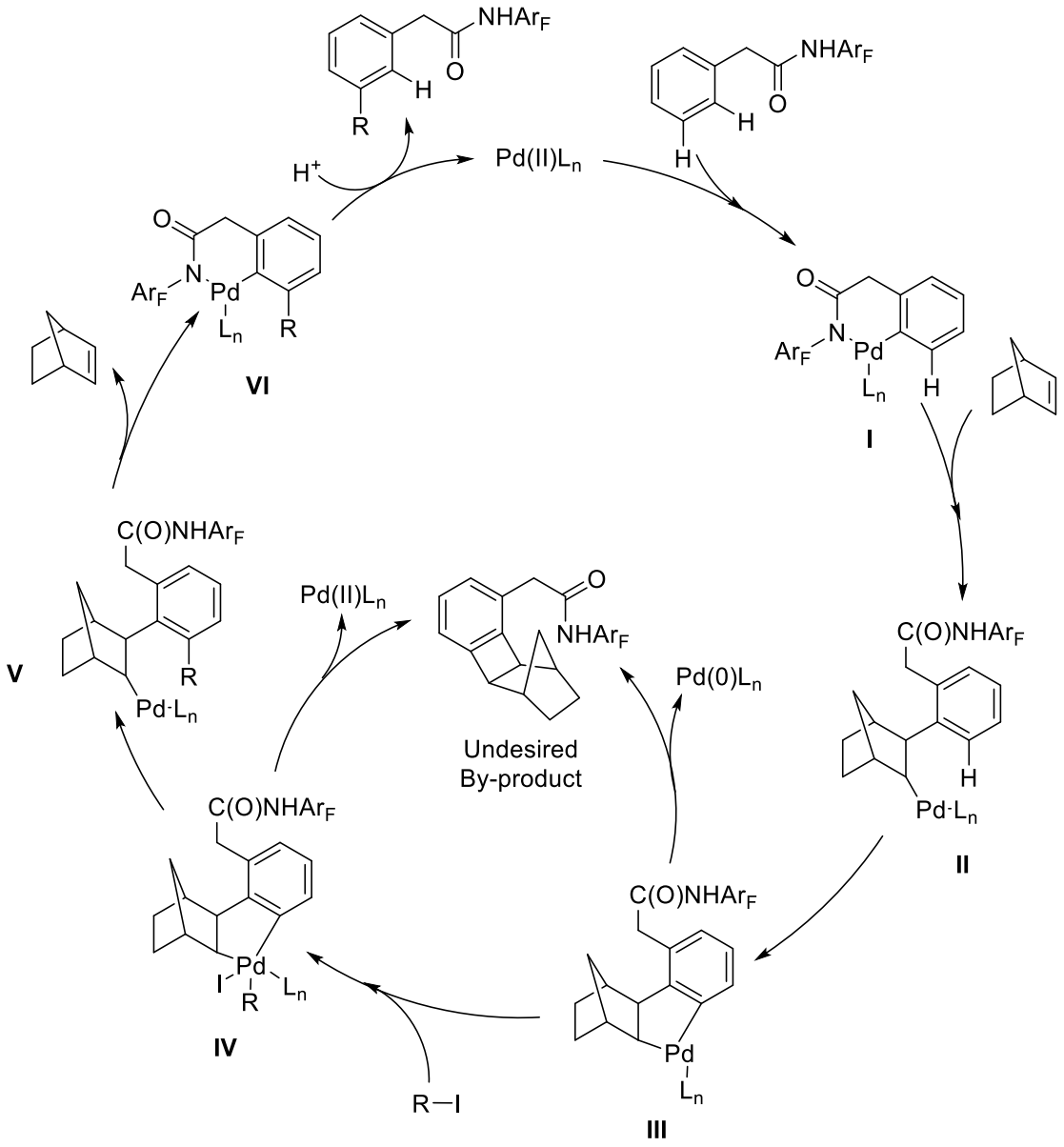

Scheme 30: Proposed catalytic cycle for the *meta* alkylation of phenylacetamides using a norbornene transient mediator.[107]

1.5.4 – Electrostatic Controlled *meta* C–H Functionalisation

A novel methodology to control the regioselectivity on the *meta* functionalisation of arene ring systems has been reported by Phipps *et al*. using ion pairing interactions to direct a metal catalyst to achieve regioselective functionalisation.[110] This methodology uses an anionic group on the metal catalyst ligand, which can then interact with a cationic group on the substrate molecule (Figure **3**).

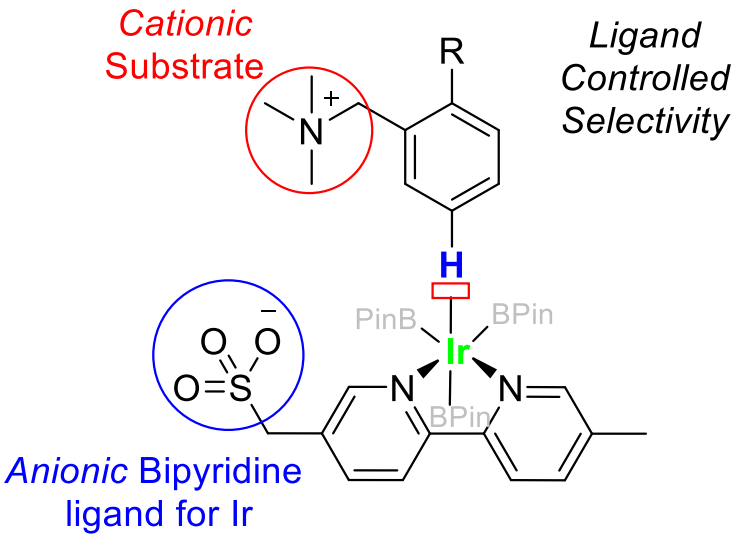

Figure 3: Ion pair-directed borylation methodology.[110]

This methodology allows for the use of benzylic amine substrates to be functionalised in a regioselective manner, and with complementary regiocontrol to what would be expected to the use of a standard S_EAr type reaction, which wold result in a mixture of *ortho*/*para* products. This interaction is achieved using an easily formed alkylammonium salt of the benzylic amine, and a sulfonate bearing tether on the Ir ligand group. The choice of the pendant ionic sulfonate group on the ligand was based on the computational work done by Singleton, Maleczka and Smith *et al.*[111,112] with a non-interacting counter ions (OTs^-, $[N(n\text{-}Bu)_4]^+$).

This ion pairing interaction then allows the *meta* proton to be proximal to the Ir centre and oxidative addition/reductive elimination events occur to borylate the *meta* position, under the reaction conditions shown in Scheme **31**.

Control experiments showed that the presence of the cationic group was essential to achieve regioselective control. Regioisomeric mixtures of the *para*:*meta* products were observed from 4:1 – >20:1, with the average being >10:1. The transformation results in diborylation when using symmetrical, unsubstituted arenes and is also possible on heterocyclic substrates, with poorer regioselectivity.

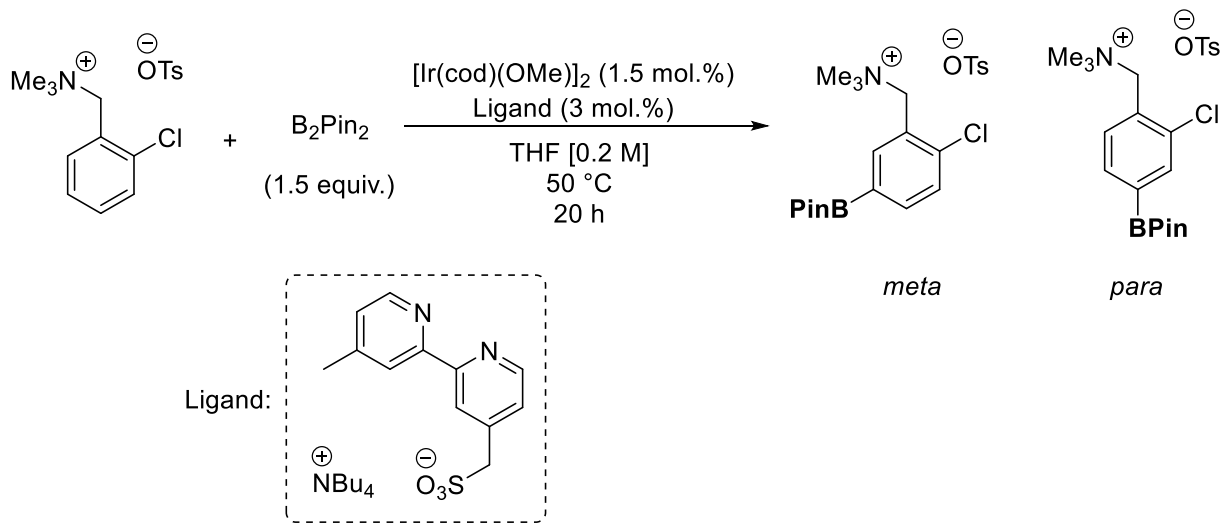

Scheme 31: Reaction conditions for the ion-pair directed borylation of quaternised benzylamines.[110]

This methodology has been extended to substrates bearing hydrogen bond donor groups and longer chain aromatic amines, to achieve the same regioselectivities.[113,114] Subsequent work by Phipps and co-workers has also expanded the range of aromatic substrates to include the use of phosphonium salts, which can then subsequently be functionalised after *meta* functionalisation.[115]

The first proposal of utilising non-covalent interactions to achieve *meta* functionalisation was made by Kanai and co-workers in 2015. In this work they demonstrate the elegant *meta* borylation of benzamide derivatives, using Ir catalysis. The regioselectivity was controlled using a meticulously designed ligand, which was shown to form a H-bond between the urea (ligand) and carbonyl (substrate), as shown in Scheme **32**. This example highlights the power of non-covalent templates as the ligand is used in such small amounts (1.5 mol.%). Low amounts of competing *para* selectivity were also observed with this reaction methodology.[116]

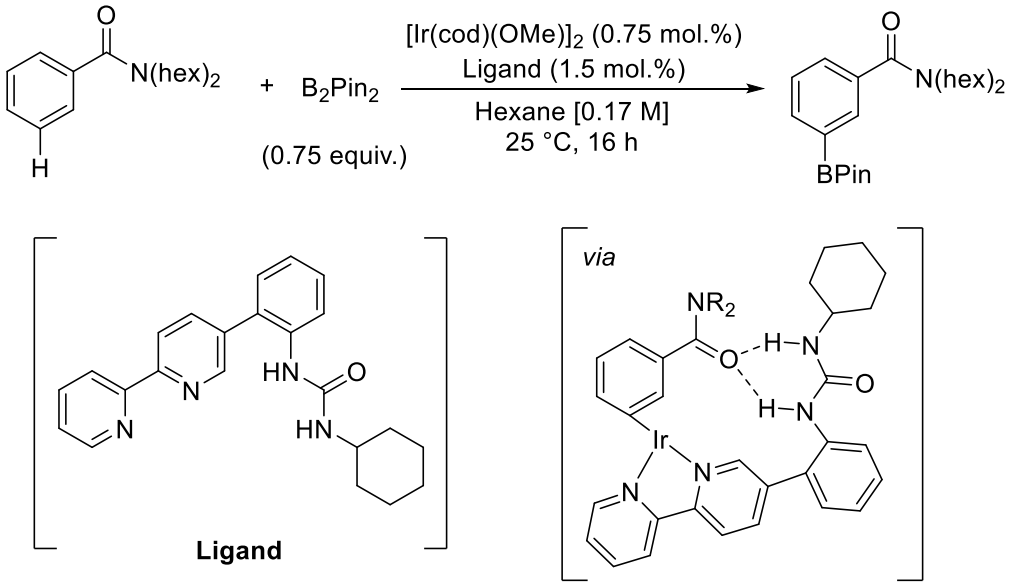

Scheme 32: Ir catalysed *meta*-borylation using a non-covalent template.[116]

Yu *et al*. have also published work whereby a Pd complex both directs and activates the *meta* C-H bond to be alkenylated with an olefin coupling partner (Scheme **25**). This work mimics the role that metal containing enzymes *in vivo*, whereby the metal centre coordinates the substrate molecule to a specific geometry around the metal ligand. This orientation then allows for the Pd to be directed to the *meta* C–H bond, under the reaction conditions shown in Scheme **33**.

The use of a Cu(II) species is thought to play a dual role as an oxidant for the Pd, as well as also being able to act as the anchor point for the substrate, as shown un Scheme **33**. However, Pd can also coordinate to the ligand as the anchor point. The acylated glycine residue is known as an effective ligand class for the promotion of CMD type reactions when coordinated to Pd.[117,118]

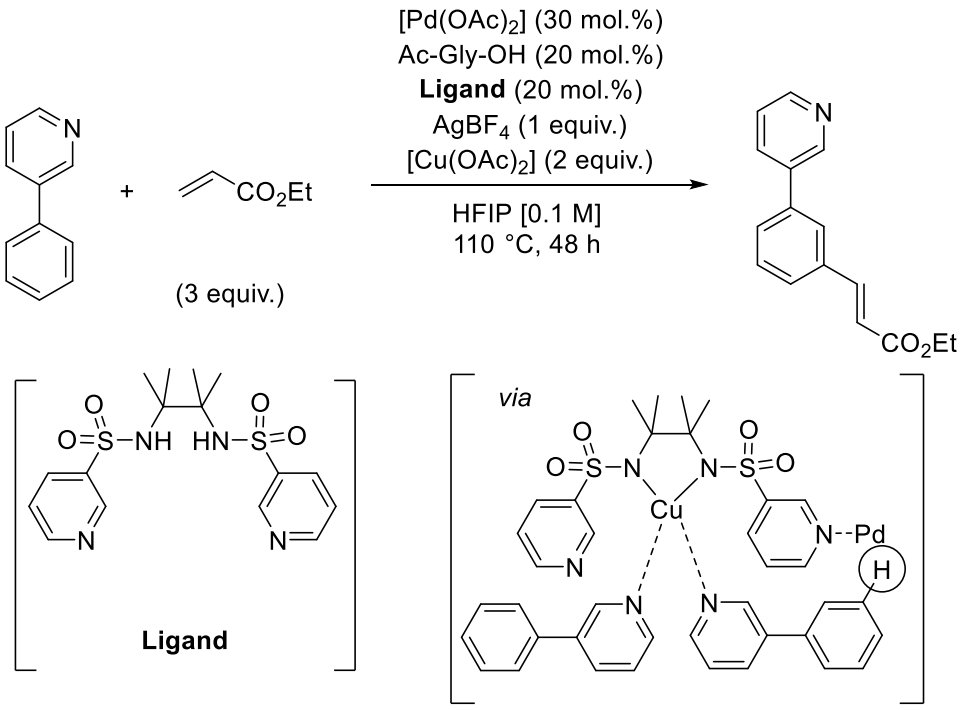

Scheme 33: Reaction conditions for the *meta* alkenylation of 3-phenylpyridine using a template directed methodology.[119] The circled proton is the one that reacts with the Pd *in situ*.

1.5.5 – *σ* Activation Enabled *meta* C–H Functionalisation

The examples mentioned in the previous section have achieved *meta* selective C–H functionalisation through the use of substrate sterics, traceless directing groups, electrostatic interactions or use of large ligands to direct the catalyst towards the *meta* proton. This occurs by making the TS necessary for the competing *ortho* functionalisation too high in energy, or through a transient blocking of the *ortho* position.

Another method for the *meta* functionalisation is through a technique known as σ-activation. As outlined previously, the insertion of Ru into C–H bonds, using a suitable directing group has been widely established for a number of years, leading to *ortho*-functionalised structures. However, in 2011 this methodology was used for the first time in a catalytic fashion to yield a *meta* product by Frost *et al*. as shown in Scheme **34**.[120]

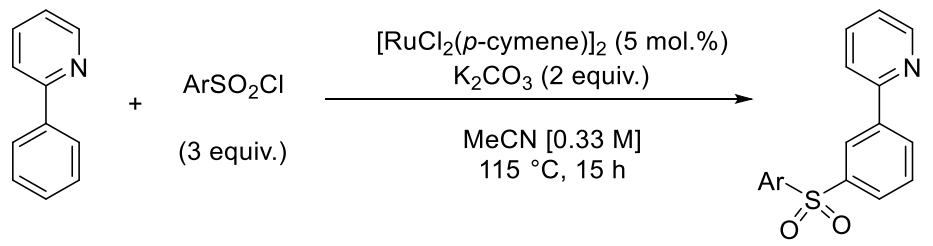

Scheme 34: Conditions for the Ru(II) catalysed *meta* sulfonation of 2-phenylpyridine.[120]

As shown in Scheme **34**, the reaction conditions for this transformation are relatively simple, in comparison to those shown for the traceless directing group and directing group methodologies (Scheme **25** and Scheme **28** respectively). It was originally suggested that this proceeded through an electrophilic-type mechanism, with the C–H bond cleavage being shown to be kinetically relevant in the reaction cycle, although no mechanism was proposed at the time.[120]

Several ruthenium complexes were studied for this transformation; however, none were found to be as effective as $[RuCl_2(p\text{-cymene})]_2$. Proof for the reaction proceeding through a σ-Ru-C_{Aryl} complex was found when isolating and reacting such an intermediate with sulfonyl chloride.[120] There is precedence for this type of reactivity in similar complexes, as seen with the modification of *fac*-(*tris*(2,2'-phenylpyridine)) iridium (III) chloride, commonly employed as an air stable photocatalyst in photochemical transformations.[121,122]

After this initial publication, a transformation involving σ-aryl Ru(II) complexes was reported by Ackermann and co-workers in 2013, detailing their work on the *meta*-selective coupling of secondary alkyl halides to 2-phenylpyridine, as shown in Scheme **35**.

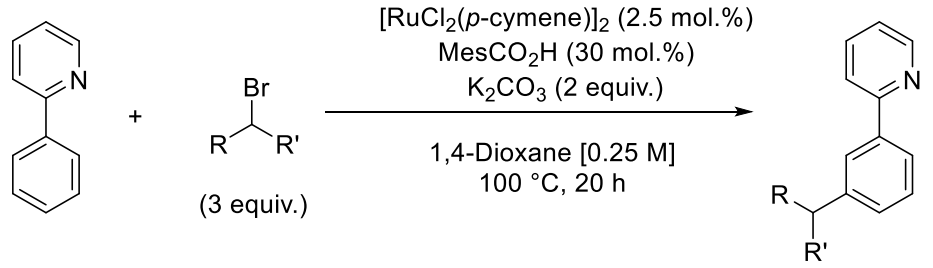

Scheme 35: Conditions for the *meta* selective secondary alkylation of 2-phenylpyridine.[123]

This expansion into the large and diverse selection of secondary alkyl halides made the scope of this transformation much more amenable to a more diverse group of possible substrates and coupling partners. During the optimisation of this reaction it was found that the addition of a carboxylate co-ligand was found to improve both the isolated yields and regioselectivity due to the more facile synthesis of a σ-aryl Ru(II) complex intermediate.[26,48,123]

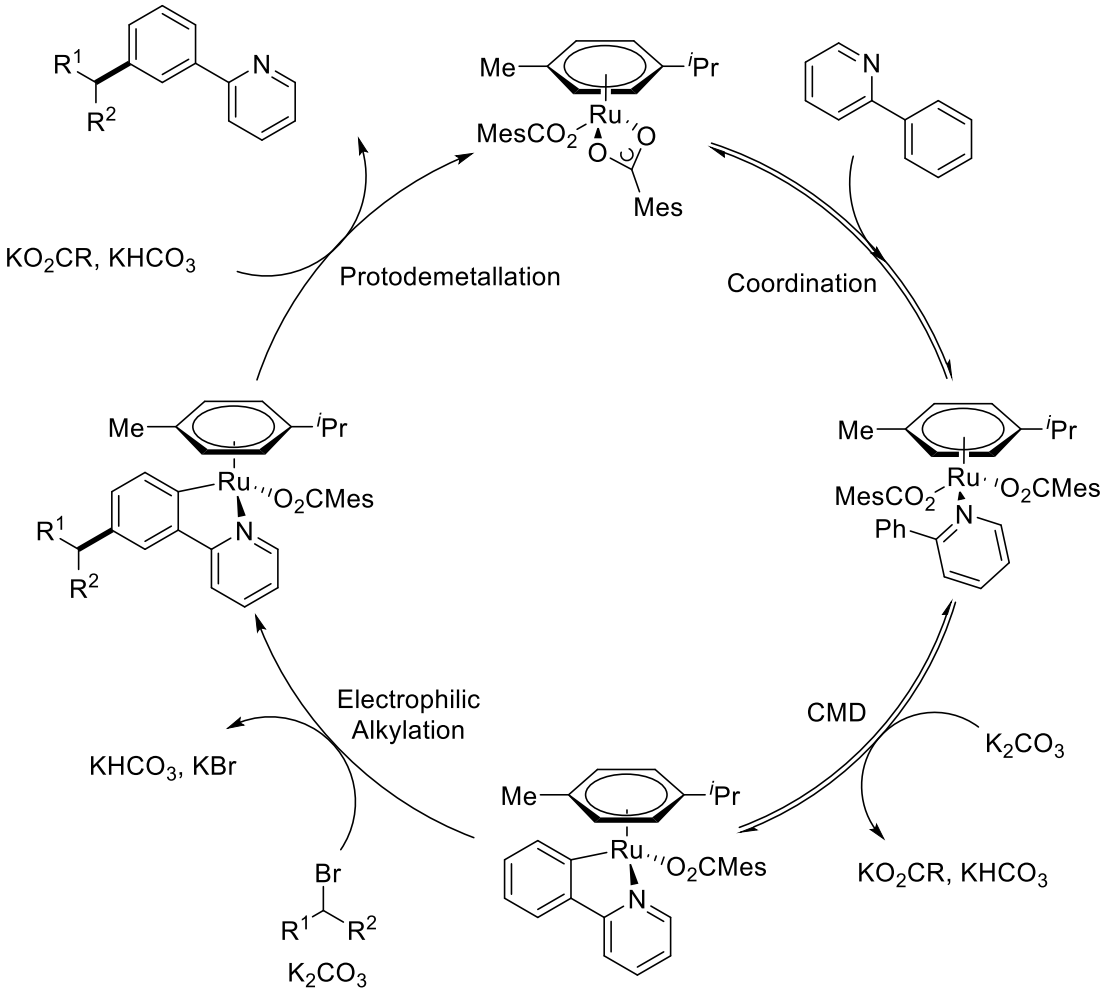

Scheme 36: Originally proposed alkylation of 2-phenylpyridine using secondary alkyl halides by Ackermann *et al*.[123]

The use of electron donating or withdrawing substituents at the *para* position on the arene ring, with respect to the pyridine were well tolerated, without effecting the observed regioselectivity.[123]

Ackermann and co-workers proposed that an S_EAr type mechanism was in operation, due to the observation that enantioenriched secondary alkyl halides resulted in racemic mixtures after reaction, along with the observation that electron rich arene derivatives react preferentially. From this data, the catalytic cycle shown in Scheme **36** was proposed.

Following these two seminal reports, the use of tertiary alkyl halide was initially published by Frost *et al*. in 2015, in the *meta* selective alkylation of 2-phenylpyridine using tertiary alkyl halides.[124] This paper cast doubt upon the proposed mechanism shown in Scheme **36**, by the inclusion of the result that addition of the radical inhibitor TEMPO ((2,2,6,6-tetramethylpiper-1-yl)oxyl) resulted in a dramatic decrease in the observed conversions. This result indicated that there is likely a radical involved in a part of the catalytic cycle.

The use of a bromoadamantane as a coupling partner as well as tertiary α-bromo esters, also showed that the mechanism likely involved a radical addition step, as S_N2 type additions are sluggish on steric grounds, S_N1 type reactions are disfavoured due to the positive charge left α to the ester carbonyl; therefore a mechanism involving a radical addition is most likely, with many examples reported using a radical formed by such an ester being utilised in the substitution of aromatics, heteroaromatics and olefins.[125–127]

The catalytic cycle that considers this inclusion of this radical species is shown in Scheme **37**, whereby CMD occurs as previously discussed, and the Ru catalyst playing a second order role in the *meta* C–H bond cleavage, as subsequently proposed by Ackermann *et al*.[128] in the CMD complex and a second Ru complex facilitating the homolytic cleavage of the C–Br bond, within a homo-bimetallic catalysis regime.[129–131]

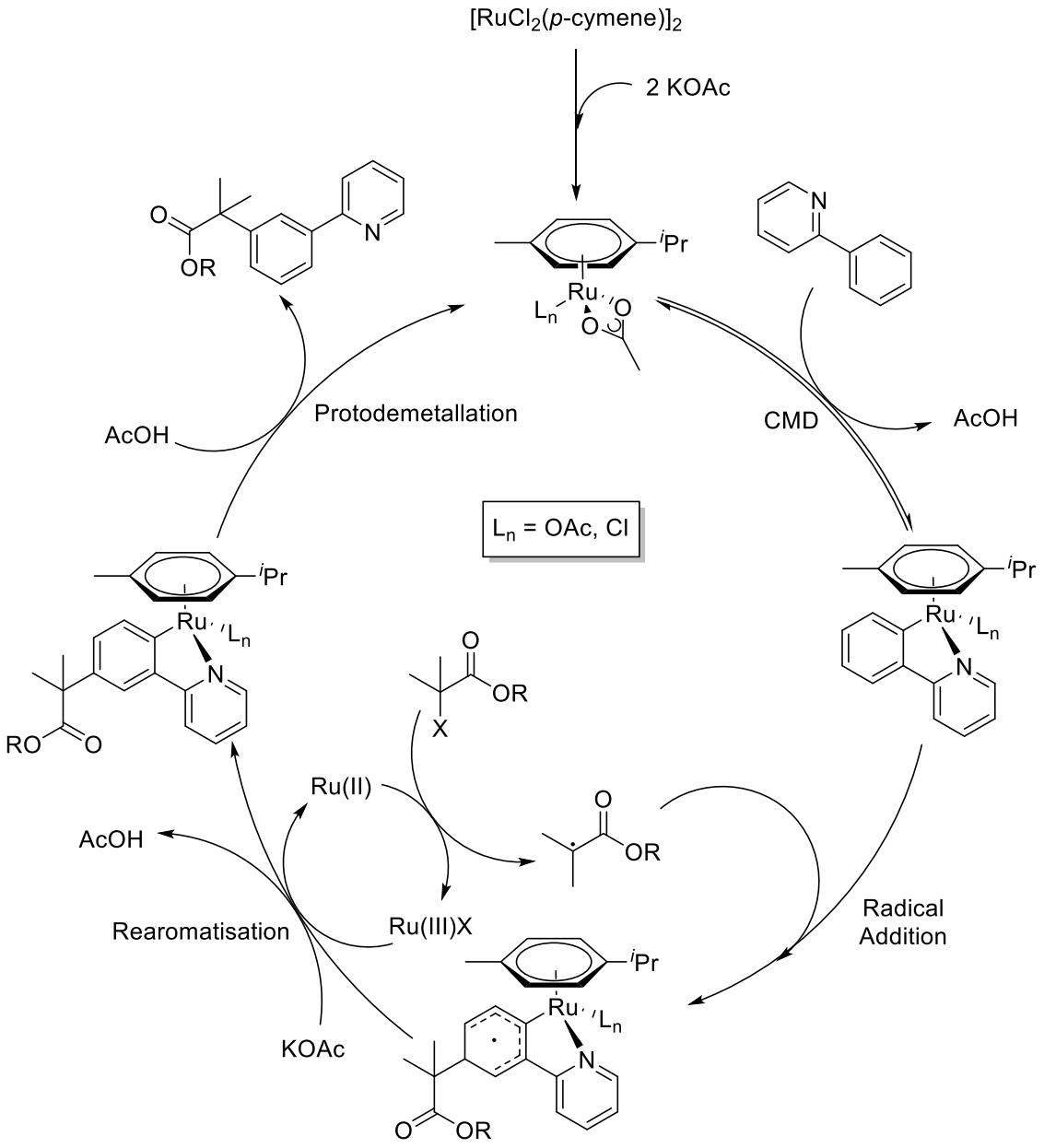

Scheme 37: Proposed catalytic cycle for the *meta* alkylation of 2-phenylpyridine using tertiary α-halo esters.[124]

Subsequent work by Frost *et al.* has more recently re-examined their original *meta*-sulfonation work in a mechanistic examination of the process.[132] As shown in Scheme **38**, the mechanism for this transformation is proposed to proceed *via* a Ru CMD complex with the 2-phenylpyridine. This complex then activates the position *para* to the C–Ru bond by inductive and mesomeric effects, due to the much higher bond polarisation.[104] The activation of this position allows it to react with the sulfonyl chloride radical.[105]

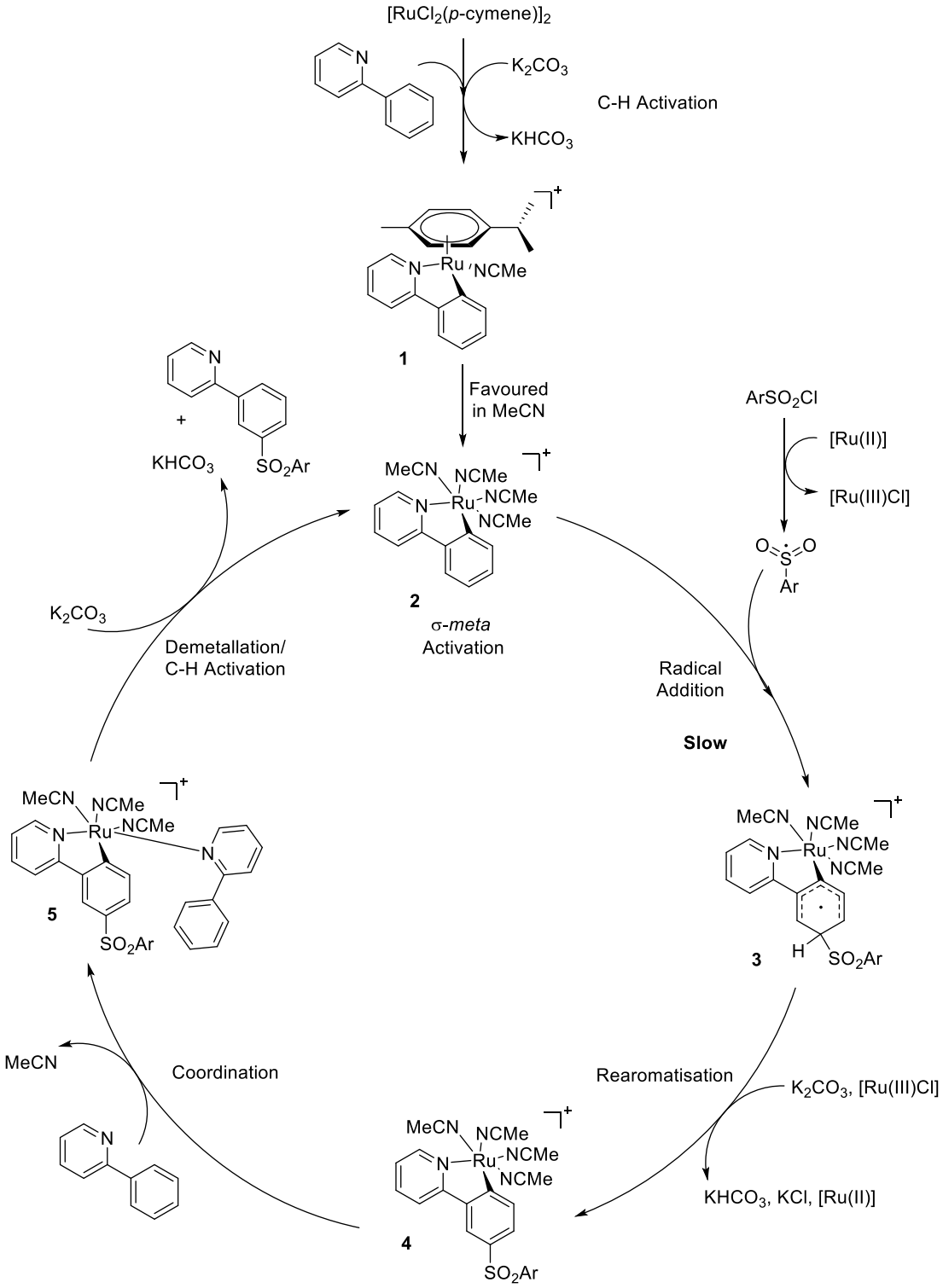

Scheme 38: Proposed mechanism for the *meta* C–H sulfonation of 2-phenylpyridine.[132]

The use of coordinating solvents such as MeCN were found to give optimal results, this indicated that an electron rich Ru species may be the optimal catalyst for the transformation; this raises the possibility of what happens to the *p*-cymene ligand in this reaction, the loss of which *in situ* was thought to be a potential deactivation pathway.[108]

Performing this reaction in the absence of sulfonyl chloride indicated that no *p*-cymene dissociation occurred, until 1.5 equivalents were added. After a short period of time , dissociation was observed. However, the exact role of *p*-cymene in the reaction is still unknown.[132]

An interesting further expansion to this methodology was achieved by Greaney *et al*. and separately by Ackermann *et al*. in using photocatalysis to achieve a *meta* selective alkylation shown in Scheme **39**.[133] This is made possible by the ruthenium being employed in a dual role, between enabling formation of a CMD intermediate, and then photoexcitation of this CMD complex to then initiate homolytic cleavage of the C–X bond on the coupling partner.[134] This radical then reacts in an identical manner shown from the "radical addition" as shown in Scheme **37**. This reaction is advantageous in comparison to the thermal *meta* alkylation methodologies, in that it has higher functional group tolerance, a broader substrate scope and most crucially a much lower reaction temperature (*e.g.* room temperature).[133,134]

The computational results indicated that for a CMD complex as shown in Scheme **39** that the Ru(III) complex gave a larger selectivity profile, using the difference in Fukui indices between the desired *meta* position and undesired *ortho* position.[134–136] Experimental evidence to support this first order role of the Ru-CMD complex was the observation that the fluorescence quenching of the CMD complex upon increasing concentrations of the alkyl halide coupling partner.[133,134] Cyclic voltammetry (CV) experiments also showed that there was a reversible oxidation event from a Ru(II) species to a Ru(III) species, further validating the first order nature of the Ru under the reaction conditions.[134]

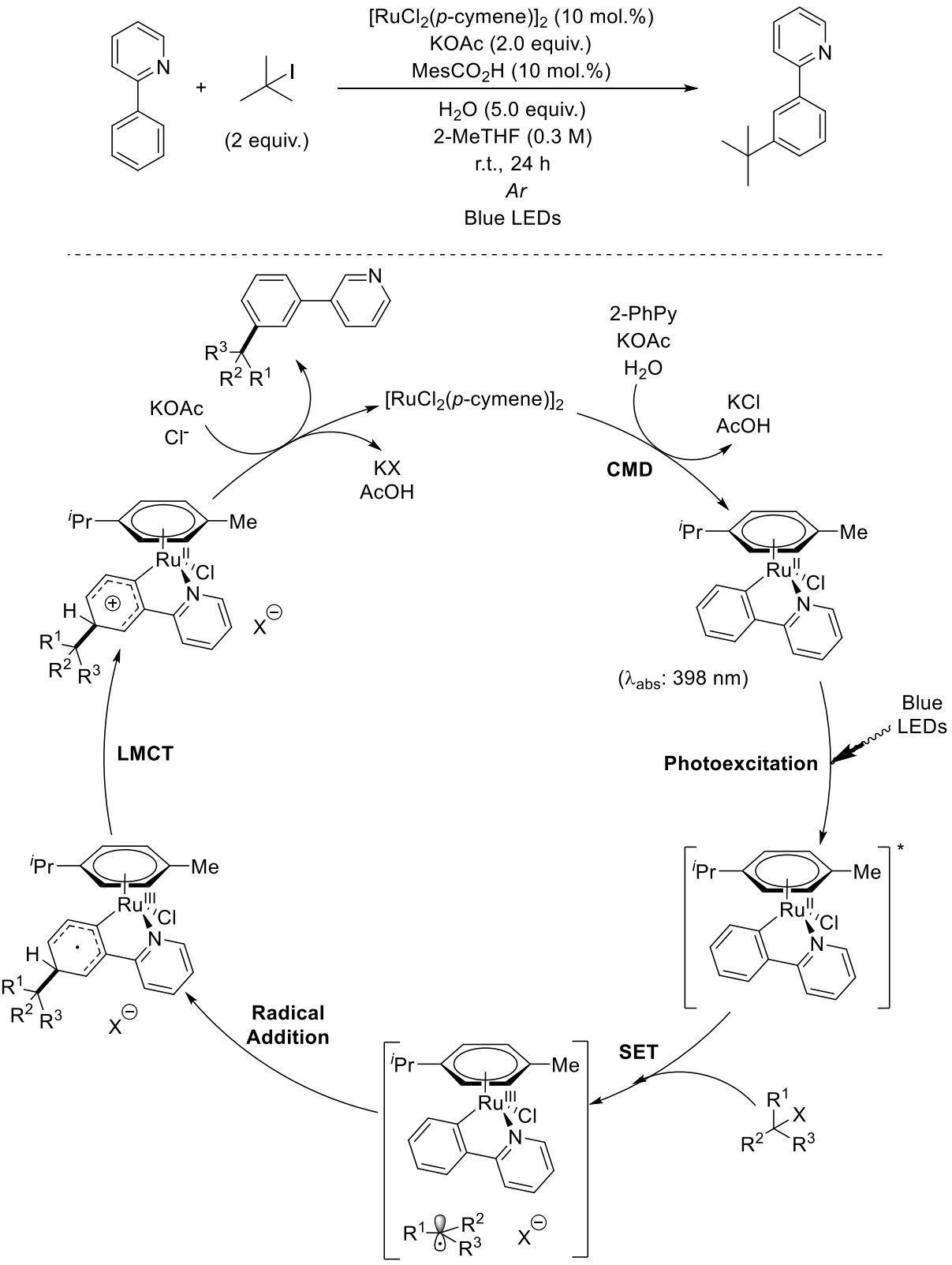

Scheme 39: Reaction conditions and mechanism for the photoactivated meta C-H alkylation of 2-phenylpyridine.[133]

Work by Ackermann and co-workers has proposed that the addition of carboxylate and/or phosphine ligands to the reaction manifold, when performing a *meta* selective functionalisations, *via* Ru(II)-σ complexes helps to stabilise the formation of a Ru–C singlet bond, which in turn stabilises the functionalised aromatic system, between functionalisation and rearomatisation as shown in Scheme 40.[137]

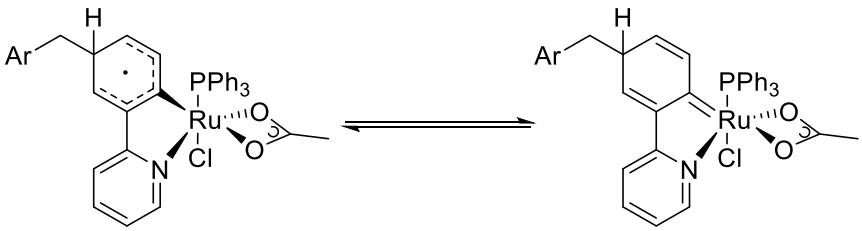

Scheme 40: Proposed stabilisation mode as a singlet species for a benzylated arene ring, through using a σ-activation methodology.[137]

Computational analysis of this process supports the conclusions, with a 20 kcal mol^{-1} stabilisation in energy when calculating the energy difference between the triplet radical and singlet carbene. This work allowed for the late stage functionalisation of highly sensitive fluorescent dyes, drugs, lipids, peptides, nucleosides and carbohydrates with high regioselectivity and functional group tolerance.[137]

In a variation of the alkylation methodologies reported, a recent publication by Cui and co-workers reported the *meta* selective difluoroalkylation of 2-phenoxypyridines by Ru catalysis. They mechanistically propose to proceed through a similar scheme to that shown in Scheme **37**, using a simple $RuCl_3$ catalyst, which forms a cyclometalated intermediate that activates the *meta* position.[138]

Beyond alkylations, alkenylations and arylations, the ability to attach other reactive functional groups in a chemo- and regioselective manner is also of great interest. The ability to halogenate the *meta* position regioselectivity has been reported by Greaney *et al*. for the *meta* bromination of 2-phenylpyridine using NBS (Scheme **41**),[139] and Huang *et al*. separately.[140] The analogous chlorination utilising *N*-chloro-2,10-camphorsultam (Scheme **42**) by Zhang *et al*.[141] The ability to regioselectively install these halides is of great use, due to their synthetic applicability in potential cross-coupling reactions.[2,142]

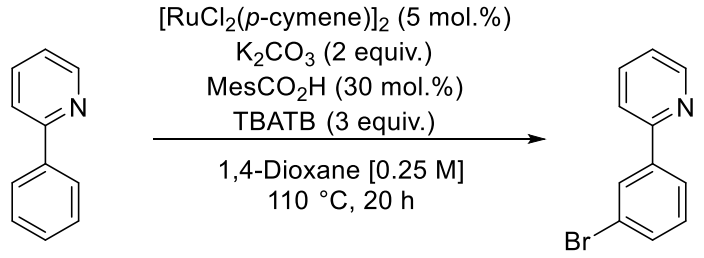

Scheme 41: Conditions for the *meta* bromination of 2-phenylpyiridne.[139]

The bromination occurs via a similar mechanistic cycle to that shown in Scheme **37**, using NBS instead of an alkyl halide, a bromination protocol utilising a heterogeneous Ru source has also been reported.[143]

Computational calculations by Ackermann *et al.* on the *meta* alkylations and bromination of purine bases has given insight to the role of the Ru in these *meta* alkylation and bromination reactions.[136] The observed first order role of the Ru concentration in the *meta* C–H alkylation and bromination reactions, suggested that a Ru(II/III) pathway may be in operation, rather than a second order reaction, whereby two molecules of Ru are involved in the formation of the active radical species.[143,144]

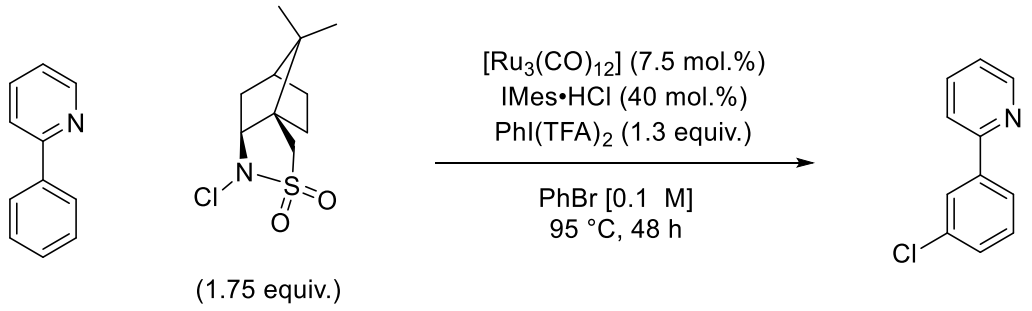

Scheme 42: Reaction conditions for the *meta* chlorination of 2-phenylpyridine.[141]

The analogous chlorination however, as shown in Scheme **42** is intriguing due to the use of a Ru(0) precatalyst, which results in a slightly differing mechanistic explanation of the process, as seen in Scheme **43**. The Ru(0) precatalyst is oxidised by the oxidant to the active Ru(II) species which then undergoes a CMD process with the 2-phenylpyridine, to form a cyclometalated intermediate.

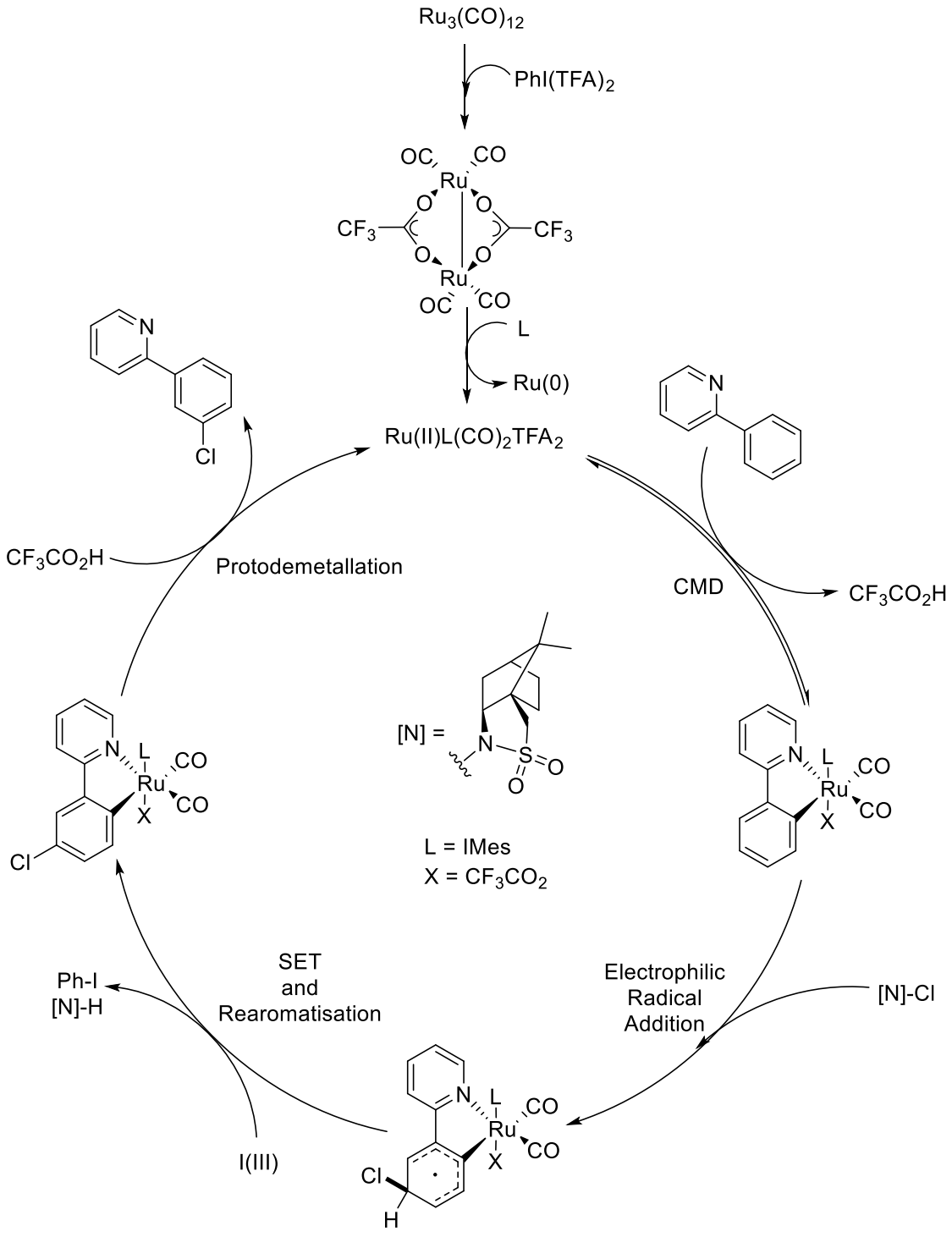

Scheme 43: Proposed mechanism for the *meta*-chlorination of 2-phenylpyridine.[141]

The chloride source then undergoes homolytic cleavage to produce the chloride radical which then attacks the position *para* to the C–Ru bond. This radical intermediate is then

oxidised and deprotonated to facilitate rearomatisation of the system, followed by protodemetallation to release the product and catalyst to begin the cycle again. Mechanistic studies indicate a reversible *ortho* metalation step and the *meta* C–H bond cleavage is not involved in the rate determining step (RDS).[141] This work also includes the use purine base and benzodiazepine derivatives as substrates, both pharmaceutically relevant motifs.

The use of a Ru(0) precatalyst has also been utilised in the *meta* nitration of 2-phenylpyridine as reported by Zhang *et al.* with the use of strongly oxidising conditions.[145] Subsequently, more mild conditions were published by Huo *et al*. which allows the transformation to proceed under milder conditions, *thus* making it more amenable to general useage.[146] A mechanistic proposal hypothesised by Zhang *et al*. is shown in Scheme **44**.

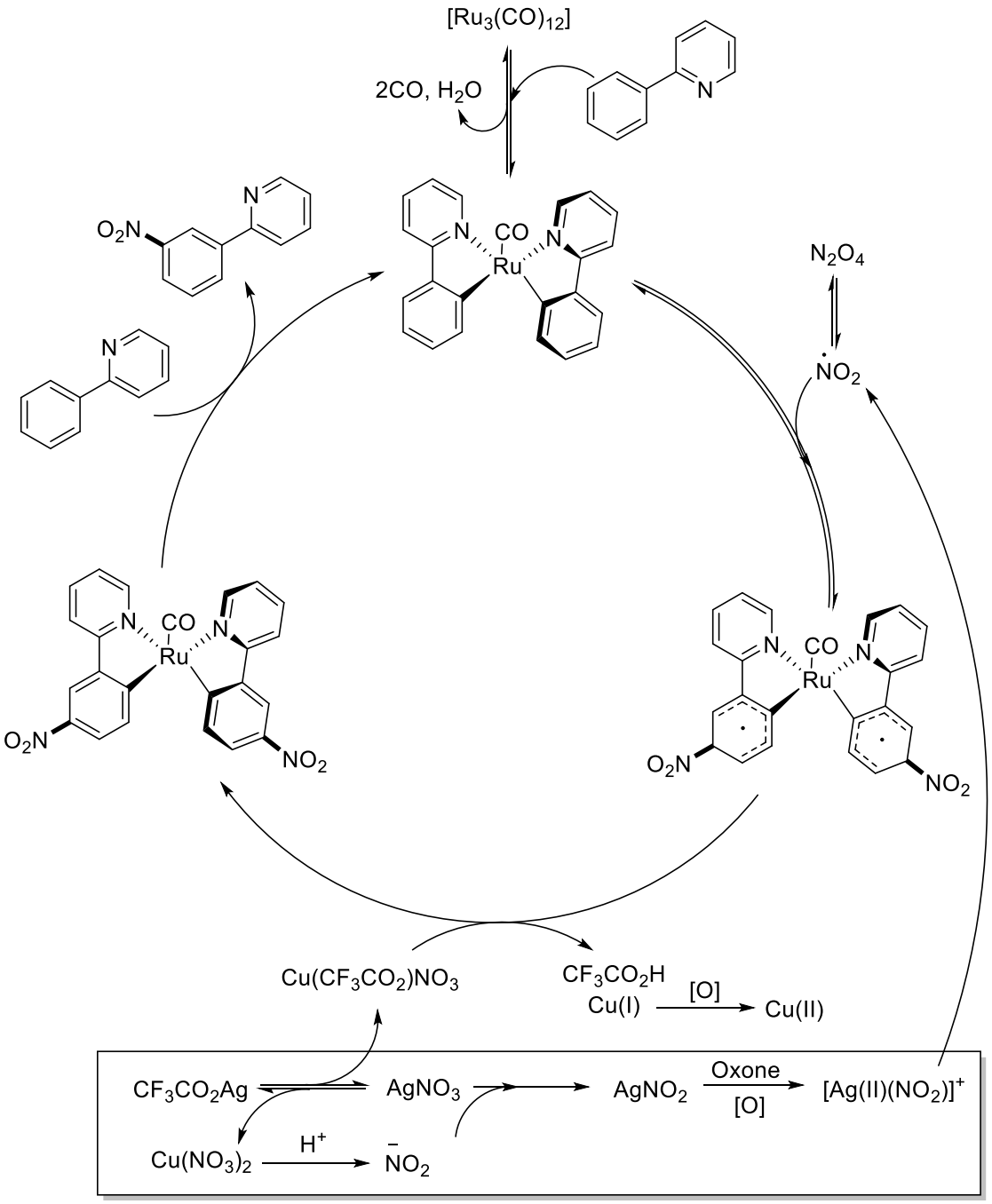

Scheme 44: Proposed mechanism for the *meta* nitration of 2-phenylpyridine.[145]

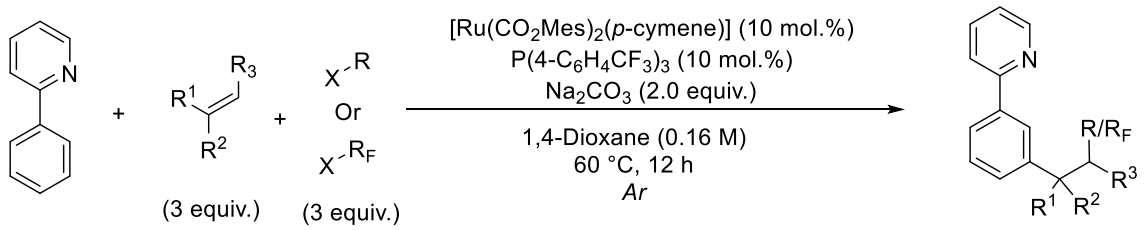

Scheme 45: Reaction conditions for the *meta* selective alkylarylation of 2-phenylpyridine.[147]

A recent report by Liang *et al*. on a alkylarylation of alkenes provides a novel new methodology on a three-component reaction, utilising the σ-activation methodology to achieve *meta* functionalisation as shown in Scheme **45**.[147] The reaction shows a wide tolerance to a range of different functional groups such as halogens and esters , as well as a variety of acrylates, vinylarenes and vinylferrocene. The mechanistic investigation for this reaction proposed that a Ru(II) CMD complex reacts with the alkyl halide, *via* an inner sphere halide transfer process to form a Ru(III) CMD complex, which then reacts *para* to the Ru–C bond as with similarly to shown in Scheme **37**. This Ru(III) CMD complex was proposed by DFT is responsible for the *meta* selectivity.[147]

The use of carbon tetrabromide as a coupling partner has also been reported by Greaney *et al*. with MeOH added to the reaction conditions, resulting in an overall *meta* carboxylation under the conditions shown in Scheme **46**.[148] This occurs by the formation of the $\cdot CBr_3$ radical, which then reacts at the *meta* position with a CMD complex, the MeOH then reacts further with the coupled $-CBr_3$ group to form the isolated $-CO_2Me$ moiety.

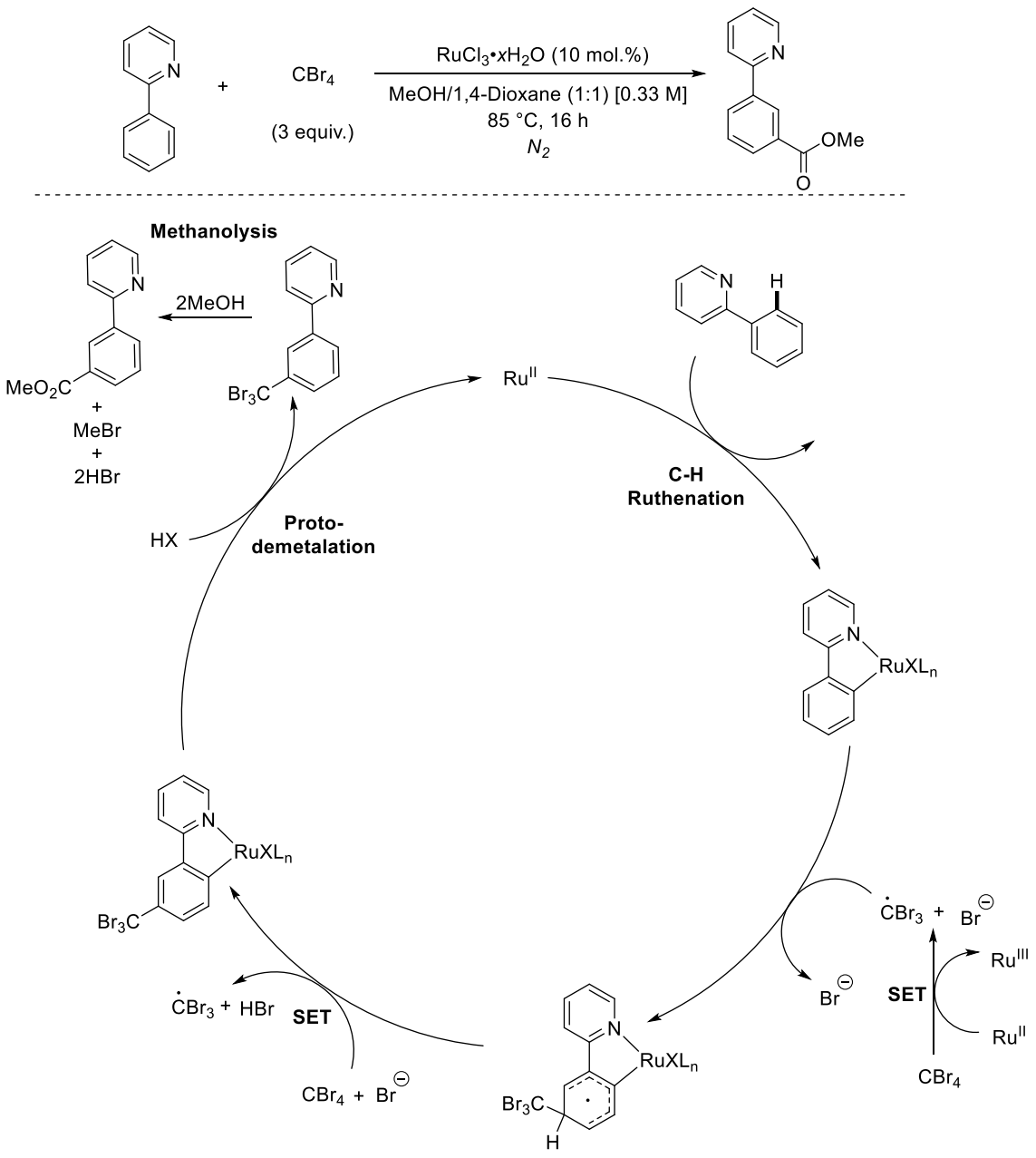

Scheme 46: Proposed mechanism and reaction conditions for the *meta* carboxylation of 2-phenylpyridine.[148]

The carboxylation work was further extended to a *meta* acylation reaction by Wang *et al.*[149] This work utilised phenylglyoxylic acid as a known *C*-centred acyl radical precursor, when reacted with a suitable single electron oxidant, collapses to produce CO_2 and the desired acyl radical, which then reacts in the normal manner of a radical addition reaction *para* to the C–Ru bond, to yield the overall *meta* acylated product, under the conditions shown in Scheme **47**.

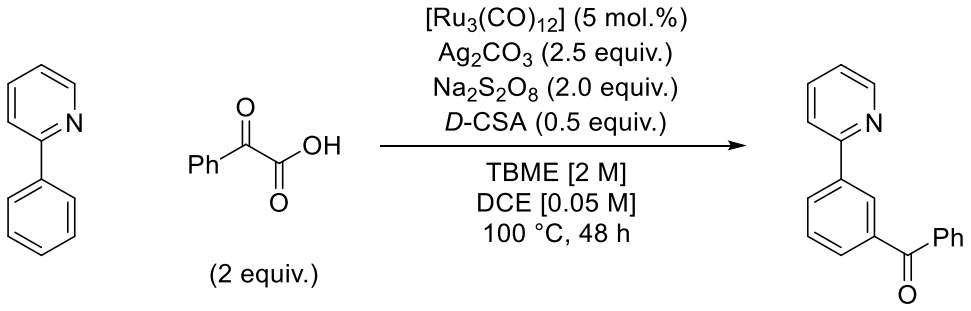

Scheme 47: Conditions for the *meta* acylation of 2-phenylpyridine.[149]

Recent work disclosed by Cui *et al*. presented a *meta* carboxylation methodology that uses a similar coupling partner to allow for a *meta* formylation.[150] This work used a $CHBr_3$ coupling partner under the conditions shown in Scheme **48**. This follows a similar mechanistic path to that shown in Scheme **46**. However, instead of methanolysis to form the carboxylated product, the coupled $–CHBr_2$ moiety reacts with the base to form the formylated product plus CO_2.

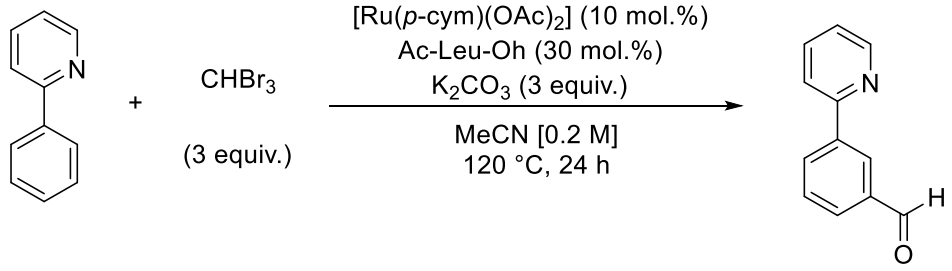

Scheme 48: Conditions for the *meta* formylation of 2-phenylpyridine.[150]

Benzylations, utilising toluene derivatives as a coupling partners have also been used by Shi *et al.*[151] This methodology requires the use of an alkyl iodide initiator to form the desired benzylic radical which can then react in a radical addition fashion, *para* to the C–Ru bond, followed by SET, rearomatisation and protodemetallation to yield a *meta* benzylated product. Examples of using complementary conditions to regioselectively select between the *ortho* and *meta* positions has also been shown by Zhao *et al*., by use of readily available Ru catalysts and oxidants shown in Scheme **49**.[152]

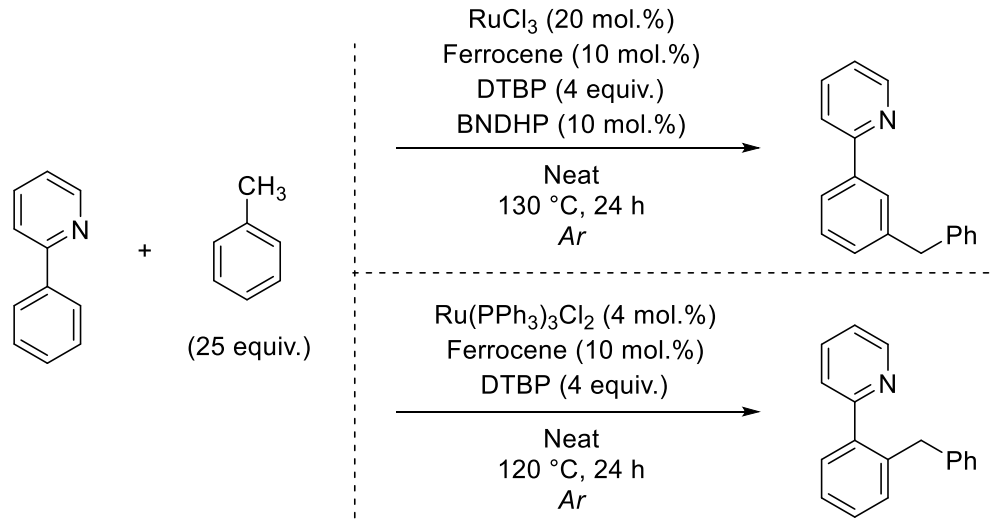

Scheme 49: Complimentary conditions for the *ortho* or *meta* benzylation of 2-phenylpyridine.[152]

1.6 – Overview of *para* C–H Functionalisation Reactions

The ability to achieve *para* regioselective functionalisations of aromatic systems represents, perhaps the most difficult position to functionalise. This is in large part due to the distal nature of the C–H bond from any potential directing groups. Due to this difficulty, may examples of *para* C–H functionalisation have used more direct C–H activation methods to achieve the desired regioselectivity, based upon the steric and electronic nature of substrate molecules.[153] Despite these difficulties, methods have been developed to achieve this C–H functionalisation that utilise directing group methods.

1.6.1 – Template Assisted *para* C–H Functionalisation

Similarly, to the work Yu *et al.* of using a "U-shaped" template to direct a TM catalyst towards the *meta* C– bond for functionalisation, this methodology has been elaborated upon by Maiti and co-workers, allowing for the realisation of a *para* alkenylation reaction as shown in Scheme **50**.

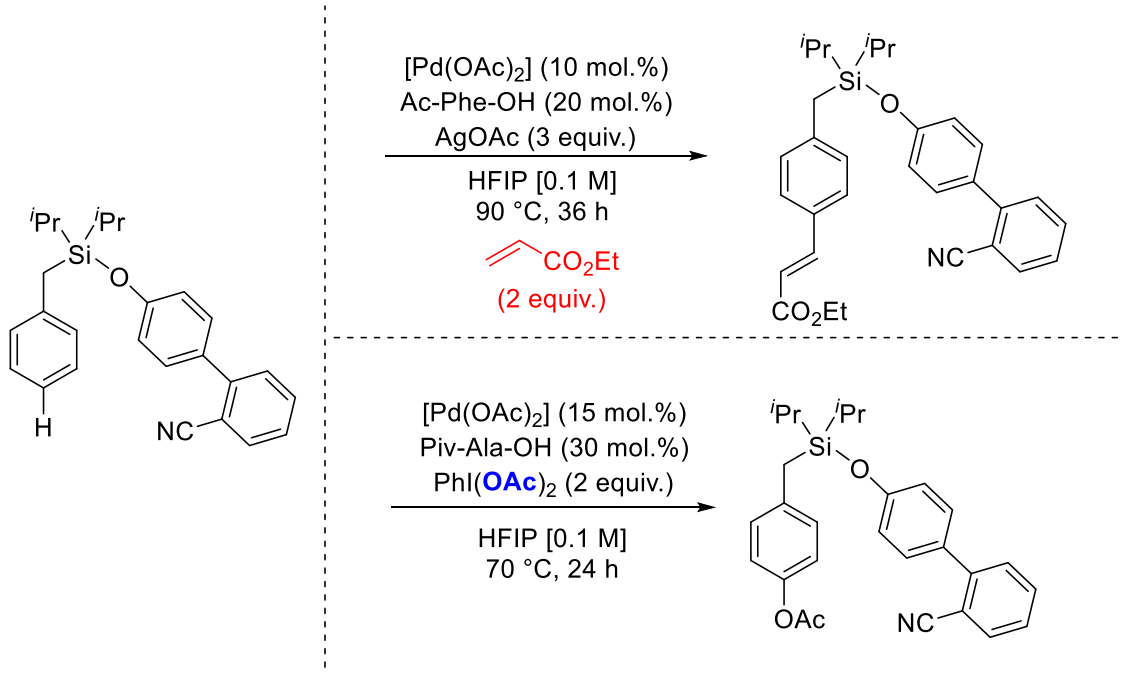

Scheme 50: *para* C–H functionalisation of toluene derivatives *via* template assistance.[154]

In the mechanistic explanation for this reaction, they proposed that they utilised the Thorpe-Ingold effect, and a longer chain length to enact selectivity for the *para* position over the *ortho* and *meta* positions. Despite this, a mixture of regioisomers was nearly always found, with *para*:others varying between 5:1 to 20:1. The same paper also described conditions for the *para* acetoxylation of same templated structures. The recovery of the template portion is vital to allow for good atom economy post C–H functionalisation, and found that treatment with TBAF allowed for the cleavage of the Si–C_{benzyl} bond in excellent yields, with near quantitative recovery of the Si–O cleaved phenol derivative.[154]

Further work published by the same group in 2016, proposed the *para* C–H alkenylation of phenol derivatives.[155] This methodology was achieved, through switching then benzyl methylene group for an oxygen, as shown in Figure **4**.[154] The reaction conditions for this *para* selective alkenylation are similar to those shown in Scheme **50**. The cleavage of this substrate is easily achieved by reaction with *p*-TSA, to produce the *para* substituted phenol and silanol-based template in good yields.[155]

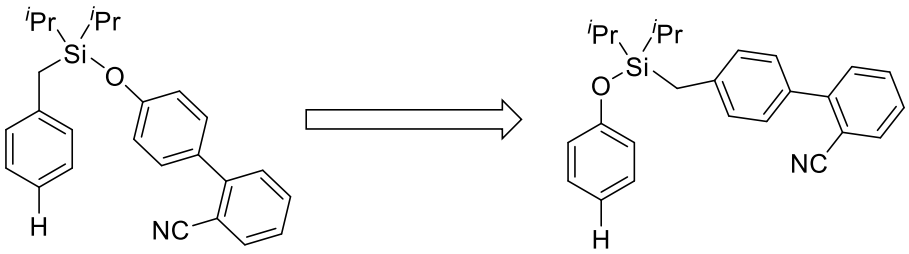

Figure 4: Substrate modification to allow for the *para* alkenylation of phenol substrates.[155]

As seen so far, the use of these non-covalent templates can be a powerful method of achieving *para* C–H functionalisations. In 2017, Chattopadhyay reported the Ir catalysed *para* C–H borylation of benzoates using a dual salt/Lewis basic chelation agent model to achieve this *para* selectivity.[156] The reaction is shown in Scheme **51**, and was found to proceed under optimised conditions on a range of substrates with regioselectivities of *para*:other of 9:1 to 99:1, with the majority >20:1. They proposed that the mechanism based on insights of using the preformed potassium alkoxide (OK) salt and comparing it to the OMe substituted ligand (cannot form the non-covalent interaction). Here, high conversions were observed in both cases however the salt gave selectivity of *para*:*meta* of 33:1, *cf*. 1.9:1 for OMe.

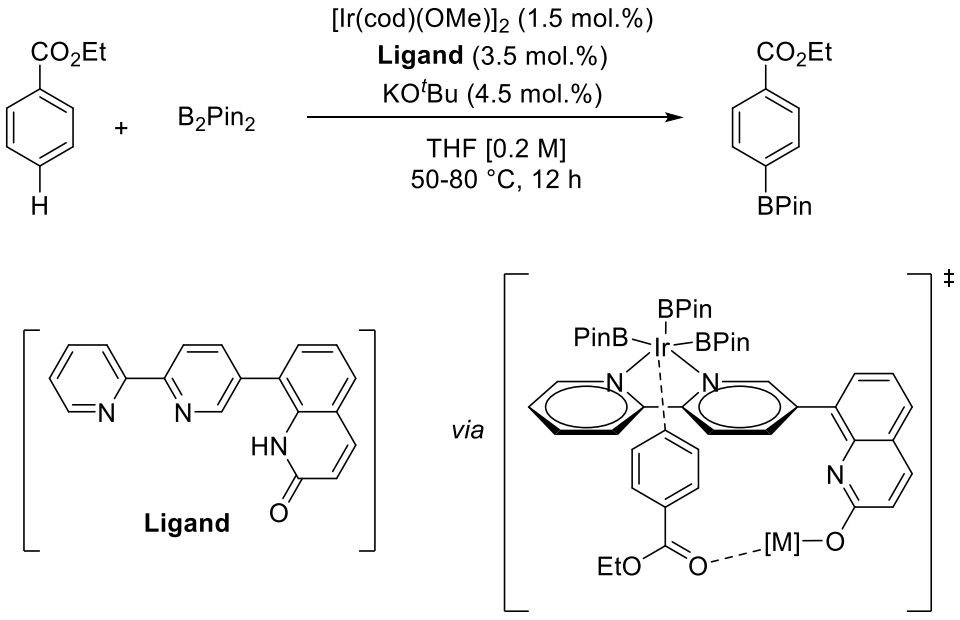

Scheme 51: Ir catalysed *para* C–H borylation of benzoates using a salt templated non-covalent interaction.[157]

Another example of template assisted *para* C–H functionalisation was published in 2019 by Phipps and co-workers, utilising an ion-pairing interaction, to direct an Ir catalyst towards the *para* C–H bond for functionalisation, in a manner akin to that shown in Figure **3**.[158] This reaction was found to work on a variety of aniline, benzylamide, phenol, benzyl alcohol, aryl and benzyl sulfonate substrates, under the conditions shown in Scheme **52**.

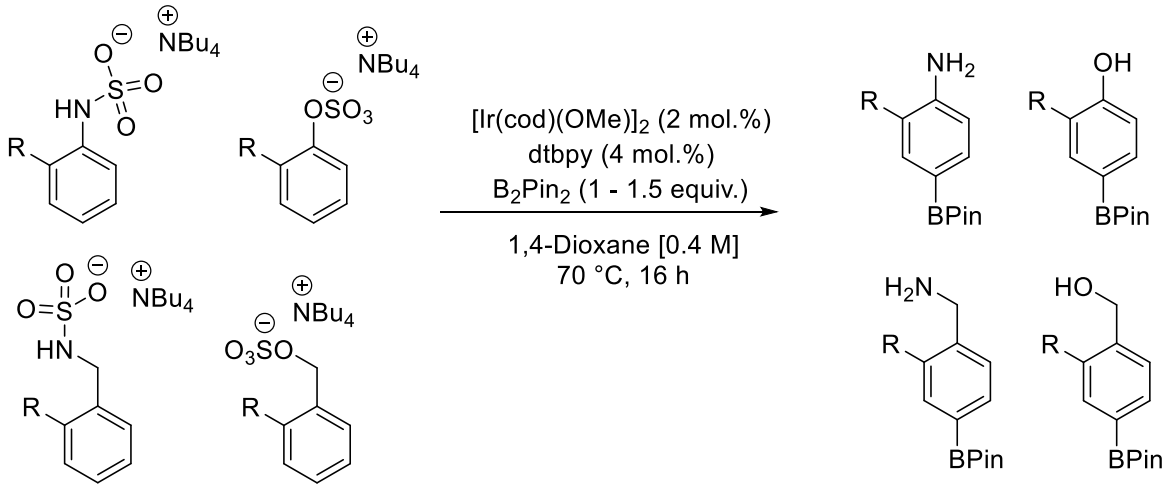

Scheme 52: Ir catalysed *para* selective C–H borylation of anilines, benzylamides, phenols and benzyl alcohols.[158]

This work found it was necessary to first convert the desired substrate into the corresponding sulfonamide or sulfate analogue, before then borylating under the conditions in Scheme **52**, and then treating with HCl in MeOH to transform back to the corresponding alcohol or amide. Selectivites for *para*:*meta* were found between 3:1 to >20:1, with bulky ammonium cations found to enhance this selectivity.[158]

A final recent example of *para* functionalisation, using a hydrogen-bonding template, was disclosed by Maiti *et al*. for the *para* selective cyanation of toluene scaffolds, as well as a few examples of phenol scaffolds.[159] This methodology utilises Pd catalysis, through the conditions shown in Scheme **53**. It was shown through NMR studies and XRD structures of reaction intermediates, of the OMe and ^{i}Pr groups on the **Tem** group increase the reactivity of the system as shown on Scheme **53**. This allows the CN group to become proximal *para* C–H bond of the substrate, through hydrogen bonding interactions with the solvent (HFIP). They then show that this template can then be easily cleaved in postreaction.[159]

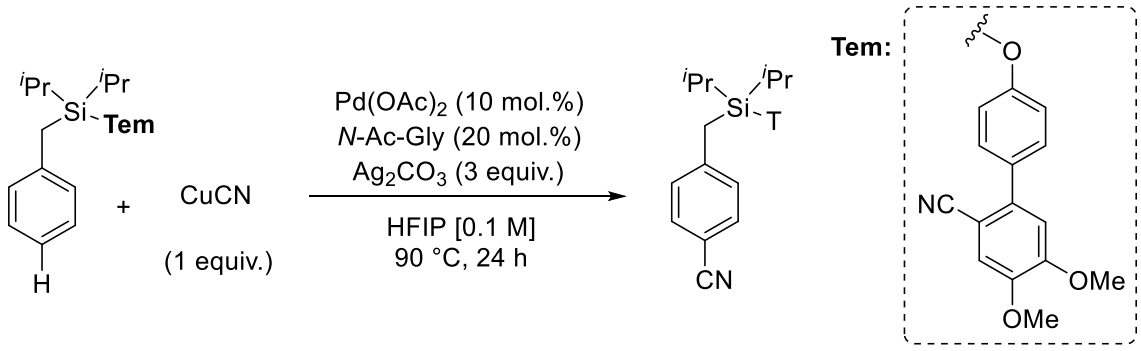

Scheme 53: Conditions for the Pd catalysed *para* cyanation of toluene scaffolds.[159]

1.6.2 – Sterically Induced *para* C–H Functionalisation

The use of sterics to influence the regioselective outcome of *para* C–H functionalisation reactions, tends to rely upon pre-existing sterically demanding functionality on the structure. Methods that utilise this methodology are however, susceptible to regioselectivity issues, due to the distal nature of the steric group(s).[17,160]

There are two reports to date which have attempted to overcome these regioselectivity issues in recent years. The first by Itami, using a bulky metal ligand to control the orientational approach of the substrate towards the metal centre. This report detailed in 2015, reported the *para* selective C–H borylation of alkylbenzene and silylbenzene derivatives.[161] Under the conditions in Scheme **54**, they use an incredibly sterically demanding bidentate phosphine ligand to favour the *para* over the *meta* functionalisation. Computational analysis of this reaction has also been done, modelling reactivity in the pocket of the Ir-ligand complex.[162]

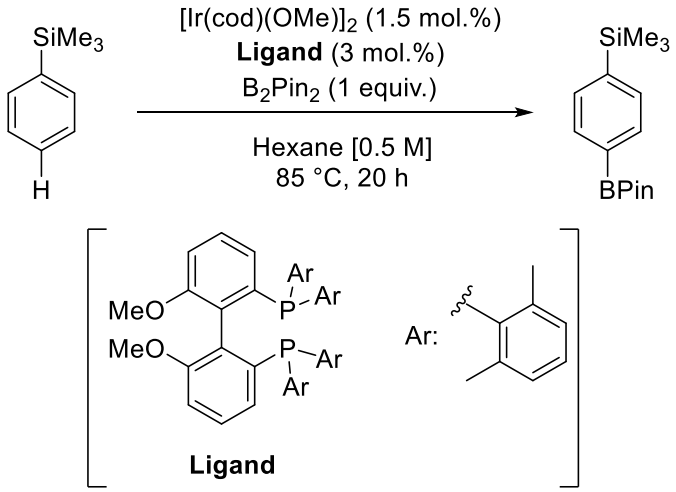

Scheme 54: Ir catalysed *para* C–H borylation, using a bulky Ir catalyst.[161]

Preliminary work by Nakao *et al*. on the C4-alkylation of pyridines, using a bulky Al Lewis acid, to enable C4 selective metalation and functionalisation,[163] led them to consider the *para* selective functionalisation of arenes, using a similar method. There methodology involved using a dual Al/Ni system to allow for the *para* C–H alkylation of benzamides and aromatic ketones.[164] The demonstrated that coordination of the carbonyl to a bulky Lewis acidic aluminium centre, coupled with a bulky nickel system enabled steric clash between the two, leading to selective para-selective C–H functionalisation, an example of this to achieve a *para* selective alkylation is shown in Scheme **55**. Following this the same group then reported the use of sulfones as substrates for the same reaction methodology.[165]

In 2017, Nakao *et al*. utilised this chemistry, to enable a *para* selective C–H borylation of benzamides.[166] The same Al Lewis acid employed previously was used again, however, a different Ir precatalyst and bipyridyl ligand were used. This borylation strategy was also applied to allow for the C4 borylation of pyridine substrates in the same paper.

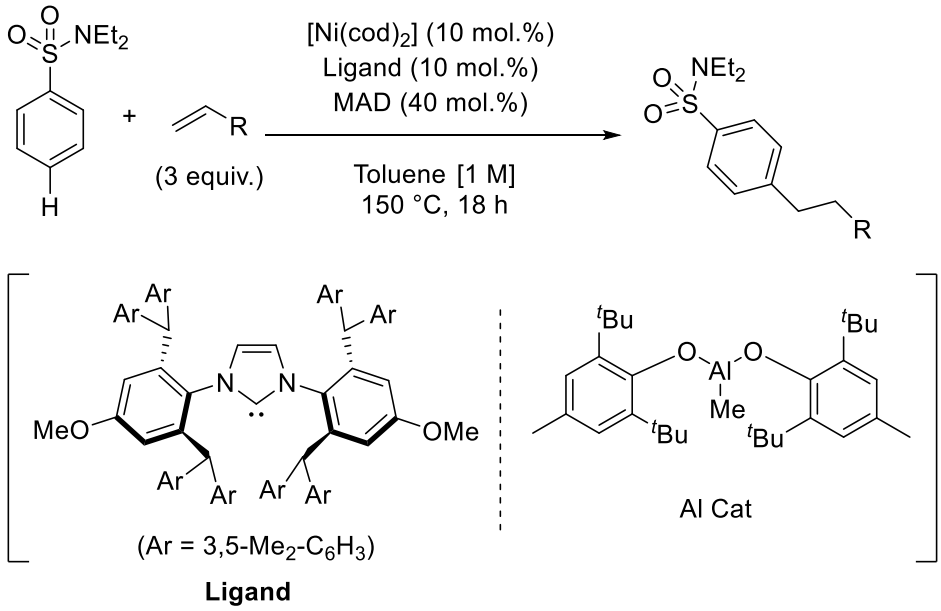

Scheme 55: Ni/Al catalysed *para* C–H alkylation of arenes.[165]

1.6.3 – Electronic Induced *para* C–H Functionalisation

A majority of *para* C–H functionalisation reactions to date, have utilised the electronic biases of substrates to dictate regioselectivity. Here, substituents which can place electron density on the *para* position of an arene can enable interaction with electrophilic metal centers or substrates.

The first such example of this type of *para* C–H functionalisation was described by Gaunt *et al*. in 2011, in the Cu-catalysed *para* arylation of anisole and aniline derivatives shown in Scheme **56**, utilising hypervalent iodine salts.[167]

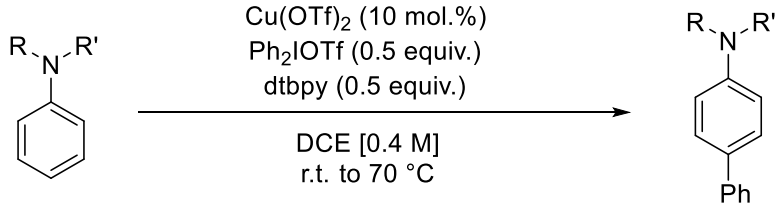

Scheme 56: Conditions for the *para* arylation of aniline derivatives.[167]

Mechanistic studies indicated that this reaction also proceeds in the absence of a Cu catalyst, albeit with lower isolated yields, longer reaction times and elevated temperatures.

The role of the Cu catalyst is believed to lower the barrier of formation of the highly electrophilic aryl cation.

Suna and co-workers have also utilised electronically activated aromatic substrates under Cu catalysis to achieve a *para* selective amination of electron rich arenes, in an Ullman-type cross-coupling fashion.[168] This methodology uses a hypervalent iodine species to react with the desired *para* proton initially in an S_EAr mechanism, to provide a pseudo halogen-type group. The Cu coordinated to the amine to be coupled, then reacts in a Cu(I/III) cycle to insert into the C–I bond, before then undergoing a reductive elimination to yield the *para* aminated product, the reaction conditions are shown in Scheme **57**. The insertion of Cu into the C–I bond is proposed by DFT calculations by Sanford *et al.*[169]

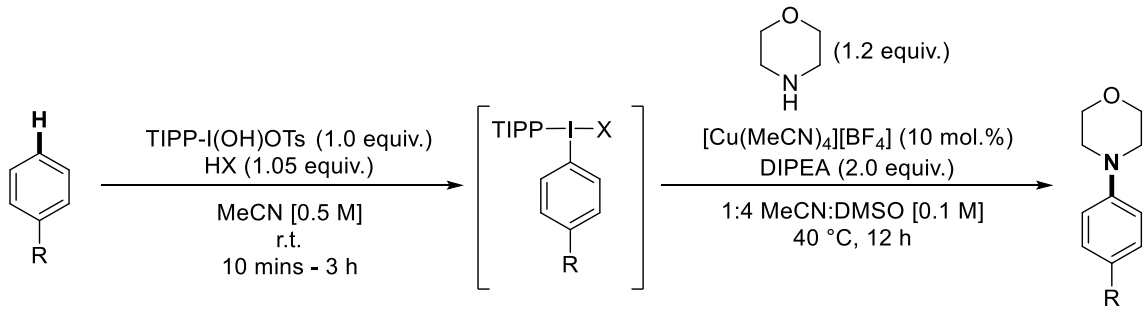

Scheme 57: Conditions for the *para* amination of electron rich arenes.[168]

Subsequent work by Zhang and co-workers reported the *para* selective sulfonimidation of anilide derivatives, utilising *N*-fluorobenzenesulfonimide (NFSI) as the sulfonimidation source using *ortho* methoxyanilides substrates.[170] Mechanistically a cyclopalladation at the *ipso* position, using a methoxy as a non-innocent arene substituent (Scheme **58**).[171,172]

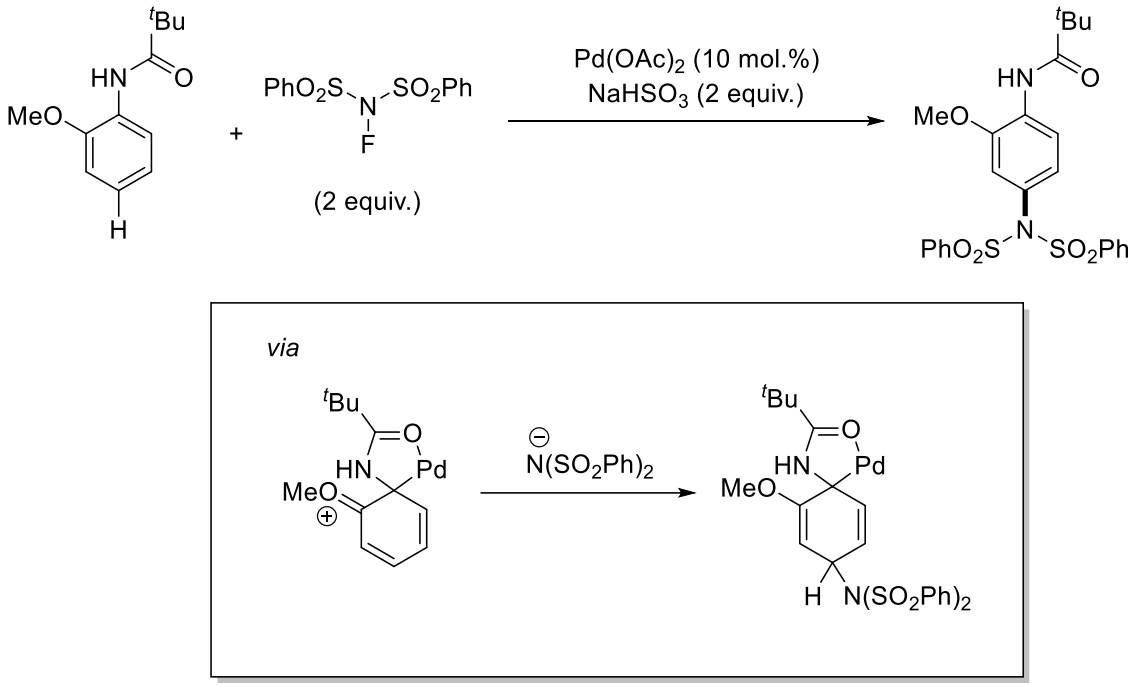

Scheme 58: Conditions for the Pd catalysed *para*-sulfonimidation of anilides.[170]

More recent work by Ritter *et al*. reported upon a method to achieve a *para* amination of electron rich arene rings.[173] This methodology used computational methods to explain the observed regioselectivity. They proposed that the selectivity was dictated by a "charge-transfer radical addition" where TS interactions between the SOMO of the coupling partner and the LUMO of the arene, enable electron shuttling, depicted in Scheme **59**.

This involved using Fukui indices to explain the relatively nucleophilicity of each atom as a simple model to explain the observed regioselectivity.[174,175] Using the calculated electron affinity of various amine radicals, it was found that theoretically and experimentally that the higher the electron affinity, the higher the *para* selectivity experimentally.[176,177] They demonstrated that the greater electron affinity of the coupling partner (more positive), the higher selectivity of functionalisation. This was rationalised as the higher electron affinity, the more readily the coupling partner will accept an electron from the arene to enable the charge transfer complex, responsible for selective C–H functionalisation.

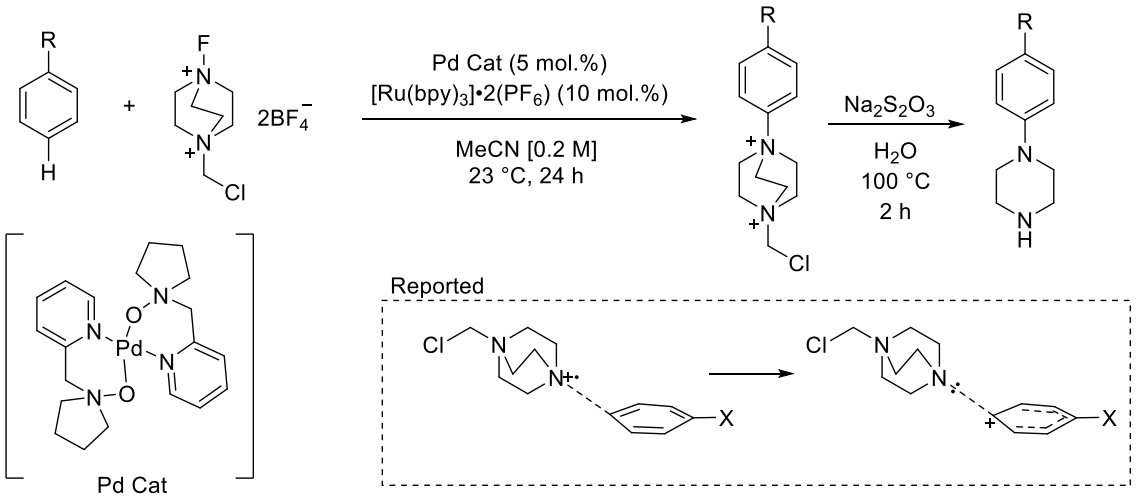

Scheme 59: Pd/Ru catalysed *para* C–H amination of electron rich arenes.[173]

Work by Ackermann *et al.* from 2013 showed that Ru catalysis can also allow for the *para* selective oxygenation of anisole derivatives (Scheme **60**). The reaction is thought to proceed *via* a radical type mechanism, as the addition of TEMPO resulted in significantly reduced yields.

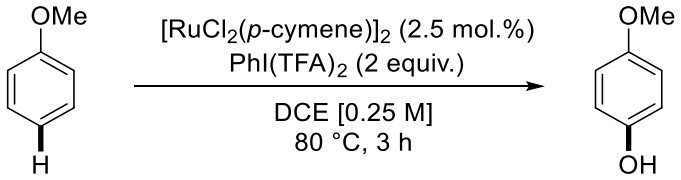

Scheme 60: Conditions for the *para* oxygenation of anilsoles.[178]

Waser and Brand described the *para* alkynylation of aniline derivatives, using Au catalysis, again as described previously in this section, utilising hypervalent iodine reagents. This transformation achieves incredibly high selectivites, under mild conditions as shown in Scheme **61**.

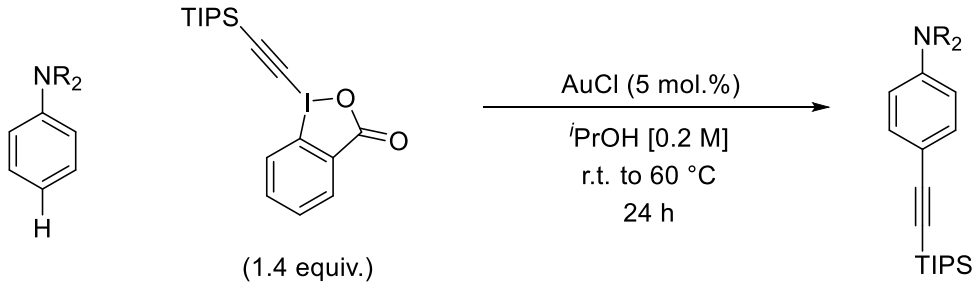

Scheme 61: Conditions for the Au catalysed *para* alkynylation of anilines.[179]

The use of cyclometalated species to achieve *para* functionalisation have recently been reported, the first by Manolikakes *et al.*, describing the *para* sulfonation of bespoke anilide derivatives.[180] The reaction is suggested to proceed through a cyclocuparated intermediate, which could allow SET with the arene ring. A radical cation, centred on the arene could then react with the sulfonyl radical, formed through reaction with a stoichiometric oxidant and sulfonate salts as shown in Scheme **62**.

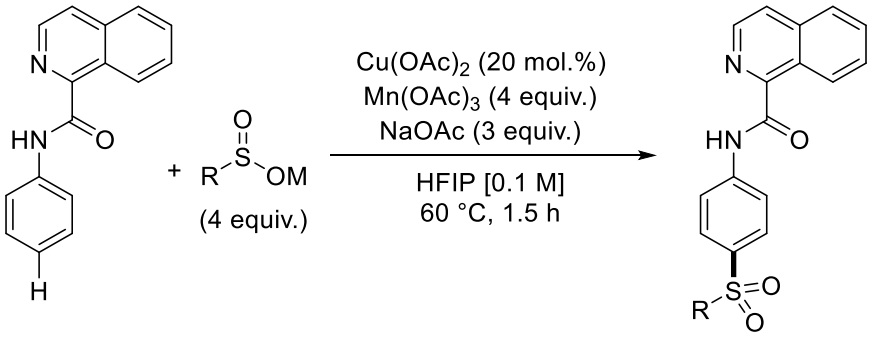

Scheme 62: Conditions for the *para* selective C-H sulfonylation of anilides.[180]

A second example of this methodology also utilises a Cu catalyst in the *para* sulfonation of 2-amino-napthalene derivatives by Lu *et al.*[181] as shown in Scheme **63**.

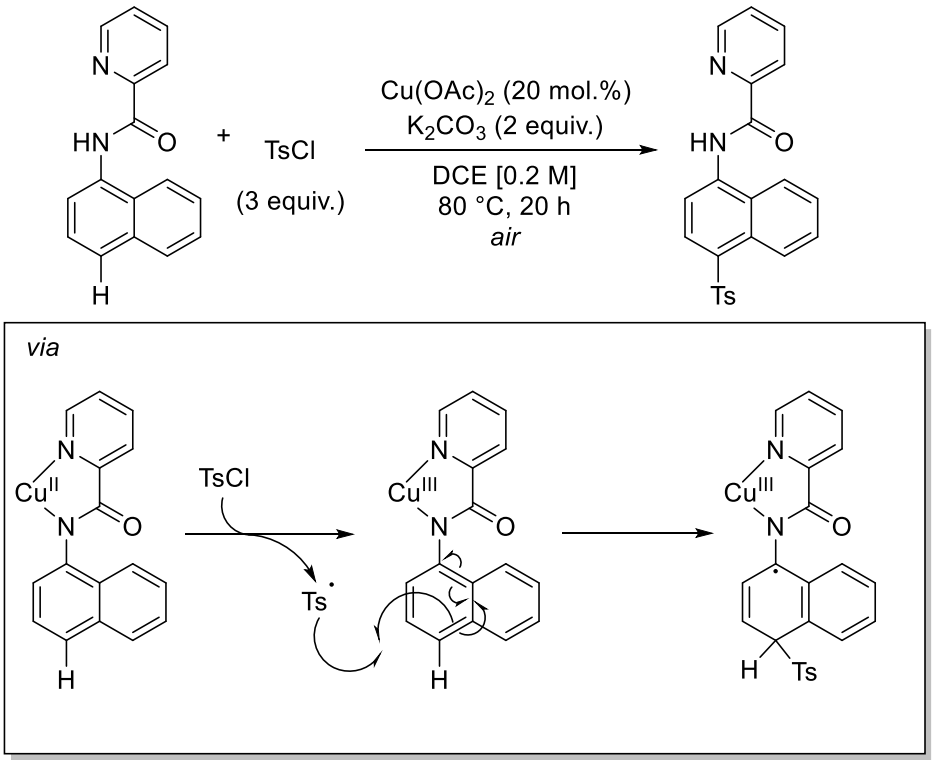

Scheme 63: Cu Catalysed *para* tosylation of aminonaphthalene derivatives.[181]

This methodology uses tosyl chloride as the coupling partner, to react with the substrate in a SET type fashion. This work used DFT and Fukui Indices to explain both the reaction mechanism and regioselectivity observed for the reaction product. This report also reported the unoptimised *para* selective acetoxylation, bromination, iodination, sulfonimidation and trifluoromethylation of the 2-aminonaphthalene derivatives.[181]

In 2017, work from within our group reported the *para* C–H alkylation of aniline derivatives using a radical methodology, as shown in Scheme **64**.[182]

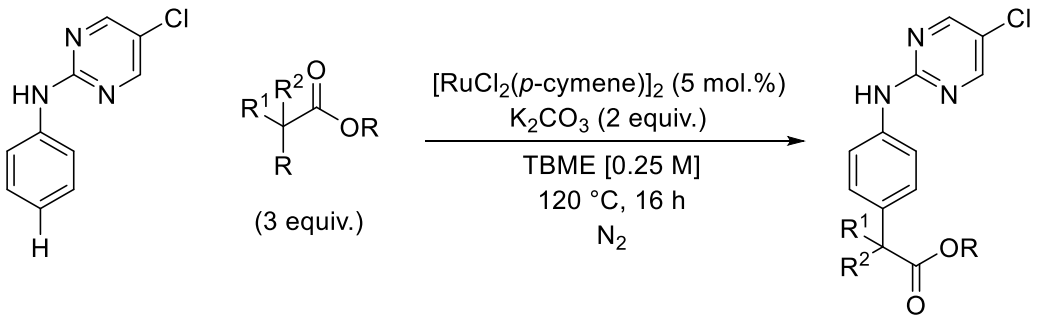

Scheme 64: Optimised conditions for the *para* selective C-H alkylation of aniline dertivatives.[182]

During the optimisation it was also discovered that increasing the reaction temperature resulted in the sole formation of the *meta* product. Under the optimised conditions no regioselectivity issues were reported, with excellent chemoselectivity also observed.

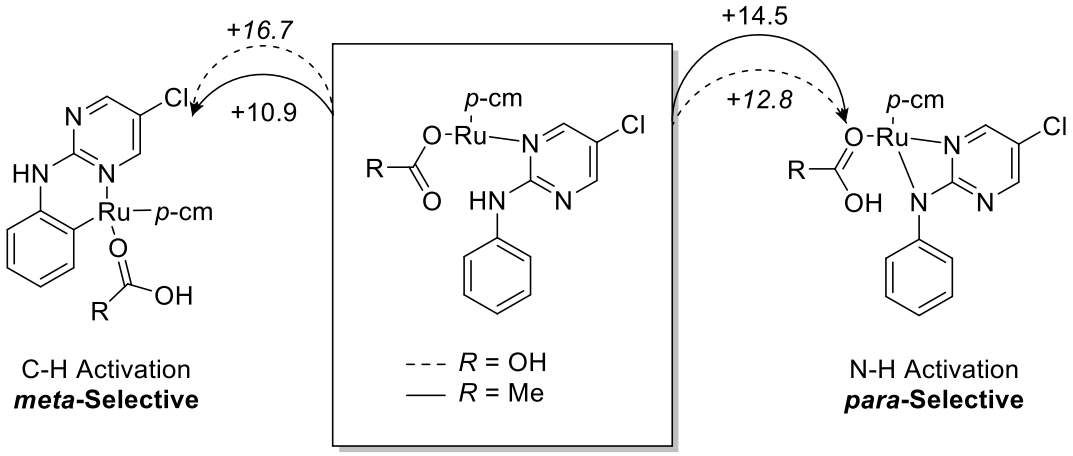

Scheme 65: Summary of DFT free energies (kcal mol^{-1}) relative to the most stable intermediate for the competing C-H and N-H activations of 5-chloro-*N*-phenylpyrimidin-2-amine at $[Ru(p\text{-cymene})(O_2CR)]^+$ in dioxane, when R = Me (acetate) or OH (carbonate).[182]

During mechanistic studies, it was determined that the regioselectivity could be changed between *meta* and *para* by simple addition or removal of an acetate ligand. DFT calculations were used to elucidate the causation of this switch in mechanism, the results of which are summarised in Scheme **65**. These calculations hinted that use of a carboxylate ligand caused the C–H activation to become more favourable and when a carbonate ligand is used the N–H activation pathway becomes more favourable. These theoretical calculations are in alignment with deuterium labelling experiments as well. Addition of stoichiometric amounts of TEMPO to the reaction causes a complete shutdown of reactivity, suggesting a radical pathway.

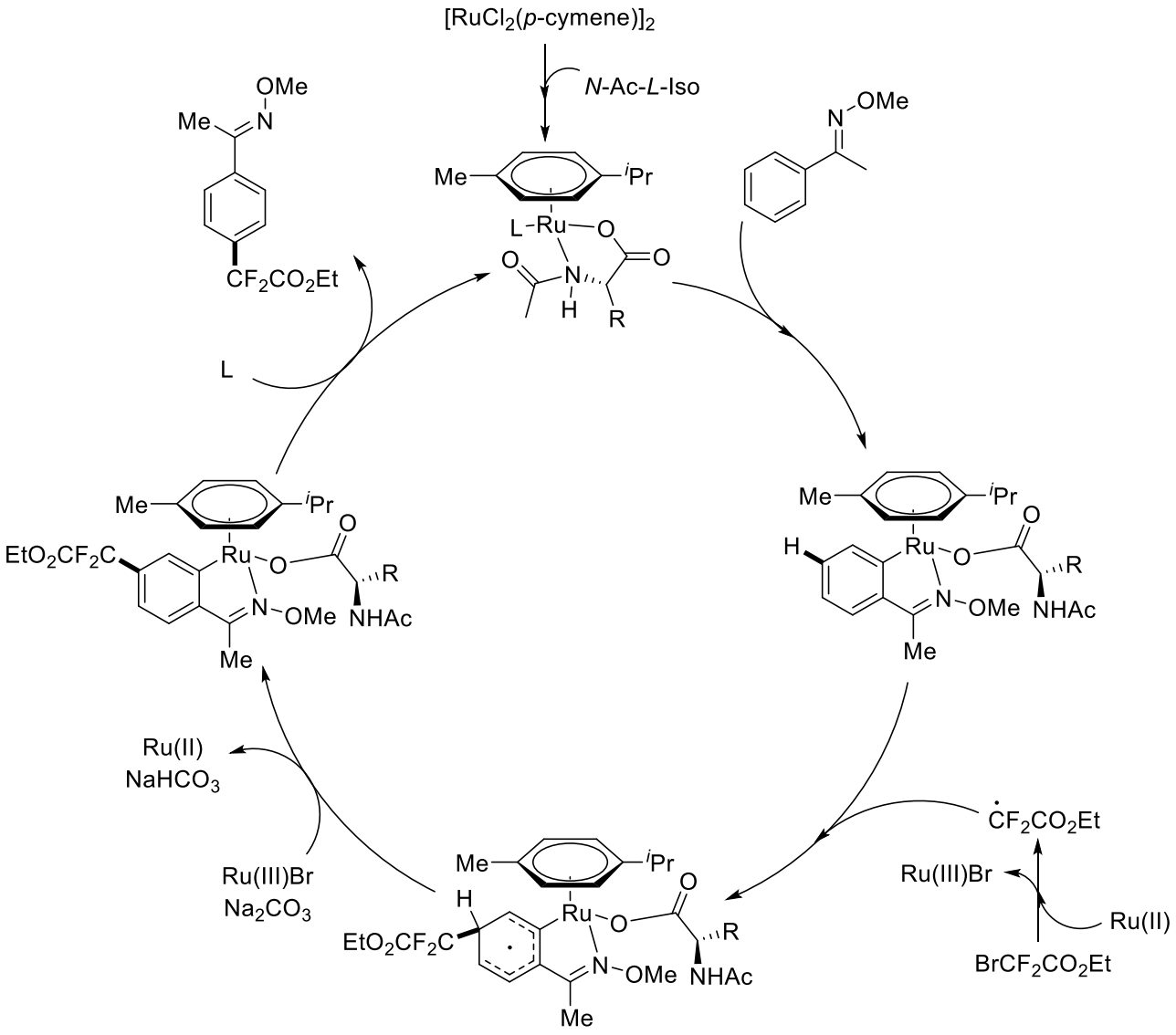

Scheme 66: Proposed catalytic cycle for the *para* difluoromethylation of ketoximes.[183]

Subsequent work by Zhao *et al.* on the *para* difluoromethylation of aromatic ketoxime derivatives proposed an alternative mechanistic pathway.[183] Their examination of the frontier orbitals involved in the reaction intermediates and transition states, suggests that C-H activation occurs preferably (through their use of *N*-Ac-*L*-Iso as a ligand, as suggested by Frost and co-workers to facilitate preferable C-H activation.[182]) with the resulting intermediate having an optimal SOMO/LUMO overlap between the *para* (LUMO) and the SOMO of the $\cdot CF_2CO_2Et$ radical; this results in the mechanistic proposal

shown in Scheme **66**. This methodology has also been extended to include examples of anilide, indoline and tetrahydroquinoline derivatives by Zhao *et al*.[184]

1.7 – Aims and Objectives

At the outset of the following research, the major aims were to develop techniques which could allow for the control of site selectivity in C–H functionalisation, using a variety of substrates and coupling partners, focusing primarily on Ru-catalysed σ-activation. To this end, the results of this thesis will be split into three distinct chapters, which will focus on the distinct regioselective and functionalisation goals as depicted below.

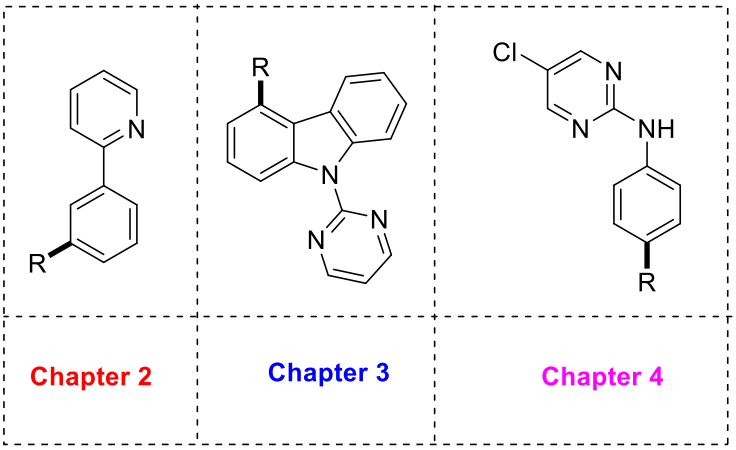

The first section will focus upon the *meta* selective, primary C–H alkylation of 2-phenylpyridine and derivatives, the realisation of this methodology and some mechanistic insights into the transformation.

The second section will focus upon the C4 selective alkylation of a carbazole derivative, the realisation of this transformation and mechanistic insights into this reaction will be focussed on.

The third and final section will focus on our efforts to achieve a *para* selective carbonylation of aniline derivatives, focussing on our attempts to enhance the reactivity of this system and rule out a few possible mechanistic pathways.

Bibliography

1 R. F. Heck and J. P. Nolley, *J. Org. Chem.*, 1972, **37**, 2320–2322.

2 A. Suzuki, *Angew. Chem Int. Ed.*, 2011, **50**, 6722–6737.

3 E. Negishi, *Angew. Chem Int. Ed.*, 2011, **50**, 6738–6764.

4 D. G. Brown and J. Boström, *J. Med. Chem.*, 2016, **59**, 4443–4458.

5 J. F. Hartwig, S. Richards, D. Barañano and F. Paul, *J. Am. Chem. Soc.*, 1996, **118**, 3626–3633.

6 M. S. Driver and J. F. Hartwig, *J. Am. Chem. Soc.*, 1995, **117**, 4708–4709.

7 M. C. Bryan, L. Diorazio, Z. Fei, K. Fraunhoffer, J. Hayler, M. Hickey, S. Hughes, M. McLaws, P. Richardson, G. D. Roiban, M. Schober, A. G. Smith, A. Steven, T. White, S. Wuyts and J. Yin, *Org. Process Res. Dev.*, 2018, **22**, 667–680.

8 K. S. Egorova and V. P. Ananikov, *Angew. Chem Int. Ed.*, 2016, **55**, 12150–12162.

9 M. C. White, *Adv. Synth. Catal.*, 2016, **358**, 2364–2365.

10 P. L. Holland, *Chem*, 2017, **2**, 443–444.

11 C. J. Li, *Chem*, 2016, **1**, 423–437.

12 H. M. L. Davies and D. Morton, *ACS Cent. Sci.*, 2017, **3**, 936–943.

13 X. S. Xue, P. Ji, B. Zhou and J. P. Cheng, *Chem. Rev.*, 2017, **117**, 8622–8648.

14 D. J. Abrams, P. A. Provencher and E. J. Sorensen, *Chem. Soc. Rev.*, 2018, **47**, 8925–8967.

15 T. Brückl, R. D. Baxter, Y. Ishihara and P. S. Baran, *Acc. Chem. Res.*, 2012, **45**, 826–839.

16 W. R. Gutekunst and P. S. Baran, *Chem. Rev. Soc.*, 2011, **40**, 1845–2040.

17 N. Kuhl, M. N. Hopkinson, J. Wencel-Delord and F. Glorius, *Angew. Chem - Int. Ed.*, 2012, **51**, 10236–10254.

18 S. S. Stahl, J. A. Labinger and J. E. Bercaw, *Angew. Chem - Int. Ed.*, 1998, **37**, 2180–2192.

19 Y. X. Luan, T. Zhang, W. W. Yao, K. Lu, L. Y. Kong, Y. T. Lin and M. Ye, *J. Am. Chem. Soc.*, 2017, **139**, 1786–1789.

20 L. T. Ball, G. C. Lloyd-Jones and C. A. Russell, *J. Am. Chem. Soc.*, 2014, **136**, 254–264.

21 I. P. Rothwell, *Acc. Chem. Res.*, 1988, **21**, 153–159.

22 V. Vidal, A. Théolier, J. Thivolle-Cazat, J. M. Basset and J. Corker, *J. Am. Chem.*

Soc., 1996, **118**, 4595–4602.

23 G. P. Niccolai and J. M. Basset, *Appl. Catal. A Gen.*, 1996, **146**, 145–156.

24 A. H. Janowicz and R. G. Bergman, *J. Am. Chem. Soc.*, 1982, **104**, 352–354.

25 J. A. Labinger and J. E. Bercaw, *Nature*, 2002, **417**, 507–14.

26 D. Lapointe and K. Fagnou, *Chem. Lett.*, 2010, **39**, 1118–1126.

27 D. L. Davies, S. M. A. Donald and S. A. Macgregor, *J. Am. Chem. Soc.*, 2005, **127**, 13754–13755.

28 J. Oxgaard, W. J. Tenn, R. J. Nielsen, R. A. Periana and W. A. Goddard, *Organometallics*, 2007, **26**, 1565–1567.

29 Y. Boutadla, D. L. Davis, S. A. MacGregor and A. I. Poblador-Bahamonde, *Dalt. Trans.*, 2009, 5887–5893.

30 S. Winstein and T. G. Traylor, *J. Am. Chem. Soc.*, 1955, **77**, 3747–3752.

31 C. W. Fung, M. Khorramdel-vahed, R. J. Ranson, R. M. G. Roberts and W. Park, *J. Chem. Soc. Perkin Trans. 2*, 1980, **0**, 267–272.

32 A. J. Kresge and J. F. Brennan, *J. Org. Chem.*, 1967, **32**, 752–755.

33 H. C. Brown and C. W. McGary, *J. Am. Chem. Soc.*, 1955, **77**, 2300–2306.

34 J. Klapproth and F. H. Westheimer, *J. Am. Chem. Soc.*, 1950, **72**, 4461–4465.

35 G. A. Olah, S. H. Yu and D. G. Parker, *J. Org. Chem.*, 1976, **41**, 1983–1986.

36 A. C. Cope and R. W. Siekman, *J. Am. Chem. Soc.*, 1965, **87**, 3272–3273.

37 A. C. Cope and E. C. Friedrich, *J. Am. Chem. Soc.*, 1968, **90**, 909–913.

38 A. D. Ryabov, *Chem. Rev.*, 1990, **90**, 403–424.

39 J. Vicente and I. Saura-Llamas, *Comments Inorg. Chem.*, 2007, **28**, 39–72.

40 M. I. Bruce, *Angew. Chem Int. Ed. English*, 1977, **16**, 73–86.

41 A. D. Ryabov, I. K. Sakodinskaya and A. K. Yatsimirsky, *J. Chem. Soc. Dalt. Trans.*, 1985, 2629–2638.

42 I. Ozdemir, S. Demir, B. Cetinkaya, C. Gourlaouen, F. Maseras, C. Bruneau and P. H. Dixneuf, *J. Am. Chem. Soc.*, 2008, **130**, 1156–7.

43 J. Oxgaard, R. P. Muller, W. A. Goddard and R. A. Periana, *J. Am. Chem. Soc.*, 2004, **126**, 352–363.

44 T. R. Cundari, T. V. Grimes and T. B. Gunnoe, *J. Am. Chem. Soc.*, 2007, **129**, 13172–13182.

45 C. Sambiagio, D. Schönbauer, R. Blieck, T. Dao-Huy, G. Pototschnig, P. Schaaf,

T. Wiesinger, M. F. Zia, J. Wencel-Delord, T. Besset, B. U. W. Maes and M. Schnürch, *Chem. Soc. Rev.*, 2018, **47**, 6603–6743.

46 X. Chen, K. M. Engle, D. H. Wang and Y. Jin-Quan, *Angew. Chem - Int. Ed.*, 2009, **48**, 5094–5115.

47 J. Yang, *Org. Biomol. Chem.*, 2015, **13**, 1930–1941.

48 P. B. Arockiam, C. Bruneau and P. H. Dixneuf, *Chem. Rev.*, 2012, **112**, 5879–5918.

49 M. Moselage, J. Li and L. Ackermann, *ACS Catal.*, 2016, **6**, 498–525.

50 E. Bill, T. Weyhermu, F. Neese, K. Wieghardt, H. B. Gray, M. D. Hopkins, V. W. W. Yam, C. C. Cummins, J. C. Price, E. W. Barr, B. Tirupati, J. M. Bollinger and C. Krebs, *Science*, 2006, **312**, 2004–2007.

51 Y. Sun, H. Tang, K. Chen, L. Hu, J. Yao, S. Shaik and H. Chen, *J. Am. Chem. Soc.*, 2016, **138**, 3715–3730.

52 K. M. Engle, T. S. Mei, M. Wasa and J. Q. Yu, *Acc. Chem. Res.*, 2012, **45**, 788–802.

53 S. De Sarkar, W. Liu, S. I. Kozhushkov and L. Ackermann, *Adv. Synth. Catal.*, 2014, **356**, 1461–1479.

54 S. Oi, Y. Ogino, S. Fukita and Y. Inoue, *Org. Lett.*, 2002, **4**, 1783–1785.

55 L. Ackermann, *Org. Lett.*, 2005, **7**, 3123–3125.

56 L. Ackermann, P. Novμk, R. Vicente and N. Hofmann, *Angew. Chem - Int. Ed.*, 2009, **48**, 6045–6048.

57 L. Ackermann, N. Hofmann and R. Vicente, *Org. Lett.*, 2011, **13**, 1875–1877.

58 G. W. Wang, M. Wheatley, M. Simonetti, D. M. Cannas and I. Larrosa, *Chem*, 2020, **6**, 1459–1468.

59 T. Kochi, A. Tazawa, K. Honda and F. Kakiuchi, *Chem. Lett.*, 2011, **40**, 1018–1020.

60 T. Kochi, S. Urano, H. Seki, E. Mizushima, M. Sato and F. Kakiuchi, *J. Am. Chem. Soc.*, 2009, **131**, 2792–2793.

61 P. M. Liu and C. G. Frost, *Org. Lett.*, 2013, **15**, 5862–5865.

62 K. Padala and M. Jeganmohan, *Org. Lett.*, 2011, **13**, 6144–6147.

63 G. Gao and J. You, *Chem. Commun.*, 2016, **52**, 4613–4616.

64 L. Ackermann, A. V. Lygin and N. Hofmann, *Angew. Chem - Int. Ed.*, 2011, **50**, 6379–6382.

65 V. S. Thirunavukkarasu, S. I. Kozhushkov and L. Ackermann, *Chem. Commun.*, 2014, **50**, 29.

66 J. C. Chu, H. C. Ai and D. F. Othmer, *Ind. Eng. Chem.*, 1953, **45**, 1266–1272.

67 V. S. Thirunavukkarasu and L. Ackermann, *Org. Lett.*, 2012, **14**, 6206–6209.

68 Y. S. Kang, P. Zhang, M. Y. Li, Y. K. Chen, H. J. Xu, J. Zhao, W. Y. Sun, J. Q. Yu and Y. Lu, *Angew. Chem - Int. Ed.*, 2019, **58**, 9099–9103.

69 N. Khatun, A. Banerjee, S. K. Santra, W. Ali and B. K. Patel, *RSC Adv.*, 2015, **5**, 36461–36466.

70 L. Wang and L. Ackermann, *Chem. Commun.*, 2014, **50**, 1083–1085.

71 S. De Sarkar, N. Y. P. Kumar and L. Ackermann, *Chem. - A Eur. J.*, 2017, **23**, 84–87.

72 S.-T. Bai, C. B. Bheeter and J. N. H. Reek, *Angew. Chem Int. Ed.*, 2019, 13173–13177.

73 T. Komuro, T. Kitano, N. Yamahira, K. Ohta, S. Okawara, N. Mager, M. Okazaki and H. Tobita, *Organometallics*, 2016, **35**, 1209–1217.

74 M. R. Cho, J.-Y., Tse, M.K., Holmes, D., Maleczka-Jr, R.E., Smith III, *Science*, 2002, **295**, 305–308.

75 J. V. Obligacion, S. P. Semproni, I. Pappas and P. J. Chirik, *J. Am. Chem. Soc.*, 2016, 10645–10653.

76 D. W. Robbins and J. F. Hartwig, *Angew. Chem. Int. Ed.*, 2013, **52**, 933–937.

77 L. Yang, N. Uemura and Y. Nakao, *J. Am. Chem. Soc.*, 2019, **141**, 7972–7979.

78 Y. Zhang, B. Shi and J. Yu, *J. Am. Chem. Soc.*, 2009, **131**, 5072–5074.

79 X. Cong, H. Tang, C. Wu and X. Zeng, *Organometallics*, 2013, **32**, 6565–6575.

80 M. H. Emmert, A. K. Cook, Y. J. Xie and M. S. Sanford, *Angew. Chem - Int. Ed.*, 2011, **50**, 9409–9412.

81 G. B. Boursalian, M. Y. Ngai, K. N. Hojczyk and T. Ritter, *J. Am. Chem. Soc.*, 2013, **135**, 13278–13281.

82 R. J. Phipps and M. J. Gaunt, *Science*, 2009, **323**, 1593–1597.

83 H. A. Duong, R. E. Gilligan, M. L. Cooke, R. J. Phipps and M. J. Gaunt, *Angew. Chem*, 2011, **123**, 483–486.

84 L. Wan, N. Dastbaravardeh, G. Li and J. Q. Yu, *J. Am. Chem. Soc.*, 2013, **135**, 18056–18059.

85 D. Leow, G. Li, T.-S. Mei and J.-Q. Yu, *Nature*, 2012, **486**, 518–522.

86 S. Lee, H. Lee and K. L. Tan, *J. Am. Chem. Soc.*, 2013, **135**, 18778–18781.

87 M. Bera, A. Modak, T. Patra, A. Maji and D. Maiti, *Org. Lett.*, 2014, **16**, 5760–

5763.

88 S. Li, H. Ji, L. Cai and G. Li, *Chem. Sci.*, 2015, **6**, 5595–5600.

89 Y. Deng and J. Q. Yu, *Angew. Chem - Int. Ed.*, 2015, **54**, 888–891.

90 M. Bera, A. Maji, S. K. Sahoo and D. Maiti, *Angew. Chem - Int. Ed.*, 2015, **54**, 8515–8519.

91 L. Chu, M. Shang, K. Tanaka, Q. Chen, N. Pissarnitski, E. Streckfuss and J.-Q. Yu, *ACS Cent. Sci.*, 2015, **1**, 394–399.

92 S. Li, L. Cai, H. Ji, L. Yang and G. Li, *Nat. Commun.*, 2016, **7**, 10443.

93 A. Maji, B. Bhaskararao, S. Singha, R. B. Sunoj and D. Maiti, *Chem. Sci.*, 2016, **7**, 3147–3153.

94 A. Modak, A. Mondal, R. Watile, S. Mukherjee and D. Maiti, *Chem. Commun.*, 2016, **52**, 13916–13919.

95 S. Maity, E. Hoque, U. Dhawa and D. Maiti, *Chem. Commun.*, 2016, **52**, 14003–14006.

96 M. Bera, S. K. Sahoo and D. Maiti, *ACS Catal.*, 2016, **6**, 3575–3579.

97 S. Bag, R. Jayarajan, R. Mondal and D. Maiti, *Angew. Chem - Int. Ed.*, 2017, **56**, 3182–3186.

98 U. Dutta, A. Modak, B. Bhaskararao, M. Bera, S. Bag, A. Mondal, D. W. Lupton, R. B. Sunoj and D. Maiti, *ACS Catal.*, 2017, **7**, 3162–3168.

99 A. Gholap, S. Bag, S. Pradhan, A. R. Kapdi and D. Maiti, *ACS Catal.*, 2020, **10**, 5347–5352.

100 S. Bag, S. K, A. Mondal, R. Jayarajan, U. Dutta, S. Porey, R. B. Sunoj and D. Maiti, *J. Am. Chem. Soc.*, , DOI:10.1021/jacs.0c05223.

101 R. R. Anugu, S. Munnuri and J. R. Falck, *J. Am. Chem. Soc.*, 2020, **142**, 5266–5271.

102 J. Luo, S. Preciado and I. Larrosa, *J. Am. Chem. Soc.*, 2014, **136**, 4109–4112.

103 J. Cornella, M. Righi and I. Larrosa, *Angew. Chem. Int. Ed.*, 2011, **50**, 9429–9432.

104 Y. Zhang, H. Zhao, M. Zhang and W. Su, *Angew. Chem - Int. Ed.*, 2015, **54**, 3817–3821.

105 X.-C. Wang, W. Gong, L.-Z. Fang, R.-Y. Zhu, S. Li, K. M. Engle and J.-Q. Yu, *Nature*, 2015, **519**, 334–338.

106 M. Catellani, F. Frignani and A. Rangoni, *Angew. Chem. Int. Ed.*, 1997, **36**, 119–122.

107 P.-X. Shen, X.-C. Wang, P. Wang, R.-Y. Zhu and J.-Q. Yu, *J. Am. Chem. Soc.*,

2015, **137**, 11574–11577.

108 L. Jiao and T. Bach, *J. Am. Chem. Soc.*, 2011, **133**, 12990–12993.

109 M. Rueping and B. J. Nachtsheim, *Beilstein J. Org. Chem.*, 2010, **6**, 1–24.

110 H. J. Davis, M. T. Mihai and R. J. Phipps, *J. Am. Chem. Soc.*, 2016, **138**, 12759–12762.

111 P. C. Roosen, V. A. Kallepalli, B. Chattopadhyay, D. A. Singleton, R. E. Maleczka and M. R. Smith, *J. Am. Chem. Soc.*, 2012, **134**, 11350–11353.

112 A. G. Green, P. Liu, C. A. Merlic and K. N. Houk, *J. Am. Chem. Soc.*, 2014, **136**, 4575–4583.

113 H. J. Davis, G. R. Genov and R. J. Phipps, *Angew. Chem - Int. Ed.*, 2017, **56**, 13351–13355.

114 M. T. Mihai, H. J. Davis, G. R. Genov and R. J. Phipps, *ACS Catal.*, 2018, **8**, 3764–3769.

115 B. Lee, M. T. Mihai, V. Stojalnikova and R. J. Phipps, *J. Org. Chem.*, 2019, **84**, 13124–13134.

116 Y. Kuninobu, H. Ida, M. Nishi and M. Kanai, *Nat. Chem.*, 2015, **7**, 712–717.

117 K. M. Engle, D. H. Wang and J. Q. Yu, *J. Am. Chem. Soc.*, 2010, **132**, 14137–14151.

118 G. Cheng, Y. Yang and P. Liu, *J. Am. Chem. Soc.*, 2014, **136**, 894–897.

119 Z. Zhang, K. Tanaka and J. Q. Yu, *Nature*, 2017, **543**, 538–542.

120 O. Saidi, J. Marafie, A. E. W. Ledger, P. M. Liu, M. F. Mahon, G. Kociok-Kohn, M. K. Whittlesey and C. G. Frost, *J. Am. Chem. Soc.*, 2011, **133**, 19298–19301.

121 J. D. Nguyen, E. M. D'Amato, J. M. R. Narayanam and C. R. J. Stephenson, *Nat. Chem.*, 2012, **4**, 854–859.

122 J. J. Devery III, J. J. Douglas, J. D. Nguyen, K. P. Cole, R. A. Flowers II and C. R. J. Stephenson, *Chem. Sci.*, 2015, **6**, 537–541.

123 N. Hofmann and L. Ackermann, *J. Am. Chem. Soc.*, 2013, **135**, 5877–5884.

124 A. J. Paterson, S. St John-Campbell, M. F. Mahon, N. J. Press and C. G. Frost, *Chem. Commun.*, 2015, **51**, 12807–12810.

125 C. Liu, D. Liu, W. Zhang, L. Zhou and A. Lei, *Org. Lett.*, 2013, **15**, 6166–6169.

126 X. Wu, J. W. T. See, K. Xu, H. Hirao, J. Roger, J. C. Hierso and J. Zhou, *Angew. Chem - Int. Ed.*, 2014, **53**, 13573–13577.

127 T. Nishikata, Y. Noda, R. Fujimoto and T. Sakashita, *J. Am. Chem. Soc.*, 2013, **135**, 16372–16375.

128 J. Li, S. Warratz, D. Zell, S. De Sarkar, E. E. Ishikawa and L. Ackermann, *J. Am. Chem. Soc.*, 2015, **137**, 13894–13901.

129 M. S. Kharasch, E. V. Jensen and W. H. Urry, *Science*, 1945, **102**, 128.

130 G. Kiefer, J. Ruiz, E. Solari, G. Hilt and K. Severin, *European J. Org. Chem.*, 2012, 93–98.

131 J. Park and S. Hong, *Chem. Soc. Rev.*, 2012, **41**, 6931–6943.

132 P. Marcé, A. J. Paterson, M. F. Mahon and C. G. Frost, *Catal. Sci. Technol.*, 2016, **6**, 7068–7076.

133 A. Sagadevan and M. F. Greaney, *Angew. Chem Int. Ed.*, 2019, **58**, 9826–9830.

134 P. Gandeepan, J. Koeller, K. Korvorapun, J. Mohr and L. Ackermann, *Angew. Chem - Int. Ed.*, 2019, 9820–9825.

135 J. A. Leitch, C. L. McMullin, M. F. Mahon, Y. Bhonoah and C. G. Frost, *ACS Catal.*, 2017, **7**, 2616–2623.

136 F. Fumagalli, S. Warratz, S. K. Zhang, T. Rogge, C. Zhu, A. C. Stückl and L. Ackermann, *Chem. - A Eur. J.*, 2018, **24**, 3984–3988.

137 K. Korvorapun, R. Kuniyil and L. Ackermann, *ACS Catal.*, 2019, acscatal.9b04592.

138 C. Jia, S. Wang, X. Lv, G. Li, L. Zhong, L. Zou and X. Cui, *European J. Org. Chem.*, 2020, **2020**, 1992–1995.

139 C. J. Teskey, A. Y. W. Lui and M. F. Greaney, *Angew. Chem - Int. Ed.*, 2015, **54**, 11677–11680.

140 Q. Yu, L. Hu, Y. Wang, S. Zheng and J. Huang, *Angew. Chem Int. Ed.*, 2015, **54**, 15284–15288.

141 Z. Fan, H. Lu, Z. Cheng and A. Zhang, *Chem. Commun.*, 2018, **54**, 6008–6011.

142 J. A. Przyojski, K. P. Veggeberg, H. D. Arman and Z. J. Tonzetich, *ACS Catal.*, 2015, **5**, 5938–5946.

143 S. Warratz, D. J. Burns, C. Zhu, K. Korvorapun, T. Rogge, J. Scholz, C. Jooss, D. Gelman and L. Ackermann, *Angew. Chem - Int. Ed.*, 2017, **56**, 1557–1560.

144 J. Li, K. Korvorapun, S. De Sarkar, T. Rogge, D. J. Burns, S. Warratz and L. Ackermann, *Nat. Commun.*, 2017, **8**, 15430.

145 Z. Fan, J. Ni and A. Zhang, *J. Am. Chem. Soc.*, 2016, **3**, 8470–8475.

146 Y. Gao, Y. Mao, B. Zhang, Y. Zhan and Y. Huo, *Org. Biomol. Chem.*, 2018, **16**, 3881–3884.

147 X. Wang, Y. Li, H. Liu, B. Zhang, X. Gou, Q. Wang, J. Ma, Y. Liang, X. Wang,

Y. Li, H. Liu, B. Zhang, X. Gou and Q. Wang, *J. Am. Chem. Soc.*, 2019, **141**, 13914–13922.

148 H. L. Barlow, C. J. Teskey and M. F. Greaney, *Org. Lett.*, 2017, **19**, 6662–6665.

149 K. Jing, Z.-Y. Li and G.-W. Wang, *ACS Catal.*, 2018, **8**, 11875–11881.

150 C. Jia, N. Wu, X. Cai, G. Li, L. Zhong, L. Zou and X. Cui, *J. Org. Chem.*, 2020, **85**, 4536–4542.

151 B. Li, S. L. Fang, D. Y. Huang and B. F. Shi, *Org. Lett.*, 2017, **19**, 3950–3953.

152 G. Li, D. Li, J. Zhang, D. Q. Shi and Y. Zhao, *ACS Catal.*, 2017, **7**, 4138–4143.

153 A. Dey, S. Maity and D. Maiti, *Chem. Commun.*, 2016, **52**, 12398–12414.

154 S. Bag, T. Patra, A. Modak, A. Deb, S. Maity, U. Dutta, A. Dey, R. Kancherla, A. Maji, A. Hazra, M. Bera and D. Maiti, *J. Am. Chem. Soc.*, 2015, **137**, 11888–11891.

155 T. Patra, S. Bag, R. Kancherla, A. Mondal, A. Dey, S. Pimparkar, S. Agasti, A. Modak and D. Maiti, *Angew. Chem - Int. Ed.*, 2016, **55**, 7751–7755.

156 M. E. Hoque, R. Bisht, C. Haldar and B. Chattopadhyay, *J. Am. Chem. Soc.*, 2017, **139**, 7745–7748.

157 R. Bisht and B. Chattopadhyay, *J. Am. Chem. Soc.*, 2016, **138**, 84–87.

158 M. T. Mihai, B. D. Williams and R. J. Phipps, *J. Am. Chem. Soc.*, 2019, **141**, 15477–15482.

159 S. Pimparkar, T. Bhattacharya, A. Maji, A. Saha, R. Jayarajan, U. Dutta, G. Lu, D. W. Lupton and D. Maiti, *Chem. - A Eur. J.*, , DOI:10.1002/chem.202001368.

160 C. Zheng and S. L. You, *RSC Adv.*, 2014, **4**, 6173–6214.

161 Y. Saito, Y. Segawa and K. Itami, *J. Am. Chem. Soc.*, 2015, **137**, 5193–5198.

162 B. E. Haines, Y. Saito, Y. Segawa, K. Itami and D. G. Musaev, *ACS Catal.*, 2016, **6**, 7536–7546.

163 Y. Nakao, Y. Yamada, N. Kashihara and T. Hiyama, *J. Am. Chem. Soc.*, 2010, **132**, 13666–13668.

164 S. Okumura, S. Tang, T. Saito, K. Semba, S. Sakaki and Y. Nakao, *J. Am. Chem. Soc.*, 2016, **138**, 14699–14704.

165 S. Okumura and Y. Nakao, *Org. Lett.*, 2017, **19**, 584–587.

166 L. Yang, K. Semba and Y. Nakao, *Angew. Chem - Int. Ed.*, 2017, **56**, 4853–4857.

167 C. L. Ciana, R. J. Phipps, J. R. Brandt, F. M. Meyer and M. J. Gaunt, *Angew. Chem - Int. Ed.*, 2011, **50**, 458–462.

168 B. Berzina, I. Sokolovs and E. Suna, *ACS Catal.*, 2015, 7008–7014.

169 N. Ichiishi, A. J. Canty, B. F. Yates and M. S. Sanford, *Organometallics*, 2014, **33**, 5525–5534.

170 K. Sun, Y. Li, T. Xiong, J. Zhang and Q. Zhang, *J. Am. Chem. Soc.*, 2011, **133**, 1694–1697.

171 C. Chen and J. F. Hartwig, *Science*, 2014, **343**, 853–857.

172 L. Gu, B. S. Neo and Y. Zhang, *Org. Lett.*, 2011, **13**, 1872–1874.

173 G. B. Boursalian, W. S. Ham, A. R. Mazzotti and T. Ritter, *Nat. Chem.*, 2016, **8**, 810–815.

174 R. G. Parr and W. Yang, *J. Am. Chem. Soc.*, 1984, **106**, 4049–4050.

175 P. W. Ayers and M. Levy, *Theor. Chem. Acc.*, 2000, **103**, 353–360.

176 J. Zhao and S. Li, *J. Org. Chem.*, 2017, **82**, 2984–2991.

177 J. Lalevée, X. Allonas, S. Genet and J. P. Fouassier, *J. Am. Chem. Soc.*, 2003, **125**, 9377–9380.

178 W. Liu and L. Ackermann, *Org. Lett.*, 2013, **15**, 2–4.

179 J. P. Brand and J. Waser, *Org. Lett.*, 2012, **14**, 744–747.

180 S. Liang, M. Bolte and G. Manolikakes, *Chem. - A Eur. J.*, 2017, **23**, 96–100.

181 J. M. Li, Y. H. Wang, Y. Yu, R. B. Wu, J. Weng and G. Lu, *ACS Catal.*, 2017, **7**, 2661–2667.

182 J. A. Leitch, C. L. McMullin, A. J. Paterson, M. F. Mahon, Y. Bhonoah and C. G. Frost, *Angew. Chem - Int. Ed.*, 2017, **56**, 15131–15135.

183 C. Yuan, L. Zhu, R. Zeng, Y. Lan and Y. Zhao, *Angew. Chem - Int. Ed.*, 2018, **57**, 1277–1281.

184 C. Yuan, L. Zhu, C. Chen, X. Chen, Y. Yang, Y. Lan and Y. Zhao, *Nat. Commun.*, 2018, **9**, 1–10.

Chapter 2 – α-Halo Carbonyls for *meta* Selective Primary C–H Alkylations

At the time of carrying this work out, the coupling partners reported for the *meta*-alkylation of 2-phenylpyridine were limited to secondary and tertiary alkyl halides and the analogous α-halo esters.[1–3] The reason for this limited scope of alkylations is due to the proposed mechanism of reaction, which involves the formation of a C-centred radical species on the coupling partner. These species are stabilised by the effects of hyperconjugation with the non-bonding orbitals of an adjacent atom or functional group.[4]

The regioselective *meta* functionalisation of arene rings, utilising directing groups had at the time of this work been limited to: alkylation (tertiary and secondary only),[1,2,5] nitrations,[6] sulfonations,[7] brominations,[8,9] and benzylations.[10,11] Since the completion of this work this has been expanded further to include carboxylations,[12] alkylarylations,[13] mono- and difluoro-alkylations,[14,15] chlorinations and iodination,[16,17] and acylations.[18]

The use of primary alkyl halides has been reported by Ackermann *et al*. as an observable by-product for the *ortho* alkylation of 2-phenylpyridine substrates, this observation is the first report of such a *meta* primary alkylation, shown in Scheme **67**.[19]

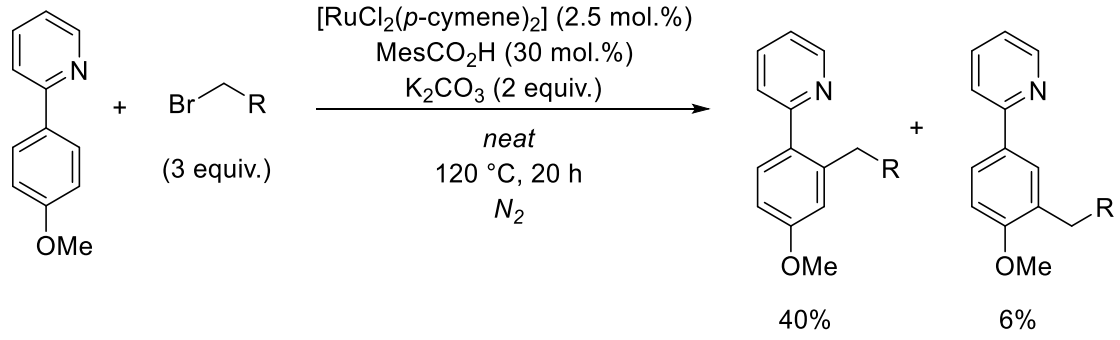

Scheme 67: Conditions used for the first report of *meta*-alkylation.[19]

As shown in Scheme **68**, the first step of the cycle shows the Ru inserting into an *ortho* C–H bond, as directed by a Lewis basic directing group, with the expulsion of a molecule of carboxylic acid.[20,21] The next step of the cycle shows a radical formed by an inner

sphere electron transfer with another molecule of Ru *in situ*., reacting with the cyclometallated phenylpyridine at the *meta* position.[2,9] However, there are also examples of this process occurring under photolytic conditions.[22,23] The next step shows the process of a single electron transfer (SET) to a Ru(III) species *in situ*,[9,11] followed by deprotonation to restore the aromaticity of the system. The final step of the cycle shows the protodemetallation of the Ru catalyst from the functionalised substrate, with acetic acid.

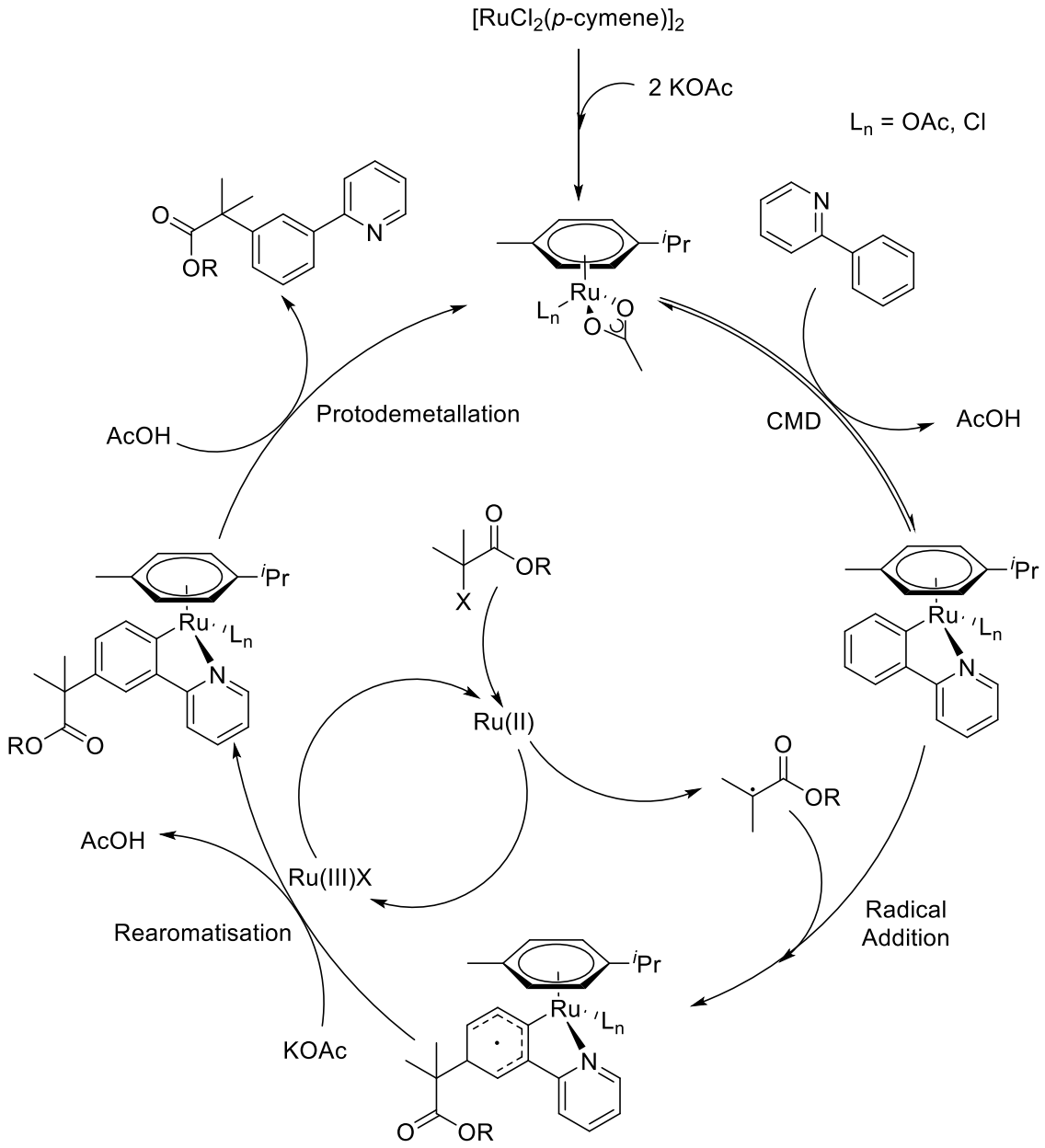

Scheme 68: Mechanistic explanation for the *meta* selective secondary and tertiary alkylation of 2-phenylpyridine.[2,24]

Work within our group had shown that α-halo ester coupling partners were effective for secondary and tertiary *meta* alkylation reactions.[2] We became intrigued as to how these substrates could be applied to include primary α-halo ester coupling partners.

The use of α-halo esters as coupling partners reduces the likelihood of electrophilic type reaction mechanisms, due to the destabilisation of any positive charge at the α-carbon and

stabilises the formation of radicals at this same position, as shown by the formation of the alkyl radical in Scheme **68**.

Preliminary investigations carried out within our group demonstrated that the use of primary alkyl halide coupling partners (such as ethyl 2-bromoacetate) under the *meta*-alkylation conditions as shown in Scheme **69**, led to a mixture of *ortho* and *meta* products in low yield, with negligible observable regioselectivity between *ortho* and *meta*, arising from a competing two-electron process, shown in Scheme **70**.

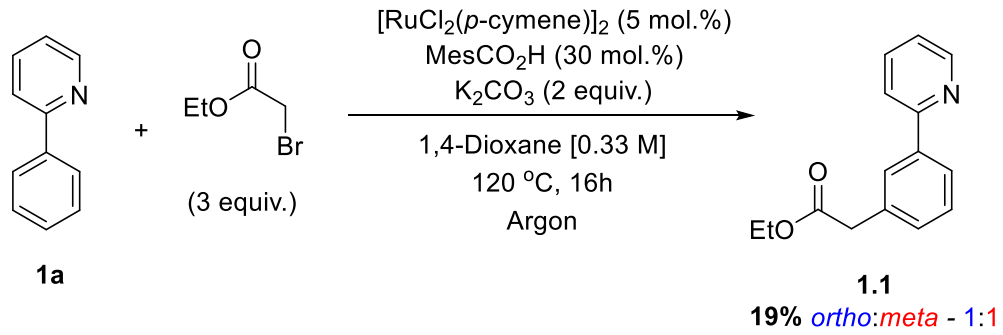

Scheme 69: Initial results of using primary alkyl halide coupling partners to access *meta*-alkylated products.

A likely mechanistic pathway leading to the *ortho* alkylated product is shown in Scheme **70**. This process begins by an identical CMD process, allowing the Ru to insert into the *ortho* C–H bond of the substrate. This Ru-CMD complex then undergoes oxidative addition into the C–Br bond of the coupling partner, rapidly followed by reductive elimination to yield the *ortho* alkylated product and the catalytically active Ru(II) species. This side reaction represents, a manner in which we hypothesis the *ortho* regioisomer is being competitively formed *in situ*.

We attributed this lack in selectivity to the fact that an *in-situ* generated primary alkyl halide radical is not sufficiently stabilised by hyperconjugation, or that two-electron oxidative addition into the C–Br bond by a Ru(II) centre is competitive.[2] This proposed radical addition of a tertiary radical to the *meta* position would initially suggest that use of primary analogue of a α-halo ester radical precursor would be inherently unstable and short-lived.[25]

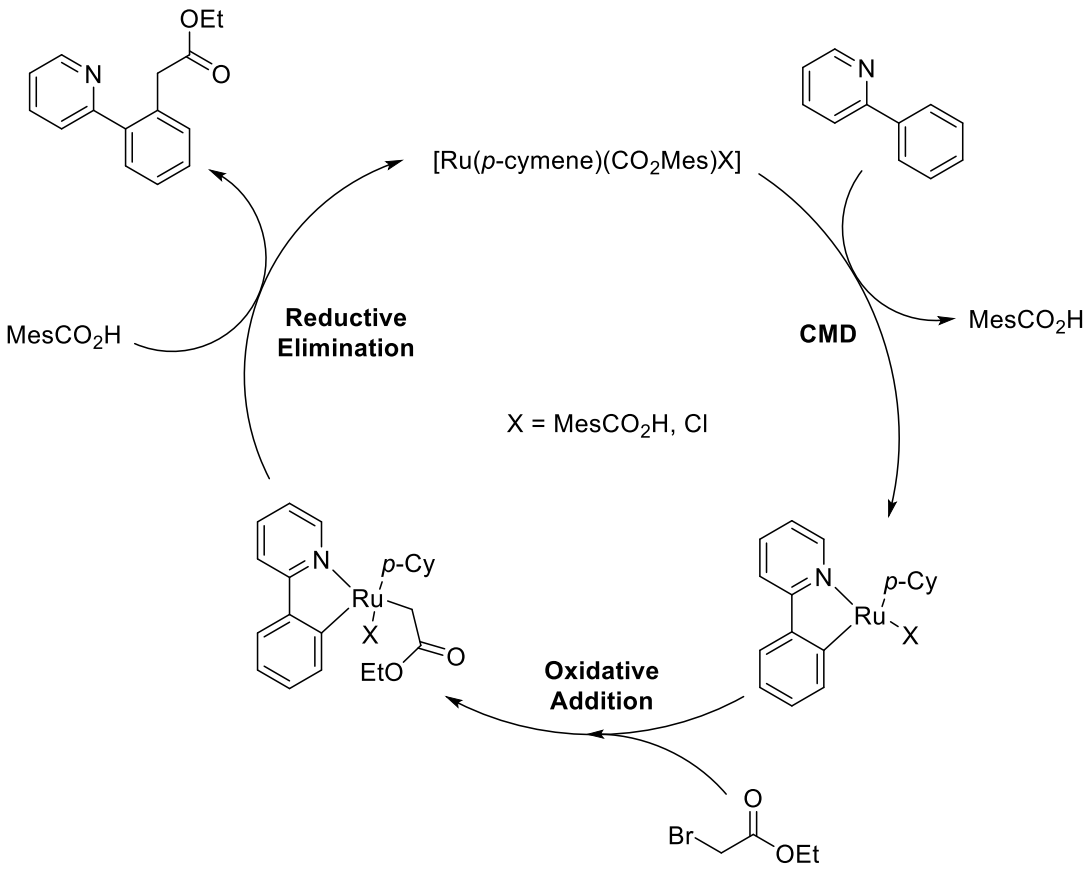

Scheme 70: Mechanistic pathway that leads to the *ortho* alkylated product, when using primary -halo ester coupling partners.

Work done within our lab sought to identify a suitable additive to the reaction, that would reduce the rate of this competing two-electron process, that leads to the *ortho* alkylated product, whilst simultaneously allowing for the *meta* addition of the coupling partner. Pleasingly, it was shown that the use of Pd based additives were effective in amplifying *meta*-selectivity and subsequent optimisation studies afforded an increased yield of C–H functionalised product and *meta*-selectivity up to 18:1 (Scheme **71**) in good yields.[26] The regioselective bias shown for the *meta* isomer suggests that this process for *ortho* functionalisation is kinetically more sluggish and that the intermediates leading to this product are reversibly formed as suggested by Itoh *et al*. for the oxidative addition/reductive elimination of allylic halides onto Ru(II) complexes under the reaction conditions shown in Scheme **71**.[27]

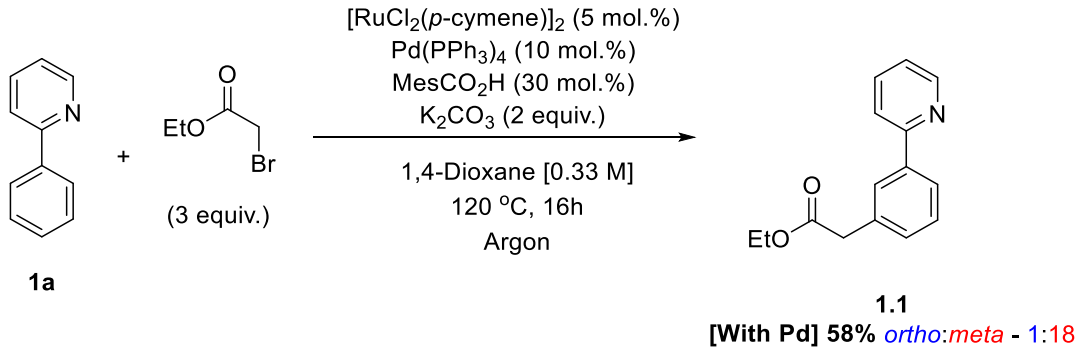

Scheme 71: Optimised conditions for the *meta* primary alkylation of 2-phenylpyridine using a palladium co-catalyst.[26]

The aim of the work carried out in this chapter was to achieve a regioselective *meta* alkylation of 2-phenylpyridine (**1a**) and related directing groups and variants thereof, using a co-catalyst to achieve this aim, whilst minimising formation of the *ortho* regioisomer. The use of an additive to increase the nucleophilicity of the desired position of reaction, or formation of a new coupling partner *in situ* amenable to radical formation, was in our view the best way to achieve this transformation, precluding the use of complex directing groups, which would then necessitate the addition of two extra steps to couple, then remove the directing group. The ability to achieve this transformation with comparable/lower catalytic loadings and a more economically sustainable cocatalyst than Pd to achieve the same regioselective and atom economical outcomes was of great importance to us, which lead us to initially base metal complexes to this end. The investigation of what was occurring mechanistically through use of experimental and computational modelling was also utilised, to allow for deeper understanding of this process. [$Pd(PPh_3)_4$] allowed this regioselectivity to be flipped in favour of the *meta* product.

Progressing from these results, we were interested in exploring more sustainable alternatives to this system as it necessitated the dual catalytic system constituting two noble/platinum group metals. As previous studies have elucidated the key role Ru plays in σ-activation methodologies, we identified that an alternative for the Pd co-catalyst may be sought. The results herein were carried out in a joint project with Dr Andrew J. Paterson, however, with a main focus on my contributions.

This reaction methodology has the potential for the rapid synthesis of a library of compounds and for the late stage functionalisation of drug candidates, two examples which contain the phenylpyridine motif are shown in Figure **5**.

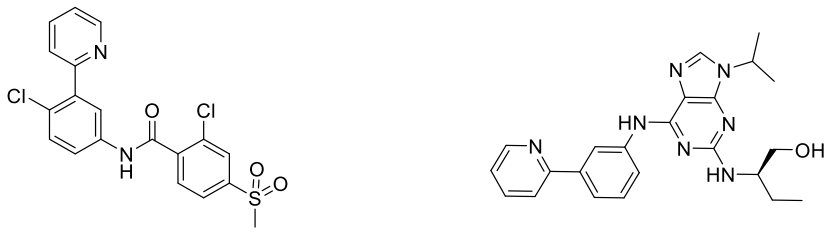

Figure 5: Pharmaceuticals containing the 2-phenylpyridine motif.

2.1 – Synthesis of Starting Materials

2-Phenylpyridine (**1a**) was chosen as our model substrate, due to its well explored "strong" directing group properties and precedent for *meta* functionalisation of this substrate *via* σ-activation methodologies in the literature.[2,3,7] To investigate the effects of electronic variations on the reaction, it was necessary to prepare a range of 2-phenylpyridine substrates.

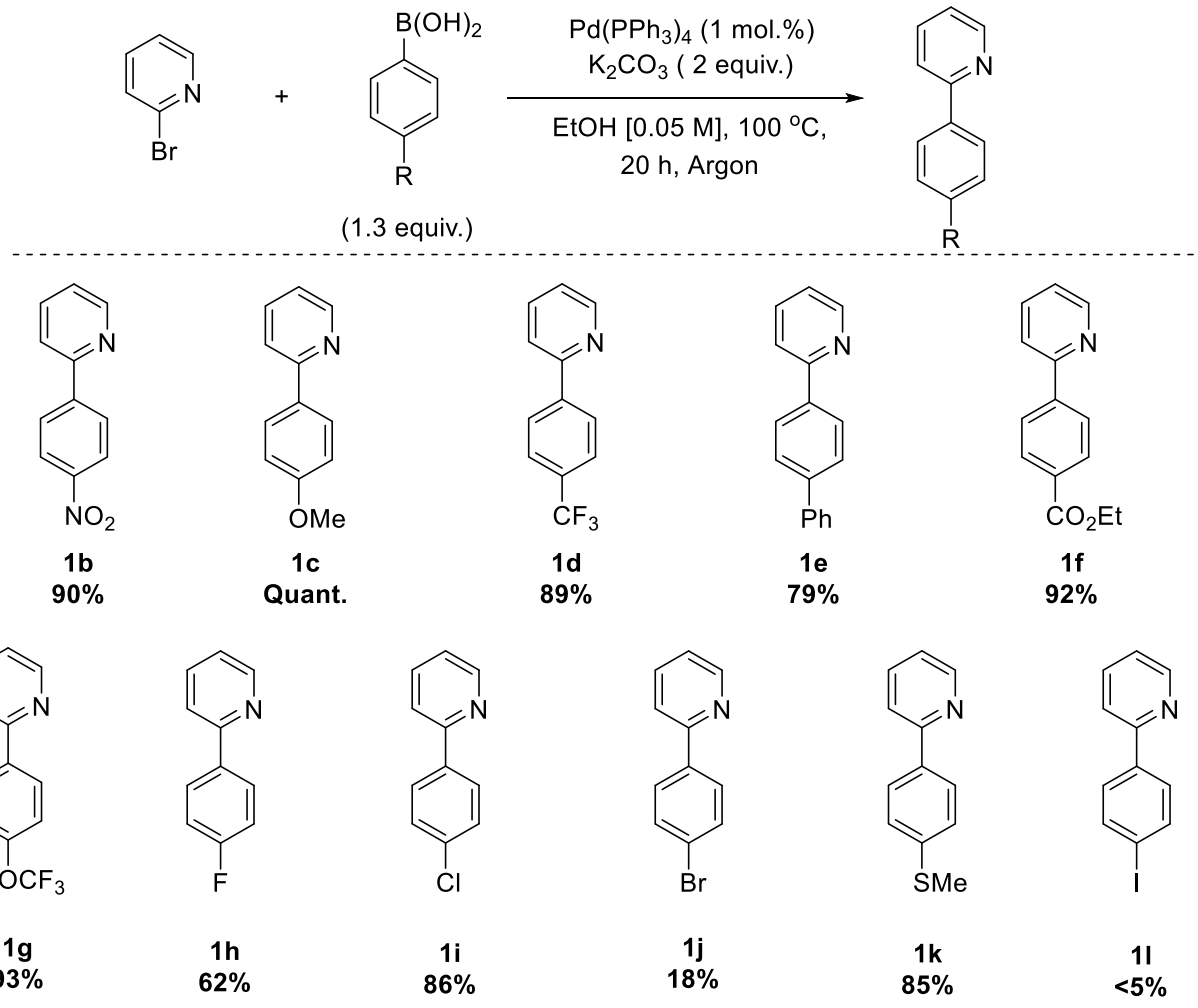

Scheme 72: Scope and results for the synthesis of *para* substituted 2-phenylpyridine substrates.

Previous work within our group and literature precedent utilising various *para*-substituted, 2-phenylpyridine derivatives were prepared *via* a Suzuki cross-coupling reaction between 2-bromopyridine and various 4-substituted phenylboronic acids.[2,28,29]

Utilising the reported conditions for the syntheses of these substrates, resulted in good to excellent yields as shown in Scheme **72**, with the exception of the bromo- and iodo-substrates, in which cases significant levels of homo-coupled by-products were observed. Due to the limited utility of the iodo- substrates as an example, its synthesis was not explored further.

For all the other substituted examples utilised in Section **2.4**, these examples were already available in house, having been prepared during the course of another project.[26]

2.2 – Optimisation of Reaction Using a Nickel Co-Catalyst

We believed that an oxidative addition event by the Pd co-catalyst and subsequent interaction with a ruthenacycle was responsible for the observed regioselectivity. On conducting a literature search we became aware of a 2013 report by Chatani *et al*. showing that the addition of Ni(II) salts with the addition of PPh_3 as a ligand, could facilitate the *ortho* addition of primary alkyl halides when using benzamide and acrylamide directing groups for both activated and unactivated alkyl halide species.[30] In their mechanistic explanation, they proposed that oxidative addition of Ni(II) into the C–X bond meant that the reaction proceeded *via* a two-electron pathway (Ni(0)/Ni(II) or Ni(II)/Ni(IV)) process.[31,32] For these reasons we believed that a Ni-based system could provide the key to unlocking a more sustainable method.

We commenced our study into more sustainable co-catalysts with Ni salts in place of $[Pd(PPh_3)_4]$. Our investigation started by using the optimal conditions from the Pd reaction and replacing the Pd with a range of Ni complexes, as seen in Table **1**.

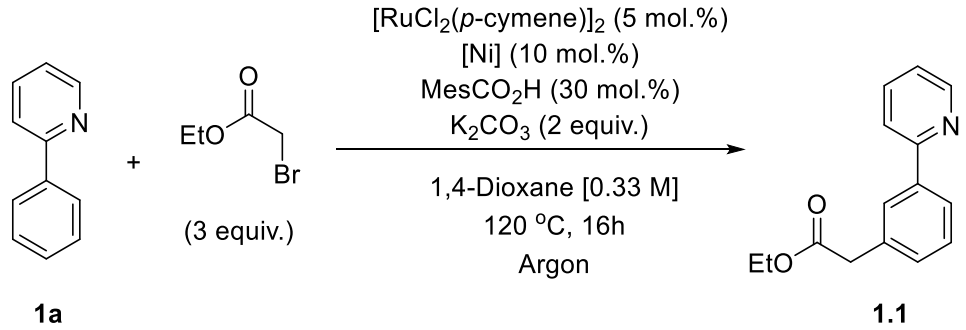

Table 1: Selected results from the investigation of Ni co-catalysts for the *meta* functionalisation of 2-phenylpyridine. IY – Isolated Yield.

Entry	Co-catalyst	Conversion to **2.1** (%) (IY) (*m*:*o*)
1	$NiCl_2 \cdot 6H_2O$	**n.r**
2	$Ni(OAc)_2 \cdot 4H_2O$	**n.r**
3	$[NiBr_2(PPh_3)_2]$	**59 (33) (8:1)**
4	$[NiCl_2(PPh_3)_2]$	**61 (38) (9:1)**
5	$[NiCl_2(dppf)]$	**<5**
6	$[Ni(COD)_2]$	**n.r**
7	$[NiCl_2(dppe)]$	**<5**

Gratifyingly, good conversion and modest regioselectivity for **1.1** were observed when employing Ni(II) co-catalysts bearing a phosphine ligand (Table **1**). A range of other Ni co-catalysts were studied but shown to be unreactive under the reaction conditions. The use of Ni(0) was attempted in the hypothesis that the Ni may be undergoing a two-electron process with the alkyl halide coupling partner to directly activate it. However, the lack of reaction led us to believe that the Ni could play a different role, which will be discussed in a later section in more detail. Use of different phosphine ligands for the Ni co-catalyst also proved to be ineffective at increasing conversions (Entries **5** and **7**, Table **1**). However, in this regard we were limited to electron rich phosphine-based ligands, due to the reported instability of such complexes bearing electron deficient phosphine ligands.[33]

After screening Ni co-catalysts, we began to investigate the optimal Ru source for this transformation as shown in Table **2**.

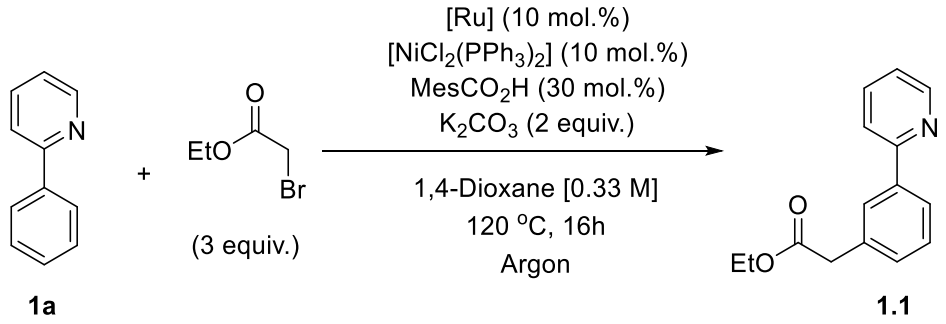

Table 2: Results from catalyst screen for the *meta* alkylation of 2-phenylpyridine. IY – Isolated Yield.

Entry	Ru source	Conversion to **2.1** (%) (IY) (*m*:*o*)
1*	$[RuCl_2(p\text{-cymene})]_2$	**61 (38) (9:1)**
2*	$[RuCl_2(benzene)]_2$	**12**
3	$RuCl_3 \cdot xH_2O$	**<5**
4	$RuCl_3(PPh_3)_2$	**<5**
5	$[Ru(1,10\text{-phen})_3] \cdot 2Cl^-$	**0**

*-5 mol.% dimer used

$[RuCl_2(p\text{-cymene})]_2$ gave the best results for conversion to **1.1**, from the catalysts screened. Ru(III) sources proved to be ineffective under the reaction conditions used; and the use of a Ru photocatalyst, with non-labile ligands showed no reactivity at all. This result hints that the formation of a CMD complex (an intermediate that is formed when a

metal species undergoes concerted metalation deprotonation (CMD) with a suitable substrate) is vital to the reactivity and that the Ru is directly used in this step.[21,34,35]

The screening of carboxylate ligands to facilitate insertion of the Ru into the *ortho* C–H bond was investigated next, with a selection of carboxylic acid/carboxylate salts tested, with the results shown in Table **3**.

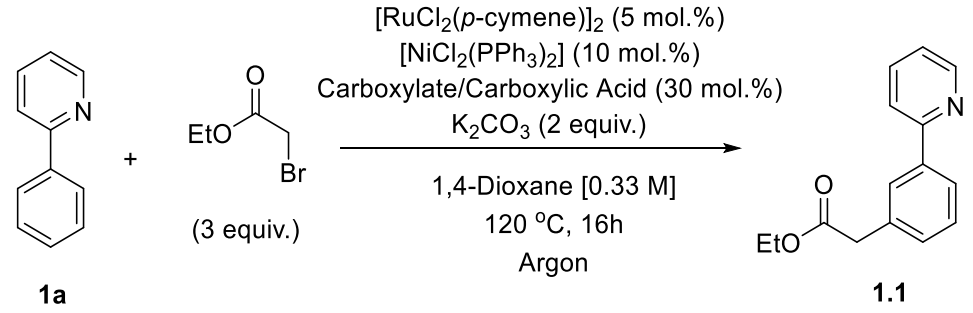

Table 3: Selected results from the optimisation of the carboxylate/carboxylic acid ligand for the *meta* functionalisation of 2-phenylpyridine. IY – Isolated Yield.

Entry	Carboxylate/Carboxylic Acid	Conversion to **2.1** (%) (IY) (*m*:*o*)
1	KOAc	**0**
2	$AdCO_2H$	**65 (54) (19:1)**
3	9-$AnthCO_2H$	**7**
4	$PhCO_2H$	**37**
5	$MesCO_2H$	**61 (38) (9:1)**
6	$PivCO_2H$	**58 (40) (6:1)**
7	Piv-Val-OH	**16**

As seen in Table **3**, the bulky acids: $PivCO_2H$, $MesCO_2H$ and $AdCO_2H$ gave the best conversions to **1.1**, these results mirror the previous work done in the group by Paterson *et al.*[26] The optimisation of this reaction component also gave the most dramatic improvement in both isolated yields and observed regioselectivities.

The use of Piv-Val-OH as utilised by Yu *et al.*,[36] and later by Ackermann *et al.*[24] successful in facilitating the CMD process between the (sp^2)C–H bond and the metal catalyst was found to be ineffective for these reaction conditions, giving a low conversion to the desired product.

The use of different bases showed that using alkali carbonate bases gave the best results, with K_2CO_3, Cs_2CO_3 and Na_2CO_3 giving near identical results (61%, 62% and 59% respectively). We decided to use K_2CO_3 as the base for this reaction, due to its common use already in similar σ-activation methodologies,[7,20,37]

The optimisation of the reaction solvent found that 1,4-dioxane was the best solvent, with other solvents giving inferior results. It could be hypothesised that this is due to the mixture of polar and non-polar reaction components, and the need for a solvent that would allow for the dissolution of both *in situ*.

2.3 – Role of [Ni] and Reoptimisation of Conditions

Upon optimisation of the reaction conditions we carried out more control experiments, in an effort to better understand the effect of each component upon the reaction. The results of these control experiments are shown in Table **4**. The addition of Ru to the reaction is critical for the reactivity of the whole system as its removal results in zero reactivity. The addition of the carboxylic acid ligand, to aid the CMD process of the Ru into the *ortho* C–H bond is essential to allow the turnover of the Ru to allow the reaction to proceed at higher yield and regioselectivity. The removal of the Ni resulted in a loss of regioselectivity of the system, and this made us question the exact role the Ni plays in the system.

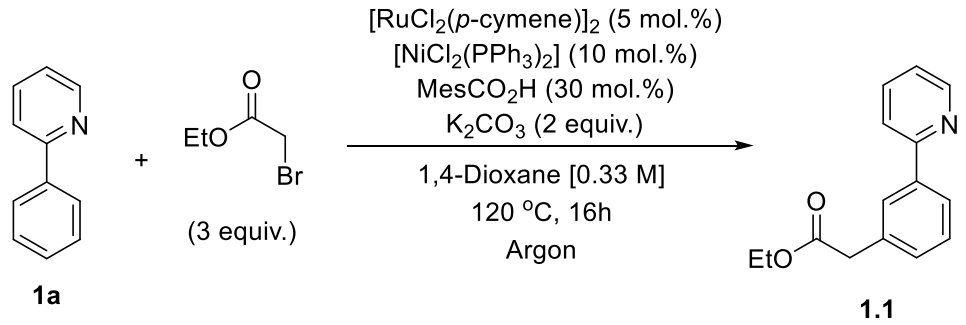

Table 4: Results of control experiments upon reaction conversions and regioselectivities. IY – Isolated Yield.

Entry	Parameter changed	Conversion to **2.1** (%) (IY) (*m*:*o*)
1	No [Ru]	**0**
2	No $AdCO_2H$	**15 (2.5:1)**
3	No [Ni]	**19 (1:1)**
4	$NiCl_2 \cdot 6H_2O$ + $2PPh_3$	**53 (30) (9:1)**
5	$NiCl_2 \cdot 6H_2O$	**0**
6*	PPh_3	**60 (57) (20:1)**

*-20 mol.% added

When we added the two components of the Ni source separately (Entry **4**, Table **4**), we seen that the reaction occurs with good regioselectivity, but lower than our observed "gold standard." We then looked at the effect of the Ni and whether it formed a heterobimetallic complex *in situ* with the Ru to form an active catalytic species,[15] or whether it was dissociating a PPh_3 ligand that then coordinated to the Ru allowing for the more powerful direction towards the desired *meta* C–H bond (Entries **5** and **6**, Table **4**). As seen in Table **4** (Entry **6**) the addition of PPh_3 alone resulted in a much higher conversion than that observed with the Ni conditions, with a comparably high regioselectivity.

We then decided to reoptimise the reaction conditions for use with a phosphine ligand. Results from this optimisation are shown in Table **5**. The use of alkyl phosphine ligands resulted in little to no observed reactivity, possibly due to increased strength of the σ-donation, resulting in much slower rates of ligand exchange required for reactivity.[38] The use of phenyl phosphine derivatives, bearing an EWG *para* to the P gave good regioselectivities, with reduced yields than compared those seen with PPh_3.

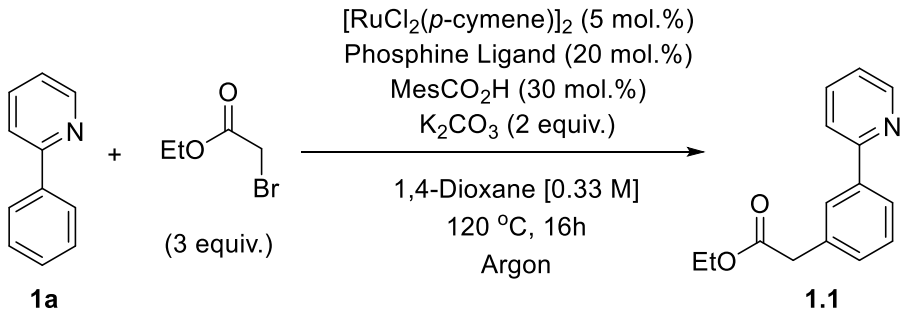

1a **1.1**

Table 5: Selected results from the optimisation for the *meta* alkylation of 2-phenylpyridine. IY – Isolated Yield.

Entry	Phosphine Ligand	Conversion to **2.1** (%) (IY) (*m*:*o*)
1	PPh_3	**60 (57) (20:1)**
2	PCy_3	**0**
3	$P(4\text{-}F(C_6H_4))_3$	**52 (38) (15:1)**
4	$P(4\text{-}(CF_3)(C_6H_4))_3$	**44 (21) (16:1)**
5	dppe	**<5**
6	dppf	**<5**
7	$P(n\text{-}Bu)_3$	**<5**

The use of bidentate phosphine ligands such as dppf and dppe (Entries **5** and **6**, Table **5**) also gave poor yields; comparable with the results seen for the alkyl phosphine ligands (Entries **2** and **7**, Table **5**).

We next began to examine the optimal carboxylate ligand for the Ru, to aid the CMD process. The results of this are shown in Table **6**, it was found that $MesCO_2H$ was the optimal ligand in this regard, with the previously used $AdCO_2H$ for the nickel reaction conditions giving an inferior yield.

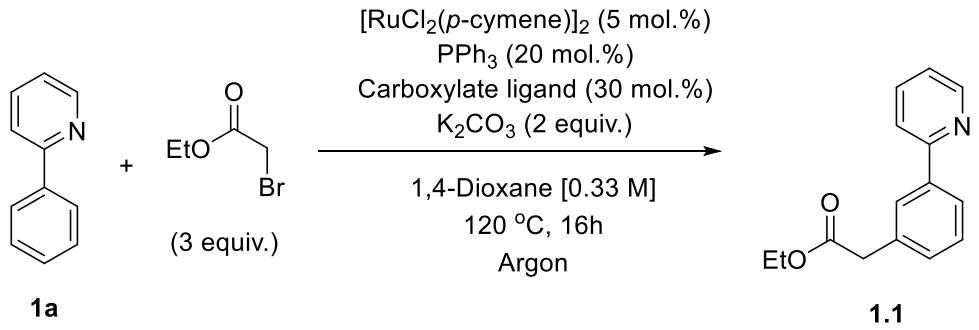

Table 6: Selected results from the carboxylate ligand optimisation for the *meta* alkylation of 2-phenylpyridine when using a phosphine ligand. IY – Isolated Yield.

Entry	Ligand	Conversion to **2.1** (IY) (%) (*m*:*o*)
1	$AdCO_2H$	**29**
2	KOAc	**54**
3	$MesCO_2H$	**60 (57) (20:1)**
4	$PivCO_2H$	**0**
5	Piv-Val-OH	**<5**

The choice of base, solvent and reaction temperature remained the same as previously used for the Ni conditions. Interestingly, an increase in reaction concentration resulted in much diminished yields, whereas such an effect when using the Ni co-catalyst, gave no such observable effect in this regard. Inclusion of air in the reaction lead to much diminished conversions by 20%, but no effect upon the regioselectivity of the reaction, but not a complete reduction in reactivity.

2.4 – Scope and Limitations

With two sets of optimised conditions in hand, we sought to explore the substrate scope of the reaction, with regards to the directing group as shown in Scheme **73**.

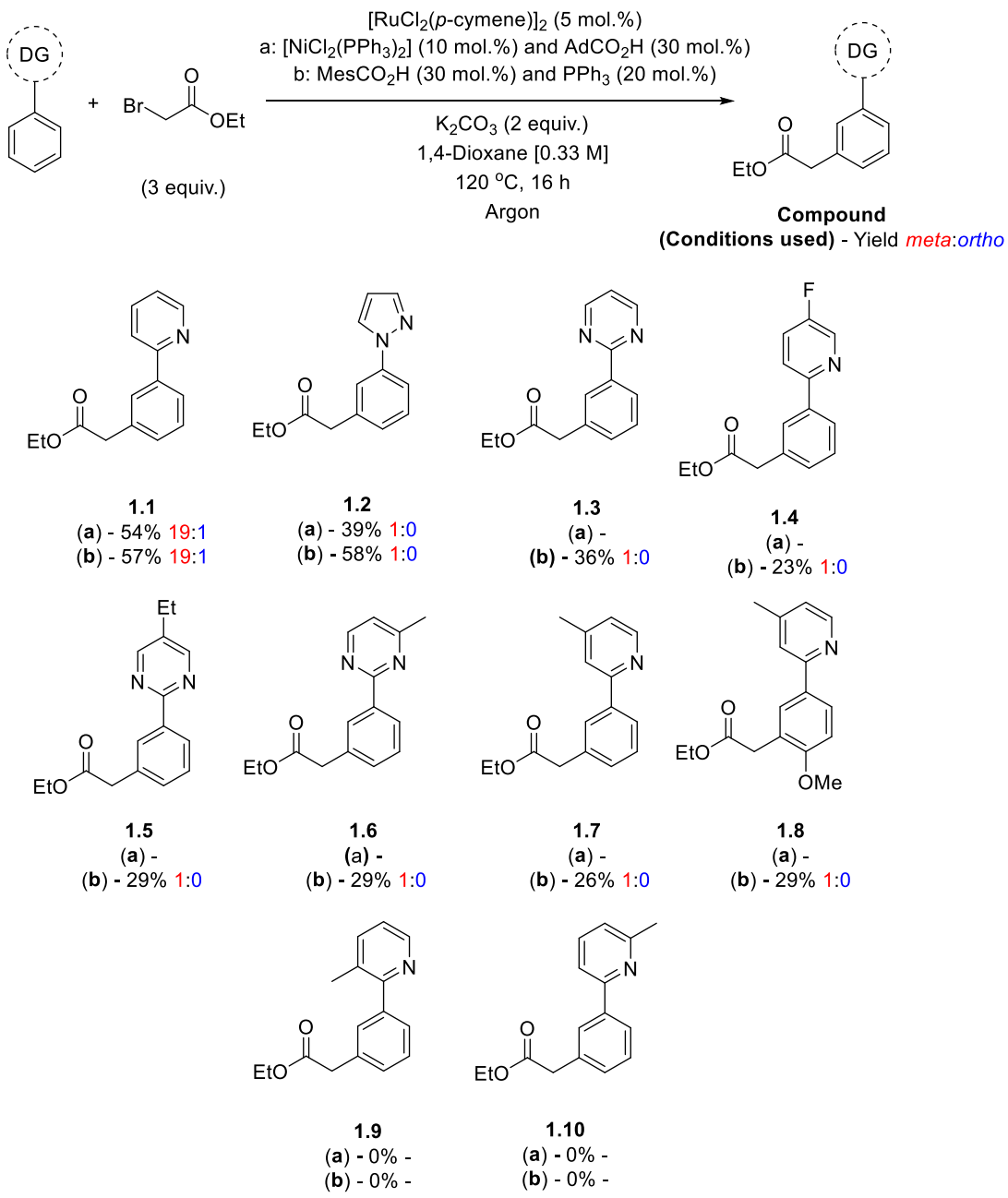

Scheme 73: Directing group scope.

In all cases, near complete regioselectivity for the desired *meta* product was observed (19:1 or greater (*m*:*o*)). Entries **1.9** and **1.10** gave no reaction under the conditions tested as the methyl group present in the pyridine rings creates a highly strained system upon CMD of the Ru into the *ortho* C–H proton, which disfavours the formation of such an intermediate.

The use of pyrimidine and pyrrole rings as directing groups work well for this methodology. However, the addition of extra functional groups to the heterocyclic portion of the molecule appears to lead to diminished yields, with no effect upon the observed regioselectivity of the isolated product. This could possibly be due to the electronic and steric effect that these groups confer upon the initial coordination of the Ru catalyst.

We then investigated the effect of substituting the arene ring and its effect upon the regioselectivity from changing the sterics and electronics of it as shown in Scheme **74**. In general, the use of electron donating groups (EDG) lead to superior regioselectivity as seen with Entries **1.11**, **1.12** and **1.16** in Scheme **74**, due to the stabilisation of the partial positive charge located in the transition state on the arene ring. Comparatively the use of electron withdrawing groups (EWG) lead to inferior regioselectivities, with the exception of the NO_2 substituted example (**1.20**) which is presumed to be too deactivated to react under this methodology. This can be attributed to their destabilising effect for S_EAr to occur at the *ortho* position directly adjacent to the strongly EWG.[39,40]

The examples bearing methyl groups in the *ortho* or *meta* positions were unreactive under the conditions attempted, despite their effectiveness as substrates in other reported Ru catalysed alkylations.[3,24] The dimethylated example (**1.26**) afforded no product either, due to its inability to form a cyclometallated complex with the Ru catalyst.

After exploring the effects of substitution on the aromatic ring systems of the substrate, we looked at the effect of using an α-chloro ester coupling partner. To our delight this furnished the desired *meta* product, **1.1** in 48% yield with an equal 19:1 (*m*:*o*) regioselectivity under the conditions shown in Scheme **75**.

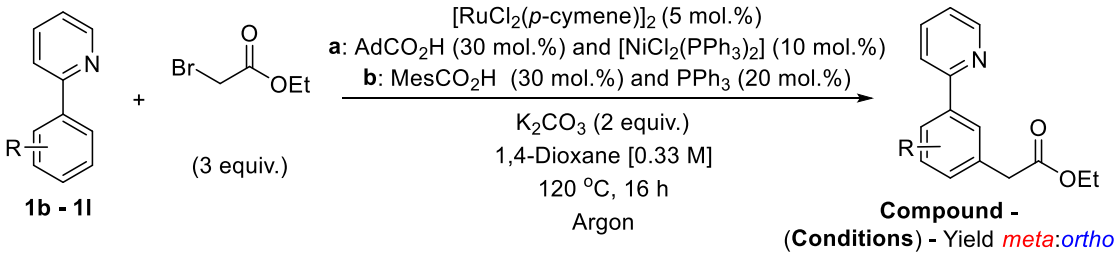

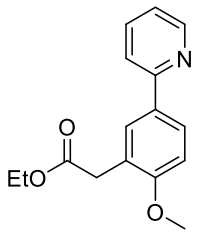

1.11
(**a**) - 47% 1:0
(**b**) - 19% 1:0

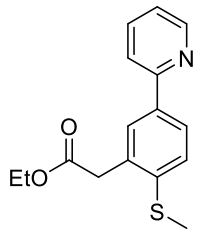

1.12
(**a**) - 29% 8:1
(**b**) - 41% 10:1

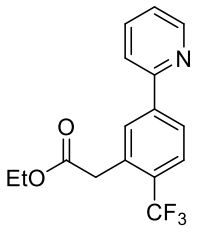

1.13
(**a**) - 20% 4:1
(**b**) - 56% 4:1

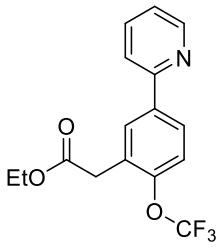

1.14
(**a**) -
(**b**) - 37% 1:1

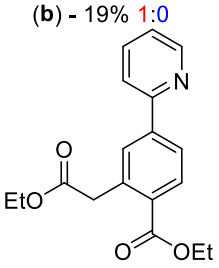

1.15
(**a**) - 37% 9:1
(**b**) - 36% 10:1

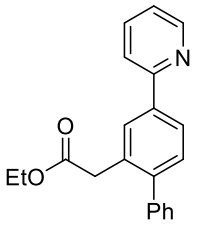

1.16
(**a**) -
(**b**) - 16% 17:1

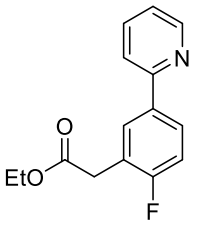

1.17
(**a**) - 42% 7:1
(**b**) - 39% 6:1

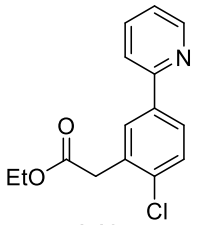

1.18
(**a**) - 48% 6:1
(**b**) - 52% 5:1

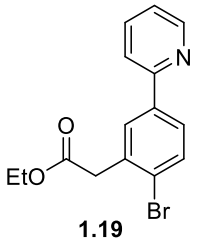

1.19
(**a**) - 23% 2:1
(**b**) -

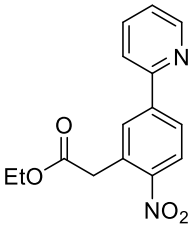

1.20
(**a**) - <5%
(**b**) - <5%

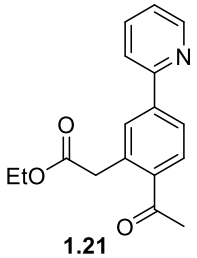

1.21
(**a**) - <5%
(**b**) - <5%

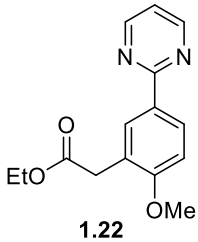

1.22
(**a**) -
(**b**) -30% 1:0

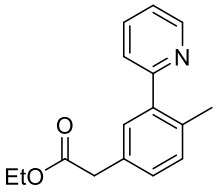

1.23
(**a**) - 0%
(**b**) - 0%

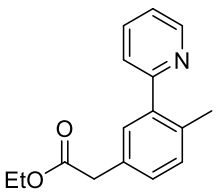

1.24
(**a**) - 0%
(**b**) - 0%

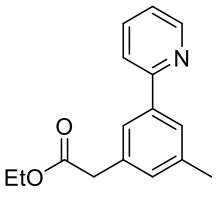

1.25
(**a**) - 0%
(**b**) - 0%

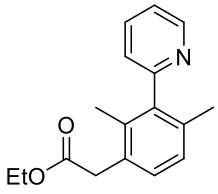

1.26
(**a**) - 0%
(**b**) - 0%

Scheme 74: Scope of substituted arene ring

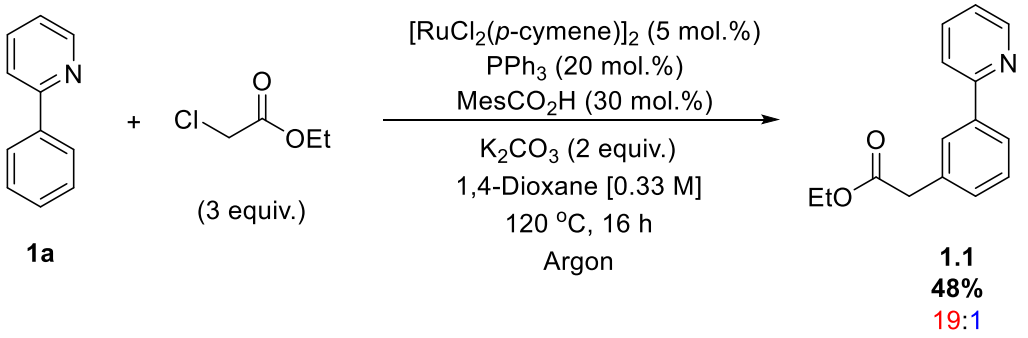

Scheme 75: Reaction conditions used for the *meta* alkylation of 2-phenylpyridine using an α-chloro ester coupling partner.

The use of activated α-halo ester coupling partners led us to question whether analogous coupling partners, lacking an adjacent group to enable captodative stabilisation, could be utilised under these reaction conditions. However, upon the testing of such coupling partners we found that no regioselective preference for the *meta* position was observed, with a 46% yield of the *ortho* alkylated product instead isolated as shown in Scheme **76**. This could be explained by the relative instability of primary alkyl radicals, resulting in a two-electron process being the most likely pathway; whereas the ester substrate radical, formed by homolytic cleavage of the C–Br bond, is much more stable, due to the donation of the C=O π bond donation into the vacant p-orbital of the adjacent radical.[41]

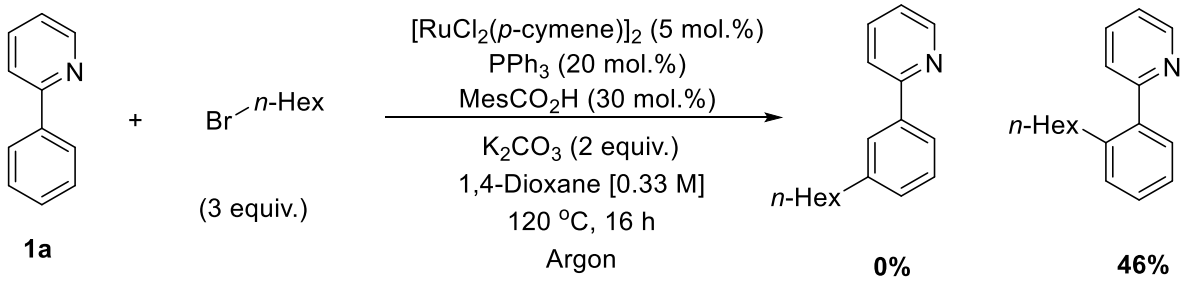

Scheme 76: Results of using an unactivated primary alkyl halide coupling partner.

2.5 – Mechanistic Considerations

Our initial thoughts upon the discovery that only a catalytic amount of PPh_3 was needed to achieve the desired yields and regioselectivities; was that the PPh_3 was either acting as a ligand or activating the coupling partner to be more amenable to the reaction conditions.

To this end we sought to determine whether the formation of a phosphonium salt was the responsible coupling partner, under the reaction conditions shown in Scheme **77**.

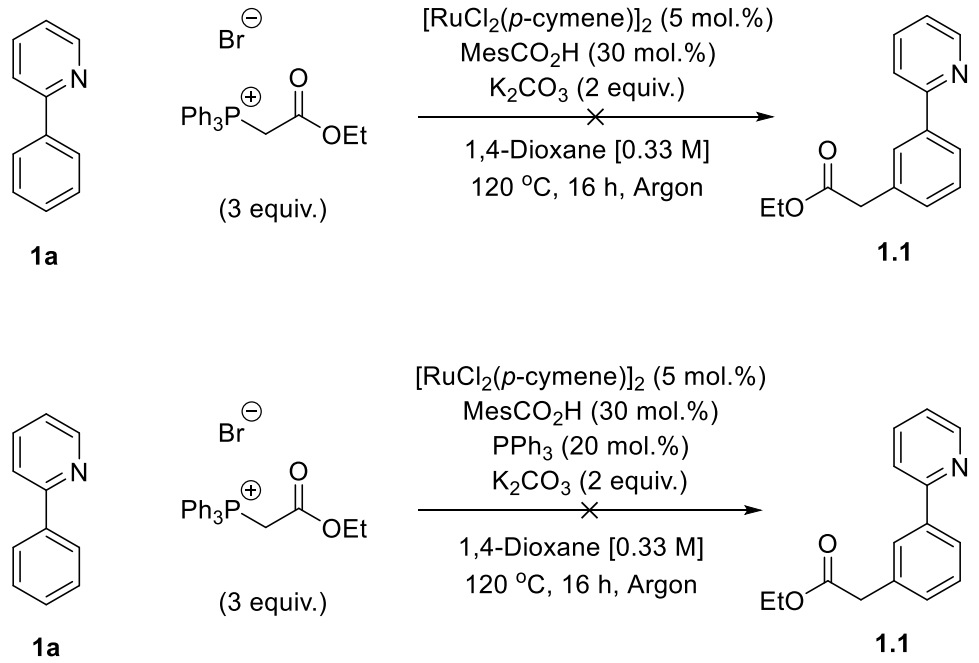

Scheme 77: Reactions to probe the role of PPh_3 in the reaction.

Under the sets of reaction conditions shown in Scheme **77**, no conversion of starting material to any products was observed. This result indicated to us that the PPh_3 was acting as a ligand for the Ru, forming an intermediate responsible for the observed *meta* selectivity *in situ*.

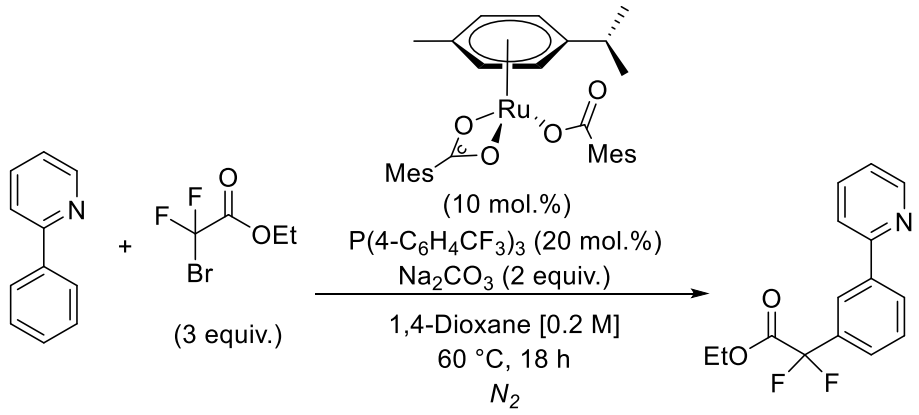

Scheme 78: Reaction conditions reported by Wang *et al*. for the *meta* di- and mono-fluoroalkylation of 2-phenylpyridine.[14]

This hypothesis is also backed up by Ackermann *et al.* in the difluroromethylation of 2-phenylpyridine which was published whilst this work was being undertaken. This work found that a phosphine source was required to achieve the desired *meta* selectivity shown in Scheme **78**.[15] Similar work by Wang *et al*. suggested that the addition of a Pd(0) co-catalyst was responsible for the formation of such a radical species, resulting in the formation of an unusual Pd(I) species, in a Pd(0)/Pd(I) catalytic cycle; albeit with no experimental evidence to prove its existence under the reaction conditions.[14]

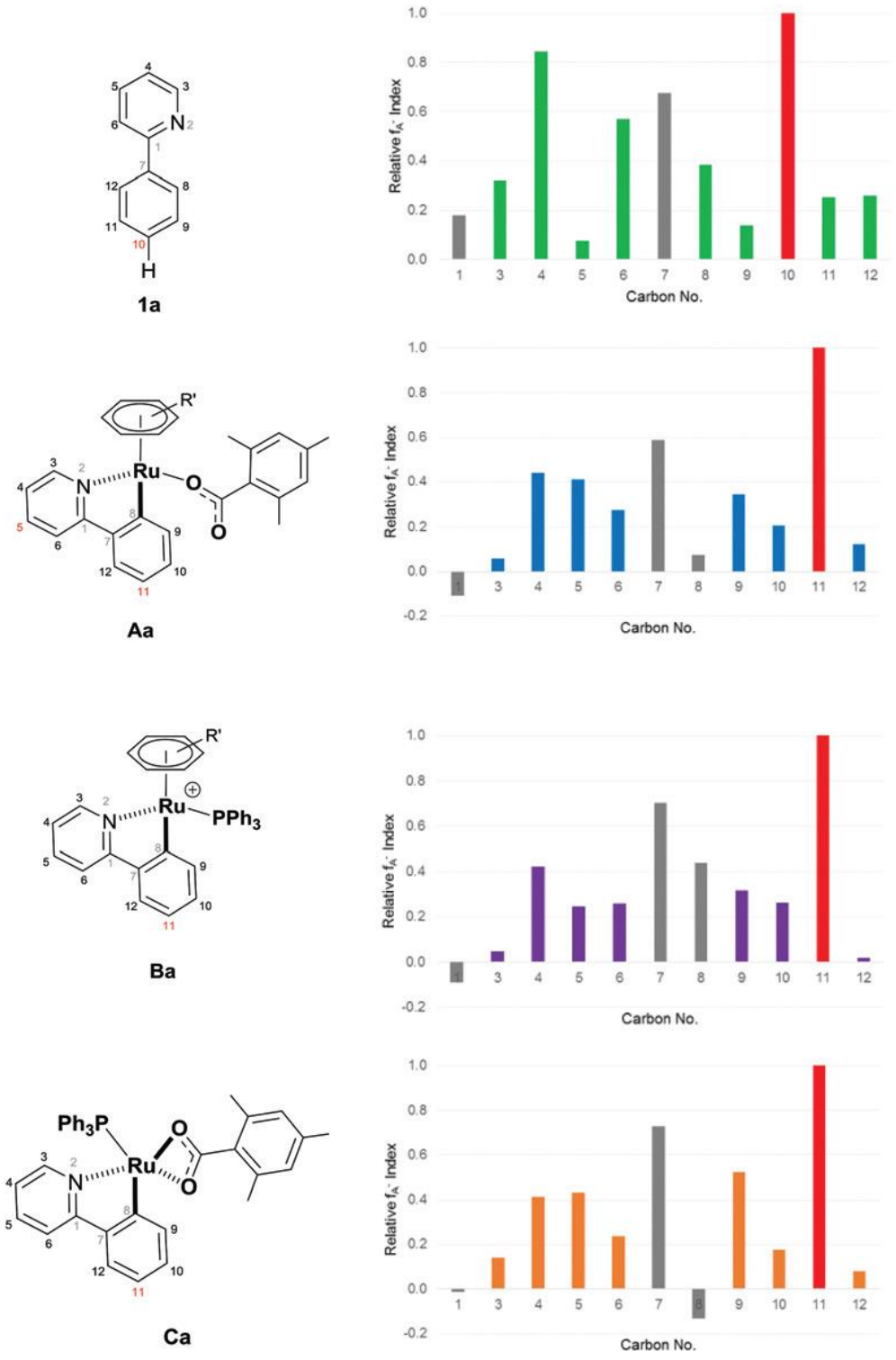

Figure 6: Relative nucleophilicity Fukui indices (fA-) calculated for the shown substrates. Calculations were performed at the BP86/6-13G** &SDD(Ru) level of theory. Fukui indices were calculated with NBO total atomic charges from the optimised neutral structure.[26]

Work by Paterson *et al*. gave an indication that the role of the phosphine in the reaction, was one as a ligand for the Ru, in the intermediate labelled **Ba** in Figure **6**. This intermediate was proposed by computational analysis of the various cyclometallated Ru complexes that could be formed *in situ* under the reaction conditions (Figure **6**). From Figure **6** it can be seen that looking at 2-phenylpyridine (**1a**), the most nucleophilic position is C10 as identified on the compound, due to the increased electron density from the inductive effects of the pyridine ring. However, upon cyclometallation this nucleophilicity switches to the *meta* C11 position, as shown in intermediates **Ba** and **Ca** in Figure **6**, which matches the observed experimental regioselective outcome of the reaction.

Comparison of the phosphine containing cyclometallated substrates (**Ba** and **Ca**) shows a similarity in electronic properties to that of **Aa**. Further computational work, carried out independently by Greaney *et al*.[22] and Ackermann *et al*.[23] suggested that analysis of the Ru(III) analogues of the possible cyclometallated intermediates was a the more likely cause for the observed regioselectivity trends between the *ortho* and *meta* regioisomers. However, our computational analysis was only used for the potential Ru(II) intermediates. However, recent work by Greaney and Ackermann independently, shows stronger enhancement for the observed regioselectivity when compared to their computational analysis of similar Ru(III) intermediates, used in their photocatalytic methodology.[22,23,26]

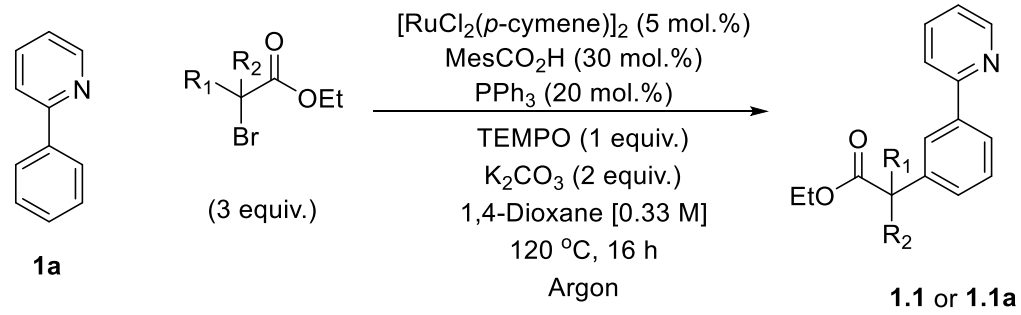

Table 7: Reactions with TEMPO.

Coupling Partner	NMR Conversion (%)
2a	41
2a[a]	0
2b	0
2b[ab]	0

1.1 ($R_1 = R_2 = H$), **1.1a** ($R_1 = R_2 = Me$). [a] 3 equivalents of TEMPO added. [b] No PPh_3 added.

Use of the radical scavenger (2,2,6,6-tetramethylpiperidin-1-yl)oxyl (TEMPO) can be used to help identify whether a reaction involves formation of a radical. Our analysis used both a primary and tertiary coupling partner under the conditions shown in Table **7**.

The addition of TEMPO to the tertiary coupling partner (**2b**) results in the complete shutdown of reaction, in line with previous results observed using this coupling partner and suggesting the formation of a radical species *in situ*.[1,2,12] However when using the primary coupling partner (**2a**) the addition of 1 equivalent of TEMPO appears not to shut the reactivity down completely. This complete shutdown of reactivity only occurs when 3 equivalents of TEMPO were added. This suggests that the mechanistic cycle for the formation of the *meta* product does not involve the formation of a radical, and this shut down of the reactivity may be due to the oxidation of the Ru catalyst to an unreactive Ru(III) that has not cyclometallated with the 2-phenylpyridine or alternatively the TEMPO reacts with the coupling partner in a radical S_N2 type reaction, removing it from the reaction completely.

To test this hypothesis, we performed DPV measurements on a variety of Ru complexes as shown in Figure **7**. We performed these measurements to determine whether the TEMPO was a strong enough oxidant to oxidise the Ru(II) to Ru(III).

As seen in Figure **7** there is an oxidation peak at 680 mV that corresponds to an oxidation event from a Ru(II) species to an Ru(III) species. In the cases of $[RuCl_2(p\text{-cymene})]_2$ and the Ru-CMD complex this oxidation occurs at a much lower potential than the other listed complexes *c.a.* ~650 mV, with the other tested complexes oxidising at a higher potential around 900 mV. The oxidation of TEMPO is reported at 490 mV (vs SCE) by Stahl *et al*.[42] This corresponds to an inability to oxidise the measured Ru species *in situ*. However, given the large excess of TEMPO in comparison to the Ru in the reaction, the deactivation is most likely due to quenching of the organic radical formed *in situ* and the reaction still proceeds in the case of Entry **1**, Table **7**, similarly to work by Greaney and Ackermann.[22,23]

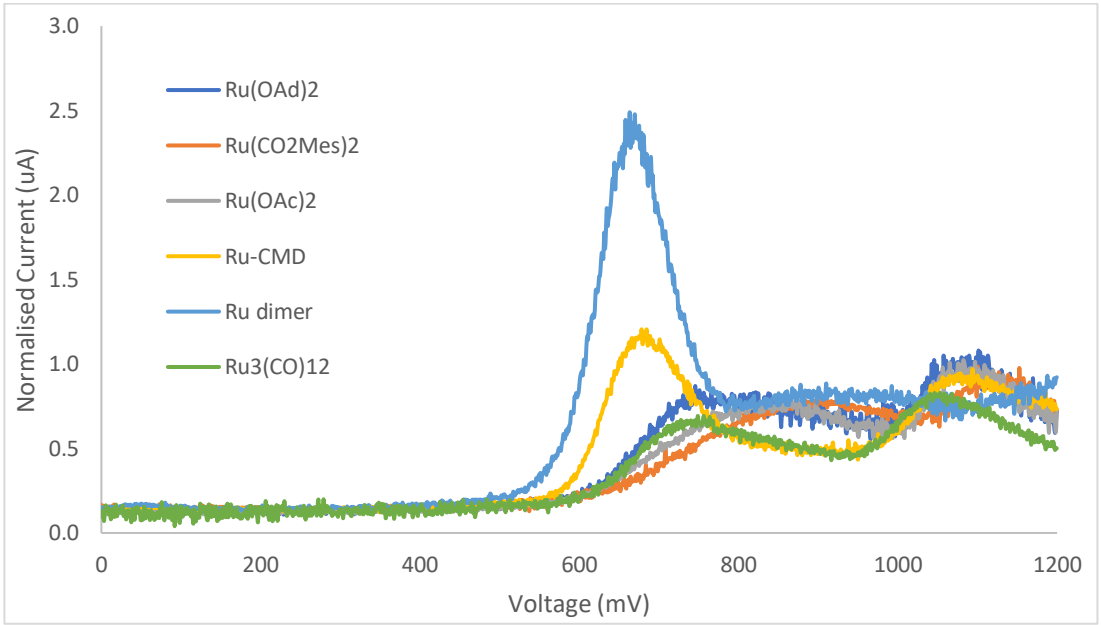

Figure 7: Differential Pulse voltammetry (DPV) at 10 mVs^{-1} in MeCN with NH_4BF_4 ([0.1 M] in MeCN) with a substrate concentration of [0.1 mM]. Voltages reported are in reference to SCE. Structures of compound tested in each graph are denoted in the scheme below.

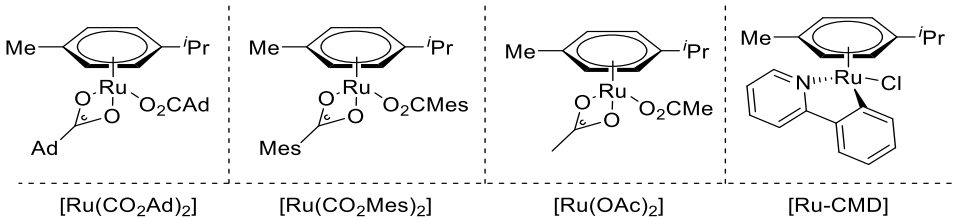

[Ru dimer] = $[RuCl_2(p\text{-cymene})]_2$
[Ru3(CO)12] = $[Ru_3(CO)_{12}]$

To this end we propose the following mechanistic cycle, based the evidence we collected, and the work of other groups on similar reactions which is shown in Scheme **79**.

The proposed catalytic cycle begins by the dissociation of the dimeric Ru species into two monomeric biscarboxylate Ru complexes, the active resting state of the catalyst *in situ*. This complex then reacts with the 2-phenylpyridine in a CMD process to insert in to the *ortho* C–H bond and form the first intermediate. A molecule of PPh_3 then ligates to the Ru and forms the complex believed to be responsible for the *meta* selectivity.[26]

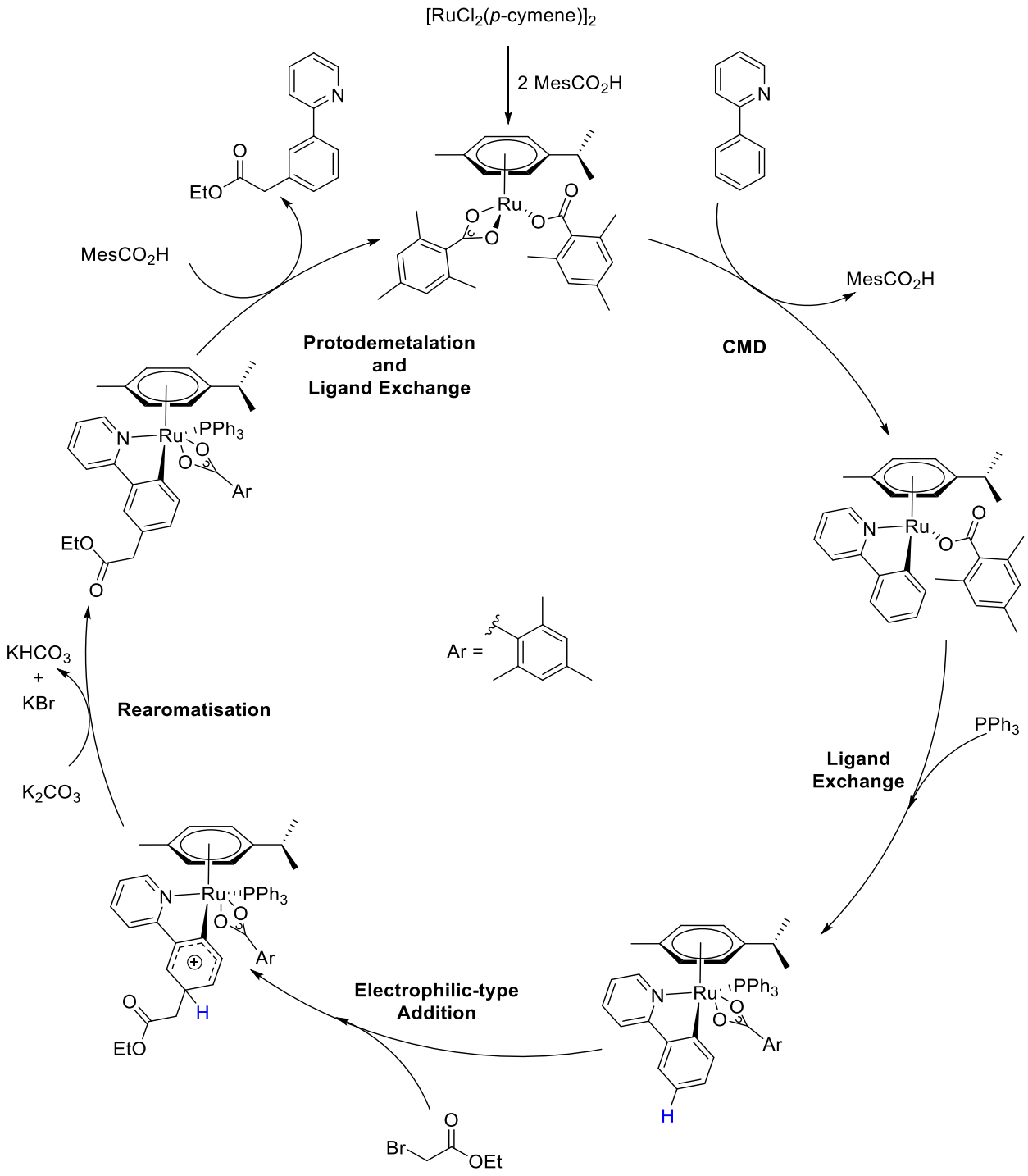

Scheme 79: Proposed catalytic cycle for the primary *meta* alkylation of 2-phenylpyridine.

This intermediate then activates the position *para* to the C–Ru bond to electrophilic attack and reacts with the alkyl halide coupling partner to form a Wheland-type intermediate, which is then quickly deprotonated to allow rearomatisation of the aromatic ring. The

final step is then protodemetallation of the *meta* substituted intermediate, followed by dissociation of the PPh_3 to form the active catalyst and re-enter the cycle.

To confirm that the reaction was reactive, under a homogeneous regime, we also carried out a mercury drop test, under the conditions shown in Scheme **80**.[43] This involves the addition of a small amount of mercury, which then acts to engulf any heterogeneous particles *in situ* and render them unreactive, thus showing whether a reaction is completely homogeneous, or whether a bi-phasic heterogeneous regime is in operation.

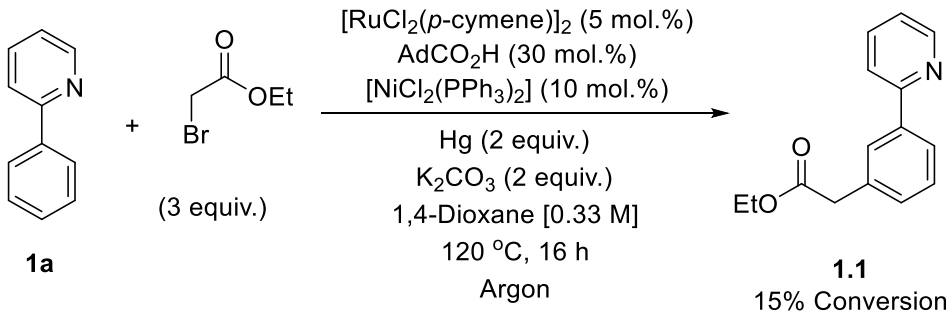

Scheme 80: Reaction conditions used for the mercury drop test.

The mercury drop test showed a large drop in conversion to *meta* product, with little effect upon the regioselectivity. This indicates that a Ru aggregate *in situ* may be responsible for the observed reactivity.

This result lines up with the use of a heterogeneous Ru_SiO_2 catalyst used by Ackermann *et al*. for the *meta* bromination of purine bases.[44] We then employed the same Ru_SiO_2 catalyst employed by Ackermann *et al*. and to our delight found that we achieved a 15% conversion to the *meta* product, with a 15:1 regioselectivity (*meta*:*ortho*). However, we did not pursue this result further as we decided not to properly analyse the made catalyst, and we therefore cannot attribute the conversion to the heterogeneous catalyst or leaching of the Ru into the solution.

2.6 – Conclusions and Future Work

In summary, we have investigated the use of primary α-halo carbonyls as versatile coupling partners for the direct *meta* primary alkylation of arene rings. This procedure is operationally simple to perform and has been shown to be possible with several substrates,

with the capacity for further synthetic elaborations to be realised. Either a Ni catalyst, bearing a phosphine ligand or sole phosphine ligand source was found to be crucial for the regioselective installation of the primary alkyl group at the *meta* position on the arene ring. The use of straight chain alkyl halides resulted in solely the *ortho* product, in contrast to the use of the privileged α-halo carbonyl coupling partners.

An investigation into the use of α-chloro carbonyl coupling partners may yield more regioselectivity for the *meta* position, as indicated by results by Itoh *et al*. by increasing the energy required to form the Ru(IV) oxidative addition intermediate, formed on the catalytic cycle for the formation of the *ortho* regioisomer.[27]

Experimental and computational mechanistic analysis highlight a dual activation pathway, whereby cyclometallation with the ruthenium catalyst activates the substrate at the position *para* to the Ru-C bond and is responsible for the *meta* selectivity observed. Through use of computational analysis, electrochemical measurements and control experiments we were able to propose a catalytic cycle for this transformation. However, further experimental work is required to fully prove our conclusions.

The expansion of the set of coupling partners and substrates that can be utilised using our developed σ-activation methodology would be of key utility and interest to groups interested in this regioselective transformation, under relatively mild conditions. The use of heterogeneous catalysis, as indicated by mercury drop experiments, may allow for lower catalytic loadings and milder conditions for this and similar transformations.

Bibliography

1 J. Li, S. Warratz, D. Zell, S. De Sarkar, E. E. Ishikawa and L. Ackermann, *J. Am. Chem. Soc.*, 2015, **137**, 13894–13901.

2 A. J. Paterson, S. St John-Campbell, M. F. Mahon, N. J. Press and C. G. Frost, *Chem. Commun.*, 2015, **51**, 12807–12810.

3 N. Hofmann and L. Ackermann, *J. Am. Chem. Soc.*, 2013, **135**, 5877–5884.

4 N. Muller and R. S. Mulliken, *J. Am. Chem. Soc.*, 1958, **80**, 3489–3497.

5 J. Li, K. Korvorapun, S. De Sarkar, T. Rogge, D. J. Burns, S. Warratz and L. Ackermann, *Nat. Commun.*, 2017, **8**, 15430.

6 Z. Fan, J. Ni and A. Zhang, *J. Am. Chem. Soc.*, 2016, **3**, 8470–8475.

7 O. Saidi, J. Marafie, A. E. W. Ledger, P. M. Liu, M. F. Mahon, G. Kociok-Kohn, M. K. Whittlesey and C. G. Frost, *J. Am. Chem. Soc.*, 2011, **133**, 19298–19301.

8 Q. Yu, L. Hu, Y. Wang, S. Zheng and J. Huang, *Angew. Chem Int. Ed.*, 2015, **54**, 15284–15288.

9 C. J. Teskey, A. Y. W. Lui and M. F. Greaney, *Angew. Chem - Int. Ed.*, 2015, **54**, 11677–11680.

10 B. Li, S. L. Fang, D. Y. Huang and B. F. Shi, *Org. Lett.*, 2017, **19**, 3950–3953.

11 G. Li, D. Li, J. Zhang, D. Q. Shi and Y. Zhao, *ACS Catal.*, 2017, **7**, 4138–4143.

12 H. L. Barlow, C. J. Teskey and M. F. Greaney, *Org. Lett.*, 2017, **19**, 6662–6665.

13 X. Wang, Y. Li, H. Liu, B. Zhang, X. Gou, Q. Wang, J. Ma, Y. Liang, X. Wang, Y. Li, H. Liu, B. Zhang, X. Gou and Q. Wang, *J. Am. Chem. Soc.*, 2019, **141**, 13914–13922.

14 G.-W. Wang, Z.-Y. Li, L. Li, Q.-L. Li, K. Jing and H. Xu, *Chem. - A Eur. J.*, 2017, 3285–3290.

15 Z. Ruan, S.-K. Zhang, C. Zhu, P. N. Ruth, D. Stalke and L. Ackermann, *Angew. Chem Int. Ed.*, 2017, **3**, 2045–2049.

16 G. M. Reddy, N. S. Rao and H. Maheswaran, *Org. Chem. Front.*, 2018, **5**, 118–1123.

17 Z. Fan, H. Lu, Z. Cheng and A. Zhang, *Chem. Commun.*, 2018, **54**, 6008–6011.

18 K. Jing, Z.-Y. Li and G.-W. Wang, *ACS Catal.*, 2018, **8**, 11875–11881.

19 L. Ackermann, N. Hofmann and R. Vicente, *Org. Lett.*, 2011, **13**, 1875–1877.

20 L. Ackermann, R. Vicente and A. Althammer, *Org. Lett.*, 2008, **10**, 2299–302.

21 D. Lapointe and K. Fagnou, *Chem. Lett.*, 2010, **39**, 1118–1126.

22 A. Sagadevan and M. F. Greaney, *Angew. Chem Int. Ed.*, 2019, **58**, 9826–9830.

23 P. Gandeepan, J. Koeller, K. Korvorapun, J. Mohr and L. Ackermann, *Angew. Chem - Int. Ed.*, 2019, 9820–9825.

24 J. Li, S. Warratz, D. Zell, S. De Sarkar, E. E. Ishikawa and L. Ackermann, *J. Am. Chem. Soc.*, 2015, **137**, 13894–13901.

25 W. Tsang, *J. Am. Chem. Soc.*, 1985, **107**, 2872–2880.

26 A. J. Paterson, C. J. Heron, C. L. McMullin, M. F. Mahon, N. J. Press and C. G. Frost, *Org. Biomol. Chem.*, 2017, **15**, 5993–6000.

27 H. Nagashima, K. Mukai, Y. Shiota, K. Yamaguchi, K.-I. Ara, T. Fukahori, H. Suzuki, M. Akita, Y. Moro-oka and K. Itoh, *Organometallics*, 1990, **9**, 799–807.

28 C. Liu, X. Lv, Y. Xing and J. Qui, *J. Mater. Chem. C*, 2015, **3**, 8010–8017.

29 S. Goggins, E. Rosevere, C. Bellini, J. C. Allen, B. J. Marsh, M. F. Mahon and C. G. Frost, *Org. Biomol. Chem.*, 2014, **12**, 47–52.

30 Y. Aihara and N. Chatani, *J. Am. Chem. Soc.*, 2013, **135**, 5308–5311.

31 A. T. Higgs, P. J. Zinn and M. S. Sanford, *Organometallics*, 2010, **29**, 5446–5449.

32 J. Terao and N. Kambe, *Acc. Chem. Res.*, 2008, **41**, 1545–1554.

33 E. A. Standley, S. J. Smith, P. Müller and T. F. Jamison, *Organometallics*, 2014, **33**, 2012–2018.

34 I. Ozdemir, S. Demir, B. Cetinkaya, C. Gourlaouen, F. Maseras, C. Bruneau and P. H. Dixneuf, *J. Am. Chem. Soc.*, 2008, **130**, 1156–7.

35 P. B. Arockiam, C. Bruneau and P. H. Dixneuf, *Chem. Rev.*, 2012, **112**, 5879–5918.

36 J. Q. Wang, D.H., Engle, K.M., Shi, B.F., Yu, *Science*, 2010, **327**, 315–319.

37 J. A. Leitch, P. B. Wilson, C. L. McMullin, M. F. Mahon, Y. Bhonoah, I. H. Williams and C. G. Frost, *ACS Catal.*, 2016, **6**, 5520–5529.

38 T. Leyssens, D. Peeters, A. G. Orpen and J. N. Harvey, *New J. Chem.*, 2005, **29**, 1424–1430.

39 G. A. Olah and J. A. Olah, *J. Am. Chem. Soc.*, 1976, **98**, 1839–1842.

40 G. A. Olah and S. Kobayashi, *J. Am. Chem. Soc.*, 1971, **93**, 6964–6967.

41 H. Yi, G. Zhang, H. Wang, Z. Huang, J. Wang, A. K. Singh and A. Lei, *Chem. Rev.*, 2017, **117**, 9016–9085.

42 J. E. Nutting, M. Rafiee and S. S. Stahl, *Chem. Rev.*, 2018, **118**, 4834–4885.

43 C. B. Reddy, R. Bharti, S. Kumar and P. Das, *RSC Adv.*, 2016, **6**, 71117–71121.

44 S. Warratz, D. J. Burns, C. Zhu, K. Korvorapun, T. Rogge, J. Scholz, C. Jooss, D.

Gelman and L. Ackermann, *Angew. Chem - Int. Ed.*, 2017, **56**, 1557–1560.

Chapter 3 – Ruthenium Catalysed Remote C4-selective C-H Functionalisation of Carbazoles

This work was started by our desire to expand the application of σ-activation methodologies to a broader range of substrates as seen previously with 2-phenylpyridine and derived substrates, to allow more commonly encountered structural motifs found in medicinal and materials chemistry to be utilised, such as *N*-pyrimidylaniline, as investigated by Ackermann *et al*.[1] Previous work from our group reported the C3/C6 alkylation of indoles (Figure **8**).[2] This work was found to proceed initially by alkylation at the C3 position, the Ru then undergoes CMD at the C2 position of the indole, as directed by the pyrimidine and ester functional group to form the intermediate shown in Figure **9** as suggested by computational analysis of the reaction.

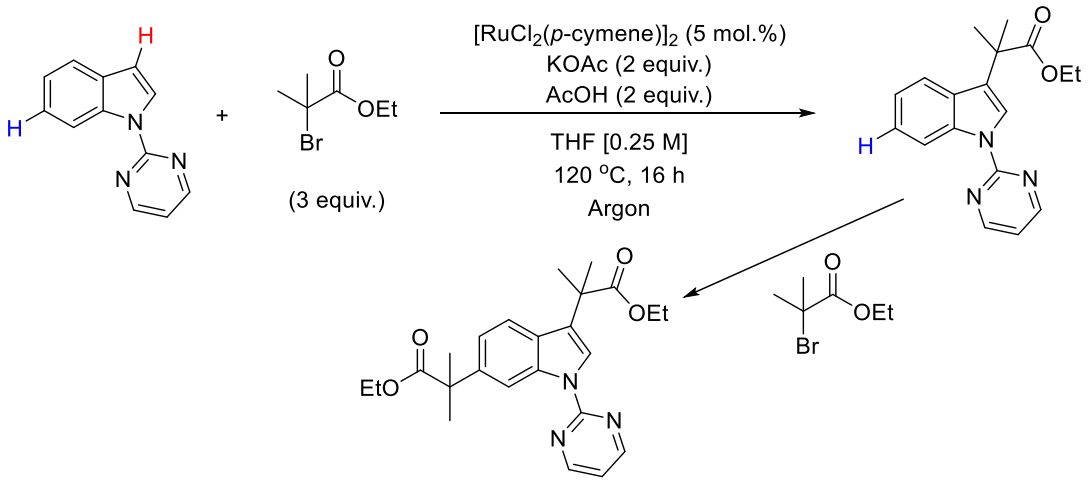

Figure 8: Reaction conditions for the one-pot C3/C6 functionalisation of indole substrates.[2]

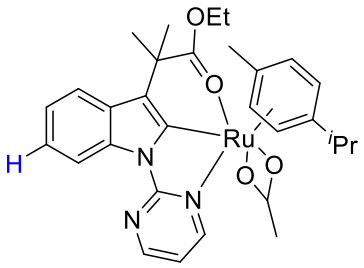

Figure 9: Computationally proposed intermediate responsible for the C6 alkylation.[2]

Following on from this work, we became interested to see how the reactivity of different heterocyclic systems, *i.e.* biologically relevant indole containing motifs, such as tryptamines and carbazoles. Carbazoles are a fused tricyclic heteroaromatic with important applications in drug discovery,[3–5] sensing,[6,7] and organic functional materials such as OLEDs (Figure **10**).[8,9] The vast majority of these techniques have been achieved by attaching a "directing group" *via* the N–H portion of the substrate.[10]

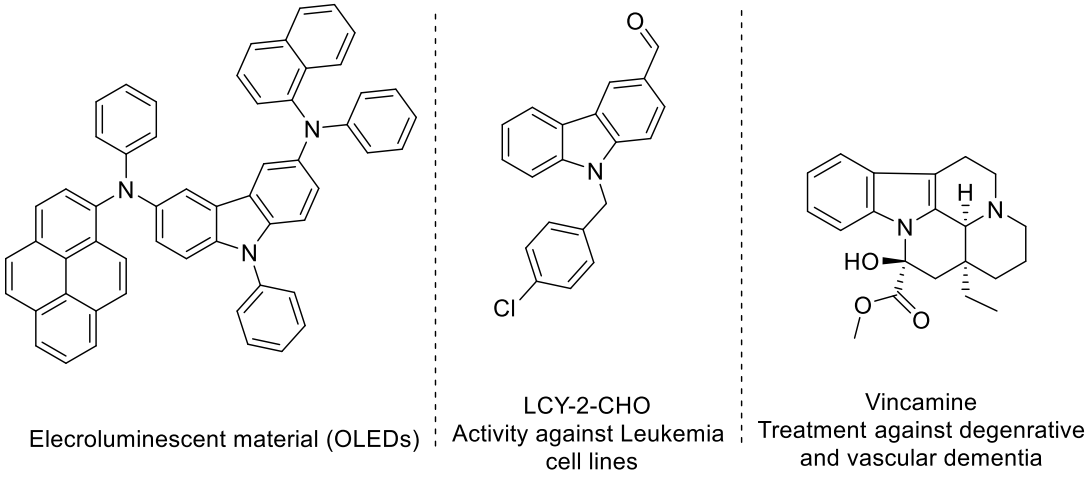

Figure 10: Molecules of commercial and academic interest containing the carbazole or tryptamine motifs.

The use of tryptamine substrates in C–H activation methodologies, utilising the intrinsic amine group as a directing group is already known. Examples of this methodology are limited to C2 functionalisation, including: the Ru catalysed C2 silylation of unprotected tryptamines,[11] the Pd catalysed norborene mediated C2 alkylation of unprotected tryptamines,[12] and the Hg catalysed C2 vinylation of unprotected tryptamines.[13] However, to date there are no examples of using a CMD intermediate, akin to that shown in Figure **9** to access C4-C7 functionalised tryptamine derivatives.

The C1, C2, and S_EAr functionalisation of carbazoles is already well known in literature, through a variety of synthetic techniques. C1 functionalisation can be achieved by utilising a directing group to direct functionalisation; this has allowed the formation of a number of C–C and C–X bonds to be created using a variety of catalytic systems.[10,14–16] C2 functionalisation has been explored in an elegant report by Baran and co-workers using a sterics-defined C2-selective C–H iridation and subsequent C–H functionalisation. This example formed part of a wider study on the functionalisation on related indole heteroaromatics.[17] C3 functionalisation has also been widely studied, due to the nucleophilic character of this carbon, enabling S_EAr chemistries to be employed.[18]

The ability to direct the cyclometallation of a Ru species towards the C1 position of a carbazole system allows us to potentially utilise a σ-activation methodology to selectively functionalise the C4 position of a carbazole system. This methodology would block functionalisation of the C2 position on steric grounds. The functionalisation of C3 would be discouraged, on electronic grounds of a C1–Ru bond, which would dominate the electronic structure of such an intermediate.

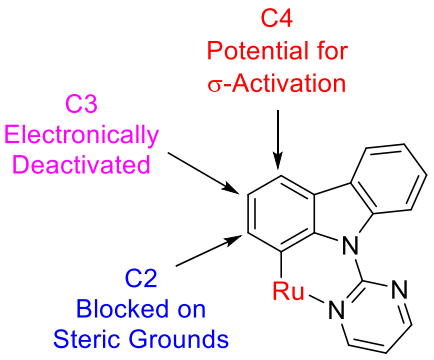

Figure 11: Thought process for carbazole substrates.

Carbazoles in particular are important classes of biological molecules. In particular, carbazoles with bulky groups attached at the C2 and/or C3 position were shown to exhibit inhibitory action on a protein involved in the function of neurons *in vivo*.[19] The ability to functionalise this C3 and C4 position has also been shown to increase the anti-tumor activity of carbazole derivatives against pancreatic cancer cell lines. Selective

functionalisation the C4 position allows for a much greater exploration of the effect of functionalisation at this position alone, on various cell lines.[20]

Initially this work was done currently with investigations into *N*-pyrimidylindoline, the structure of which is shown in Figure **12**. This substrate bore no reactivity under the conditions tried, however, it led us to believe that a directing group must be attached to the indole structure through the *N* position to drive the Ru to cyclometallate at the C7 position. This led us to begin investigating carbazole structures, which contain two aromatic rings, held together in a "bowl" type shape. This makes the pyrimidine group more proximal to the desired C1 position on the carbazole, meaning a CMD process could occur more easily, allowing us to investigate the σ-activation chemistry of such a substrate.

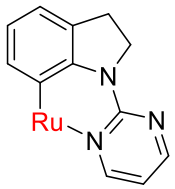

Figure 12: Structure of the indoline functional group, bearing an *N*-bound pyrimidine directing group, directing a potential Ru catalyst to cyclometallate at the C7 position.

The work discussed herein constitutes, to our knowledge, the first known example that allows the direct access to C–H functionalisation at the C4 position of carbazole derivatives.[21] This work is part of a joint study with Dr J. A. Leitch, however this chapter will be focused upon my own contributions to this work.[21]

3.1 – Synthesis of Starting Materials

The beginning of this project sought to identify a suitable directing group that could be easily coupled with the tryptamine, *via* the non-aromatic N–H bond, which could then be used to successfully functionalise the C4–C7 position of the system, *via* the methodology shown in Figure **13**.

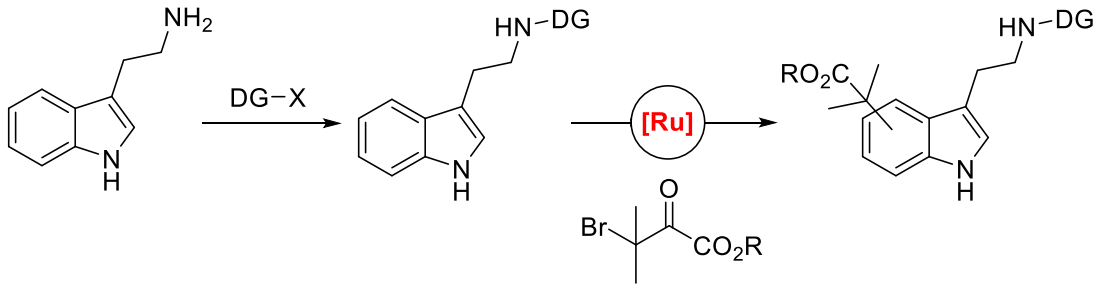

Figure 13: General idea for the application of σ-activation methodologies on tryptamine substrates.

We initially began by looking at the use of pyrimidine directing groups to direct a Ru catalyst to undergo CMD with the indole heterocycle. The synthesis of these substrates proceeded smoothly, utilising methodology by Moody *et al.*, yielding the **2a** and **2b** in good yields as shown in Scheme **81**.[22]

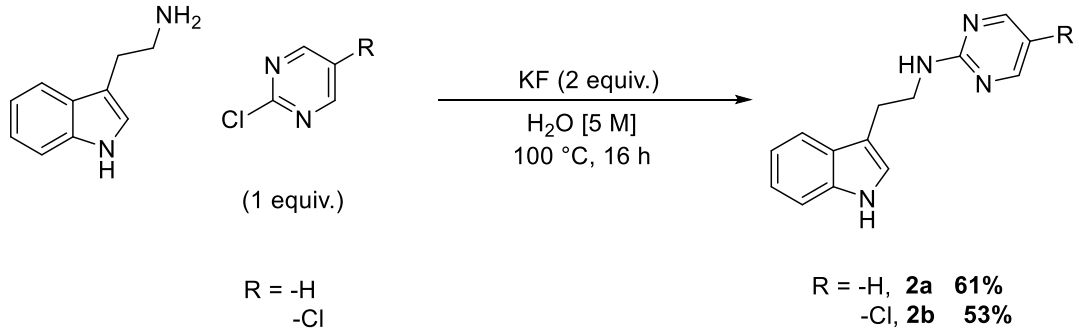

Scheme 81: Reaction conditions for the synthesis of **2a** and **2b**.

However, when subjected to a variety of reported conditions, reported for the C–H functionalisation of indoles and 2-phenylpyridine substrates, shown in Scheme **86**; no reactivity was observed using **2a**; and **2b** resulted in the alkylation of the pyrimidine ring, at the "–R" position as seen in Scheme **81**. We then decided to try other directing groups, such as pyridine, **2c**. The synthesis proceeded smoothly in excellent yield, as shown in Scheme **82** to isolate the HCl salt of **2c**.[23]

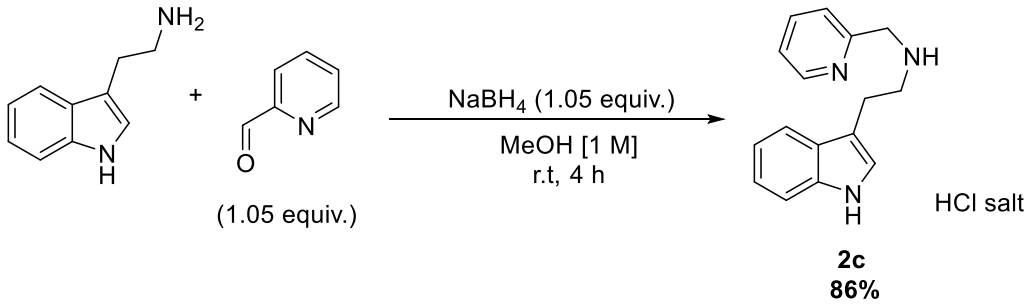

Scheme 82: Reaction conditions for the synthesis of **2c**.

The use of the aforementioned alkylation conditions (Scheme **86**) resulted in no observed reactivity when using **2c** as a substrate. We questioned whether the use of a non-aromatic directing group would aid the reactivity. We decided to use a nitrile group to test this, **2d**. The synthesis of **2d** is shown in Scheme **83** under conditions reported by Prasad *et al.*[24]

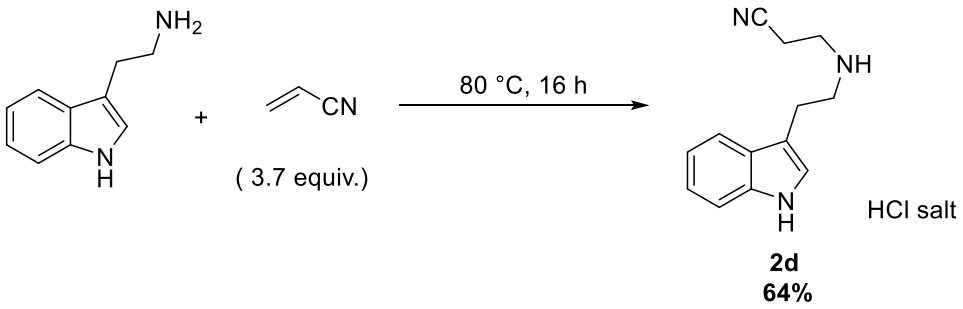

Scheme 83: Reaction conditions for the synthesis of **2d**.

The use of a nitrile group also resulted in no observable reactivity under the conditions shown in Scheme **86**, and with this we decided to focus our attentions towards carbazole substrates. We began by employing a pyrimidine group in the N–H position (Scheme **84**), which had superior activity to the corresponding pyridine in the previous work on indoles done within our group.[2] The procedure we used to access this motif for the desired carbazole example (**2e**) was adapted from a route by Kambe *et al*. shown in Scheme **84**.

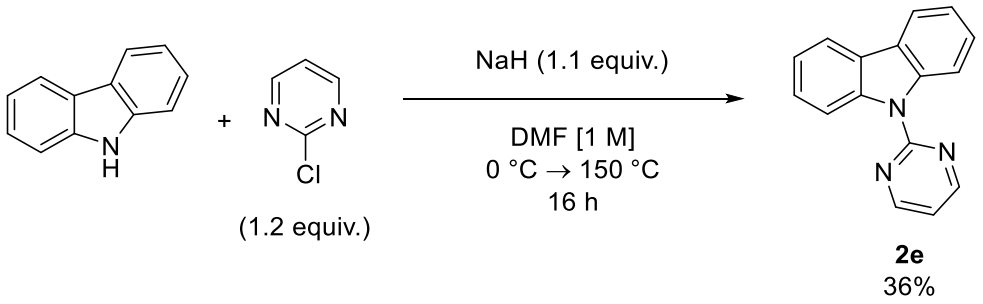

Scheme 84: Synthesis of 9-(pyrimidin-2-yl)-9*H*-carbazole, **2e**.[16]

This synthetic pathway proceeds *via* deprotonation of the N–H bond of the carbazole, which then reacts through an S_NAr type reaction to displace the chloride leaving group, yielding **2e** as shown in Scheme **84**. We then turned our attention to a pyridine analogue of **2e**, however, there are no known literature examples of synthesising this *via* analogous S_NAr type reactions and attempts to adapt the above method were largely unsuccessful. To synthesise 9-(pyridine-2-yl)-9*H*-carbazole, **2f**, we used a protocol reported by Xu *et al*.[25] by which a Pd catalyst is used to perform a tandem *ortho* arylation and then annulation reaction to form the desired product **2f**, under the conditions shown in Scheme **85**.

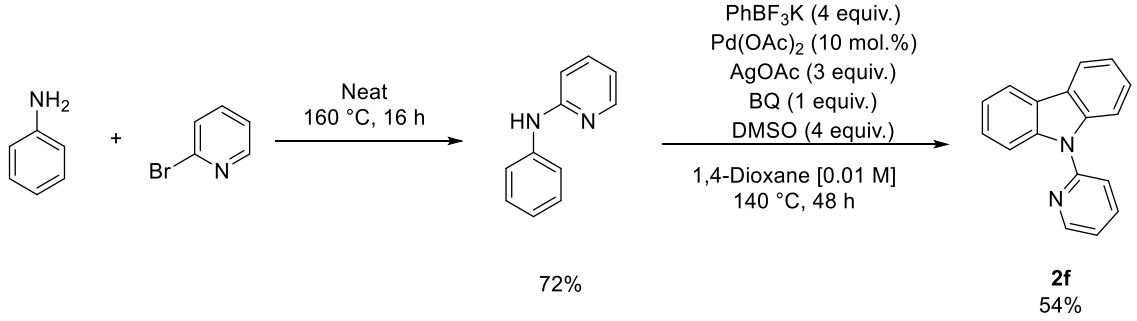

Scheme 85: Synthesis of 9-(pyridin-2-yl)-9*H*-carbazole, **2f**.[25]

As seen in Scheme **85**, the initial step of this synthesis involves an S_NAr reaction between aniline and 2-bromopyridine under reflux overnight to yield pyridylaniline in good yield.[25] This is then subjected to the conditions reported by Xu *et al*. to yield product **2f**.[25] It must be noted however, that a small amount of uncyclized by-product was formed during the reaction (~5%), that was not possible to separate *via* chromatographic methods,

however, we still decided to use it to test its feasibility as a substrate for our reaction conditions.

Our investigation of reaction conditions tested for each substrate used optimised conditions, reported for a variety of methodologies that we had developed in our group for *meta* alkylation and dual C3/C6 alkylation of indoles.[2,21,26,27] These conditions are shown in Scheme **86**.

As stated before, the use of these reaction conditions resulted in no observable products when utilising substrates **2a**–**2d** and **2f**. Compound **2b** is an exception to this observation however, with a small observation of tryptamine containing by-product observable by NMR (<5%) and polymeric species. Attempts to isolate this by-product were unsuccessful however, and we did not pursue this result further.

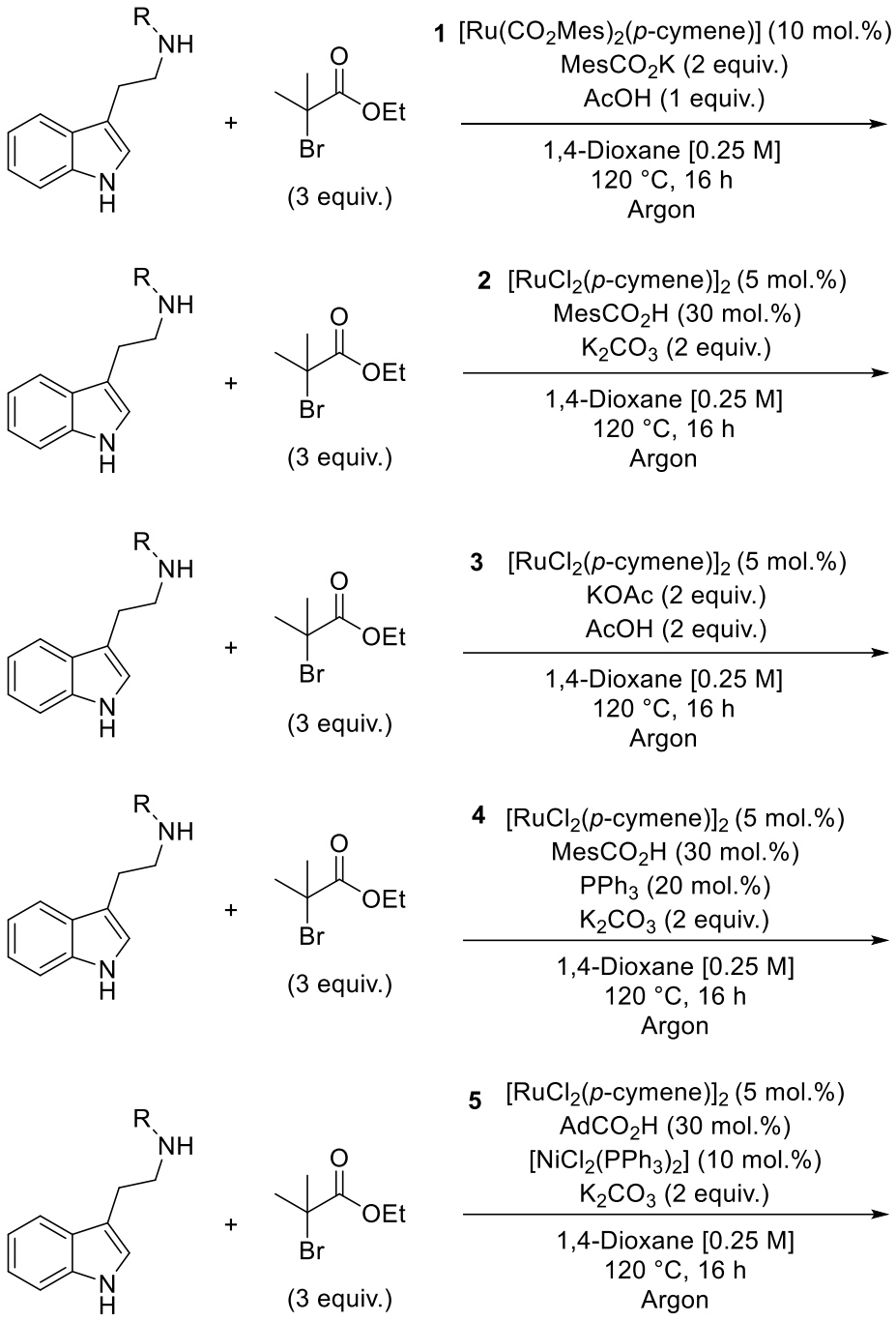

Scheme 86: Reaction conditions used to test tryptamine derivatives.

3.2 – Reaction Optimisation

Optimisation of the reaction began by using product **2e** as our standard substrate, using reaction conditions previously developed within our group, for the C6 alkylation of

indoles (Conditions **3** from Scheme **86**).[2] To our delight, using these conditions we managed to isolate the C4 alkylated product in a 48% yield, under the reaction conditions shown in Scheme **87**.

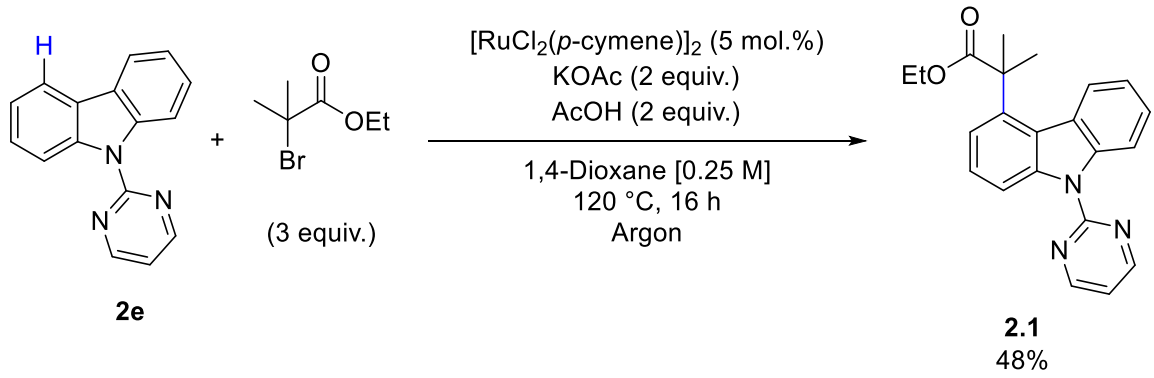

Scheme 87: Initial reaction conditions for the C4 alkylation of the carbazole substrate.

With this promising result in hand, we commenced our optimisation studies by varying the Ru catalyst. The use of a preformed Ru acetate monomer complex was also shown to work (entry **6**, Table **8**) albeit in lower yields than those observed from using the Ru dimer (entry **1**, Table **8**).

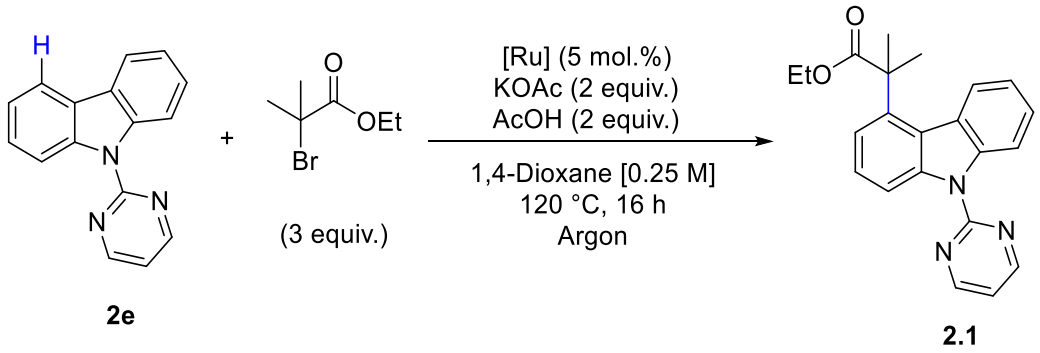

Table 8: Results from the optimisation of the Ru catalyst. IY – Isolated Yield.

Entry	Ru Source	NMR Conversion to **2.1** (IY) (%)
1	$[RuCl_2(p\text{-cymene})]_2$	**68** (**48**)
2	$RuCl_2(benzene)]_2$	**<5**
3[a]	$RuCl_3 \cdot xH_2O$	**0**
4[a]	$RuCl_3(PPh_3)_2$	**11**
5[a]	$[Ru(1,10\text{-phen})_3] \cdot 2Cl^-$	**0**
6[a]	$[Ru(OAc)_2(p\text{-cymene})]$	**63** (**36**)

[a] 10 mol.% of catalyst used

Following this, we looked at the choice of base in the reaction mixture. Pleasingly, an increase in product formation was observed using the mesitylcarboxylic acid, potassium salt, $MesCO_2K$ (Entry **1**, Table **9**). The use of inorganic bases (Entries **2** and **4**, Table **9**) gave poor results in comparison to the organic bases tested.

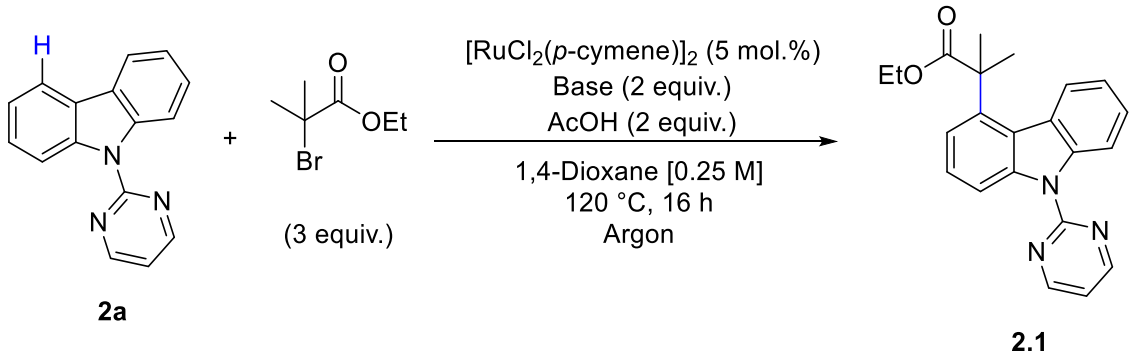

Table 9: Results from the optimisation of the base. IY – Isolated Yield.

Entry	Base	NMR Conversion to **2.1** (IY) (%)
1	KCO_2Mes	**80** (**61**)
2	$KHCO_3$	**25**
3	$NaCO_2Ad$	**58**
4	K_2CO_3	**0**
5	$NaCO_2Mes$	**70** (**60**)
6	K_3Citrate	**45**

We studied the effect of changing the cation used with the base (potassium vs. sodium), but little effect was observed with regards to product formation, with potassium performing marginally better. The use of a base with more of an ability to extract more than one proton, such as potassium citrate tribasic (Entry **6**, Table **9**), also gave inferior results. This suggested that bulky monobasic bases, were the ideal candidates for this reaction methodology.

We next began to look at the optimisation of the acid on the reaction, using a variety of organic and inorganic acids. Interestingly, despite the basic additive used, we found that AcOH gave rise to the highest conversion to the product, with $MesCO_2H$ and $AdCO_2H$ giving slightly inferior conversions and yields, with some selected results shown in Table **10**. The use of stronger organic and inorganic acids led to much poorer observed conversions.

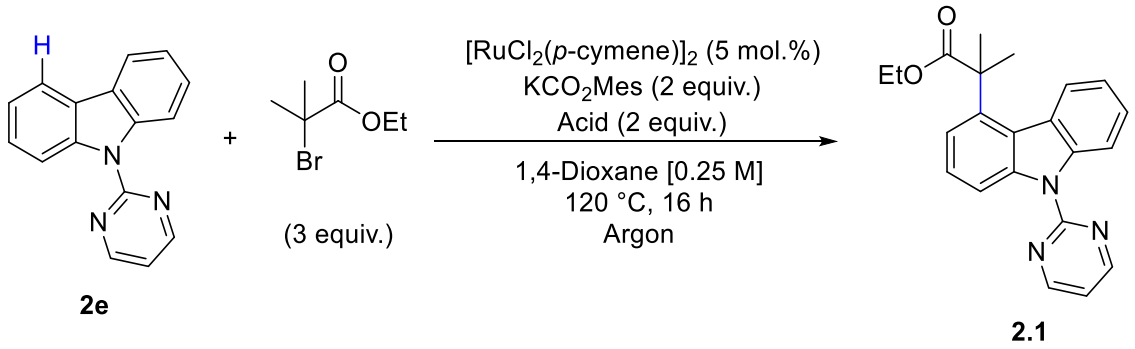

Table 10: Results from the optimisation of the acid. IY – Isolated Yield.

Entry	Acid	NMR Conversion to **2.1** (IY) (%)
1	AcOH	**80** (**61**)
2	$MesCO_2H$	**64** (**51**)
3	$AdCO_2H$	**66** (**50**)
4	HCl	**17**
5	CF_3CO_2H	**15**

The equivalents of acid added to the reaction became our next area of exploration for the optimisation of this reaction. Our previous work benefitted from the use of an equimolar quantity of acid and base,[2] however, in this case when changing the acid/base equilibrium, notably the use of less acid led to higher reaction conversions (Entry **2**, Table **11**), with 1 equivalent of acid performing most effectively.

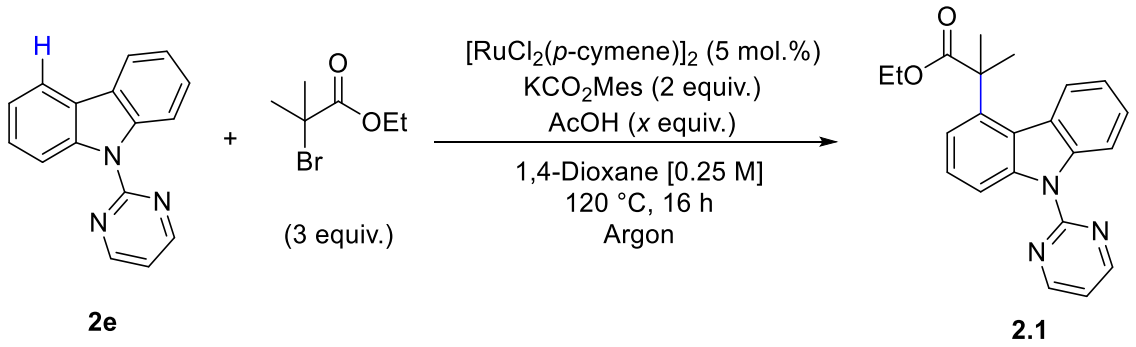

Table 11: Optimisation of acid equivalencies. IY – Isolated Yield.

Entry	Equivalents of AcOH added	NMR Conversion to **2.1** (IY) (%)
1	0.5	**80**
2	1	**84** (**68**)
3	2	**80** (**61**)
4	4	**68**
5	8	**<5**

The optimisation of the reaction solvent gave perhaps one of the most interesting discoveries, the results of which are shown in Table **12**.

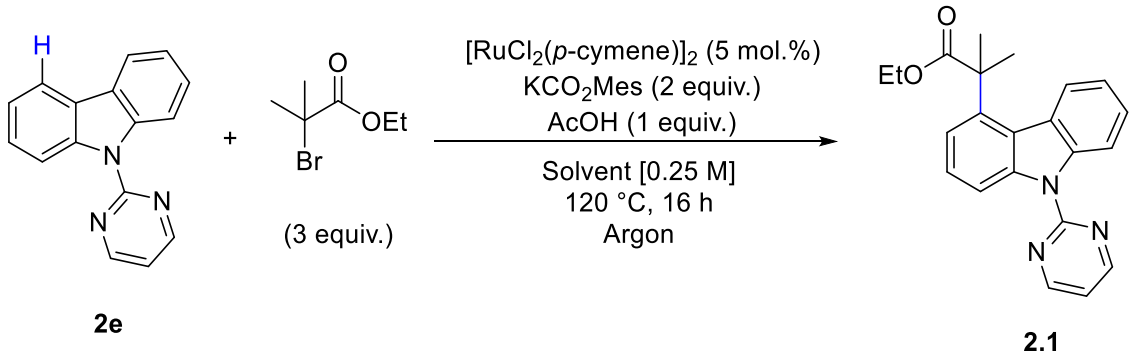

Table 12: Optimisation of the reaction solvent. IY – Isolated Yield.

Entry	Solvent	NMR Conversion to **2.1** (IY) (%)
1	2-MeTHF	**55**
2	Toluene	**0**
3	MeCN	**72** (**55**)
4	AcOH	**31**
5	1,4-Dioxane	**84** (**68**)
6	2-Butanone	**55**

We found that our original choice of 1,4-dioxane as our reaction solvent was superior to the other solvents tested. Despite this, the use of toluene (Entry **2**, Table **12**) showed a 21% conversion to a C3 alkylated product.

Control experiments without the Ru catalyst (Entry **5**, Table **12**) demonstrated low amounts of C3-alkylated products (<10%). For these reasons, we believe the result in toluene is due to an inefficient background S_EAr reaction.

Lowering of the reaction temperature to 100 °C led to a significant drop in conversion (61%). Interestingly, the use of [Ru(CO_2Mes)$_2$(*p*-cymene)] as a catalyst gave comparably excellent yields under the conditions shown in Scheme **88**. This catalyst system was also shown to be more effective for certain substrates (see later).The presence of air in the reaction led to a complete drop-off in reactivity, with no products observed.

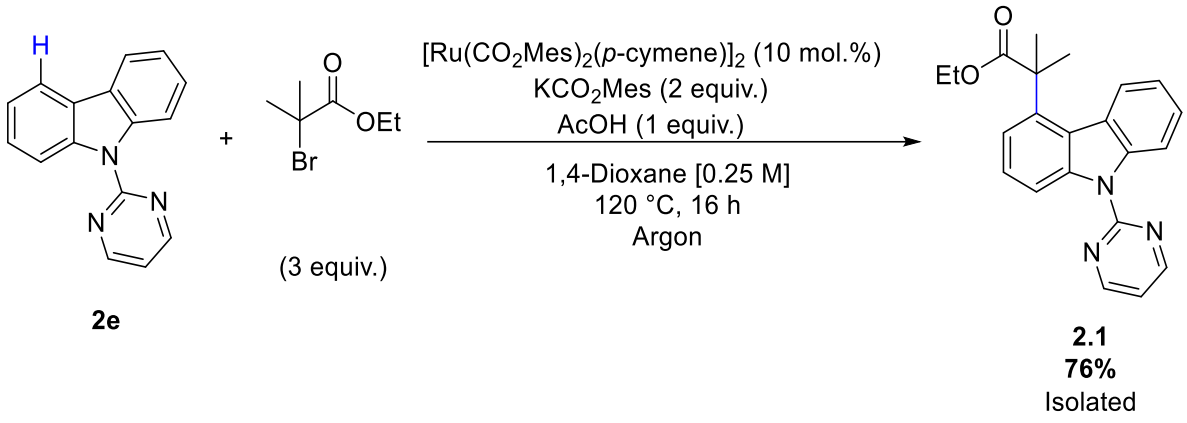

Scheme 88: Optimised conditions for the C4 alkylation of carbazoles using a Ru monomer catalyst.

3.3 – Scope and Limitations

We began exploring the reaction conditions employing both the commercially available dimer (conditions **A**) and the pre-synthesised monomer (conditions **B**) (Scheme **89**).

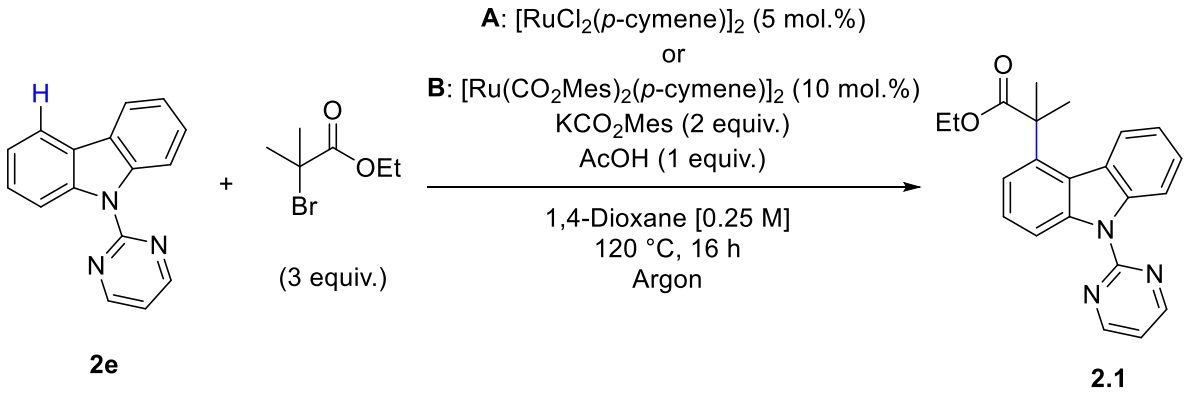

Scheme 89: Optimised conditions for the C4 alkylation of carbazoles.[21]

A variety of ester substituents were shown to be very well tolerated in the remote functionalisation methodology (**2.1**–**2.7**, **2.9**), with impressive yields up to 92% for the *tert*-butyl ester variant, **2.3**. It was noteworthy to note that *tert*-butyl bromide, utilised by numerous groups in σ-activation methodologies was not amenable to this methodology, **2.6** (Scheme **90**).[26–31]

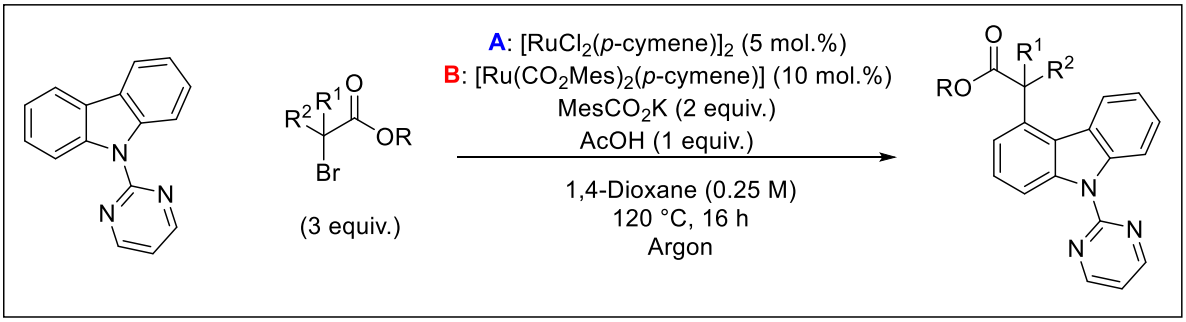

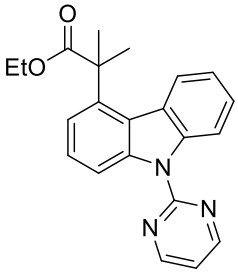

2.1
A: 68%
B: 76%

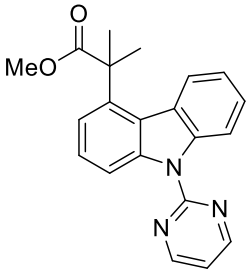

2.2
A: 70%
B: 65%

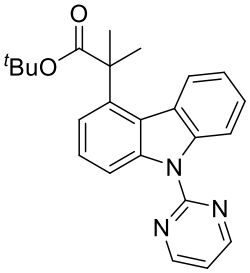

2.3
A: 72%
B: 92%

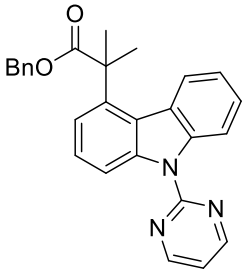

2.4
A: 51%
B: 74%

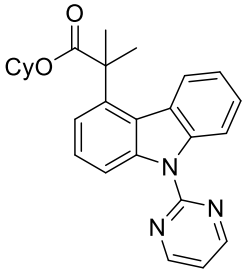

2.5
A: 54%
B: 74%

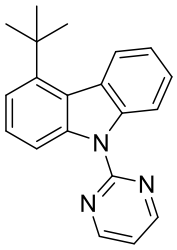

2.6
A: 0%
B: 0%

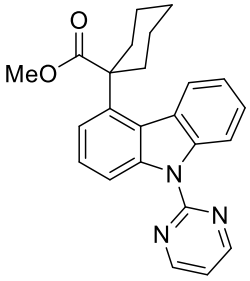

2.7
A: 35%
B: 42%

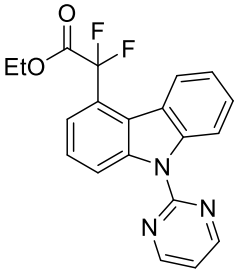

2.8
A: 0%
A+PPh_3: Trace

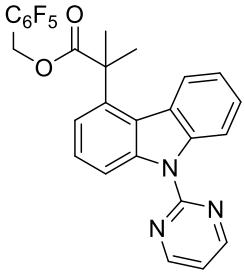

2.9
A: 41%
B: 39%

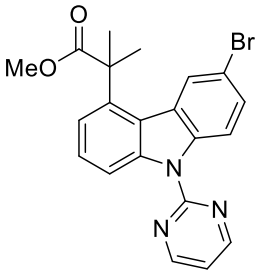

2.10
A: 54%
B: 49%

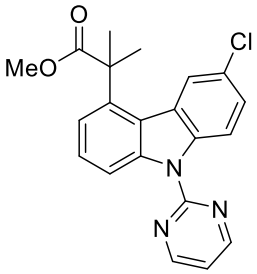

2.11
A: 60%
B: 71%

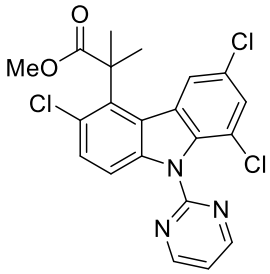

2.12
A: 10%
B: 7%

Scheme 90: Scope of C4 alkylation of carbazoles.[21]

When we investigated the use of the difluoro ester coupling partner, as utilised by Ackermann and Xu independently,[30,32] as seen with **2.8**, we found no conversion to the desired product, even upon the addition of a co-catalytic amounts of PPh_3 which have been shown to be vital in such transformations. Further studies on the remote C4-selective sulfonation, alkylation and bromination, using reported σ-activation protocols were also ineffective. We believe this highlights the uniqueness of the transformation we have achieved.

The synthesis of decorated carbazoles still remains a challenge and therefore limited variation on the aromatic rings in the scope could be achieved. However, when using mono bromo- and chloro- (**2.10** and **2.11** respectively) examples we have shown that these are also effective substrates for the transformation, with the regioselectivity for the non-functionalised ring exclusively. The trichlorinated example (**2.12**) gave poor yields, but this may be more a function of its poor solubility under the reaction conditions, rather than a facet of the transformation reactivity.

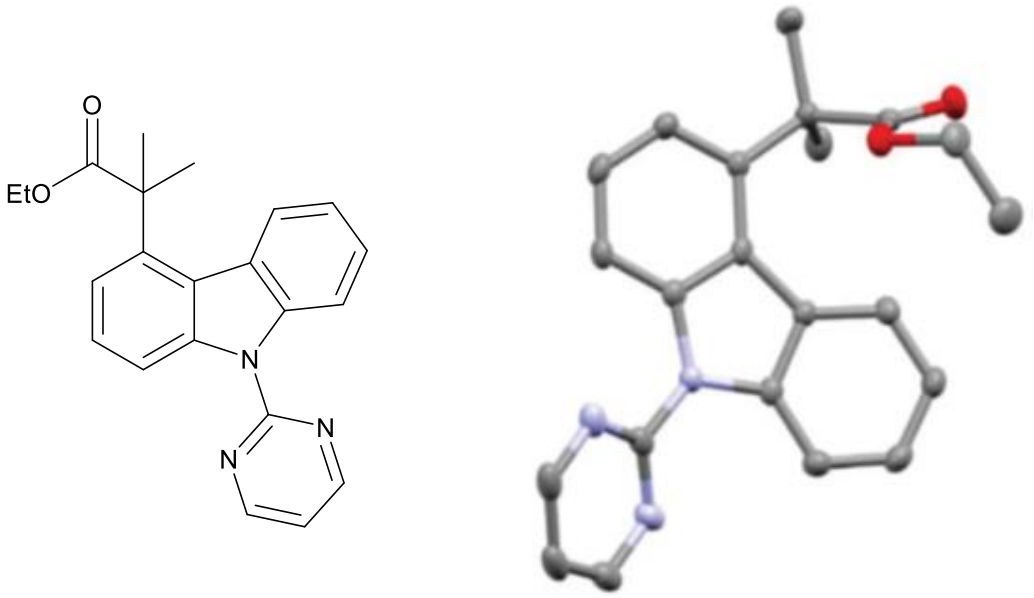

2.1

Figure 14: SCXRD structure of the C4 alkylated product **2.1**, confirming the regioselectivity of functionalisation, the hydrogen atoms have been omitted for clarity. *CCDC 1574475*. Colour Scheme – Grey: Carbon, Blue: Nitrogen, Red: Oxygen. Crystals for this structure were grown by Dr J. A. Leitch.

To confirm the regioselectivity of the reaction, we obtained a crystal structure of the EtO-ester product **2.1**, as shown in Figure **14**. The use of other directing groups such as pivalate or pyridine in place of the pyrimidine led to no observable reaction, demonstrating the necessity of a strongly coordinating directing group. The use of 2,3-dialkylated indoles and indolines (Scheme **91**) led to no reaction under the developed conditions. We believe this is due to the indole substituent at the C2 position interfering with the stable and planar cyclometallate or the Et at the C3 position blocking the C4 position sterically thus, preventing addition of the radical.

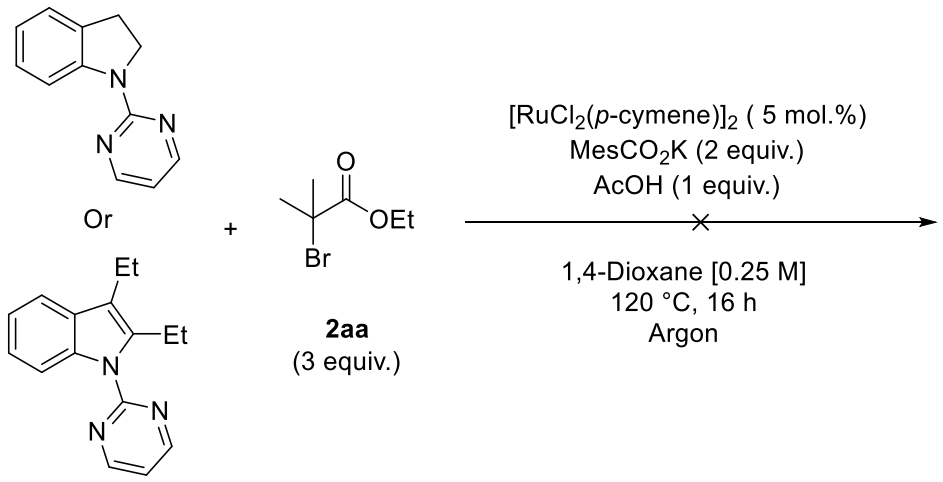

Scheme 91: Failed substrates under reaction conditions.[21]

The cleavage of directing groups is often a desirable property in the investigation of DG enabled C–H functionalisation methodologies. In the case when a pyrimidine is attached to the substrate *via* a C–C bond, this cleavage is generally not possible. However, when attached through a heteroatom, this removal is more straightforward. Heating the substrate with NaOEt in DMSO is an often utilised method for the removal of such pyrimidine DGs as shown in Scheme **92**. However, in the presence of an ester group, means this methodology would most likely result in the de-esterification of the substrate.

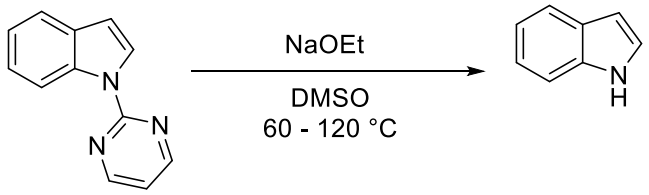

Scheme 92: General conditions used to cleave pyrimidine directing groups as shown on a pyrimidine-indole substrate.

More recent methodologies published by Chatani *et al*. have also shown that the removal of a pyrimidine DG from benzimidazoles can be achieved under the reaction conditions shown in Scheme **93**.[33]

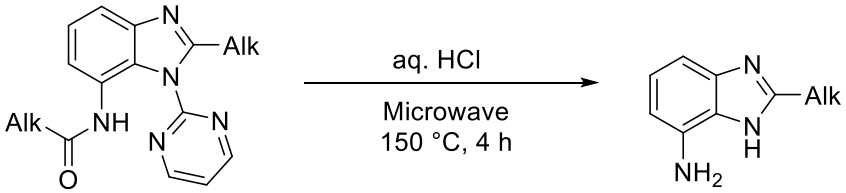

Scheme 93: Deprotection of pyrimidines on benzimidazole substrates.[33]

3.4 – Mechanistic considerations

Our investigation into the role of the ruthenium source in this reaction began by consideration of the directing groups attached to the carbazole nitrogen. When submitting *N*-benzylcarbazole under the developed conditions no product was observed under the developed conditions seen in Scheme **94**, demonstrating that a directing group is required. This is reinforced by the observation, that the omission of Ru in the reaction also led to no reaction at the desired C4 position, and only a small amount of the C3 alkylated product was isolated. These two pieces of information, along with the data from Scheme **91** lend themselves towards a σ-activation pathway in the way that they completely change the innate reactivity of the substrate molecule and its fundamental regioselectivity under a given set of conditions.

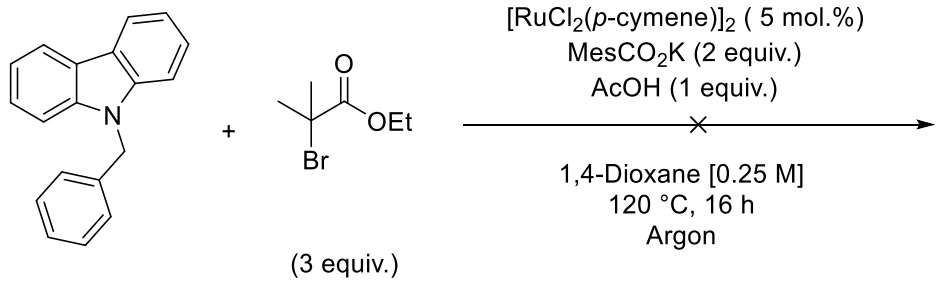

Scheme 94: Reaction conditions used to test *N*-benzylcabazole as a reaction substrate.

However, to probe this hypothesis further we ran a radical trapping experiment using TEMPO, whereby we observed a reduced conversion of product when using catalytic amounts (30 mol.%). The use of stoichiometric amounts of TEMPO (1 equivalent and 3 equivalents) led to similar observations whereby we observed conversions of 15% and 0% respectively. These results suggest a single electron transfer process being present under the reaction conditions. We then decided that it would be of interest to run H/D scrambling experiments using isotopically labelled acetic acid (AcOD) (Scheme **95**).

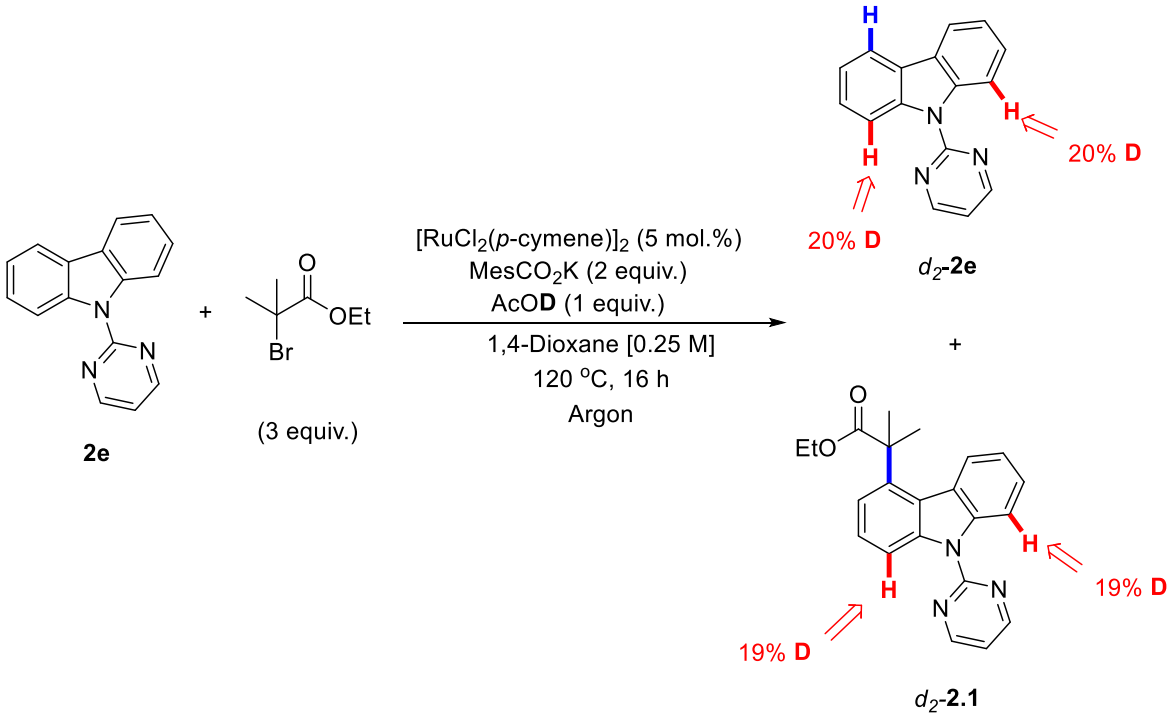

Scheme 95: Deuterium labelling experiment.

Deuterium incorporation was observed at both at the C1 and C8 positions in both the starting material, d_2-**2e** (20%) and product, d_2-**2.1** (19%). These observations lend themselves to a reversible C-H activation at both *ortho*-positions, under the conditions shown in Scheme **95**. Gratifyingly, the lack of scrambling at the C5 position in the product and at the C4/C5 position in the product rules out a readily reversible C-H metalation at these positions and lends itself to a C1 σ-activation protocol.

The addition of mercury into the reaction, as discussed in the previous chapter resulted in no change in conversions or observed regioselectivity. This result suggests a homogeneous catalytic regime is in operation.

From these mechanistic considerations, and previous insights into similar methodologies, a plausible mechanism for the remote C4 alkylation of carbazole derivatives is proposed (Scheme **96**). [27,29]

We propose that the ruthenium monomer undergoes a reversible CMD type insertion into the C-H at the C1 position *ortho* to the pyrimidine directing group. A single electron transfer process with an equivalent of a Ru species *via* an outer-sphere process to form the stabilised tertiary alkyl radical, α to the ester group. This radical then interacts with the sterically encumbered ruthenacycle species at the *para* position to the metal centre *via* a σ-activation process (most likely due to a shift in electron density to the C4 position).[34] Another SET process to reform the Ru(II) species and proton abstraction enables rearomatisation of the heterocyclic system. Protodemetallation then occurs to regenerate the catalyst and release the functionalised carbazole derivative.

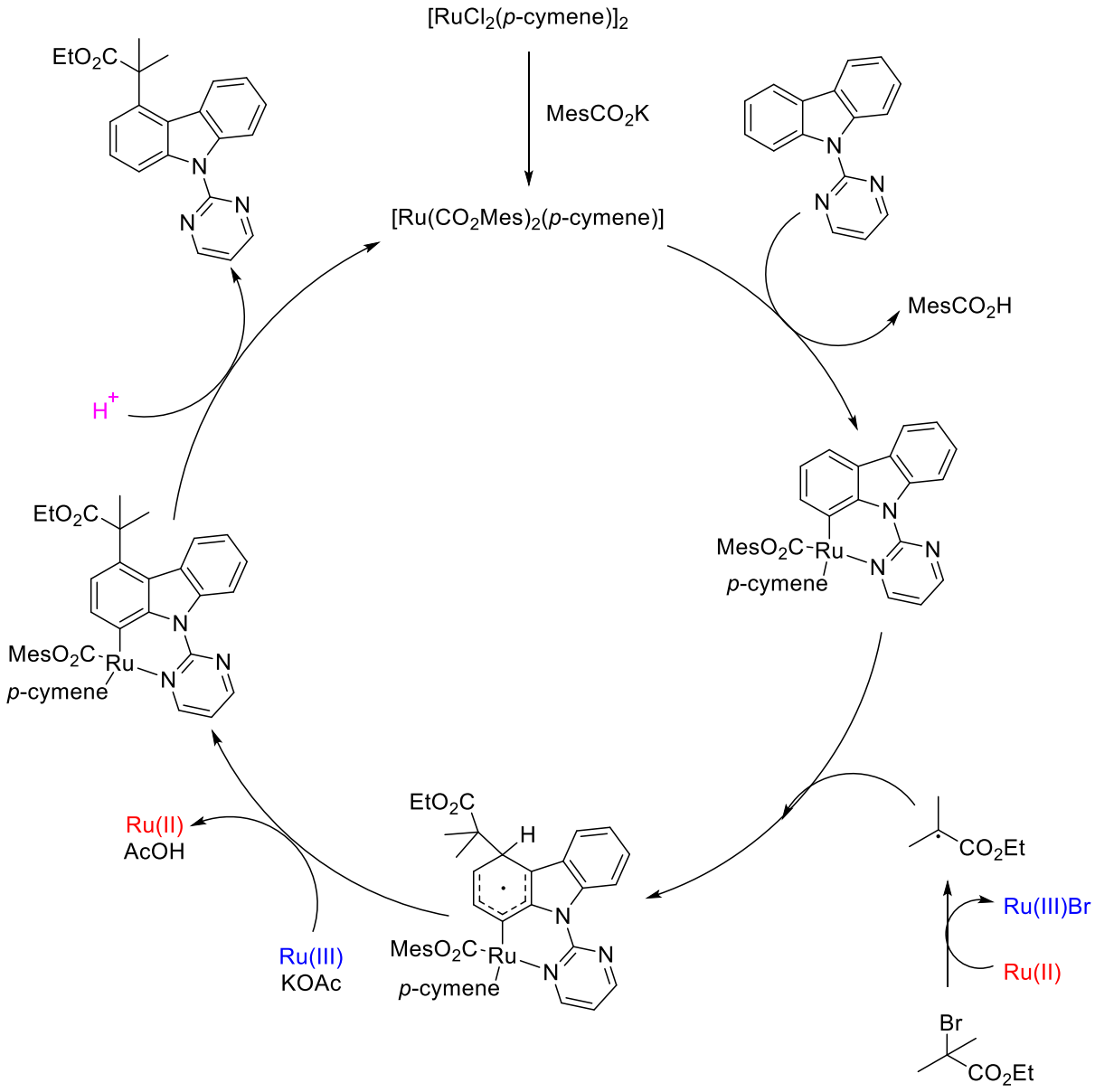

Scheme 96: Plausible mechanism for the C4 alkylation of carbazole derivatives.

3.5 – Conclusions and future work

In this section we have presented the remote C4-selective C-H alkylation of carbazole derivatives, at the time and to date the only example of the selective C4-functionalisation of the carbazole heteroaromatic. We have demonstrated that furnishing the carbazole heteroaromatic with a pyrimidine directing group is essential to allow the σ-activation process, whereby a stable and planar ruthenacycle at the C1 position, allows the

interaction of the *para* position (C4) with a tertiary alkyl radical. We also demonstrated the unique reactivity of α-halo carbonyl coupling partners *cf.* aliphatic alkyl halides.

Further investigations of the tryptamine substrates shown, utilising an easily added/cleaved blocking group on the indole N-atom, would remove a Lewis acidic, blocking group from coordinating to the Ru and leading to deactivation.

In future it would be of interest to extend the scope of available coupling partners to regioselectively couple to the carbazole ring system, under similarly mild conditions. Particularly attempting to utilise some of the other reported coupling partners, utilised in σ-activation reactions coupling partners which have been reported already in the literature.[35–38]

It would also be of interest to utilise a more easily cleavable directing group than pyrimidine, to allow for a more expansive set of derivatives that could be synthesised more easily from the C4 alkylated products, this could be achieved by use of computational modelling to examine potential directing groups that could be utilised. To this end the use of a more easily cleaved directing group, such as a sulfonamide could be used for this purpose, the cleavage of which is easily achieved under mild conditions (hydrolysis with TFA).[39]

Bibliography

1 J. Li, S. Warratz, D. Zell, S. De Sarkar, E. E. Ishikawa and L. Ackermann, *J. Am. Chem. Soc.*, 2015, **137**, 13894–13901.

2 J. A. Leitch, C. L. McMullin, M. F. Mahon, Y. Bhonoah and C. G. Frost, *ACS Catal.*, 2017, **7**, 2616–2623.

3 F. F. Zhang, L. L. Gan and C. H. Zhou, *Bioorganic Med. Chem. Lett.*, 2010, **20**, 1881–1884.

4 C. C. Chang, I. C. Kuo, J. J. Lin, Y. C. Lu, C. T. Chenc, H. T. Back, P. J. Lou and T. C. Chang, *Chem. Biodivers.*, 2004, **1**, 1377–1384.

5 M. H. Block, S. Boyer, W. Brailsford, D. R. Brittain, D. Carroll, S. Chapman, D. S. Clarke, C. S. Donald, K. M. Foote, L. Godfrey, A. Ladner, P. R. Marsham, D. J. Masters, C. D. Mee, M. R. O'Donovan, J. E. Pease, A. G. Pickup, J. W. Rayner, A. Roberts, P. Schofield, A. Suleman and A. V. Turnbull, *J. Med. Chem.*, 2002, **45**, 3509–3523.

6 C. C. Chang, I. C. Kuo, I. F. Ling, C. T. Chen, H. C. Chen, P. J. Lou, J. J. Lin and T. C. Chang, *Anal. Chem.*, 2004, **76**, 4490–4494.

7 C. C. Chang, J. Y. Wu, C. W. Chien, W. S. Wu, H. Liu, C. C. Kang, L. J. Yu and T. C. Chang, *Anal. Chem.*, 2003, **75**, 6177–6183.

8 K. Brunner, A. Van Dijken, H. Börner, J. J. A. M. Bastiaansen, N. M. M. Kiggen and B. M. W. Langeveld, *J. Am. Chem. Soc.*, 2004, **126**, 6035–6042.

9 J. Ding, J. Gao, Y. Cheng, Z. Xie, L. Wang, D. Ma, X. Jing and F. Wang, *Adv. Funct. Mater.*, 2006, **16**, 575–581.

10 J. A. Leitch, Y. Bhonoah and C. G. Frost, *ACS Catal.*, 2017, **7**, 5618–5627.

11 K. Devaraj, C. Sollert, C. Juds, P. J. Gates and L. T. Pilarski, *Chem. Commun.*, 2016, **52**, 5868–5871.

12 L. Jiao and T. Bach, *J. Am. Chem. Soc.*, 2011, **133**, 12990–12993.

13 H. Mizoguchi, H. Oikawa and H. Oguri, *Org. Biomol. Chem.*, 2012, **10**, 4236–4242.

14 V. P. Reddy, R. Qiu, T. Iwasaki and N. Kambe, *Org. Lett.*, 2013, **15**, 1290–1293.

15 R. Qiu, V. P. Reddy, T. Iwasaki and N. Kambe, *J. Org. Chem.*, 2015, **80**, 367–374.

16 L. Zhu, X. Cao, R. Qiu, T. Iwasaki, V. P. Reddy, X. Xu, S. F. Yin and N. Kambe, *RSC Adv.*, 2015, **5**, 39358–39365.

17 Y. Feng, D. Holte, J. Zoller, S. Umemiya, L. R. Simke and P. S. Baran, *J. Am. Chem. Soc.*, 2015, **137**, 10160–10163.

18 M. Majchrzak, M. Grzelak and B. Marciniec, *Org. Biomol. Chem.*, 2016, **14**, 9406–9415.

19 T. Takeuchi, S. Oishi, T. Watanabe, H. Ohno, J. I. Sawada, K. Matsuno, A. Asai, N. Asada, K. Kitaura and N. Fujii, *J. Med. Chem.*, 2011, **54**, 4839–4846.

20 S. Issa, A. Prandina, N. Bedel, P. Rongved, S. Yous, M. Le Borgne and Z. Bouaziz, *J. Enzyme Inhib. Med. Chem.*, 2019, **34**, 1321–1346.

21 J. A. Leitch, C. J. Heron, J. McKnight, G. Kociok-Köhn, Y. Bhonoah and C. G. Frost, *Chem. Commun.*, 2017, **53**, 13039–13042.

22 K. Walsh, H. F. Sneddon and C. J. Moody, *ChemSusChem*, 2013, **6**, 1455–1460.

23 T. Yajima, M. Okajima, A. Odani and O. Yamauchi, *Inorganica Chim. Acta*, 2002, **339**, 445–454.

24 G. A. Swan, K. B.; Prasad, *J Chem Soc*, 1958, **0**, 2045–2051.

25 X. Huang, S. Xu, Q. Tan, M. Gao, M. Li and B. Xu, *Chem. Commun.*, 2014, **50**, 1465–1468.

26 A. J. Paterson, C. J. Heron, C. L. McMullin, M. F. Mahon, N. J. Press and C. G. Frost, *Org. Biomol. Chem.*, 2017, **15**, 5993–6000.

27 A. J. Paterson, S. St John-Campbell, M. F. Mahon, N. J. Press and C. G. Frost, *Chem. Commun.*, 2015, **51**, 12807–12810.

28 N. Hofmann and L. Ackermann, *J. Am. Chem. Soc.*, 2013, **135**, 5877–5884.

29 J. Li, S. Warratz, D. Zell, S. De Sarkar, E. E. Ishikawa and L. Ackermann, *J. Am. Chem. Soc.*, 2015, **137**, 13894–13901.

30 G.-W. Wang, Z.-Y. Li, L. Li, Q.-L. Li, K. Jing and H. Xu, *Chem. - A Eur. J.*, 2017, 3285–3290.

31 S. Warratz, D. J. Burns, C. Zhu, K. Korvorapun, T. Rogge, J. Scholz, C. Jooss, D. Gelman and L. Ackermann, *Angew. Chem - Int. Ed.*, 2017, **56**, 1557–1560.

32 Z. Ruan, S.-K. Zhang, C. Zhu, P. N. Ruth, D. Stalke and L. Ackermann, *Angew. Chem Int. Ed.*, 2017, **3**, 2045–2049.

33 S. M. Khake and N. Chatani, *Org. Lett.*, 2020, **22**, 3655–3660.

34 L. Zhang, L. Yu, J. Zhou and Y. Chen, *European J. Org. Chem.*, 2018, **2018**, 5268–5277.

35 Q. Yu, L. Hu, Y. Wang, S. Zheng and J. Huang, *Angew. Chem Int. Ed.*, 2015, **54**, 15284–15288.

36 H. L. Barlow, C. J. Teskey and M. F. Greaney, *Org. Lett.*, 2017, **19**, 6662–6665.

37 O. Saidi, J. Marafie, A. E. W. Ledger, P. M. Liu, M. F. Mahon, G. Kociok-Kohn,

M. K. Whittlesey and C. G. Frost, *J. Am. Chem. Soc.*, 2011, **133**, 19298–19301.

38 B. Li, S. L. Fang, D. Y. Huang and B. F. Shi, *Org. Lett.*, 2017, **19**, 3950–3953.

39 H. X. Dai, A. F. Stepan, M. S. Plummer, Y. H. Zhang and J. Q. Yu, *J. Am. Chem. Soc.*, 2011, **133**, 7222–7228.

Chapter 4 – Studies into New Coupling Partners and Substrates

The work discussed in the following section began as an attempt to investigate alternative coupling partners for the recently published methodology for the selective *para* alkylation of aniline derivatives, **3a**, with tertiary α-halo esters, with the Ru coordinated *via* the two N-atoms as shown in Scheme **62** (Section **1.6.3**). The reaction conditions for this transformation are shown in Scheme **97**.[1]

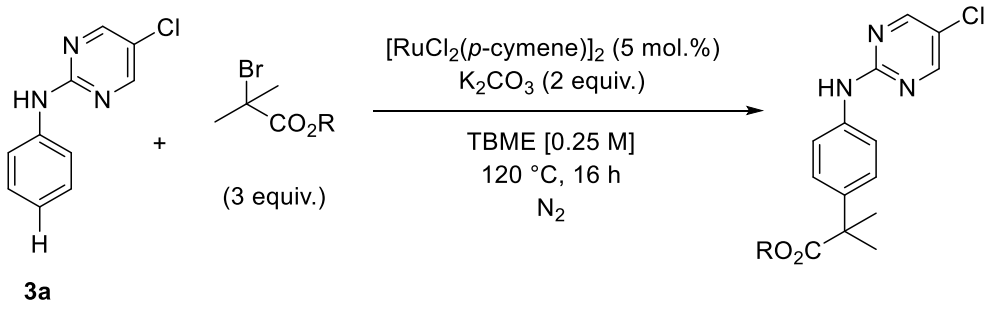

Scheme 97: Optimised conditions for the Ru catalysed *para*-selective C–H alkylation of aniline derivatives.[1]

To build on previous work carried out in the group and expand the range of functionality that could be successfully and selectively coupled to such substrates, we began to examine different radical precursors as coupling partners that could be successfully coupled at the *para* position of the aniline, with potentially similar electronic and electrochemical properties to α-halo ester substrates.[1–5] To this end, we were inspired by a study from Greaney and co-workers, using CBr_4 as a coupling partner for the *meta* carboxylation of 2-phenylpyridine (**1a**), under the conditions shown in Scheme **98**.[6] The mechanistic explanation of this carboxylation is shown in Scheme **45** (Section **1.5.5**).

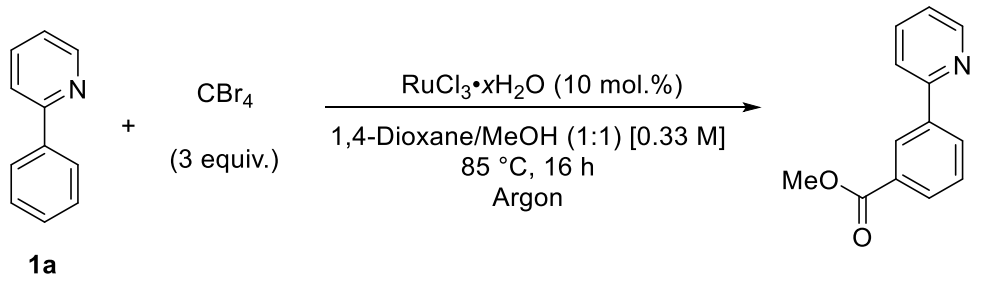

Scheme 98: Optimised conditions for the Ru catalysed *meta* carboxylation of 2-phenylpyridine.[6]

Anilines are ubiquitous in many biologically relevant motifs, with examples of this shown in Figure **15**.[7,8] This relevance therefore makes the use of such substrates for functionalisation reactions of great interest and importance in the area of transition metal mediated C–H activation reactions.

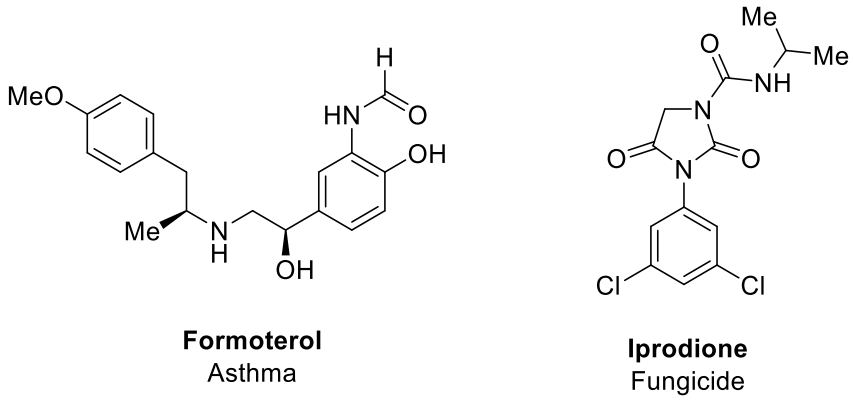

Figure 15: Selected examples of biologically relevant compounds containing the aniline motif.

As a vast majority of previous σ-activation based transformations have generated the formation of $C(sp^3)$–$C(sp^2)$ bonds, this elegant approach using an acyl surrogate particularly interested us as a route into the selective construction of $C(sp^2)$–$C(sp^2)$ bonds. Notably, reaction conditions for this transformation are unusual in that the use of the commonly used Ru(II) sources commonly used in σ-activation methodologies and the previous chapters of this thesis did not give the desired reactivity; only simple $RuCl_3 \cdot xH_2O$ gave any observable conversion. This is the first example that we are aware of that such a transformation has been achieved.

We were intrigued to see whether we could marry together the above report with our *para*-selective C–H functionalisation method, resulting in a *para* selective carboxylation of

anilines. We hypothesis that a mechanism similar to the one shown in Scheme **99**, would be in action. This would begin by a coordination of the Ru to the two N atoms on the substrate, as proposed by computational analysis of the *para* selective alkylation by Frost *et al*.[1] The CBr_4 would then undergo an SET process with a Ru species *in situ* to form a CBr_3 radical, which would then react at the most electrophilic position on the arene ring (*para*). A rearomatisation would then occur with the formed Br^- anion acting as a base and the Ru(III) species formed by the radical formation would be reduced back to Ru(II). A molecule of acid formed *in situ* would then remove the Ru from the molecule by protodemetallation, and the $–CBr_3$ group undergoes methanolysis to form the *para* carboxylated product.[1,6]

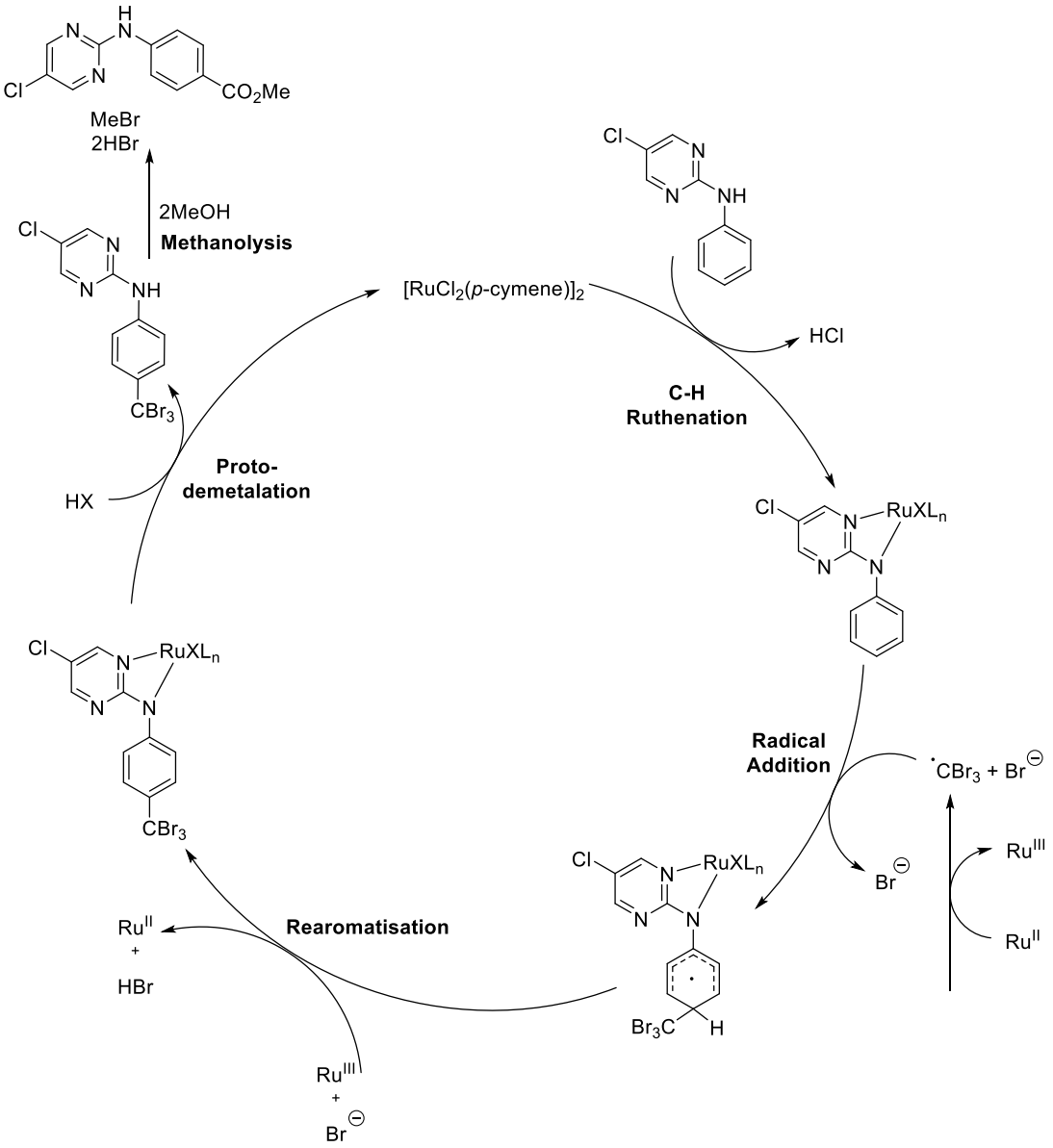

Scheme 99: A hypothetical mechanistic explanation for the *para* selective carboxylation of 5-chloropyrimidinenanliline (5–CPA), **3a**.

4.1 – Synthesis of Substrates for Studying the Proposed Reaction Design

We identified an *N*-pyrimidylaniline derivative as our model substrate for method development (5-CPA), **3a**.[1] This substrate is readily synthesised in one step using easily sourced starting materials as shown in Scheme **100**. From previous studies, we were aware that the blocking of the 5-position on the pyrimidine ring with a chloro group was found

to be necessary, due to the observed competing alkylation of this position when it is unprotected.[1]

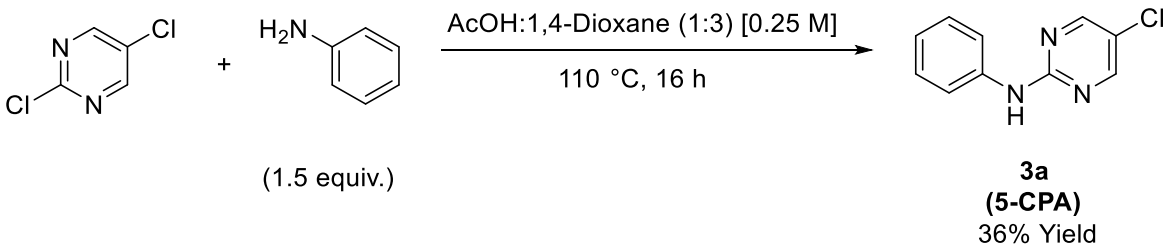

Scheme 100: Synthesis of 5-chloro-*N*-phenylpyrimidin-2-amine (5-CPA), **3a**.[1]

We also synthesised a similar pyridine variant of this substrate, **3b**, under the conditions in Scheme **101**.

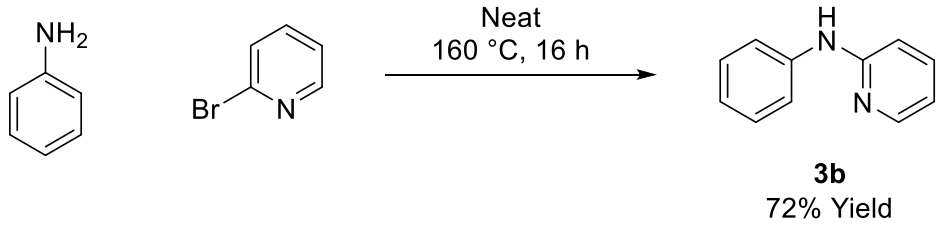

Scheme 101: Synthesis of N-phenylpyridin-2-amine (PPA), **3b**.

4.2 – Reaction Optimisation

Preliminary reaction investigations using substrate, **3b**, testing a series of reaction conditions demonstrated this structure afforded no productive C–H functionalisation products. Due to this, we decided to use **3a** (5-CPA) as our model substrate, based on its previous use within the group.

We first began this optimisation process by looking at the optimal catalyst for the process, as shown in Table **13**.

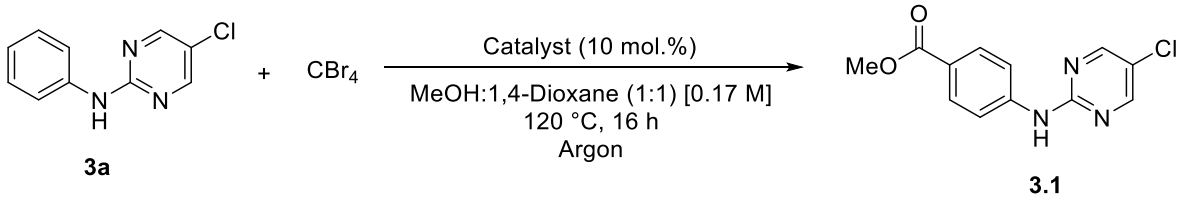

Table 13: Selected results for the catalyst optimisation on the *para*-carboxylation of **3a**. IY – Isolated yield.

Entry	Catalyst	NMR Conversion (IY) (%)
1	$RuCl_3 \cdot xH_2O$	**34** (**20**)
2[1]	$[RuCl_2(p\text{-cymene})]_2$	**20**
3	$[Ru(OAc)_2(p\text{-cymene})]$	**12**
4	$[Fe(acac)_3]$	**19**
5	Fe_2O_3	**29**
6	$FeCl_2$	**Trace**
7	$FeCl_3$	**33** (**23**)
8	$ZnCl_2$	**0**
9	AgCl	**0**
10[1]	No catalyst	**5**

[1]- *5 mol.% used*, [2]- 48 h

With a desired substrate in hand, we began to investigate the catalyst activity for this reaction. Initially we began by testing various Ru(II) sources and to our delight, from the first conditions we observed conversion to the desired *para* carboxylated product. Interestingly, addition of no catalyst at all resulted in a 5% conversion to the *para* product, this resulted also in formation of significant amounts of the *N*-carboxylated product *c.a.* 20%, **3.2**, as well as requiring a longer reaction time, these two products under the used reaction conditions are shown in Scheme **102**.

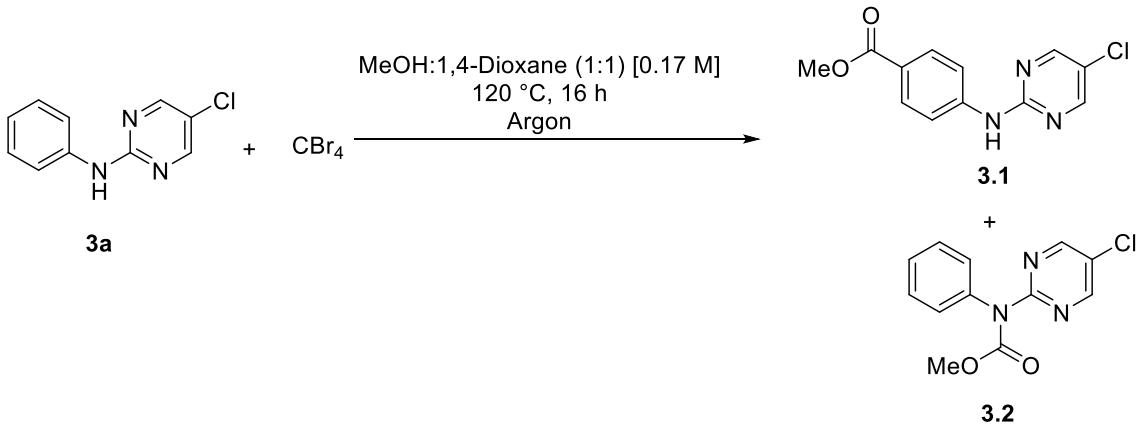

Scheme 102: Products formed when the reaction is run in the absence of a catalyst.

As a matter of curiosity during this optimisation we wanted to check whether this reactivity was inherent for Ru only, or if it was a facet of group 8 metals in general, the results of this are shown in Table **13**. To our surprise, the use of $FeCl_3$ gave a slightly improved isolated yield when compared to $RuCl_3$, and therefore we decided to proceed further with this result as Fe based catalysts are more sustainable in an economical and environmental sense. The use of Fe(II) and Fe(III) catalysts have been reported previously by Mukminov and co-workers, for the carboxylation of benzofurans.[9] Use of different Lewis acids also proved unreactive under the conditions tested.

We next elected to vary the amount of catalyst utilised in the reaction medium. As seen in Table **14**, a surprising inverse trend was observed where higher quantities of catalyst suppressed reactivity. The results gathered here indicate that the iron catalyst might play further, alternative roles in the reaction, and in higher quantities promote alternative pathways. More information must be collected to ascertain this, however. It must be noted also that the reaction proceeds, albeit very sluggishly and in low yield in the absence of any catalyst, showing that the iron is acting in a positive way to catalyse the system.

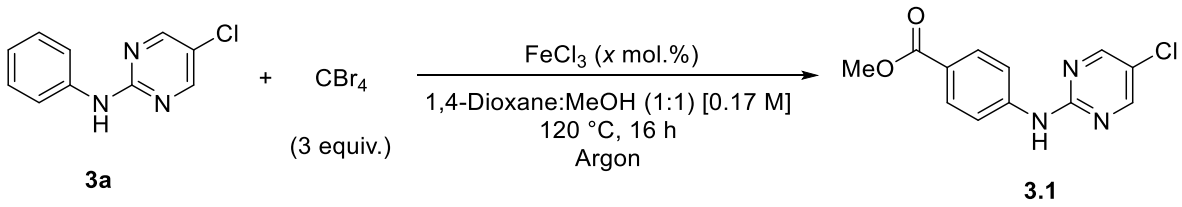

Table 14: Results from optimisation of catalyst loading for the *para* carboxylation of **3a**. IY – Isolated Yield.

Entry	mol.% of catalyst used	NMR Conversion (IY) (%)
1	5	**37** (**18**)
2	10	**33** (**23**)
3	15	**26**
4	20	**21**
5	25	**18**
6	30	**15**
7	100	**0**

Furthermore, reducing the number of CBr_4 equivalents had no positive effect upon the reaction outcome.

We next began to optimise the solvent choice used in conjunction with MeOH. Results by Greaney *et al*. showed a large decrease in yields when moving away from using simple alcohols as co-solvent.[6] Some preliminary results in the lab also showed that using other alcohols for this reaction gave no observed product, therefore the scope of the alcohol co-solvent was not investigated further.

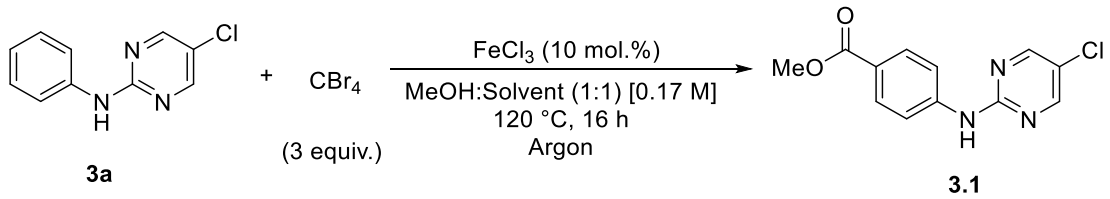

Table 15: Selected results from the solvent optimisation of the *para*-carboxylation of **3a**. IY – Isolated Yield.

Entry	Solvent	NMR Conversion (IY) (%)
1	MeCN	**0**
2	DCE	**<5**
3	2-Butanone	**17**
4	Toluene	**17**
5	2-MeTHF	**27** (**20**)
6	H_2O	**0**
7	HFIP	**17**

The use of MeCN resulted in no observable reaction (Entry **1**, Table **15**), this may be due to the coordinative saturation of the Fe *in situ* making the kinetics of ligation with the substrate very slow.[10] The use of other polar solvents also led to poor conversions, although the use of 2-MeTHF (Entry **5**, Table **15**) gave good results, with yields comparable to using 1,4-dioxane as solvent. The use of water gave no observable reaction.

The effect of the solvent ratios on the reaction also became of interest to us, in our attempts to increase the yields. The results of this study are shown in Table **16**. As seen in Table **16**, decreasing the concentration of MeOH in the solvent mixture led to a complete shutdown in reactivity. However, increasing the MeOH concentration led to an increase in conversions from Entry **6** to Entry **7**, Table **16**, before the reactivity shut down again.

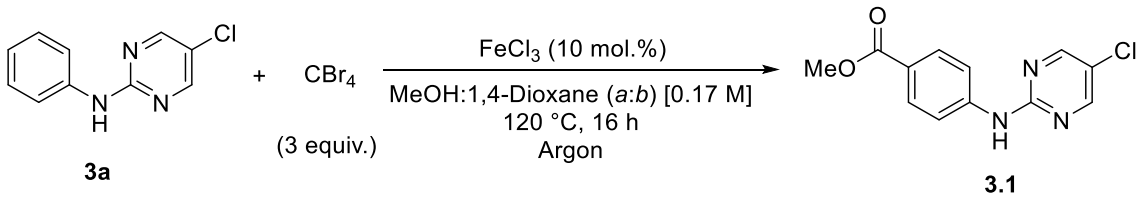

Table 16: Results for the optimisation of the solvent ratio, for the *para* carboxylation of **3a**. IY – Isolated Yield.

Entry	*a*:*b*	NMR Conversion (IY) (%)
1	1:2	**0**
2	1:4	**0**
3	1:5	**0**
4	1:10	**0**
5	2:1	**<5**
6	4:1	**48** (**20**)
7	5:1	**39**
8	10:1	**0**

The variation of reaction concentration of was next investigated, with the results as shown in Table **17**. The use of either 0.50 M or 0.17 M (Entry **2** and **4**, Table **17**) as the concentration resulted in identical isolated yields of the desired product. With a view to efficient use of materials during the optimisation, we decided the use of 0.50 M as our standard concentration would be used. The used of vigorously dried solvents also led to no observable reaction. This might indicate that residual moisture in the solvents aid in solubility of the reagents, or aid in a step of the reaction cycle.

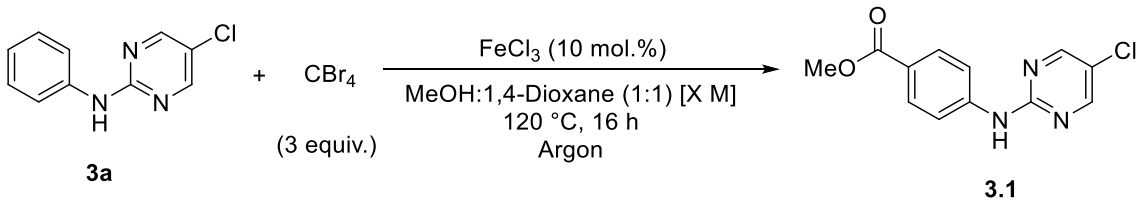

Table 17: Results from the concentration optimisation of the *para*-carboxylation of **3a**. IY – Isolated Yield.

Entry	Concentration (mol L^{-1})	NMR Conversion (IY) (%)
1	1.0	**<5**
2	0.50	**44** (**23**)
3	0.25	**10**
4	0.17	**33** (**23**)
5	0.10	**11**
6	0.01	**<5**

After exhausting all avenues to us, in terms of optimisation of reaction parameters; we then decided to investigate the effect of conversion against reaction time. Our initial thought was that the reaction could have very poor kinetics, and therefore by increasing the time we may begin to realise larger isolated yields. The results of this investigation are shown in graphical form in Figure **16**. The graph in Figure **16** show that a maximum conversion to the desired *para* product is achieved after approximately 40 hours. However, upon using a 48 hour reaction time we still only achieved a 23% isolated yield, identical to the best yield achieved using a 16 hour reaction period.

Dropping of the reaction temperature from 120 °C to 90 °C resulted in only trace conversion to the desired product. The presence of oxygen in the reaction led to a small conversion to *para* product, albeit under much diminished conversions. Analogously, increase of the reaction temperature from 120 °C to 160 °C also resulted in no improvement of reaction yield or conversion.

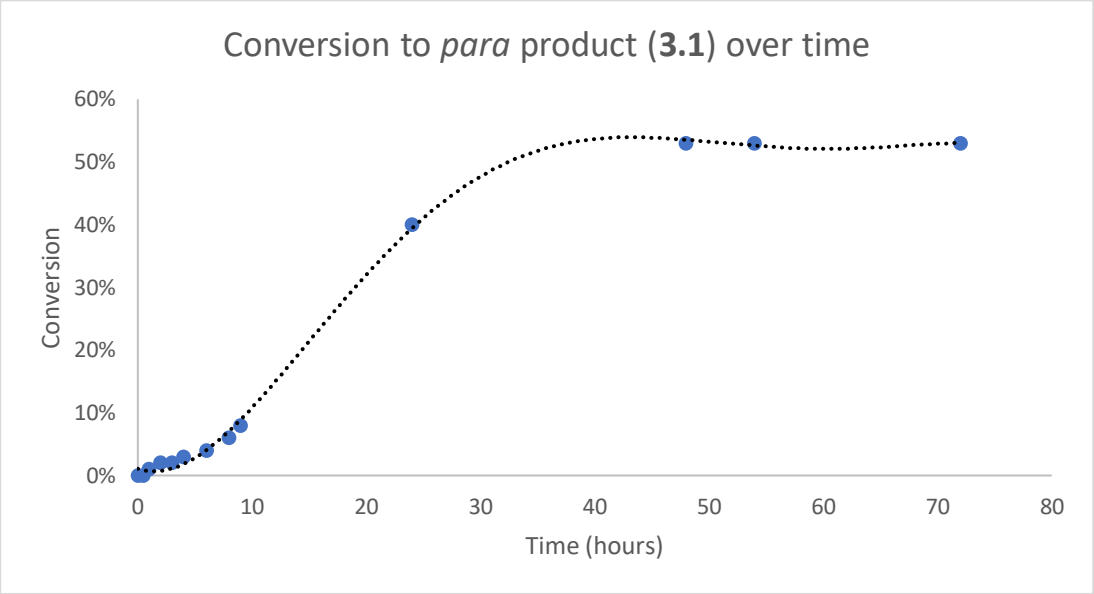

Figure 16: Graph showing conversion of starting material (**3a**) to *para* product (**3.1**) over time.

4.3 – Mechanistic Considerations

In an effort to try and understand the role of Fe in this reaction we questioned whether a separate Fe complex or a free, uncoordinated $FeCl_3$ molecule was responsible for the formation of the $\cdot CBr_3$ radical *in situ*. We decided to add a series of ligands which could enhance the redox properties of the Fe centre, in order to alter the HOMO-LUMO of the $FeCl_3$, the results of this are shown in Table **18**.

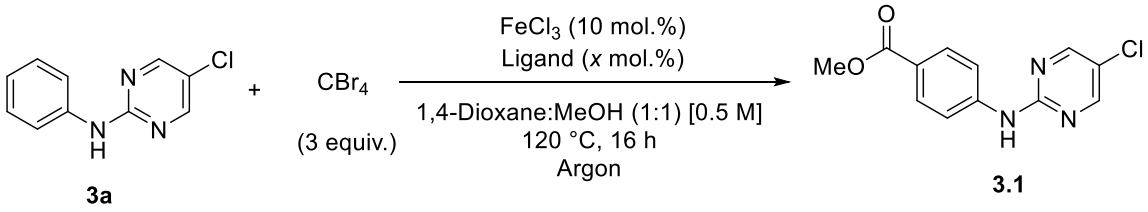

Table 18: Results from the ligand screen for the *para*-carboxylation of **3a**. IY – Isolated Yield.

Entry	Ligand	Ligand Equivalents (mol.%)	NMR Conversion (IY) (%)
1	2,2'-bipy	10	**20**
2	2,2'-bipy	20	**27** (**12**)
3	1,10-phen	10	**16**
4	1,10-phen	20	**7**
5	PyBox-Ph	10	**5**
6	PyBox-Ph	20	**7**

As seen in Table **18**, the addition of ligands to the reaction led to reduced conversions, and in the case of our best observed result (Entry **2**, Table **18**) reduced isolated yields.

An observation of the reaction vessel after cooling, showed the presence of small, heterogeneous particles, presumable formed by the aggregation of the Fe. This observation made us question whether the reaction was at all homogeneous or heterogeneous, or whether the aggregation of the metal particles was a by-product from a catalyst deactivation pathway. To answer the first question, we performed a mercury drop test, under the conditions shown in Scheme **103**.

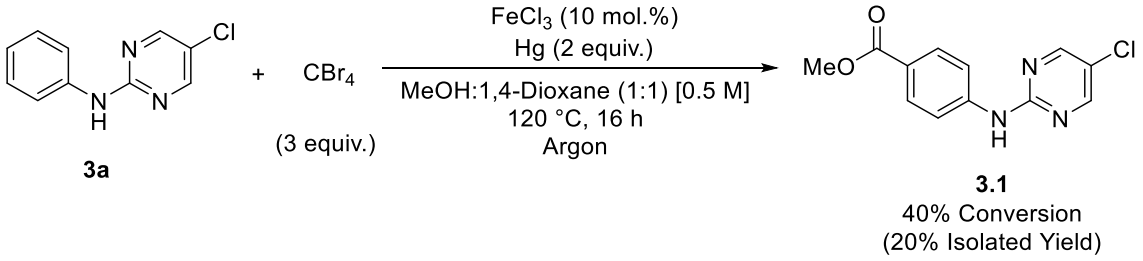

Scheme 103: Mercury drop test on the *para*-carboxylation of **3a**.

As shown in Scheme **103** the addition of mercury resulted in little, to no effect upon the observed conversions or yields. This result implies that the reaction proceeds *via* a

homogeneous regime. Attempts at growing an adduct of the substrate with the $FeCl_3$ have not yet, yielded diffraction quality crystals.

At this point we pondered whether a directing group was required for this transformation, or whether the electronics of the substrate were a more important aspect towards yield/regioselectivity. To this end, we decided to use acetamide as a model comparison, due to similar electronic influences of the ring, similar pK_a of the N–H and that it contains a metal coordinating group.[1] This reaction is shown in Scheme **104**.

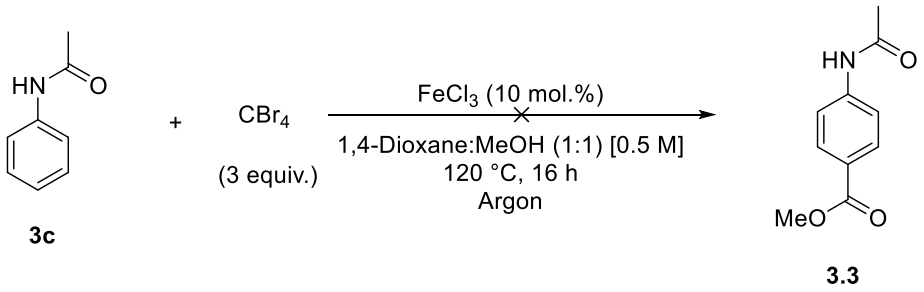

Scheme 104: Testing acetamide, **3c**, as a reaction substrate.

The use of acetamide as a substrate yielded no reactivity. This suggests that the coordination of Fe in the system is critical to the observed regioselectivity of the product.

4.4 – Conclusions and Future Work

The *para*-carboxylation of aniline derivatives, as discussed in Section **4.1** gives an avenue for future investigation, with an isolated yield of 23% under lead conditions. The ability to regioselectively couple together two substrates together, is of potential benefit to any possible molecules of interest containing such a motif. Figure **17** shows two potential post-synthetic modification routes that coupled be applied to the *para*-carboxylated substrate.

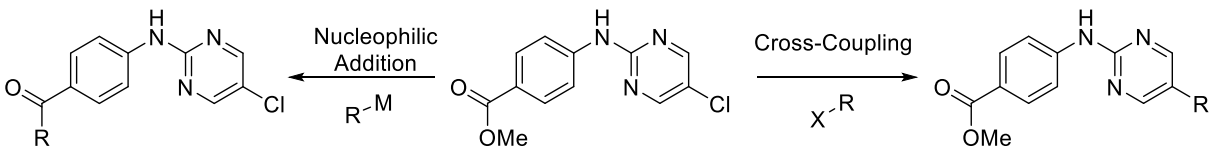

Figure 17: Examples of potential post-synthetic modifications on *para*-carboxylated substrates.

The scope of the catalysts tested for this transformation would be an ideal place to begin any future work on this transformation, by extending the scope of such catalyst to other transitions metals and main-group Lewis acids, in an effort to elucidate whether this reaction is specifically catalysed by Fe, or if it is a Lewis acid catalysed transformation.

The use of computational modelling based on recent work by Ritter *et al*. would also be of interest, in an attempt to gain more understanding of this transformation, with regards to whether a Fe(II)/Fe(III) redox couple is in operation, or whether a redox neutral process is occuring.[11,12] Further investigation of new and possibly fruitful coupling partners to further expand the synthetic capability of such a methodology would also be of interest in future.

Bibliography

1 J. A. Leitch, C. L. McMullin, A. J. Paterson, M. F. Mahon, Y. Bhonoah and C. G. Frost, *Angew. Chemie - Int. Ed.*, 2017, **56**, 15131–15135.

2 J. Li, S. Warratz, D. Zell, S. De Sarkar, E. E. Ishikawa and L. Ackermann, *J. Am. Chem. Soc.*, 2015, **137**, 13894–13901.

3 N. Hofmann and L. Ackermann, *J. Am. Chem. Soc.*, 2013, **135**, 5877–5884.

4 A. J. Paterson, S. St John-Campbell, M. F. Mahon, N. J. Press and C. G. Frost, *Chem. Commun.*, 2015, **51**, 12807–12810.

5 A. J. Paterson, C. J. Heron, C. L. McMullin, M. F. Mahon, N. J. Press and C. G. Frost, *Org. Biomol. Chem.*, 2017, **15**, 5993–6000.

6 H. L. Barlow, C. J. Teskey and M. F. Greaney, *Org. Lett.*, 2017, **19**, 6662–6665.

7 W. Ma, H. Dong, D. Wang and L. Ackermann, *Adv. Synth. Catal.*, 2017, **359**, 966–973.

8 J. A. Leitch and C. G. Frost, *Synth.*, 2018, **50**, 2693–2706.

9 R. I. Khusnutdinov, A. R. Baiguzina and R. R. Mukminov, *Russ. J. Org. Chem.*, 2011, **47**, 437–441.

10 L. McGhee, R. M. Siddique and J. M. Winfield, *J. Chem. Soc. Dalt. Trans.*, 1988, 1309–1314.

11 G. B. Boursalian, W. S. Ham, A. R. Mazzotti and T. Ritter, *Nat. Chem.*, 2016, **8**, 810–815.

12 F. Berger, M. B. Plutschack, J. Riegger, W. Yu, S. Speicher, M. Ho, N. Frank and T. Ritter, *Nature*, 2019, **567**, 223–228.

5 - Experimental

5.1 – General

All reagents were used were purchased from Sigma-Aldrich, Acros Organics, Alfa-Aesar or Strem Chemicals without further purification, unless otherwise stated. All solvents used were purchased directly from VWR or Sigma-Aldrich without further purification. All dried solvents used (except EtOH), were dried and deoxygenated by passing over anhydrous activated alumina columns using an Innovative Technology Inc. Ps-400-7 solvent purification (SPS) and stored under an atmosphere of nitrogen prior to use. EtOH was dried and deoxygenated by storing over dried 4 Å molecular sieves (Sigma-Aldrich) for 2 days and purging with a stream of argon gas for 30 mins.

Temperatures quoted are external. Solvents were removed under reduced pressure using a Büchi-Rotorvapor apparatus.

Analytical thin-layer chromatography (TLC) was performed on aluminium-backed plates coated with Alugram® SIL G/UV254 purchased from Macherey-Nagel and visualised with ultraviolet light (254 nm). Silica gel column chromatography was performed using 60 Å, 200-400 mesh particle size silica gel purchased from Sigma-Aldrich. Samples were loaded as saturated solutions in an appropriate solvent system.

All NMR measurements unless otherwise stated were performed at 25 °C (unless otherwise stated) on a Bruker 300 MHz or Agilent Technologies 500 MHz spectrometer (^{1}H NMR at 300 MHz or 500 MHz, ^{13}C NMR at 126 MHz or 75 MHz and ^{19}F NMR at 470 MHz and ^{11}B at 160 MHz and ^{31}P at 202 MHz). All ^{13}C spectra are ^{1}H decoupled unless stated otherwise. Shift values were reported in parts per million (ppm) relative to $Si(CH_3)_4$ or set internal solvent signals. ^{1}H chemical shifts are reported in ppm relative to $Si(CH_3)_4$ (δ 0) and were referenced internally with respect to the residual protic solvent impurity for $CDCl_3$, d^6-DMSO, d^3-MeOD or CD_3CN (δ 7.27 for $CHCl_3$, δ 2.62 for DMSO, δ 3.49 for MeOH, δ 1.94 for CH_3CN). ^{13}C chemical shifts are reported in ppm relative to $SiMe_4$ (δ 0) and were referenced internally with respect to the solvent for $CDCl_3$, d^6-DMSO or d^3-MeOD (δ 77.4 for $CDCl_3$, δ 40.5 for DMSO or δ 49.9 for MeOH). ^{19}F

chemical shifts are reported in ppm relative to $CFCl_3$ (δ 0). ^{31}P chemical shifts are reported in ppm relative to 85% H_3PO_4 in H_2O (δ 0). ^{11}B chemical shifts are reported in ppm relative to 15% $BF_3 \cdot Et_2O$ in $CDCl_3$ (δ 0). NMR data are presented in the following format: chemical shift, (number of apparent nuclei by integration, multiplicity [app = apparent, br=broad, d=doublet, t=triplet, q=quartet, dd=doublet of doublets, dt=doublet of triplets, dq=doublet of quartets, ddd=doublet of doublets of doublets, m=multiplet], coupling constant [in Hz], assignment).

Mass spectra were obtained using a micrOTOF electrospray time-of-flight (ESI-TOF) mass spectrometer (Bruker Daltonik) collecting data in the positive mode and using acetonitrile as a solvent. The peaks quoted correspond to the calculated exact mass, the correct isotope patterns are present where the peak is quoted. Infrared (IR) spectra were recorded on a Perkin-Elmer 1600 FT (Fourier transform) IR spectrophotometer, with absorbencies as reciprocal wavelength (ν [in cm^{-1}]). Melting points were obtained on a Bibby Sterilin SMP10 melting point machine and are uncorrected.

All differential pulse voltammograms (DPV's) were run in HPLC grade acetonitrile with ammonium tetrafluoroborate (NH_4BF_4), [0.1 M] as a supporting electrolyte. The concentration of samples was 100 μM throughout. Experiments were carried out using a Metrohm Autolab PGSTAT30 potentiostat controlled by a laptop running General Purpose Electrochemical System (GPES) software. All electrochemical experiments were run under ambient conditions (STP). A three-electrode cell was employed which consisted of a glassy carbon working electrode, a Pt wire auxiliary electrode and a saturated calomel electrode (SCE) reference electrode. A scan rate of 10 mV s^{-1} was used, unless otherwise stated. Cited potentials are referenced relative to a saturated calomel electrode (SCE). The electrochemical cell was not degassed before use on all experiments.

5.2 – Synthesis of 2-Aryl Pyridine Derivatives

5.2.1 – General Procedure **A**

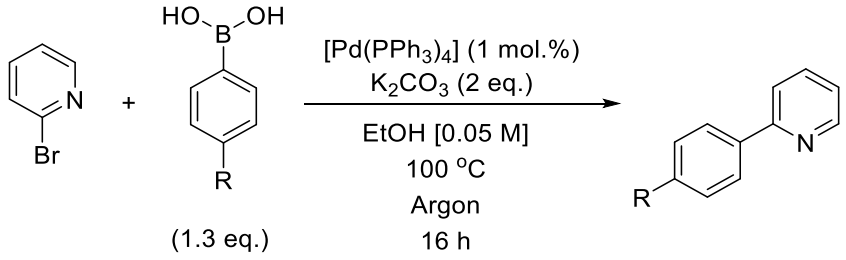

To an oven-dried, round bottomed flask equipped with a magnetic stirrer and condenser was added palladium tetrakis(triphenylphosphine) (1 mol.%), potassium carbonate (2 eq.), boronic acid (1.5 eq.) and ethanol (0.05 M). The flask and condenser were then purged with argon for *c.a.* 15 mins, and the 2-bromopyridine reagent (1 equiv.) were then added *via* syringe through a rubber septum located at the top of the condenser. The reaction was then heated to 100 °C and refluxed for 16 hours. After cooling the reaction to room temperature, the reaction mixture was filtered through a plug of celite, washing the solids with ethyl acetate. The crude reaction mixture was then dried over $MgSO_4$, filtered and concentrated under reduced pressure to yield crude product. The crude product was then purified by flash chromatography (40-60 Petroleum Ether/EtOAc) to yield the desired product.

5.2.2 – Synthesis of 2-(4-nitrophenyl)pyridine, **1b**

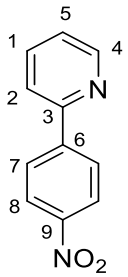

General Procedure **A** was followed using: 2-bromopyridine (0.43 mL, 4.5 mmol), 4-nitrophenyl boronic acid (1.00 g, 6.0 mmol), $[Pd(PPh_3)_4]$ (52 mg, 0.045 mmol), K_2CO_3 (1.24 g, 9.0 mmol) and EtOH (90 mL). Column chromatography (5% EtOAc/ Hexanes) yielded an amorphous yellow solid **1b**, 90% (806 mg).

^{1}H NMR (500 MHz, $CDCl_3$): δ 8.76–8.75 (1H, m, C(5)-*H*), 8.34–8.32 (2H, m, C(8)-*H*), 8.19–8.17 (2H, m, C(2)-*H*, C(6)-*H*), 7.84–7.82 (2H, m, C(7)-*H*), 7.36–7.33 (1H, m, C(1)-*H*).

^{13}C{^{1}H} NMR (126 MHz, $CDCl_3$): δ 154.9 (Ar*C*), 150.1 (Ar*C*H), 148.1 (Ar*C*), 145.2 (Ar*C*H), 137.1 (Ar*C*H), 127.7 (Ar*C*H), 124.0 (Ar*C*H), 123.5 (Ar*C*H), 121.2 (Ar*C*H).

These are in accordance with literature data.[1]

5.2.3 - Synthesis of 2-(4-methoxypenyl) pyridine, **1c**

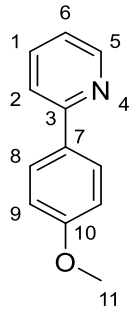

General Procedure **A** was followed using: 2-bromopyridine (0.47 mL, 4.95 mmol),4-methoxyphenyl boronic acid (1.00 g, 6.6 mmol), $[Pd(PPh_3)_4]$ (57 mg, 0.05 mmol), K_2CO_3 (1.37 g, 9.9 mmol) and EtOH (55 mL). Column chromatography (5% EtOAc/ Hexanes) yielded an amorphous white solid, **1c**, >99% (917 mg).

^{1}H NMR (500 MHz, $CDCl_3$): δ 8.67–8.64 (1H, ddd, J = 4.8, 1.7, 1.3 Hz ,C-(5)-*H*), 7.95 (2H, d, J = 8.9 Hz, C(8)-*H*), 7.73–7.65 (2H, m, C(1)-*H*, C(6)-*H*), 7.19–7.15 (1H, ddd, J = 7.2, 4.8, 1.3 Hz, C(2)-*H*), 7.00 (2H, d, J = 8.9 Hz, C(9)-*H*), 3.87 (3H, s, C(11)-*H*).

^{13}C{^{1}H} NMR (126 MHz, $CDCl_3$): δ 160.4 (Ar*C*), 157.1 (Ar*C*), 149.5 (Ar*C*H), 136.6 (Ar*C*H), 132.0 (Ar*C*), 128.2 (Ar*C*H), 121.4 (Ar*C*H), 119.8 (Ar*C*H), 114.1 (Ar*C*H), 55.3 (O*C*H_3).

These are in accordance with literature data.[1]

5.2.4 – Synthesis of 2-(4-(trifluoromethyl)phenyl) pyridine, **1d**

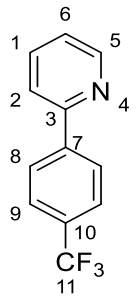

General procedure **A** was followed using: 2-bromopyridine (0.38 mL, 3.95 mmol), (4-(trifluoromethyl) phenyl) boronic acid (1.00 g, 5.27 mmol), [$Pd(PPh_3)_4$] (46 mg, 0.04 mmol), K_2CO_3 (1.09 g, 7.9 mmol) and EtOH (60 mL). Column chromatography (5% EtOAc/ Hexanes) yielded a white amorphous solid, **1d**, 89% (785 mg).

^{1}H NMR (500 MHz, $CDCl_3$): δ 8.75–8.71 (1H, d, J = 4.7 Hz, C(5)-*H*), 8.13–8.10 (2H, m, C(8)-*H*), 7.83–7.76 (2H, m, C(1)-*H*, C(2)-*H*), 7.73 (2H, d, J = 8.2 Hz, C(9)-*H*), 7.30 (1H, dd, J = 4.7, 1.4 Hz, C(6)-*H*).

^{13}C{^{1}H} NMR (126 MHz, $CDCl_3$): δ 156.1 (Ar*C*), 149.8 (Ar*C*H), 143.0 (Ar*C*H), 138.1 (Ar*C*H), 131.3 (q, J = 32.5 Hz, Ar*C*), 127.8 (Ar*C*H), 124.9 (q, J = 3.8 Hz, Ar*C*H), 123.7 (q, J = 272.0 Hz, Ar-*C*F_3), 122.9 (Ar*C*H), 121.0 (Ar*C*H).

^{19}F NMR (470 MHz, $CDCl_3$): δ -62.62 (s, 3F).

These are in accordance with literature data.[2]

5.2.5 – Synthesis of Ethyl 4-(pyridin-2-yl) benzoate, **1e**

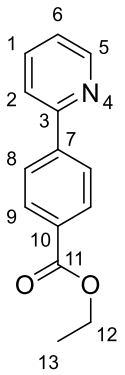

General procedure **A** was followed using: 2-bromopyridine (0.38 mL, 3.86 mmol), (4-(ethoxycarbonyl) phenyl) boronic acid (1.00 g, 5.15 mmol), [$Pd(PPh_3)_4$] (45 mg, 0.039 mmol), K_2CO_3 (1.07 g, 7.72 mmol) and EtOH (60 mL). Column chromatography (5% EtOAc/ Hexanes) yielded an amorphous white solid, **1e**, 79% (689 mg).

^{1}H NMR (500 MHz, $CDCl_3$): δ 8.73 (1H, d, J = 4.8 Hz, C(5)-*H*), 8.16–8.13 (2H, m, C(8)-*H*), 8.08–8.06 (2H, m, C(9)-*H*), 7.79–7.77 (2H, m, C(1)-*H*, C(2)-*H*), 7.31–7.27 (1H, m, C(6)-*H*), 4.41 (2H, q, J = 7.1 Hz, C(12)-*H*), 1.42 (3H, t, J = 7.1 Hz, C(13)-*H*).

^{13}C{^{1}H} NMR (126 MHz, $CDCl_3$): δ 166.6 (*C*=O), 156.4 (Ar*C*), 149.9 (Ar*C*H), 143.4 (Ar*C*), 137.2 (Ar*C*), 130.9 (Ar*C*H), 130.2 (Ar*C*H), 127.0 (Ar*C*H), 123.0 (Ar*C*H), 121.2 (Ar*C*H), 61.2 (*C*(17)), 14.5 (*C*(18)).

These are in accordance with literature data.[3]

5.2.6 – Synthesis of 2-([1,1'-biphenyl]-4-yl) pyridine, 1f

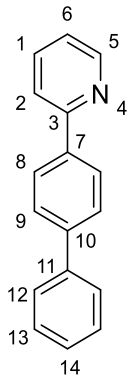

General procedure **A** was followed using: 2-bromopyridine (0.36 mL, 3.79 mmol), [1,1'-biphenyl]-4-yl boronic acid (1.00 g, 5.05 mmol), [$Pd(PPh_3)_4$] (44 mg, 0.038 mmol), K_2CO_3 (1.05 g, 7.58 mmol) and EtOH (60 mL). Column chromatography (5% EtOAc/ Hexanes) yielded an amorphous pink solid, **1f**, 92% (803 mg).

^{1}H NMR (500 MHz, $CDCl_3$): δ 8.73–8.71 (1H, m, C(5)-*H*), 8.10–8.07 (2H, m, C(8)-*H*), 7.79–7.76 (2H, m, C(9)-*H*), 7.74–7.71 (2H, m, C(12)-*H*), 7.67 (1H, dd, J = 2.2, 1.4 Hz, C(1)-*H*), 7.67–7.65 (1H, m, C(14)-*H*), 7.49–7.45 (2H, m, C(13)-*H*), 7.39–7.35 (1H, m, C(2)-*H*), 7.25 (1H, dd, J = 4.8, 2.2 Hz, C(6)-*H*).

$^{13}C\{^{1}H\}$ NMR (126 MHz, $CDCl_3$): δ 157.0 (Ar*C*), 149.7 (Ar*C*H), 141.7 (Ar*C*), 140.6 (Ar*C*), 138.3 (Ar*C*), 136.7 (Ar*C*H), 128.8 (Ar*C*H), 127.5 (Ar*C*H), 127.4 (Ar*C*H), 127.3 (Ar*C*H), 127.1 (Ar*C*H), 122.1 (Ar*C*H), 120.4 (Ar*C*H).

These are in accordance with literature data.[4]

5.2.7 – Synthesis of 2-(4-(trifluoromethoxy) phenyl) pyridine, **1g**

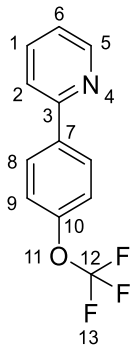

General procedure **A** was followed using: 2-bromopyridine (0.35 mL, 3.64 mmol), (4-(trifluoromethoxy) phenyl) boronic acid (1.00 g, 4.86 mmol), $[Pd(PPh_3)_4]$ (42 mg, 0.036 mmol), K_2CO_3 (1.01 g, 7.28 mmol) and EtOH (60 mL). Column chromatography (5% EtOAc/ Hexanes) yielded a white solid, **1g**, 93% (807 mg).

Melting point: 53–55 ˚C.

^{1}H NMR (500 MHz, $CDCl_3$): δ 8.70 (1H, ddd, *J* = 4.8, 1.8, 1.0 Hz, C(5)-*H*), 8.04–8.01 (2H, m, C(8)-*H*), 7.79–7.70 (2H, m, C(1)-*H*, C(2)-*H*), 7.32–7.31 (2H, m, C(9)-*H*), 7.27–7.26 (1H, m, C(6)-*H*).

$^{13}C\{^{1}H\}$ NMR (126 MHz, $CDCl_3$): δ 156.1 (Ar*C*), 149.9 (Ar*C*H), 149.8 (q, *J* = 2.4 Hz, ArC), 138.0 (Ar*C*H), 136.9 (Ar*C*H), 128.4 (Ar*C*), 122.4 (Ar*C*H), 121.0 (Ar*C*H), 120.4 (q, *J* = 255 Hz, Ar-O*C*F_3), 119.9 (Ar*C*H).

^{19}F NMR (470 MHz, $CDCl_3$): δ -57.77 (3F, s).

These are in accordance with literature data. [5]

5.2.8 – Synthesis of 2-(4fluorophenyl) pyridine, **1h**

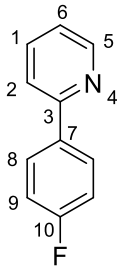

General procedure **A** was followed using: 2-bromopyridine (0.51 mL, 5.36 mmol), (4-fluorophenyl) boronic acid (1.00 g, 7.15 mmol), $[Pd(PPh_3)_4]$ (62 mg, 0.054 mmol), K_2CO_3 (1.48 g, 10.72 mmol) and EtOH (60 mL). Column chromatography (5% EtOAc/ Hexanes) yielded a white solid, **1h**, 62% (580 mg).

Melting point: 40–42 °C.

^{1}H NMR (500 MHz, $CDCl_3$): δ 8.68 (1H, ddd, *J* = 4.8, 1.6, 0.9 Hz, C(5)-*H*), 7.98 (2H, dd, *J* = 8.7, 5.4 Hz, C(8)-*H*), 7.77–7.72 (1H, m, C(1)-*H*), 7.68-7.64 (1H, m, C(2)-*H*), 7.22 (1H, ddd, *J* = 7.4, 4.8, 1.1 Hz, C(6)-*H*), 7.18-7.14 (2H, m, C(9)-*H*).

^{13}C{^{1}H} NMR (126 MHz, $CDCl_3$): δ 164.5 (d, *J* = 248 Hz, Ar*C*-F), 156.5 (Ar*C*), 149.7 (Ar*C*H), 136.8 (d, *J* = 4.1 Hz, Ar*C*H), 128.6 (d, *J* = 9.0 Hz, ArCH), 122.0 (Ar*C*), 120.2 (Ar*C*H), 115.5 (d, *J* = 21.6 Hz, Ar*C*H), 110.0 (Ar*C*H).

^{19}F NMR (470 MHz, $CDCl_3$): δ -113.23 (1F, ddd, *J* = 21.6, 9.0, 4.1 Hz).

These are in accordance with literature data.[6]

5.2.9 – Synthesis of 2-(4-chlorophenyl) pyridine, **1i**

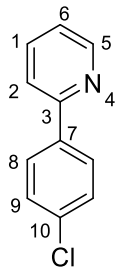

General procedure **A** was followed using: 2-bromopyridine (0.46 mL, 4.79 mmol), (4-chlorophenyl) boronic acid (1.00 g, 6.39 mmol), [$Pd(PPh_3)_4$] (55 mg, 0.048 mmol), K_2CO_3 (1.32 g, 9.58 mmol) and EtOH (60 mL). Column chromatography (5% EtOAc/ Hexanes) yielded an amorphous white solid, **1i**, 86% (782 mg).

Melting point: 49–51 °C.

^{1}H NMR (500 MHz, $CDCl_3$): δ 8.69 (1H, ddd, J = 4.8, 1.8, 1.0 Hz, C(5)-*H*), 7.95 (2H, d, J = 8.4 Hz, C(8)-*H*), 7.77–7.69 (2H, m, C(1)-*H*, C(2)-*H*), 7.46–7.43 (2H, d, J = 8.4 Hz, C(9)-*H*), 7.24 (1H, ddd, J = 7.4, 4.8, 1.2 Hz, C(6)-*H*).

^{13}C{^{1}H} NMR (126 MHz, $CDCl_3$): δ 156.2 (Ar*C*), 149.7 (Ar*C*H), 137.8 (Ar*C*), 136.8 (Ar*C*), 135.1 (Ar*C*H), 128.9 (Ar*C*H), 128.2 (Ar*C*H), 122.3 (Ar*C*H), 120.3 (Ar*C*H).

These are in accordance with literature data.[7]

5.2.10 – Synthesis of 2-(4-bromophenyl) pyridine, **1j**

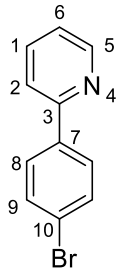

General procedure **A** was followed using: 2-bromopyridine (0.36 mL, 3.73 mmol), (4-bromophenyl) boronic acid (1.00 g, 4.98 mmol), [$Pd(PPh_3)_4$] (43 mg, 0.037 mmol), K_2CO_3 (1.03 g, 7.46 mmol) and EtOH (50 mL). Column chromatography (5% EtOAc/ Hexanes) yielded an off-white solid, **1j**, 18% (161 mg).

Melting point: 60–62 °C.

^{1}H NMR (500 MHz, $CDCl_3$): δ 8.72 – 8.71 (1H, d, J = 4.8 Hz, C(5)-*H*), 8.08 – 8.07 (2H, d, J = 8.1 Hz, C(8)-*H*), 7.78 – 7.77 (1H, m, C(1)-*H*), 7.68 – 7.65 (1H, m, C(2)-*H*), 7.49 – 7.45 (2H, d, J = 8.1 Hz, C(9)-*H*), 7.25 – 7.23 (1H, m, C(6)-*H*).

$^{13}C\{^1H\}$ NMR (126 MHz, $CDCl_3$): δ 156.2 (Ar*C*), 149.7 (Ar*C*H), 136.8 (Ar*C*), 131.9 (Ar*C*H), 128.8 (Ar*C*H), 128.7 (Ar*C*H), 127.4 (Ar*C*H), 127.1 (Ar*C*H), 122.1 (Ar*C*), 117.2 (Ar*C*H).

These are in accordance with literature data.[7]

5.2.11 – Synthesis of 2-(4-(methylthio)phenyl) pyridine, **1k**

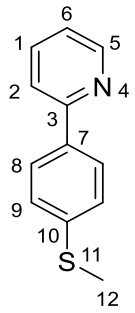

General procedure **A** was followed using: 2-bromopyridine (0.19 mL, 1.99 mmol), (4-(methylthio)phenyl) boronic acid (555 mg, 3.3 mmol), $[Pd(PPh_3)_4]$ (23 mg, 0.020 mmol), K_2CO_3 (0.55 g, 4 mmol) and EtOH (30 mL). Column chromatography (5% EtOAc/ Hexanes) yielded a pink solid, **1k**, 85% (471 mg).

Melting point: 50-52 °C.

^1H NMR (500 MHz, $CDCl_3$): δ 8.67 (1H, dd, *J* = 4.9, 1.9 Hz, C(5)-*H*), 7.93 (2H, d, *J* = 8.5 Hz, C(8)-*H*), 7.76 – 7.68 (2H, m, C(1)-*H*, C(2)-*H*), 7.34 (2H, d, *J* = 7.4 Hz, C(9)-*H*), 7.21 (1H, ddd, *J* = 7.0, 4.9, 1.3 Hz, C(6)-*H*), 2.53 (3H, s, C(12)-*H*).

$^{13}C\{^1H\}$ NMR (126 MHz, $CDCl_3$): δ 156.8 (Ar*C*), 149.6 (Ar*C*H), 139.8 (Ar*C*), 136.8 (Ar*C*H), 136.0 (Ar*C*), 127.2 (Ar*C*H), 126.4 (Ar*C*H), 121.9 (Ar*C*H), 120.1 (Ar*C*H), 15.6 (-S*C*H_3).

These are in accordance with literature data.[8]

5.3 – Optimisation for the *meta* alkylation of primary substrates

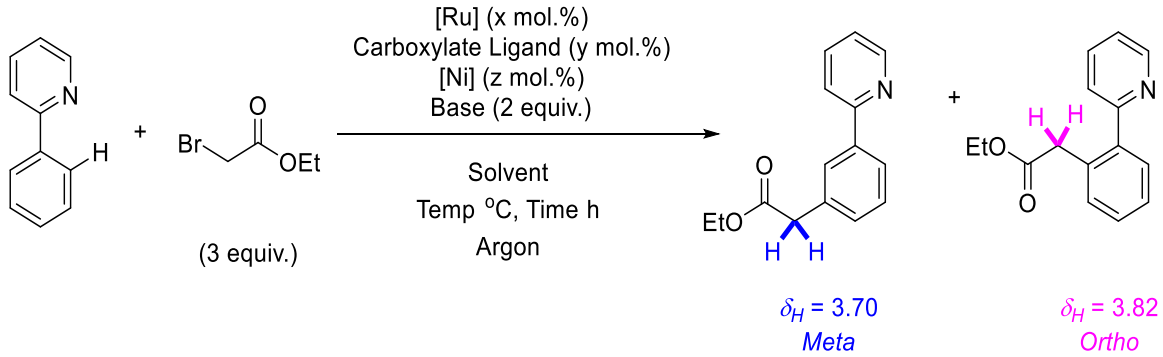

Proton NMR conversions were taken from the *ortho* diagnostic protons. Two products were formed over the course of the reaction (competing *ortho* and *meta* selectivity, predominantly *meta* product) lead to ^{1}H NMR conversions being indicative of combined yield of alkylated products. *Ortho*:*meta* calculated using the corresponding benzyl peaks: *ortho* δ 3.82 ppm (s, 2H): *meta* δ 3.70 ppm (s, 2H). Major product consistent with *meta* substituted product and is fully characterised later (Section **5.3.3**). Minor isomer consistent with the *ortho* substituted product. An example of the ^{1}H NMR spectrum of the *ortho* substituted product is shown in Figure **18**. Conversion by ^{1}H NMR of Crude Reaction Mixture: Signal at 7.93 ppm (1H, s) from *meta* product and signal at 8.02 – 7.98 (2H, m) from starting material used for conversion calculation.

$$\%\ \text{Conversion from Starting Material} = \frac{2 \times \int \text{Starting Material (ortho)}}{\int \text{meta Product (ortho)}} \times 100$$

The ratio of *ortho*:*meta* product was then calculated using the ratio of the benzyl peaks of each product, as denoted above.

Entry	Ruthenium Catalyst	Carboxylate Ligand	Additive	Base	Solvent	Conversion (%) (IY) (*m*:o)
1	$RuCl_3{\cdot}xH_2O$	1-$AdCO_2H$	$[NiCl_2(PPh_3)_2]$	K_2CO_3	1,4-Dioxane	**18**
2	$[RuCl_2(benzene)]_2$	1-$AdCO_2H$	$[NiCl_2(PPh_3)_2]$	K_2CO_3	1,4-Dioxane	**12**
3	$[RuCl_2(PPh_3)_3]$	1-$AdCO_2H$	$[NiCl_2(PPh_3)_2]$	K_2CO_3	1,4-Dioxane	**17**
4	$[RuH(CO)(PPh_3)_3]$	1-$AdCO_2H$	$[NiCl_2(PPh_3)_2]$	K_2CO_3	1,4-Dioxane	**0**
5	Grubbs 1st Gen	1-$AdCO_2H$	$[NiCl_2(PPh_3)_2]$	K_2CO_3	1,4-Dioxane	**20**
6	**$[RuCl_2$(*p*-cymene)$]_2$**	**1-$AdCO_2H$**	**$[NiCl_2(PPh_3)_2]$**	**K_2CO_3**	**1,4-Dioxane**	**61 (38) (9:1)**
7	$[RuCl_2$(*p*-cymene)$]_2$	KOAc	$[NiCl_2(PPh_3)_2]$	K_2CO_3	1,4-Dioxane	**0**
8	$[RuCl_2$(*p*-cymene)$]_2$	9-AnthCO_2H	$[NiCl_2(PPh_3)_2]$	K_2CO_3	1,4-Dioxane	**7**
9	$[RuCl_2$(*p*-cymene)$]_2$	PhCO_2H	$[NiCl_2(PPh_3)_2]$	K_2CO_3	1,4-Dioxane	**37**
10	$[RuCl_2$(*p*-cymene)$]_2$	PivCO_2H	$[NiCl_2(PPh_3)_2]$	K_2CO_3	1,4-Dioxane	**61**

11	$[RuCl_2(p\text{-cymene})]_2$	Piv-Val-OH	$[NiCl_2(PPh_3)_2]$	K_2CO_3	1,4-Dioxane	**16**
12	$[RuCl_2(p\text{-cymene})]_2$	$MesCO_2H$	$[NiCl_2(PPh_3)_2]$	K_2CO_3	1,4-Dioxane	**58**
13	$[RuCl_2(p\text{-cymene})]_2$	1-$AdCO_2H$	$[NiCl_2(PPh_3)_2]$	Na_2CO_3	1,4-Dioxane	**59**
14	$[RuCl_2(p\text{-cymene})]_2$	1-$AdCO_2H$	$[NiCl_2(PPh_3)_2]$	Ag_2CO_3	1,4-Dioxane	**20**
15	$[RuCl_2(p\text{-cymene})]_2$	1-$AdCO_2H$	$[NiCl_2(PPh_3)_2]$	Cs_2CO_3	1,4-Dioxane	**62**
16	$[RuCl_2(p\text{-cymene})]_2$	1-$AdCO_2H$	$[NiCl_2(PPh_3)_2]$	$AdCO_2Na$	1,4-Dioxane	**28**
17	$[RuCl_2(p\text{-cymene})]_2$	1-$AdCO_2H$	$Ni(OAc)_2{\cdot}4H_2O$	K_2CO_3	1,4-Dioxane	**0**
18	$[RuCl_2(p\text{-cymene})]_2$	1-$AdCO_2H$	$[NiCl_2(DME)]$	K_2CO_3	1,4-Dioxane	**0**
19	$[RuCl_2(p\text{-cymene})]_2$	1-$AdCO_2H$	$[NiBr_2(PPh_3)_2]$	K_2CO_3	1,4-Dioxane	**59 (33) (8:1)**
20	$[RuCl_2(p\text{-cymene})]_2$	1-$AdCO_2H$	$[Ni(COD)_2]$	K_2CO_3	1,4-Dioxane	**0**
21	$[RuCl_2(p\text{-cymene})]_2$	1-$AdCO_2H$	$[Ni(acac)_2]$	K_2CO_3	1,4-Dioxane	**0**
22	$[RuCl_2(p\text{-cymene})]_2$	1-$AdCO_2H$	$[NiCl_2(dppe)]$	K_2CO_3	1,4-Dioxane	**trace**
23	$[RuCl_2(p\text{-cymene})]_2$	1-$AdCO_2H$	$[NiCl_2(dppf)]$	K_2CO_3	1,4-Dioxane	**trace**
24	$[RuCl_2(p\text{-cymene})]_2$	1-$AdCO_2H$	$[NiCl_2(PCy_3)_2]$	K_2CO_3	1,4-Dioxane	**5**
25	$[RuCl_2(p\text{-cymene})]_2$	1-$AdCO_2H$	$Ni(NO_3)_2{\cdot}6H_2O$	K_2CO_3	1,4-Dioxane	**0**
26	$[RuCl_2(p\text{-cymene})]_2$	1-$AdCO_2H$	$NiCl_2{\cdot}6H_2O$	K_2CO_3	1,4-Dioxane	**0**
27	$[RuCl_2(p\text{-cymene})]_2$	1-$AdCO_2H$	$Ni(SO_4)_2{\cdot}6H_2O$	K_2CO_3	1,4-Dioxane	**11**
28	$[RuCl_2(p\text{-cymene})]_2$	1-$AdCO_2H$	$[NiCl_2(PPh_3)_2]$	K_2CO_3	2-MeTHF	**12**
29	$[RuCl_2(p\text{-cymene})]_2$	1-$AdCO_2H$	$[NiCl_2(PPh_3)_2]$	K_2CO_3	H_2O	**0**
30	$[RuCl_2(p\text{-cymene})]_2$	1-$AdCO_2H$	$[NiCl_2(PPh_3)_2]$	K_2CO_3	MePh	**3**
31	$[RuCl_2(p\text{-cymene})]_2$	1-$AdCO_2H$	$[NiCl_2(PPh_3)_2]$	K_2CO_3	MeCN	**0**
32	$[RuCl_2(p\text{-cymene})]_2$	1-$AdCO_2H$	$[NiCl_2(PPh_3)_2]$	K_2CO_3	DCE	**26**
33	$[RuCl_2(p\text{-cymene})]_2$	1-$AdCO_2H$	$[NiCl_2(PPh_3)_2]$	K_2CO_3	NMP	**2**
34	$[RuCl_2(p\text{-cymene})]_2$	1-$AdCO_2H$	$[NiCl_2(PPh_3)_2]$	K_2CO_3	DME	**22**
35	$[RuCl_2(p\text{-cymene})]_2$	1-$AdCO_2H$	$[NiCl_2(PPh_3)_2]$	K_2CO_3	*t*-BuOMe	**33**
36	$[RuCl_2(p\text{-cymene})]_2$	1-$AdCO_2H$	$[NiCl_2(PPh_3)_2]$	K_2CO_3	Cumene	**11**
37	$[RuCl_2(p\text{-cymene})]_2$	1-$AdCO_2H$	$[NiCl_2(PPh_3)_2]$	K_2CO_3	Diglyme	**17**
38	$[RuCl_2(p\text{-cymene})]_2$	1-$AdCO_2H$	$[NiCl_2(PPh_3)_2]$	K_2CO_3	*t*-amylOH	**48**
39[a]	$[RuCl_2(p\text{-cymene})]_2$	1-$AdCO_2H$	$[NiCl_2(PPh_3)_2]$	K_2CO_3	1,4-Dioxane	**43**
40[b]	$[RuCl_2(p\text{-cymene})]_2$	1-$AdCO_2H$	$[NiCl_2(PPh_3)_2]$	K_2CO_3	1,4-Dioxane	**0**
41	-	1-$AdCO_2H$	$[NiCl_2(PPh_3)_2]$	K_2CO_3	1,4-Dioxane	**0**
42	$[RuCl_2(p\text{-cymene})]_2$	1-$AdCO_2H$	-	K_2CO_3	1,4-Dioxane	**19***
43	**$[RuCl_2(p\text{-cymene})]_2$**	**$MesCO_2H$**	**PPh_3**	**K_2CO_3**	**1,4-Dioxane**	**60 (58) (19:1)**
44	$[RuCl(OAc)(p\text{-cymene})]$	-	PPh_3	K_2CO_3	1,4-Dioxane	**12**
45	$[Ru(OAc)_2(p\text{-cymene})]$	-	PPh_3	K_2CO_3	1,4-Dioxane	**15**
46	$[Ru(O_2CAd)_2(p\text{-cymene})]$	-	PPh_3	K_2CO_3	1,4-Dioxane	**20**
47	$[Ru(O_2CMes)_2(p\text{-cymene})]$	-	PPh_3	K_2CO_3	1,4-Dioxane	**23**
48	$[RuCl_2(p\text{-cymene})]_2$	$MesCO_2H$	PCy_3	K_2CO_3	1,4-Dioxane	**0**
49	$[RuCl_2(p\text{-cymene})]_2$	$MesCO_2H$	dppe	K_2CO_3	1,4-Dioxane	**<5**
50	$[RuCl_2(p\text{-cymene})]_2$	$MesCO_2H$	dppf	K_2CO_3	1,4-Dioxane	**<5**
51	$[RuCl_2(p\text{-cymene})]_2$	$MesCO_2H$	$P(4\text{-}(CF_3)(C_6H_4))_3$	K_2CO_3	1,4-Dioxane	**21**
52	$[RuCl_2(p\text{-cymene})]_2$	$MesCO_2H$	$P(4\text{-}F(C_6H_4))_3$	K_2CO_3	1,4-Dioxane	**38**
53	$[RuCl_2(p\text{-cymene})]_2$	$MesCO_2H$	PCy_3	K_2CO_3	1,4-Dioxane	**<5**
54	$[RuCl_2(p\text{-cymene})]_2$	$PhCO_2H$	PPh_3	K_2CO_3	1,4-Dioxane	**23**
55	$[RuCl_2(p\text{-cymene})]_2$	$AdCO_2H$	PPh_3	K_2CO_3	1,4-Dioxane	**29**
56	$[RuCl_2(p\text{-cymene})]_2$	KOAc	PPh_3	K_2CO_3	1,4-Dioxane	**54**
57	$[RuCl_2(p\text{-cymene})]_2$	$PivCO_2H$	PPh_3	K_2CO_3	1,4-Dioxane	**57**
58	$[RuCl_2(p\text{-cymene})]_2$	Piv-Val-OH	PPh_3	K_2CO_3	1,4-Dioxane	**<5**
59	$[RuCl_2(p\text{-cymene})]_2$	$MesCO_2H$	PPh_3	Na_2CO_3	1,4-Dioxane	**40**
60	$[RuCl_2(p\text{-cymene})]_2$	$MesCO_2H$	PPh_3	Ag_2CO_3	1,4-Dioxane	**17**
61	$[RuCl_2(p\text{-cymene})]_2$	$MesCO_2H$	PPh_3	Cs_2CO_3	1,4-Dioxane	**33**
62	$[RuCl_2(p\text{-cymene})]_2$	$MesCO_2H$	PPh_3	H_2KPO_4	1,4-Dioxane	**0**
63	$[RuCl_2(p\text{-cymene})]_2$	-	PPh_3	KOAc	1,4-Dioxane	**13**
64	$[RuCl_2(p\text{-cymene})]_2$	$NaCO_2Ad$	PPh_3	K_2CO_3	1,4-Dioxane	**21**
65	$[RuCl_2(p\text{-cymene})]_2$	$MesCO_2H$	PPh_3	K_2CO_3	2-MeTHF	**15**
66	$[RuCl_2(p\text{-cymene})]_2$	$MesCO_2H$	PPh_3	K_2CO_3	H_2O	**0**
67	$[RuCl_2(p\text{-cymene})]_2$	$MesCO_2H$	PPh_3	K_2CO_3	MePh	**26**
68	$[RuCl_2(p\text{-cymene})]_2$	$MesCO_2H$	PPh_3	K_2CO_3	MeCN	**0**
69	$[RuCl_2(p\text{-cymene})]_2$	$MesCO_2H$	PPh_3	K_2CO_3	NMP	**0**
70	$[RuCl_2(p\text{-cymene})]_2$	$MesCO_2H$	PPh_3 (10 mol.%)	K_2CO_3	1,4-Dioxane	**67 (47) (19:1)**
71	$[RuCl_2(p\text{-cymene})]_2$	$MesCO_2H$	PPh_3 (50 mol.%)	K_2CO_3	1,4-Dioxane	**68 (46) (>20:1)**
72	$[RuCl_2(p\text{-cymene})]_2$	$MesCO_2H$	PPh_3 (100 mol.%)	K_2CO_3	1,4-Dioxane	**6**
73[b]	$[RuCl_2(p\text{-cymene})]_2$	$MesCO_2H$	PPh_3	K_2CO_3	1,4-Dioxane	**0**
74[c]	$[RuCl_2(p\text{-cymene})]_2$	1-$AdCO_2H$	$NiCl_2{\cdot}6H_2O$ + PPh_3	K_2CO_3	1,4-Dioxane	**53 (30) (9:1)**

[a] Reaction done in air [b] 100 ˚C * 1:1 (*ortho:meta*)

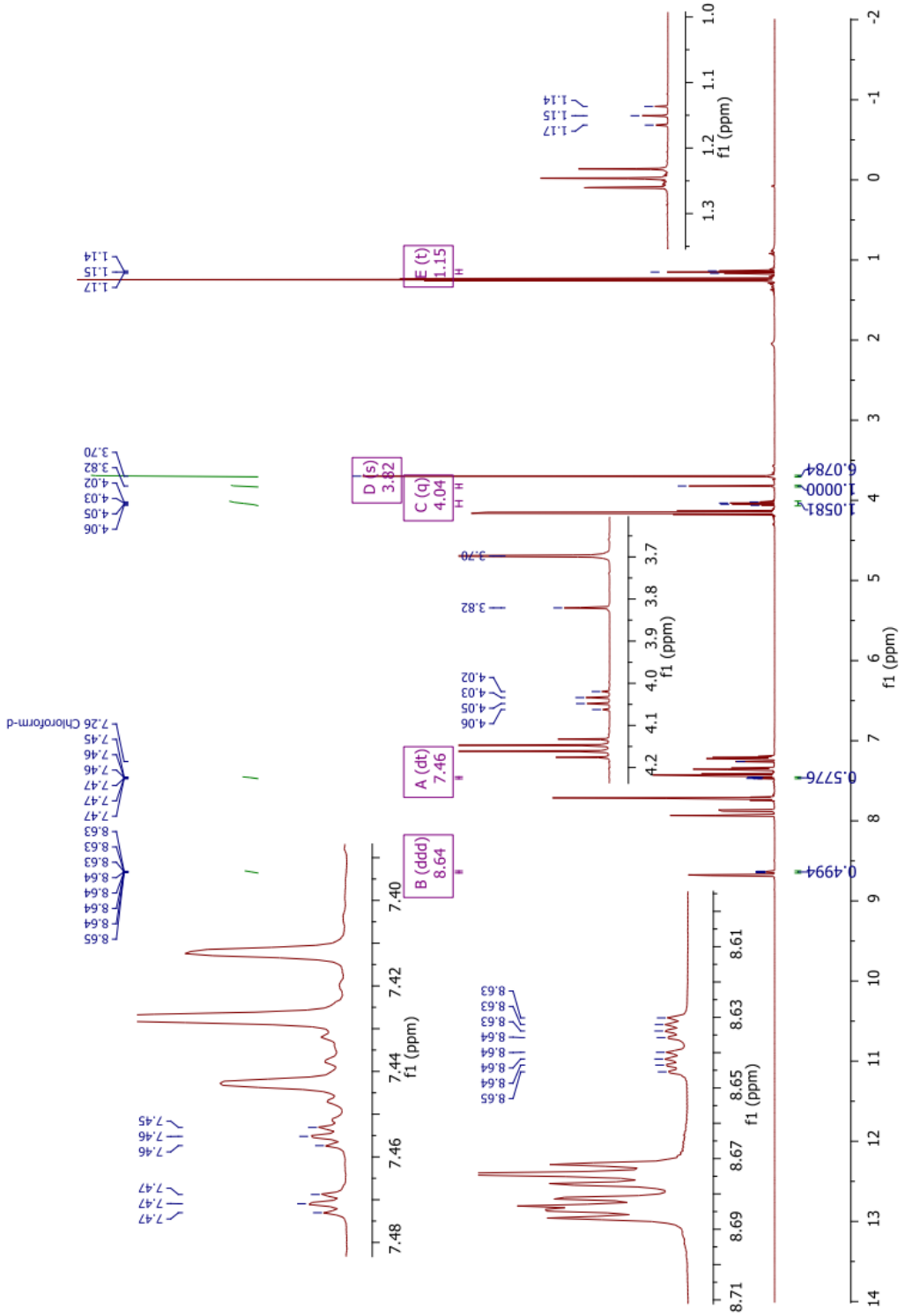

Figure 18: Example spectrum of mixed *ortho* and *meta* alkylation products, with the *ortho* and *meta* peaks used to determine the regioselectivity shown.

5.4 – Scope of Ruthenium Catalysed *meta* C-H Alkylation of Primary Substrates

5.4.1 – General Procedure **A** for the Formation of ethyl 2-(3-(pyridin-2-yl) phenyl) acetates

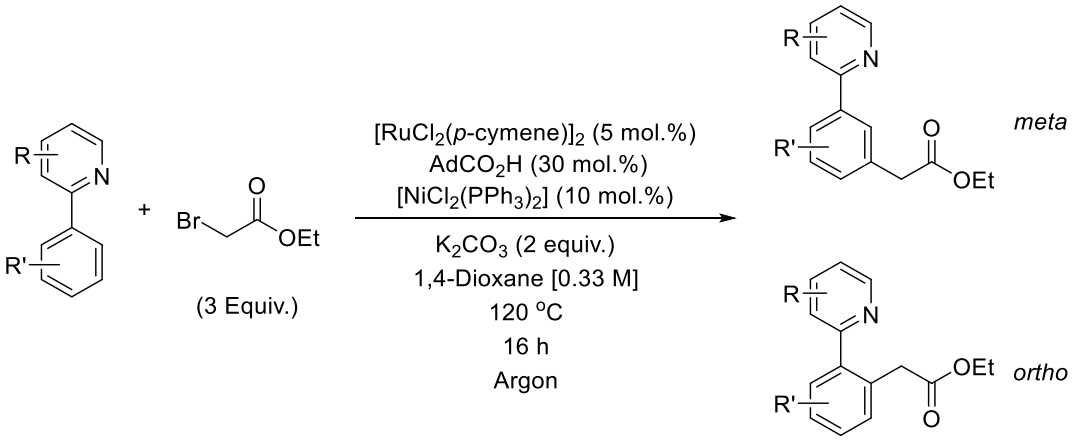

To an oven dried, argon purged carousel tube equipped with magnetic stirrer was added $[RuCl_2(p\text{-cymene})]_2$ (15 mg, 0.025 mmol), 1-adamantane carboxylic acid (27 mg, 0.15 mmol), $[NiCl_2(PPh_3)_2]$ (33 mg, 0.05 mmol), K_2CO_3 (138 mg, 1.0 mmol), phenylpyridine derivative (0.5 mmol), 1,4-dioxane (1.5 mL) and ethyl bromoacetate (0.17 mL, 1.5 mmol). The carousel tube was then sealed and refluxed in a carousel reactor at 120 °C for 16 h. After cooling to room temperature, the reaction mixture was dry loaded onto silica and purified by flash chromatography (40/60 Petroleum Ether/ Ethyl Acetate) to yield the desired product.

5.4.2 – General procedure **B** for the formation of ethyl 2-(3-(pyridine-2-yl) phenyl) acetates

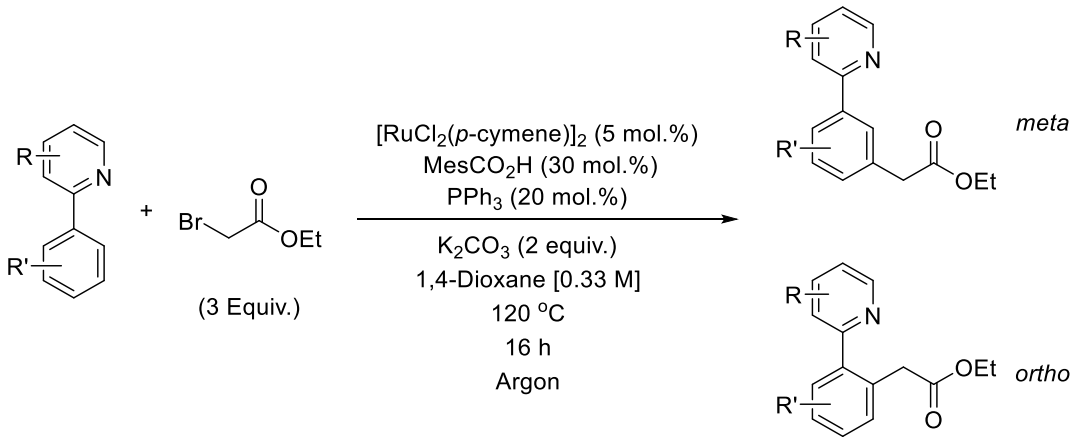

To an oven dried, argon purged carousel tube equipped with magnetic stirrer was added $[RuCl_2(p\text{-cymene})]_2$ (15 mg, 0.025 mmol), 2,4,6-trimethylbenzoic acid (25 mg, 0.15 mmol), PPh_3 (26 mg, 0.10 mmol), K_2CO_3 (138 mg, 1.0 mmol), the substrate molecule (0.5 mmol), 1,4-dioxane (1.5 mL) and ethyl bromoacetate (0.17 mL, 1.5 mmol). The carousel tube was then sealed and refluxed in a carousel reactor at 120 ˚C for 16 h. After cooling to room temperature, the reaction mixture was dry loaded onto silica and purified by flash chromatography (40/60 Petroleum Ether/ Ethyl Acetate) to yield the desired product.

5.4.3 – Synthesis of ethyl 2-(3-(pyridin-2-yl)phenyl)acetate, **1.1**

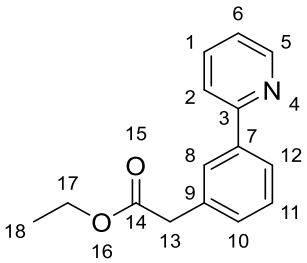

General procedure **A** was followed using the following compounds: 2-phenylpyridine (0.07 mL, 0.5 mmol), ethyl bromoacetate (0.17 mL, 1.5 mmol), $[RuCl_2(p\text{-cymene})]_2$ (15 mg, 0.025 mmol), $[NiCl_2(PPh_3)_2]$ (33 mg, 0.05 mmol), 1-adamantanecarboxylic acid (27 mg, 0.15 mmol), K_2CO_3 (138 mg, 1 mmol) and 1,4-dioxane (1.5 mL). Column

chromatography (10% EtOAc/ hexanes) yielded the title compound as a colourless oil, **1.1**, 38% (45 mg).

*When general conditions **B** were used with the following reagents: PPh_3 (26 mg, 0.1 mmol) and 2,4,6-trimethylbenzoic acid (25 mg, 0.15 mmol) were used instead of $[NiCl_2(PPh_3)_2]$ and 1-adamantanecarboxylic acid respectively, the title compound was obtained as a colourless oil, 54% (69 mg).

^{1}H NMR (500 MHz, $CDCl_3$): δ 8.68 (1H, dd, J = 5.0, 1.2 Hz, C(5)-*H*), 7.93 (1H, s, C(8)-*H*), 7.87 (1H, d, J = 7.8 Hz, C(12)-*H*), 7.75 – 7.69 (2H, m, C(10)-*H*, C(11)-*H*), 7.43 (1H, dd, J = 7.7, 5.4 Hz, C(1)-*H*), 7.35 (1H, d, J = 7.7 Hz, C(2)-*H*), 7.21 (1H, ddd, J = 5.4, 5.0, 2.8 Hz, C(6)-*H*), 4.15 (2H, q, J = 7.1 Hz, C(17)-*H*), 3.70 (2H, s, C(13)-*H*), 1.25 (3H, t, J = 7.1 Hz, C(18)-*H*).

^{13}C{^{1}H} NMR (126 MHz, $CDCl_3$): δ 171.6 (*C*=O), 157.3 (Ar*C*), 149.7 (Ar*C*H), 139.8 (Ar*C*), 136.8 (Ar*C*), 134.8 (Ar*C*H), 129.9 (Ar*C*H), 129.0 (Ar*C*H), 128.0 (Ar*C*H), 125.7 (Ar*C*H), 122.3 (Ar*C*H), 120.7 (Ar*C*H), 61.0 (O-*C*H_2), 41.5 ((C=O)-*C*H_2-), 14.3 (*C*H_3)

HR-MS (ESI) *m/z*: calculated for $C_{15}H_{15}NO_2$ requires 264.1000 for $[M+Na]^+$ found 264.1005.

FTIR (thin film): ν_{max} = 3021, 2160, 2029, 1729, 1587, 1464, 1369, 1335 cm^{-1}.

5.4.4 - Synthesis of ethyl 2-3-(1*H*-pyrazol-1-yl)phenyl)acetate, 1.2

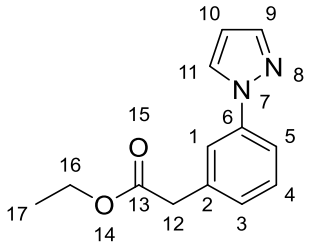

General procedure **B** was followed using the following compounds: 1-phenylpyrazole (0.07 mL, 0.5 mmol), ethyl bromoacetate (0.17 mL, 1.5 mmol), $[RuCl_2(p\text{-cymene})]_2$ (15 mg, 0.025 mmol), $[NiCl_2(PPh_3)_2]$ (33 mg, 0.05 mmol), 1-adamantanecarboxylic acid (27 mg, 0.15 mmol), K_2CO_3 (138 mg, 1 mmol) and 1,4-dioxane (1.5 mL). Column

chromatography (10% EtOAc/ hexanes) yielded the title compound as a yellow oil, **1.2**, 58% (67 mg).

*When general conditions **A** were used with the following reagents: PPh_3 (26 mg, 0.1 mmol) and 2,4,6-trimethylbenzoic acid (25 mg, 0.15 mmol) were used instead of $[NiCl_2(PPh_3)_2]$ and 1-adamantanecarboxylic acid respectively, the title compound was obtained as a colourless oil, 39% (45 mg).

^{1}H NMR (500 MHz, $CDCl_3$): δ 7.92 (1H, d, J = 2.3 Hz, C(11)-*H*), 7.70 (1H, d, J = 1.5 Hz, C(9)-*H*), 7.65 (1H, t, J = 1.5 Hz, C(1)-*H*), 7.58 (1H, dd, J = 8.1, 1.2 Hz, C(5)-*H*), 7.38 (1H, d, J = 8.1 Hz, C(3)-*H*), 7.20 (1H, dd, J = 8.1, 1.5 Hz, C(4)-*H*), 6.45 (1H, d, J = 2.3 Hz, C(10)-*H*), 4.15 (2H, q, J = 7.1 Hz, C(16)-*H*), 3.66 (2H, s, C(12)-*H*), 1.25 (3H, t, J = 7.1 Hz, C(17)-*H*).

^{13}C{^{1}H} NMR (126 MHz, $CDCl_3$): δ 171.0 (*C*=O), 141.1 (Ar*C*H), 140.4 (Ar*C*) 129.5 (Ar*C*), 127.3 (Ar*C*H), 126.8 (Ar*C*H), 126.1 (Ar*C*H), 120.2 (Ar*C*H), 117.8 (Ar*C*H), 107.6 (Ar*C*H), 61.0 (O-*C*H_2-CH_3), 41.2 ((C=O)-*C*H_2-), 14.6 (O-CH_2-*C*H_3).

HR-MS (ESI) *m/z*: calculated for $C_{13}H_{14}N_2O_2$ requires 253.0953 for $[M+Na]^+$ found 253.0960.

FTIR (thin film): ν_{max} = 2981, 2254, 2161, 2031, 1730, 1610, 1595, 1520, 1502, 1476, 1454, 1394, 1370, 1331 cm^{-1}.

5.4.5 – Synthesis of ethyl 2-(3-(pyrimidin-2-yl)phenyl)acetate, 1.3

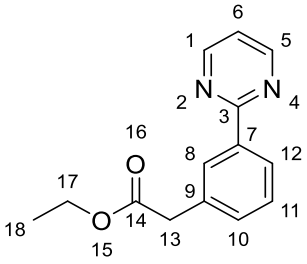

General procedure **B** was followed using the following compounds: 2-phenylpyrimidine (78 mg, 0.5 mmol), ethyl bromoacetate (0.17 mL, 1.5 mmol), $[RuCl_2(p\text{-cymene})]_2$ (15 mg, 0.025 mmol), PPh_3 (26 mg, 0.1 mmol), 2, 4, 6-trimethylbenzoic acid (25 mg, 0.15

mmol), K_2CO_3 (138 mg, 1 mmol) and 1,4-dioxane (1.5 mL). Column chromatography (10% EtOAc/ hexanes) yielded the title compound a colourless oil, **1.3**, 36% (44 mg).

^{1}H NMR (500 MHz, $CDCl_3$): δ 8.79 (2H, d, J = 4.8 Hz, C(1)-*H*, C(5)-*H*), 8.37 (1H, d, J = 1.6 Hz, C(8)-*H*), 8.35 (1H, dd, J = 7.4, 1.6 Hz, C(12)-*H*), 7.48 – 7.41 (2H, m, C(10)-*H*, C(11)-*H*), 7.17 (1H, t, J = 4.8 Hz, C(6)-*H*), 4.16 (2H, q, J = 7.1 Hz, C(17)-*H*), 3.71 (2H, s, C(13)-*H*), 1.24 (3H, t, J = 7.1 Hz, C(18)-*H*).

^{13}C{^{1}H} NMR (126 MHz, $CDCl_3$): δ 171.6 (*C*=O), 164.6 (Ar*C*), 157.3 (2C, Ar*C*H), 138.0 (Ar*C*), 134.7 (Ar*C*), 131.8 (Ar*C*H), 129.2 (Ar*C*H), 129.0 (Ar*C*H), 127.0 (Ar*C*H), 119.3 (Ar*C*H), 61.0 (O-*C*H_2-CH_3), 41.5 ((C=O)-*C*H_2-), 14.3(O-CH_2-*C*H_3).

HR-MS (ESI) *m/z*: calculated for $C_{14}H_{14}N_2O_2$ requires 243.1134 for $[M+H]^+$ found 243.1121.

FTIR (thin film): ν_{max} = 2981, 2252, 2165, 2025, 1730, 1603, 1568, 1556, 1498, 1454, 1374 cm^{-1}.

5.4.6 – Synthesis of ethyl 2-(3-(5-fluoropyridin-2-yl)phenyl)acetate, 1.4

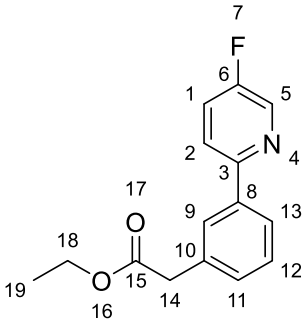

General procedure **B** was followed using the following compounds: 5-fluoro-2-phenylpyridine (87 mg, 0.5 mmol), ethyl bromoacetate (0.17 mL, 1.5 mmol), $[RuCl_2(p\text{-cymene})]_2$ (15 mg, 0.025 mmol), PPh_3 (26 mg, 0.1 mmol), 2, 4, 6-trimethylbenzoic acid (25 mg, 0.15 mmol), K_2CO_3 (138 mg, 1 mmol) and 1,4-dioxane (1.5 mL). Column chromatography (10% EtOAc/ hexanes) yielded the title compound a colourless oil, **1.4**, 23% (30 mg).

^{1}H NMR (500 MHz, $CDCl_3$): δ 8.54 (1H, d, *J* = 2.9 Hz, C(5)-*H*), 7.88 (1H, t, *J* = 1.5 Hz, C(9)-*H*), 7.84 – 7.79 (1H, m, C(13)-*H*), 7.72 (1H, ddd, *J* = 8.8, 4.2, 0.4 Hz, C(12)-*H*), 7.49 – 7.45 (2H, m, C(1)-*H*, C(11)-*H*), 7.43 (1H, t, *J* = 7.5 Hz, C(2)-*H*), 4.17 (2H, q, *J* = 7.1 Hz, C(18)-*H*), 3.70 (2H, s, C(14)-*H*), 1.26 (3H, t, *J* = 7.1 Hz, C(19)-*H*).

^{13}C{^{1}H} NMR (126 MHz, $CDCl_3$): δ 171.6 (*C*=O), 159.0 (d, *J* = 256.2 Hz, (Ar*C*-F), 153.7, (d, *J* = 3.9 Hz, Ar*C*), 138.9 (Ar*C*H), 137.9 (d, *J* = 23.5 Hz, Ar*C*H), 134.9 (Ar*C*), 130.0 (Ar*C*H), 129.2 (Ar*C*H), 128.0 (Ar*C*H), 125.7 (Ar*C*H), 123.7 (d, *J* = 18.5 Hz, Ar*C*H), 121.6 (d, *J* = 4.3 Hz, Ar*C*H), 61.1 (O-*C*H_2-CH_3), 41.5 ((C=O)-*C*H_2-), 14.4 (O-CH_2-*C*H_3).

^{19}F NMR (470 MHz, $CDCl_3$): δ -129.64 – -129.69 (m, 1F).

HR-MS (ESI) *m/z*: calculated for $C_{15}H_{14}NO_2F$ requires 260.1087 for $[M+H]^+$ found 260.1085.

FTIR (thin film): ν_{max} = 2981, 1733, 1580 cm^{-1}.

5.4.7 – Synthesis of ethyl 2-(3-(5-ethylpyrimidin-2-yl)phenyl)acetate, 1.5

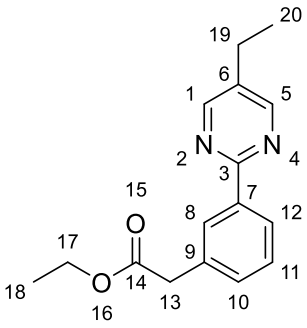

General procedure **B** was followed using the following compounds: 5-ethyl-2-phenylpyrimidine (92 mg, 0.5 mmol), ethyl bromoacetate (0.17 mL, 1.5 mmol), $[RuCl_2(p\text{-cymene})]_2$ (15 mg, 0.025 mmol), PPh_3 (26 mg, 0.1 mmol), 2, 4, 6-trimethylbenzoic acid (25 mg, 0.15 mmol), K_2CO_3 (138 mg, 1 mmol) and 1,4-dioxane (1.5 mL). Column chromatography (10% EtOAc/ hexanes) yielded the title compound as a colourless oil, **1.5**, 29% (39 mg).

^{1}H NMR (500 MHz, $CDCl_3$): δ 8.62 (2H, d, *J* = 3.5 Hz, C(1)-*H*, C(5)-*H*), 8.34 – 8.32 (1H, m, C(8)-*H*), 8.31 (1H, dd, *J* = 7.6, 1.5 Hz, C(12)-*H*), 7.44 (1H, t, *J* = 7.6 Hz, C(11)-

H), 7.39 (1H, dd, *J* = 7.6, 1.5 Hz, C(10)-*H*), 4.15 (2H, q, *J* = 7.1 Hz, C(17)-*H*), 3.70 (2H, s, C(13)-*H*), 2.65 (2H, q, *J* = 7.6 Hz, C(19)-*H*), 1.28 (3H, t, *J* = 7.6 Hz, C(20)-*H*), 1.24 (3H, t, *J* = 7.1 Hz, C(18)-*H*).

^{13}C{^{1}H} NMR (126 MHz, $CDCl_3$): δ 171.6 (*C*=O), 162.5 (Ar*C*), 156.7 (2C, Ar*C*H), 138.0 (Ar*C*), 134.6 (Ar*C*), 134.3 (Ar*C*H), 131.3 (Ar*C*H), 128.9 (Ar*C*H), 128.9 (Ar*C*H), 126.7 (Ar*C*H), 60.9 (O-*C*H_2-CH_3), 41.5((C=O)-*C*H_2-), 23.5(ArC-*C*H_2-CH_3), 15.0 (ArC-CH_2-*C*H_3), 14.3 (O-CH_2-*C*H_3).

HR-MS (ESI) *m/z*: calculated for $C_{16}H_{18}N_2O_2$ requires 293.1266 for $[M+Na]^+$ found 293.1276.

FTIR (thin film): ν_{max} = 2971, 1731, 1586, 1544 cm^{-1}.

5.4.8 – Synthesis of ethyl 2-(3-(4-methylpyrimidin-2-yl)phenyl)acetate, 1.6

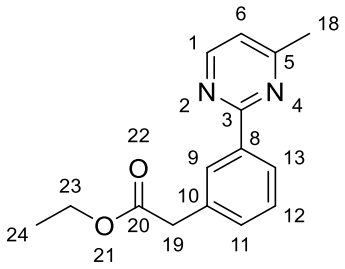

General procedure **B** was followed using the following compounds: 4-methyl-2-phenylpyrimidine (85 mg, 0.5 mmol), ethyl bromoacetate (0.17 mL, 1.5 mmol), $[RuCl_2(p\text{-cymene})]_2$ (15 mg, 0.025 mmol), PPh_3 (26 mg, 0.1 mmol), 2, 4, 6-trimethylbenzoic acid (25 mg, 0.15 mmol), K_2CO_3 (138 mg, 1 mmol) and 1,4-dioxane (1.5 mL). Column chromatography (10% EtOAc/ hexanes) yielded the title compound as a colourless oil, **1.6**, 29% (37 mg).

^{1}H NMR (500 MHz, $CDCl_3$): δ 8.62 (1H, d, *J* = 5.2 Hz, C(1)-*H*), 8.37 – 8.36 (1H, m, C(9)-*H*), 8.34 (1H, dd, *J* = 7.4, 1.6 Hz, C(13)-*H*), 7.47 – 7.39 (2H, m, C(11)-*H*, C(12)-*H*), 7.02 (1H, d, *J* = 5.2 Hz, C(6)-*H*), 4.15 (2H, q, *J* = 7.1 Hz, C(23)-*H*), 3.71 (2H, s, C(19)-*H*), 2.56 (3H, s, C(18)-*H*), 1.24 (3H, t, *J* = 7.1 Hz, C(24)-*H*).

$^{13}C\{^1H\}$ NMR (126 MHz, $CDCl_3$): δ 171.6 (*C*=O), 167.3 (Ar*C*), 164.2 (Ar*C*), 156.8 (Ar*C*H), 138.2 (Ar*C*), 134.5 (Ar*C*), 131.5 (Ar*C*H), 129.2 (Ar*C*H), 128.8 (Ar*C*H), 127.0 (Ar*C*H), 118.7 (Ar*C*H), 60.9 (O-*C*H_2-CH_3), 41.5 ((C=O)-*C*H_2-), 24.5 (ArC-*C*H_3), 14.3 (O-CH_2-*C*H_3).

HR-MS (ESI) *m/z*: calculated for $C_{15}H_{16}N_2O_2$ requires 279.1109 for $[M+Na]^+$ found 279.1101.

FTIR (thin film): ν_{max} = 2981, 1731, 1573, 1554 cm^{-1}.

5.4.9 – Synthesis of ethyl 2-(3-(4-methylpyridin-2-yl)phenyl)acetate, 1.7

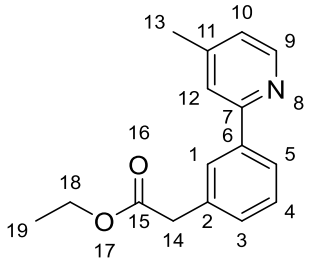

General procedure **B** was followed using the following compounds: 4-methyl-2-phenylpyridine (85 mg, 0.5 mmol), ethyl bromoacetate (0.17 mL, 1.5 mmol), $[RuCl_2(p\text{-cymene})]_2$ (15 mg, 0.025 mmol), PPh_3 (26 mg, 0.1 mmol), 2, 4, 6-trimethylbenzoic acid (25 mg, 0.15 mmol), K_2CO_3 (138 mg, 1 mmol) and 1,4-dioxane (1.5 mL). Column chromatography (10% EtOAc/ hexanes) yielded the title compound a colourless oil, **1.7**, 26% (33 mg).

^1H NMR (500 MHz, $CDCl_3$): δ 8.53 (1H, d, *J* = 4.9 Hz, C(9)-*H*), 7.91 (1H, t, *J* = 1.4 Hz, C(1)-*H*), 7.88 – 7.84 (1H, m, C(5)-*H*), 7.57 – 7.50 (1H, m, C(4)-*H*), 7.42 (1H, t, *J* = 7.6 Hz, C(3)-*H*), 7.36 – 7.30 (1H, m, C(12)-*H*), 7.08 – 7.02 (1H, m, C(10)-*H*), 4.16 (2H, q, *J* = 7.1 Hz, C(18)-*H*), 3.70 (2H, s, C(14)-*H*), 2.40 (3H, s, C(13)-*H*), 1.25 (3H, t, *J* = 7.1 Hz, C(19)-*H*).

$^{13}C\{^1H\}$ NMR (126 MHz, $CDCl_3$): δ 171.7 (*C*=O), 157.2 (Ar*C*), 149.5 (Ar*C*H), 147.9 (Ar*C*), 139.9 (Ar*C*H), 134.7 (Ar*C*), 129.8 (Ar*C*H), 129.0 (Ar*C*H), 128.0 (Ar*C*H), 125.8 (Ar*C*H), 123.3 (Ar*C*H), 121.7 (Ar*C*H), 61.0 (O-*C*H_2-CH_3), 41.5 ((C=O)-*C*H_2-), 21.3 (ArC-*C*H_3), 14.3 (O-CH_2-*C*H_3).

HR-MS (ESI) *m/z*: calculated for $C_{16}H_{17}NO_2$ requires 278.1157 for $[M+Na]^+$ found 278.1179.

FTIR (thin film): ν_{max} = 2980, 1731, 1601 cm^{-1}.

5.4.10 – Synthesis of ethyl 2-(2-methoxy-5-(4-methylpyridin-2-yl)phenyl)acetate, 1.8

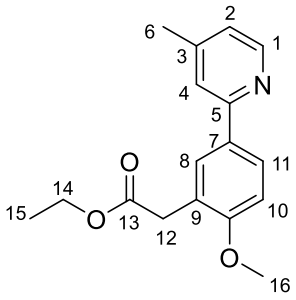

General procedure **B** was followed using the following compounds: 2-(4-methoxyphenyl)-4-methylpyridine (100 mg, 0.5 mmol), ethyl bromoacetate (0.17 mL, 1.5 mmol), $[RuCl_2(p\text{-cymene})]_2$ (15 mg, 0.025 mmol), PPh_3 (26 mg, 0.1 mmol), 2, 4, 6-trimethylbenzoic acid (25 mg, 0.15 mmol), K_2CO_3 (138 mg, 1 mmol) and 1,4-dioxane (1.5 mL). Column chromatography (10% EtOAc/ hexanes) yielded the title compound a colourless oil, **1.8**, 30% (43 mg).

^{1}H NMR (500 MHz, $CDCl_3$): δ 8.49 (1H, d, *J* = 5.0 Hz, C(1)-*H*), 7.89 (1H, dd, *J* = 8.5, 2.3 Hz, C(11)-*H*), 7.85 (1H, d, *J* = 2.3 Hz, C(8)-*H*), 7.52 – 7.46 (1H, m, C()-*H*), 6.99 (1H, dd, *J* = 5.0, 0.8 Hz, C(2)-*H*), 6.95 (1H, d, *J* = 8.5 Hz, C(10)-*H*), 4.16 (2H, q, *J* = 7.1 Hz, C(14)-*H*), 3.87 (3H, s, C(16)-*H*), 3.69 (2H, s, C(12)-*H*), 2.39 (3H, s, C(6)-*H*), 1.25 (3H, t, *J* = 7.1 Hz, C(15)-*H*).

^{13}C{^{1}H} NMR (126 MHz, $CDCl_3$): δ 171.9 (*C*=O), 158.5 (Ar*C*), 157.0 (Ar*C*), 149.4 (Ar*C*H), 132.0 (Ar*C*H), 129.8 (Ar*C*), 127.2 (Ar*C*), 123.6 (Ar*C*H), 122.6 (Ar*C*H), 120.9 (Ar*C*H), 110.7 (Ar*C*H), 60.7 (O-*C*H_2-CH_3), 55.7 (O-*C*H_3), 36.4 ((C=O)-*C*H_2-ArC), 21.4 (Ar-*C*H_3), 14.4 ((C=O)-CH_2-*C*H_3).

HR-MS (ESI) *m/z*: calculated for $C_{17}H_{19}NO_3$ requires 308.1263 for $[M+H]^+$ found 308.1259.

FTIR (thin film): ν_{max} = 2978, 1733, 1604, 1559 cm^{-1}.

5.4.11 – Synthesis of ethyl 2-(2-methoxy-5-(pyridin-2-yl)phenyl)acetate, **1.11**

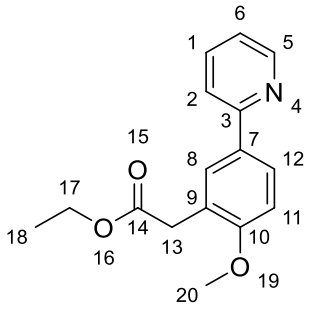

General procedure **A** was followed using the following compounds: 2-(4-methoxypenyl) pyridine (**1c)** (93 mg, 0.5 mmol), ethyl bromoacetate (0.17 mL, 1.5 mmol), $[RuCl_2(p\text{-cymene})]_2$ (15 mg, 0.025 mmol), $[NiCl_2(PPh_3)_2]$ (33 mg, 0.05 mmol), 1-adamantanecarboxylic acid (27 mg, 0.15 mmol), K_2CO_3 (138 mg, 1 mmol) and 1,4-dioxane (1.5 mL). Column chromatography (10% EtOAc/ hexanes) yielded the title compound as a colourless oil, **1.11**, 47% (64 mg).

*When general conditions **B** were used with the following reagents: PPh_3 (26 mg, 0.1 mmol) and 2,4,6-trimethylbenzoic acid (25 mg, 0.15 mmol) were used instead of $[NiCl_2(PPh_3)_2]$ and 1-adamantanecarboxylic acid respectively, the title compound was obtained as a colourless oil, 19% (26 mg).

^{1}H NMR (500 MHz, $CDCl_3$): δ 8.64 (1H, ddd, *J* = 4.8, 1.8, 1.1 Hz, C(5)-*H*), 7.90 (1H, dd, *J* = 8.5, 2.3 Hz, C(12)-*H*), 7.87 (1H, d, *J* = 2.3 Hz, C(8)-*H*), 7.71 – 7.65 (1H, m, C(2)-*H*), 7.16 (1H, ddd, *J* = 7.1, 4.8, 1.5 Hz, C(6)-*H*), 6.96 (1H, d, *J* = 8.5 Hz, C(11)-*H*), 4.17 (2H, q, *J* = 7.1 Hz, C(17)-*H*), 3.87 (3H, s, C(20)-*H*), 3.70 (2H, s, C(13)-*H*), 1.25 (3H, t, *J* = 7.1 Hz, C(18)-*H*).

^{13}C{^{1}H} NMR (126 MHz, $CDCl_3$): δ 171.8 (*C*=O), 158.6 (Ar*C*), 157.2 (Ar*C*), 149.6 (Ar*C*H), 136.7 (Ar*C*H), 131.9 (Ar*C*H), 129.8 (Ar*C*), 127.3 (Ar*C*), 123.7 (Ar*C*H), 121.5 (Ar*C*H), 120.0 (Ar*C*H), 110.7 (Ar*C*H), 60.8 (O-*C*H_2-CH_3), 55.8 (O-*C*H_3), 36.4 ((C=O)-*C*H_2-), 14.4 (OCH_2-*C*H_3).

HR-MS (ESI) *m/z*: calculated for $C_{16}H_{17}NO_3$ requires 294.1106 for $[M+Na]^+$ found: 294.1127.

FTIR (thin film): ν_{max} = 3019, 2159, 2027, 1729, 1611, 1591, 1566, 1508, 1466 cm^{-1}.

5.4.12 – Synthesis of ethyl 2-(2-(methylthio)-5-(pyridin-2-yl)phenyl)acetate, 1.12

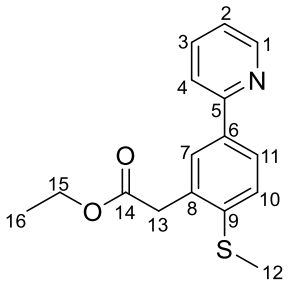

General procedure **B** was followed using the following compounds: 1-phenylpyrazole (0.07 mL, 0.5 mmol), ethyl bromoacetate (0.17 mL, 1.5 mmol), $[RuCl_2(p\text{-cymene})]_2$ (15 mg, 0.025 mmol), PPh_3 (26 mg, 0.1 mmol), 2, 4, 6-trimethylbenzoic acid (25 mg, 0.15 mmol), K_2CO_3 (138 mg, 1 mmol) and 1,4-dioxane (1.5 mL). Column chromatography (10% EtOAc/ hexanes) yielded the title compound as a yellow oil, **1.11**, 41% (41 mg).

*When general conditions **A** were used with the following reagents: PPh_3 (26 mg, 0.1 mmol) and 2,4,6-trimethylbenzoic acid (25 mg, 0.15 mmol) were used instead of $[NiCl_2(PPh_3)_2]$ and 1-adamantanecarboxylic acid respectively, the title compound was obtained as a colourless oil, 29% (29 mg).

^{1}H NMR (500 MHz, $CDCl_3$): δ 8.69 (1H, m, C(1)-*H*), 7.91 (1H, dd, *J* = 8.2, 2.1 Hz, C(11)-*H*), 7.80 – 7.72 (2H, m, C(7)-*H*, C(1)-*H*), 7.49 (1H, d, *J* = 8.3 Hz, C(3)-*H*), 7.37 (1H, d, *J* = 8.3 Hz, C(4)-*H*), 7.25 – 7.21 (1H, m, C(2)-*H*), 4.18 (2H, q, *J* = 7.1 Hz, C(15)-*H*), 3.85 (2H, s, C(13)-*H*), 2.51 (3H, s, C(12)-*H*), 1.26 (3H, t, *J* = 7.1 Hz, C(16)-*H*).

^{13}C{^{1}H} NMR (126 MHz, $CDCl_3$): δ 171.0 (*C*=O), 156.4 (Ar*C*), 149.4 (Ar*C*H), 149.1 (Ar*C*), 133.3 (Ar*C*), 129.5 (Ar*C*), 128.9 (Ar*C*H), 127.4 (Ar*C*H), 126.8 (Ar*C*H), 126.3 (Ar*C*H), 122.3 (Ar*C*H), 120.4 (Ar*C*H), 61.0 (O-*C*H_2-CH_3), 39.5 ((C=O)-*C*H_2-), 16.3 (S-*C*H_3), 14.1 (O-CH_2-*C*H_3).

HR-MS (ESI) *m/z*: calculated for $C_{16}H_{17}NO_2S$ requires 310.0872 for $[M+Na]^+$ found 310.0896.

FTIR (thin film): ν_{max} = 2182, 2009, 1730, 1589, 1466, 1433 cm^{-1}.

5.4.13 – Synthesis of ethyl 2-(5-(pyridin-2-yl)-2-(trifluoromethyl)phenyl)acetate, 1.13

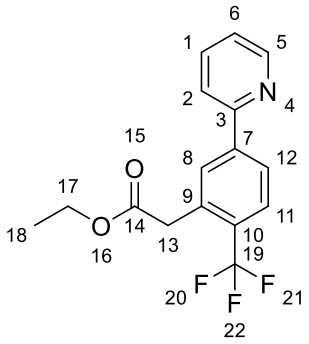

General procedure **B** was followed using the following compounds: 2-(4-(trifluoromethyl)phenyl) pyridine (**1d**) (112 mg, 0.5 mmol), ethyl bromoacetate (0.17 mL, 1.5 mmol), $[RuCl_2(p\text{-cymene})]_2$ (15 mg, 0.025 mmol), PPh_3 (26 mg, 0.1 mmol), 2, 4, 6-trimethylbenzoic acid (25 mg, 0.15 mmol), K_2CO_3 (138 mg, 1 mmol) and 1,4-dioxane (1.5 mL). Column chromatography (10% EtOAc/ hexanes) yielded the title compound as a yellow oil, **1.13**, 56% (87 mg).

*When general conditions **A** were used with the following reagents: $[NiCl_2(PPh_3)_2]$ (33 mg, 0.05 mmol) and 1-adamantanecarboxylic acid (27 mg, 0.15 mmol) were used instead of PPh_3 and 2,4,6-trimethylbenzoic acid respectively, the title compound was obtained as a colourless oil, 20% (31 mg).

^{1}H NMR (500 MHz, $CDCl_3$): δ 8.72 (1H, ddd, *J* = 4.8, 1.7, 1.1 Hz, C(5)-*H*), 8.05 (1H, s, C(8)-*H*), 7.99 (1H, dd, *J* = 8.2, 0.8 Hz, C(12)-*H*), 7.82 – 7.73 (3H, m, C(1)-*H*, C(11)-*H*, C(2)-*H*), 7.30 (1H, ddd, *J* = 6.7, 4.8, 2.0 Hz, C(6)-*H*), 4.18 (2H, q, *J* =7.1 Hz, C(17)-*H*), 3.91 (2H, d, *J* = 0.9 Hz, C(13)-*H*), 1.25 (3H, t, *J* = 7.1 Hz, C(18)-*H*).

^{13}C NMR: Is not reported due to complex splitting making the spectrum peaks difficult to differentiate from each other.

^{19}F NMR (470 MHz, $CDCl_3$): δ -59.91 (3F, s).

HR-MS (ESI) *m/z*: calculated for $C_{16}H_{14}NO_2F_3$ requires 310.1055 for $[M+H]^+$ found 310.1097.

FTIR (thin film): ν_{max} = 3021, 2314, 2161, 2030, 1731, 1590, 1469, 1421, 1370, 1328, 1317 cm^{-1}.

5.4.14 – Synthesis of ethyl 2-(5-((pyridin-2-yl)-2-(trifluoromethoxy)phenyl)acetate, 1.14

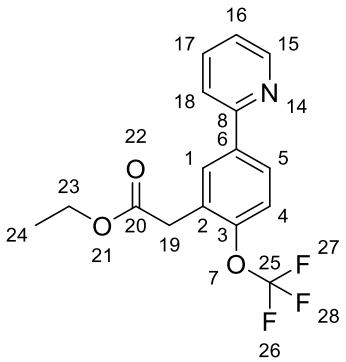

General procedure **B** was followed using the following compounds: 2-(4-(trifluoromethoxy) phenyl) pyridine (**1g**) (120 mg, 0.5 mmol), ethyl bromoacetate (0.17 mL, 1.5 mmol), $[RuCl_2(p\text{-cymene})]_2$ (15 mg, 0.025 mmol), $[NiCl_2(PPh_3)_2]$ (33 mg, 0.05 mmol), 1-adamantanecarboxylic acid (27 mg, 0.15 mmol), K_2CO_3 (138 mg, 1 mmol) and 1,4-dioxane (1.5 mL). Column chromatography (10% EtOAc/ hexanes) yielded the title compound a brown oil, **1.14**, 37% (60 mg).

^{1}H NMR (500 MHz, $CDCl_3$): δ 8.68 (1H, ddd, *J* = 4.9, 1.8, 1.0 Hz, C(15)-*H*), 8.00 (1H, d, *J* = 2.3 Hz, C(1)-*H*), 7.92 (1H, dd, *J* = 8.6, 2.3 Hz, C(5)-*H*), 7.77 – 7.74 (1H, m, C(4)-*H*), 7.72 (1H, t, *J* = 1.0 Hz, C(17)-*H*), 7.48 – 7.44 (1H, m, C(18)-*H*), 7.35 (1H, dd, *J* = 8.6, 1.8 Hz, C(16)-*H*), 4.18 (2H, q, *J* = 7.1 Hz, C(23)-*H*), 3.82 (2H, s, C(19)-*H*), 1.25 (3H, t, *J* = 7.1 Hz, C(24)-*H*).

^{13}C{^{1}H} NMR (126 MHz, $CDCl_3$): δ 171.0 (*C*=O), 158.2 (Ar*C*), 155.8 (Ar*C*), 149.7 (Ar*C*H), 149.0 (Ar*C*H), 136.6 (Ar*C*H), 131.2 (Ar*C*), 130.5 (q, O-*C*F_3), 127.2 (Ar*C*), 123.9

(Ar*C*H), 122.1 (Ar*C*H), 120.5 (Ar*C*H), 119.5 (Ar*C*H), 60.8 (O-*C*H_2-CH_3), 39.2 ((C=O)-*C*H_2), 14.1 (CH_2-*C*H_3).

^{19}F NMR (470 MHz, $CDCl_3$): δ -57.72 (3F).

HR-MS (ESI) *m/z*: calculated for $C_{16}H_{14}F_3NO_3$ requires 348.0823 for $[M+Na]^+$ found 348.0828.

FTIR (thin film): ν_{max} = 2986, 2159, 2009, 1733, 1612, 1588, 1567, 1504, 1467, 1433, cm^{-1}.

5.4.15 – Synthesis of ethyl 2-(2-ethoxy-2-oxoethyl)-4-(pyridin-2-yl)benzoate, **1.15**

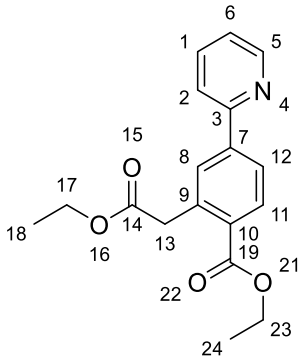

General procedure **A** was followed using the following compounds: ethyl 4-(pyridin-2-yl) benzoate (**1e**) (113 mg, 0.5 mmol), ethyl bromoacetate (0.17 mL, 1.5 mmol), $[RuCl_2(p\text{-cymene})]_2$ (15 mg, 0.025 mmol), $[NiCl_2(PPh_3)_2]$ (33 mg, 0.05 mmol), 1-adamantanecarboxylic acid (27 mg, 0.15 mmol), K_2CO_3 (138 mg, 1 mmol) and 1,4-dioxane (1.5 mL). Column chromatography (10% EtOAc/ hexanes) yielded the title compound as a brown oil, **1.15**, 37% (58 mg).

*When general conditions **B** were used with the following reagents: PPh_3 (26 mg, 0.1 mmol) and 2,4,6-trimethylbenzoic acid (25 mg, 0.15 mmol) were used instead of $[NiCl_2(PPh_3)_2]$ and 1-adamantanecarboxylic acid respectively, the title compound was obtained as a colourless oil, 36% (56 mg).

^{1}H NMR (500 MHz, $CDCl_3$): δ 8.71 (1H, dd, *J* = 4.8, 1.4 Hz, C(5)-*H*), 8.12 (1H, d, *J* = 8.1 Hz, C(11)-*H*), 7.94 (1H, dd, *J* = 8.1, 1.9 Hz, C(12)-*H*), 7.91 (1H, d, *J* = 1.9 Hz, C(8)-*H*), 7.78–7.76 (2H, m, C(1)-*H*, C(2)-*H*), 7.27 (1H, dd, *J* = 4.8, 3.5 Hz, C(6)-*H*), 4.35 (2H,

q, *J* = 7.1 Hz, C(17)-*H*), 4.16 (2H, q, *J* = 7.1 Hz, C(23)-*H*), 4.11 (2H, s, C(13)-*H*), 1.39 (3H, t, *J* = 7.1 Hz, C(24)-*H*), 1.25 (3H, t, *J* = 7.1 Hz, C(18)-*H*).

^{13}C{^{1}H} NMR (126 MHz, $CDCl_3$): δ 171.5 (*C*=O), 167.1 (*C*=O), 156.1 (Ar*C*), 150.0 (Ar*C*H), 142.8 (Ar*C*), 137.0 (Ar*C*), 136.6 (Ar*C*H), 131.7 (Ar*C*H), 130.8 (Ar*C*H), 130.5 (Ar*C*), 125.7 (Ar*C*H), 123.0 (Ar*C*H), 121.1 (Ar*C*H), 61.2 (-*C*H_2-), 60.9 (-*C*H_2-), 41.1 ((C=O)-*C*H_2-), 14.4 (-*C*H_3), 14.3 (-*C*H_3).

HR-MS (ESI) *m/z*: calculated for $C_{18}H_{19}NO_4$ requires 314.1392 for $[M+H]^+$ found 314.1410.

FTIR (thin film): ν_{max} = 3020, 2162, 2033, 1717, 1589, 1467, 1369 cm^{-1}.

5.4.16 – Synthesis of ethyl 2-(4-(pyridin-2-yl)-[1,1'-biphenyl]-2-yl)acetate, 1.16

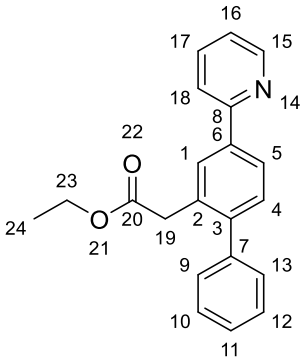

General procedure **B** was followed using the following compounds: 2-([1,1'-biphenyl]-4-yl) pyridine (**1f**) (116 mg, 0.5 mmol), ethyl bromoacetate (0.17 mL, 1.5 mmol), $[RuCl_2(p\text{-cymene})]_2$ (15 mg, 0.025 mmol), $[NiCl_2(PPh_3)_2]$ (33 mg, 0.05 mmol), 1-adamantanecarboxylic acid (27 mg, 0.15 mmol), K_2CO_3 (138 mg, 1 mmol) and 1,4-dioxane (1.5 mL). Column chromatography (10% EtOAc/ hexanes) yielded the title compound as a brown oil, **1.16**, 16% (26 mg).

^{1}H NMR (500 MHz, $CDCl_3$): δ 8.72 – 8.70 (1H, m, C(15)-*H*), 8.01 (1H, d, *J* = 1.8 Hz, C(1)-*H*), 7.94 (1H, dd, *J* = 8.0, 1.8 Hz, C(5)-*H*), 7.78–7.77 (1H, m, C(4)-*H*), 7.56–7.52 (1H, m, C(17)-*H*), 7.46–7.34 (6H, m, C(9)-*H*, C(10)-*H*, C(11)-*H*, C(12)-*H*, C(13)-*H*, C(18)-*H*), 7.24 (1H, ddd, *J* = 6.3, 4.9, 2.5 Hz, C(16)-*H*), 4.07 (2H, q, *J* = 7.1 Hz, C(23)-*H*), 3.69 (2H, s, C(19)-*H*), 1.19 (3H, t, *J* = 7.1 Hz, C(24)-*H*).

^{13}C{^{1}H} NMR (126 MHz, $CDCl_3$): δ 171.8 (*C*=O), 156.6 (Ar*C*), 149.6 (Ar*C*H), 143.2 (Ar*C*H), 140.7 (Ar*C*), 136.8 (Ar*C*H), 132.4 (Ar*C*), 130.7 (Ar*C*), 129.2 (Ar*C*), 129.0 (Ar*C*H), 128.8 (Ar*C*H), 128.2 (Ar*C*H), 127.3 (Ar*C*H), 127.2 (Ar*C*H), 126.1 (Ar*C*H), 125.6 (Ar*C*H), 122.2 (Ar*C*H), 120.6 (Ar*C*H), 60.8 (O-*C*H_2-CH_3) 39.1 ((C=O)-*C*H_2), 14.1 (CH_2-*C*H_3).

HR-MS (ESI) *m/z*: calculated for $C_{21}H_{19}NO_2$ requires 340.1313 for $[M+Na]^+$ found 340.1308.

FTIR (thin film): ν_{max} = 3020, 2159, 1979, 1729, 1589, 1467, 1432, 1365, 1335 cm^{-1}.

5.4.17 – Synthesis of ethyl 2-(2-fluoro-5-(pyridin-2-yl)phenyl)acetate, 1.17

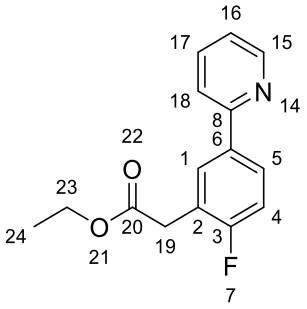

General procedure **A** was followed using the following compounds: 2-(4fluorophenyl) pyridine (**1e**) (113 mg, 0.5 mmol), ethyl bromoacetate (0.17 mL, 1.5 mmol), $[RuCl_2(p\text{-cymene})]_2$ (15 mg, 0.025 mmol), $[NiCl_2(PPh_3)_2]$ (33 mg, 0.05 mmol), 1-adamantanecarboxylic acid (27 mg, 0.15 mmol), K_2CO_3 (138 mg, 1 mmol) and 1,4-dioxane (1.5 mL). Column chromatography (10% EtOAc/ hexanes) yielded the title compound as a brown oil, **1.17**, 42% (55 mg).

*When general conditions **B** were used with the following reagents: PPh_3 (26 mg, 0.1 mmol) and 2,4,6-trimethylbenzoic acid (25 mg, 0.15 mmol) were used instead of $[NiCl_2(PPh_3)_2]$ and 1-adamantanecarboxylic acid respectively, the title compound was obtained as a colourless oil, 39% (51 mg).

^{1}H NMR (500 MHz, $CDCl_3$): δ 8.67 (1H, ddd, *J* = 4.8, 1.8, 1.1 Hz, C(15)-*H*), 7.94 (1H, dd, *J* = 7.4, 2.3 Hz, C(1)-*H*), 7.88 (1H, ddd, *J* = 7.4, 4.8, 1.2 Hz, C(5)-*H*), 7.76 – 7.71 (1H, m, C(4)-*H*), 7.68 (1H, dd, *J* = 7.4, 1.1 Hz, C(17)-*H*), 7.22 (1H, ddd, *J* = 7.4, 4.8, 1.1 Hz,

C(18)-*H*), 7.18 – 7.13 (1H, m, C(16)-*H*), 4.18 (2H, q, *J* = 7.1 Hz, C(23)-*H*), 3.74 (2H, d, *J* = 0.8 Hz, C(19)-*H*), 1.26 (3H, t, *J* = 7.1 Hz, C(24)-*H*).

^{13}C{^{1}H} NMR (126 MHz, $CDCl_3$): δ 170.7 (*C*=O), 162.0 (d, *J* = 249.4 Hz, Ar*C*-F), 156.4 (Ar*C*), 149.8 (Ar*C*H), 137.0 (Ar*C*H), 135.7 (d, *J* = 3.4 Hz, Ar*C*), 130.4 (d, *J* = 4.5 Hz, Ar*C*H), 127.8 (d, *J* = 8.6 Hz, Ar*C*H), 122.2 (Ar*C*H), 122.1 (d, *J* = 16.4 Hz, Ar*C*), 120.4 (Ar*C*), 115.8 (d, *J* = 22.4 Hz, Ar*C*H), 61.2 (O-*C*H_2-CH_3), 35.0 (d, *J* = 2.7 Hz, ((C=O)-*C*H_2), 14.3 (CH_2-*C*H_3).

^{19}F NMR (470 MHz, $CDCl_3$): δ -116.97 – -117.30 (1F, m).

HR-MS (ESI) *m/z*: calculated for $C_{15}H_{14}FNO_2$ requires 282.0906 for $[M+Na]^+$ found 282.0908.

FTIR (thin film): ν_{max} = 3020, 2161, 2033, 1730, 1592, 1506, 1496, 1434, 1370 cm^{-1}.

5.4.18 – Synthesis of ethyl 2-(2-chloro-5-(pyridin-2-yl)phenyl)acetate, 1.18

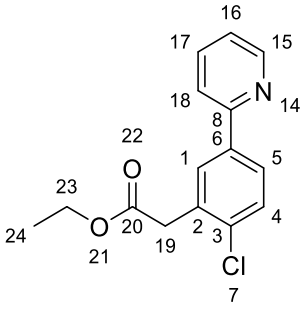

General procedure **B** was followed using the following compounds: 2-(4-chlorophenyl) pyridine (**1i**) (94 mg, 0.5 mmol), ethyl bromoacetate (0.17 mL, 1.5 mmol), $[RuCl_2(p\text{-cymene})]_2$ (15 mg, 0.025 mmol), PPh_3 (26 mg, 0.1 mmol), 2, 4, 6-trimethylbenzoic acid (25 mg, 0.15 mmol), K_2CO_3 (138 mg, 1 mmol) and 1,4-dioxane (1.5 mL). Column chromatography (10% EtOAc/ hexanes) yielded the title compound as a yellow oil, **1.18**, 52% (72 mg).

*When general conditions **A** were used with the following reagents: PPh_3 (26 mg, 0.1 mmol) and 2,4,6-trimethylbenzoic acid (25 mg, 0.15 mmol) were used instead of $[NiCl_2(PPh_3)_2]$ and 1-adamantanecarboxylic acid respectively, the title compound was obtained as a colourless oil, 48% (66 mg).

^{1}H NMR (500 MHz, $CDCl_3$): δ 8.68 (1H, ddd, *J* = 4.8, 1.8, 1.1 Hz, C(15)-*H*), 7.96 (1H, d, *J* = 2.2 Hz, C(1)-*H*), 7.84 (1H, dd, *J* = 8.3, 2.2 Hz, C(5)-*H*), 7.77–7.73 (1H, m, C(4)-*H*), 7.71 (1H, dd, *J* = 8.3, 1.1 Hz, C(17)-*H*), 7.48 (1H, d, *J* = 8.3 Hz, C(18)-*H*), 7.24 (1H, ddd, *J* = 8.3, 4.8, 1.1 Hz, C(16)-*H*), 4.19 (2H, q, *J* = 7.1 Hz, C(23)-*H*), 3.85 (2H, s, C(19)-*H*), 1.27 (3H, t, *J* = 7.1 Hz, C(24)-*H*).

^{13}C{^{1}H} NMR (126 MHz, $CDCl_3$): δ 170.6 (*C*=O), 156.2 (Ar*C*), 149.9 (Ar*C*H), 138.3 (Ar*C*H), 137.0 (Ar*C*H), 135.6 (Ar*C*), 133.1 (Ar*C*), 130.1 (Ar*C*H), 129.9 (Ar*C*H), 127.1 (Ar*C*H), 122.6 (Ar*C*H), 120.6 (Ar*C*H), 61.2 (O-*C*H_2-CH_3), 39.5 ((C=O)-*C*H_2-), 14.3 (OCH_2-*C*H_3).

HR-MS (ESI) *m/z*: calculated for $C_{15}H_{14}ClNO_2$ requires 276.0791 for $[M+H]^+$ found 276.0799.

FTIR (thin film): ν_{max} = 2981, 2158, 2039, 1731, 1589, 1465, 1430, 1369, 1334 cm^{-1}.

5.4.19 – Synthesis of ethyl 2-(2-bromo-5-(pyridin-2-yl)phenyl)acetate, 1.19

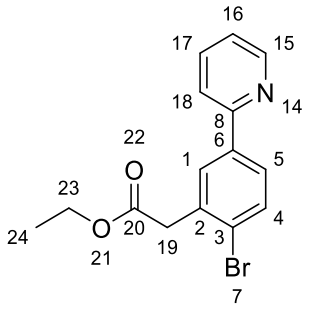

General procedure **A** was followed using the following compounds: 2-(4-bromophenyl) pyridine (**1j**) (117 mg, 0.5 mmol), ethyl bromoacetate (0.17 mL, 1.5 mmol), $[RuCl_2(p\text{-cymene})]_2$ (15 mg, 0.025 mmol), $[NiCl_2(PPh_3)_2]$ (33 mg, 0.05 mmol), 1-adamantanecarboxylic acid (27 mg, 0.15 mmol), K_2CO_3 (138 mg, 1 mmol) and 1,4-dioxane (1.5 mL). Column chromatography (10% EtOAc/ hexanes) yielded the title compound as a green oil, **1.19**, 23% (37 mg).

^{1}H NMR (500 MHz, $CDCl_3$): δ 8.71 (1H, dt, *J* = 4.8, 1.4 Hz, C(15)-*H*), 8.02 (1H, d, *J* = 1.9 Hz, C(1)-*H*), 7.94 (1H, dt, *J* = 8.0, 1.9 Hz, C(5)-*H*), 7.77 (1H, d, *J* = 8.0 Hz, C(4)-*H*), 7.57 – 7.54 (1H, m, C(17)-*H*), 7.39 – 7.33 (1H, m, C(18)-*H*), 7.25 – 7.24 (1H, m, C(16)-

H), 4.09 (2H, q, *J* = 7.1 Hz, C(23)-*H*), 3.66 (2H, s, C(19)-*H*), 1.20 (3H, t, *J* = 7.1 Hz, C(24)-*H*).

$^{13}C\{^{1}H\}$ NMR (126 MHz, $CDCl_3$): δ 171.6 (*C*=O), 156.7 (Ar*C*), 149.7 (Ar*C*H), 136.8 (Ar*C*), 131.4 (Ar*C*), 130.9 (Ar*C*H), 130.5 (Ar*C*H), 129.2 (Ar*C*H), 128.2 (Ar*C*H), 125.7 (Ar*C*H), 122.3 (Ar*C*), 120.6 (Ar*C*H), 60.9 (O-*C*H_2-CH_3), 39.1 ((C=O)-*C*H_2-), 14.1 (O-CH_2-*C*H_3).

HR-MS (ESI) *m/z*: calculated for $C_{15}H_{14}ClNO_2$ requires 276.0791 for $[M+H]^+$ found 276.0799.

FTIR (thin film): ν_{max} = 2980, 2358, 2164, 2030, 1927, 1729, 1586, 1464, 1432, 1389, 1368 cm^{-1}.

5.4.20 – Synthesis of ethyl 2-(2-methoxy-5-(pyrimidin-2-yl)phenyl)acetate, 1.22

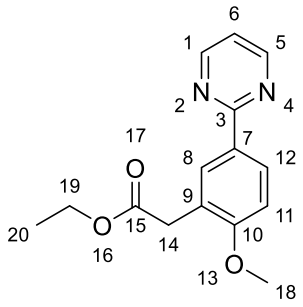

General procedure **B** was followed using the following compounds: 2-(4-methoxyphenyl) pyrimidine (93 mg, 0.5 mmol), ethyl bromoacetate (0.17 mL, 1.5 mmol), $[RuCl_2(p\text{-cymene})]_2$ (15 mg, 0.025 mmol), PPh_3 (26 mg, 0.1 mmol), 2, 4, 6-trimethylbenzoic acid (25 mg, 0.15 mmol), K_2CO_3 (138 mg, 1 mmol) and 1,4-dioxane (1.5 mL). Column chromatography (10% EtOAc/ hexanes) yielded the title compound as a colourless oil, **1.22**, 30% (41 mg).

^{1}H NMR (500 MHz, $CDCl_3$): δ 8.73 (2H, d, *J* = 4.8 Hz, C(1)-*H*, C(5)-*H*), 8.37 (1H, dd, *J* = 8.6, 2.3 Hz, C(12)-*H*), 8.29 (1H, d, *J* = 2.3 Hz, C(8)-*H*), 7.09 (1H, t, *J* = 4.8 Hz, C(6)-*H*), 6.96 (1H, d, *J* = 8.6 Hz, C(11)-*H*), 4.16 (2H, q, *J* = 7.1 Hz, C(19)-*H*), 3.88 (s, C(18)-*H*), 3.70 (2H, s, C(14)-*H*), 1.24 (3H, t, *J* = 7.1 Hz, C(20)-*H*).

$^{13}C\{^{1}H\}$ NMR (126 MHz, $CDCl_3$): δ 171.7 (*C*=O), 164.5 (Ar*C*), 160.0 (Ar*C*), 157.2 (Ar*C*H), 131.1 (Ar*C*), 130.0 (Ar*C*H), 129.0 (Ar*C*), 123.5 (Ar*C*H), 118.4 (Ar*C*H), 110.4 (Ar*C*H), 60.7 (O-*C*H_2-CH_3), 55.7 (O-*C*H_3), 36.3 ((C=O)-*C*H_2-), 14.3 (O-CH_2-*C*H_3).

HR-MS (ESI) *m/z*: calculated for $C_{15}H_{16}N_2O_3$ requires 273.1239 for $[M+H]^+$ found 273.1223.

FTIR (thin film): ν_{max} = 2978, 1730, 1608, 1591 cm^{-1}.

5.5 – Mechanistic experiments for the *meta* alkylation with primary substrates

5.5.1 – Radical Inhibitor experiments

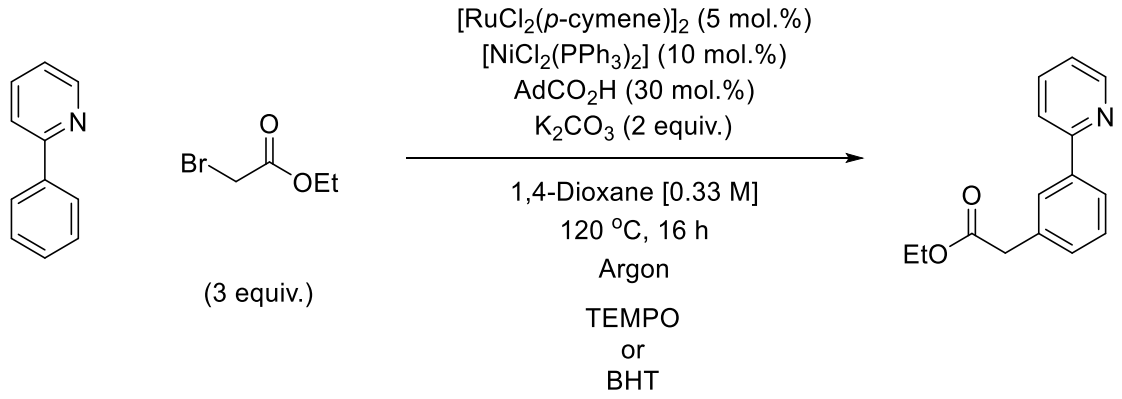

General procedure **B** was followed using the following compounds: 2-phenylpyridine (0.07 mL, 0.5 mmol), ethyl bromoacetate (0.17 mL, 1.5 mmol), $[RuCl_2(p\text{-cymene})]_2$ (15 mg, 0.025 mmol), $[NiCl_2(PPh_3)_2]$ (33 mg, 0.05 mmol), 1-adamantanecarboxylic acid (27 mg, 0.15 mmol), K_2CO_3 (138 mg, 1 mmol) and 1,4-dioxane (1.5 mL). To each reaction was then added TEMPO: 30 mol.% (0.10 mmol, 16 mg), 100 mol.% (1.0 mmol, 156 mg) and 300 mol.% (3.00 mmol, 469 mg) or BHT: 30 mol.% (0.10 mmol, 22 mg), 100 mol.% (1.0 mmol, 220 mg) and 300 mol.% (3.0 mmol, 660 mg).

After stirring for 16 h, an aliquot was taken from each reaction and analysed *via* ^{1}H NMR to determine the reaction conversion. The results are shown in the table below.

Entry	Radical inhibitor used	Equivalents	Conversion (%)
1	TEMPO	0.1	51
2	TEMPO	1.0	34
3	TEMPO	3.0	<5
4	BHT	0.1	39
5	BHT	1.0	27
6	BHT	3.0	25

5.5.2 – Testing Phosphonium salt as active coupling species *in situ*

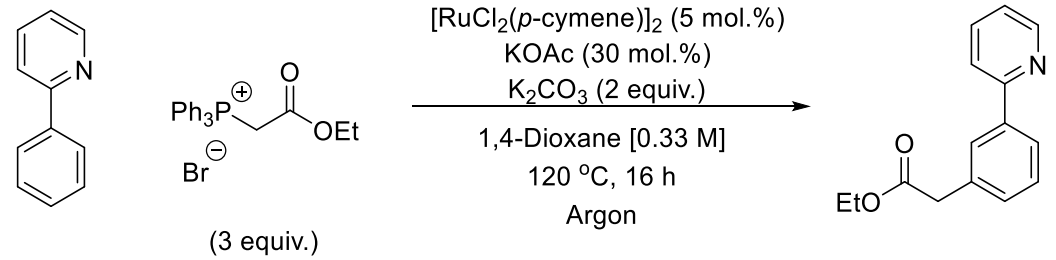

General procedure **A** was followed using the following compounds: 2-phenylpyridine (0.07 mL, 0.5 mmol), (2-ethoxy-2-oxoethyl)triphenylphosphonium bromide (644 mg, 1.5 mmol), $[RuCl_2(p\text{-cymene})]_2$ (15 mg, 0.025 mmol), KOAc (15 mg, 0.15 mmol), K_2CO_3 (138 mg, 1 mmol) and 1,4-dioxane (1.5 mL).

After stirring for 16 h, an aliquot was taken and then analysed *via* ^{1}H NMR, which showed zero conversion of the starting material.

5.5.3 – Mercury drop test

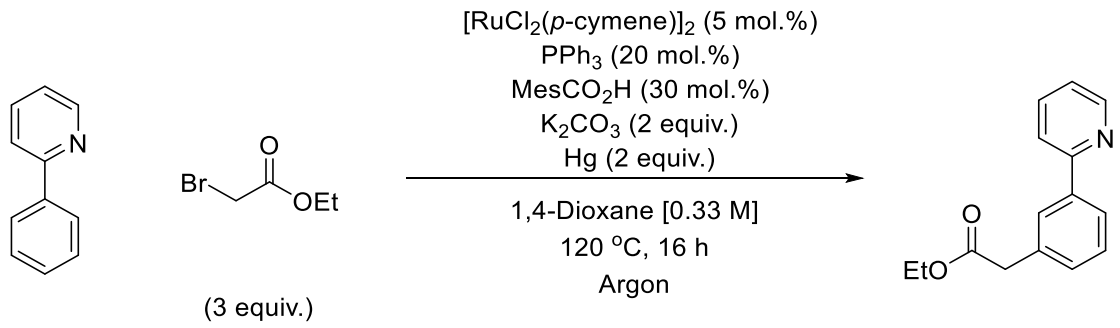

General procedure **B** was followed using the following compounds: 2-phenylpyridine (0.07 mL, 0.5 mmol), ethyl bromoacetate (0.17 mL, 1.5 mmol), $[RuCl_2(p\text{-cymene})]_2$ (15 mg, 0.025 mmol), 2, 4, 6-trimethylbenzoic acid (25 mg, 0.15 mmol), PPh_3 (26 mg, 0.1 mmol), K_2CO_3 (138 mg, 1 mmol), 1,4-dioxane (1.5 mL) and Hg (0.50 mmol, 100 mg).

After stirring for 16 h, an aliquot was taken and then analysed *via* ^{1}H NMR, which showed 14% conversion to the *meta* product.

5.6 – Synthesis of carbazole and tryptamine substrates for testing

5.6.1 – Synthesis of *N*-(2-(1*H*-indol-3-yl)ethyl)pyrimidin-2-amine, **2a**

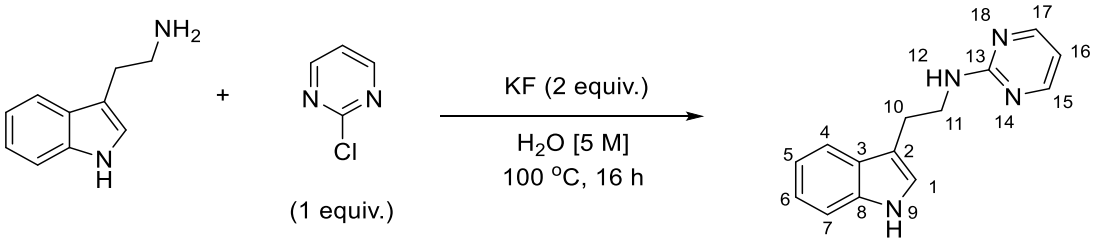

To a 50 mL round-bottomed flask, charged with magnetic stirrer bar was added: tryptamine (5 mmol, 801 mg), 2-chloropyrimidine (5 mmol, 573 mg), KF (10 mmol, 581 mg) and water (5 mL). A condenser was then attached, and the reaction refluxed at 100 °C for 16 hours. After allowing to cool back to room temperature, $NaHCO_3$ (sat.) (aq.) (120 mL) was added to quench the reaction and the product extracted with EtOAc (3 × 80 mL). The combined organic extracts were then dried over anhydrous $MgSO_4$, filtered and concentrated under reduced pressure to yield crude product. This was then purified by flash chromatography (20% EtOAc/hexanes) to yield the title compound as a pale yellow crystalline solid, **2a**, 61% (725 mg).

^{1}H NMR (500 MHz, $CDCl_3$): δ 8.29 (2H, d, J = 4.8 Hz, C(15)-*H*, C(17)-*H*), 8.01 (1H, s, N(12)-*H*), 7.66 (1H, dd, J = 8.0, 1.0 Hz, C(4)-*H*), 7.35 (1H, d, J = 8.2 Hz, C(7)-*H*), 7.21 (1H, ddd, J = 8.2, 7.0, 1.0, C(6)-*H*), 7.13 (1H, ddd, J = 8.0, 7.0, 1.0 Hz, C(5)-*H*), 7.03 (1H, d, J = 2.3 Hz, C(1)-*H*), 6.54 (1H, t, J = 4.8 Hz, C(16)-*H*), 5.56 (1H, s, N(9)-*H*), 3.78 (2H, td, J = 6.8, 5.8 Hz, C(11)-*H*), 3.10 (2H, td, J = 6.9, 0.9 Hz, C(10)-*H*).

^{13}C{^{1}H} NMR (126 MHz, $CDCl_3$): δ 162.3 (Ar*C*), 158.0 (Ar*C*H), 136.4 (Ar*C*), 127.4 (Ar*C*), 122.1 (Ar*C*H), 122.0 (Ar*C*H), 119.4 (Ar*C*H), 118.8 (Ar*C*H), 113.2 (Ar*C*), 111.2 (Ar*C*H), 110.5 (Ar*C*H), 41.5 (NH-*C*H_2-CH_2), 25.3 (NH-CH_2-*C*H_2).

Melting Point: 164 – 166 °C.

This data is in accordance with literature precedent.[12]

5.6.2 – Synthesis of *N*-(2-(1*H*-indol-3-yl)ethyl)-5-chloropyrimidin-2-amine, **2b**

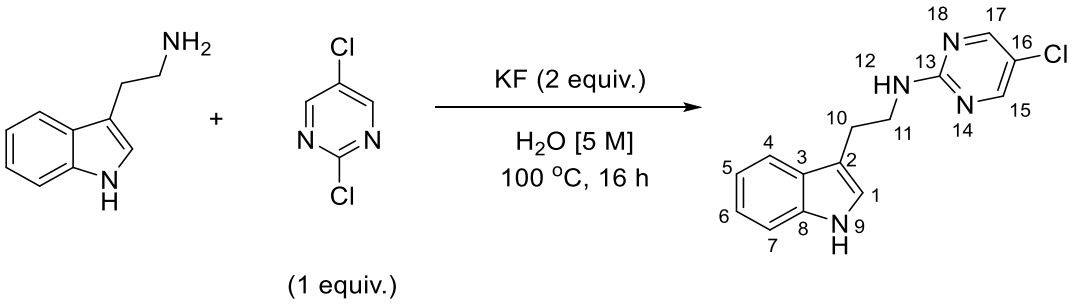

(1 equiv.)

To a 50 mL round-bottomed flask, charged with magnetic stirrer bar was added: tryptamine (5 mmol, 801 mg), 2,5-dichloropyrimidine (5 mmol, 745 mg), KF (10 mmol, 581 mg) and water (5 mL). A condenser was then attached, and the reaction refluxed at 100 °C for 16 hours. After allowing to cool back to room temperature, $NaHCO_3$ (sat.) (aq.) (120 mL) was added to quench the reaction and the product extracted with EtOAc (3 × 80 mL). The combined organic extracts were then dried over anhydrous $MgSO_4$, filtered and concentrated under reduced pressure to yield crude product. This was then purified by flash chromatography (20% EtOAc/hexanes) to yield the title compound as a pale pink/red crystalline solid, **2b**, 53% (722 mg).

^{1}H NMR (500 MHz, $CDCl_3$): δ 8.23 (2H, s, C(15)-*H*, C(17)-*H*), 8.02 (1H, s, N(12)-*H*), 7.64 (1H, d, *J* = 7.8 Hz, C(4)-*H*), 7.38 (1H, d, *J* = 8.1 Hz, C(7)-*H*), 7.21 (1H, ddd, *J* = 8.1, 7.0, 1.1 Hz, C(6)-*H*), 7.13 (1H, ddd, *J* = 8.1, 7.0, 1.1 Hz, C(5)-*H*), 7.03 (1H, d, *J* = 2.3 Hz, C(1)-*H*), 3.77 (2H, q, *J* = 6.6 Hz, C(11)-*H*), 3.09 (2H, td, *J* = 6.6, 0.8 Hz, C(10)-*H*).

^{13}C{^{1}H} NMR (126 MHz, $CDCl_3$): δ 160.6 (Ar*C*), 156.2 (2C, Ar*C*H), 136.4 (Ar*C*), 127.3 (Ar*C*), 122.2 (Ar*C*H), 122.0 (Ar*C*H), 119.5 (Ar*C*), 118.8 (Ar*C*H), 118.7 (Ar*C*H), 113.1 (Ar*C*), 111.2 (Ar*C*H), 41.8 (NH-*C*H_2-CH_2), 25.2 (NH-CH_2-*C*H_2).

HR-MS (ESI) *m/z*: calculated for $C_{14}H_{13}N_4Cl$ requires 273.0902 for $[M+H]^+$ found 273.0896.

FTIR (thin film): ν_{max} = 3262, 3121, 2919, 2873, 2853, 1918, 1877, 1603, 1570, 1478, 1441, 1384, 1352 cm^{-1}.

Melting Point: 156 – 157 °C.

5.6.3 – Synthesis of 2-(1*H*-indol-3-yl)-*N*-(pyridin-2-ylmethyl)ethan-1-ammonium chloride, **2c**

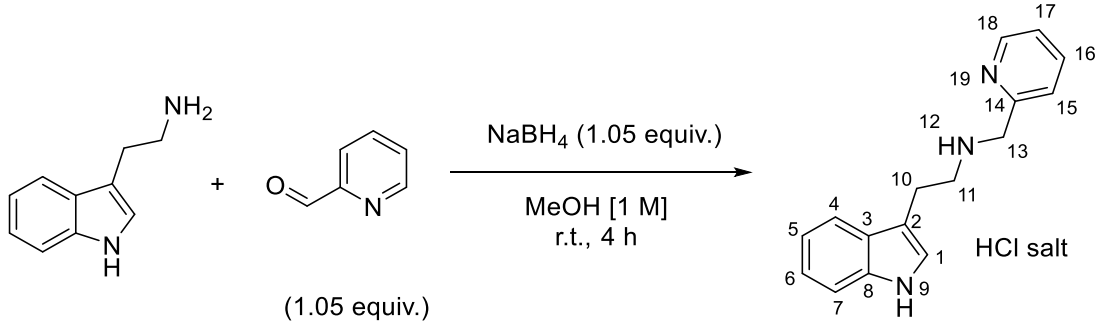

To a 100 mL round bottomed flask was added: tryptamine (10 mmol, 1.60 g), 2-formylpyridine (10.5 mmol, 1.125 g) and MeOH (10 mL). This mixture was allowed to stir for 10 minutes, before adding $NaBH_4$ (10.5 mmol, 397 mg) in one portion. The reaction was then left to stir at room temperature for 4 hours, before the addition of 6 M HCl (aq.) (20 mL). The reaction mixture was then evaporated to dryness under reduced pressure. The remaining residue was redissolved in H_2O (20 mL) and washed with $CHCl_3$ (3 × 15 mL), and the aqueous layer then basified by addition of sat. $NaHCO_3$ (aq.) before then washing again with $CHCl_3$ (3 × 20 mL). The combined organic extracts were then dried over $MgSO_4$, filtered and concentrated under reduced pressure to yield a pale-yellow oil. This was then purified by first adding HCl/EtOH to precipitate out a solid, which was then collected by vacuum filtration. This was then recrystallised from hot methanol to yield the title compound as a dark brown crystalline solid, **2c**, 86% (2.46 g).

^{1}H NMR (500 MHz, D_2O): δ 8.64 (1H, d, J = 4.7 Hz, C(18)-*H*), 8.28 (1H, td, J =7.4, 3.6 Hz, C(16)-*H*), 7.79 (2H, d, J = 7.4 Hz, C(15)-*H*, C(17)-*H*), 7.62 – 7.59 (1H, m, C(4)-*H*), 7.53 (1H, d, J = 8.2 Hz, C(7)-*H*), 7.32 (1H, s, C(1)-*H*), 7.28 (1H, dd, J = 8.2, 6.9 Hz, C(6)-*H*), 7.17 (1H, dd, J = 8.2, 6.9 Hz, C(5)-*H*), 4.54 (2H, s, C(13)-*H*), 3.54–3.51 (2H, t, J = 7.1 Hz, C(11)-*H*), 3.26 (2H, t, J = 7.1 Hz, C(10)-*H*).

^{13}C{^{1}H} NMR (126 MHz, $CDCl_3$): δ 146.4 (Ar*C*), 145.4 (Ar*C*H), 143.7 (Ar*C*H), 136.3 (Ar*C*), 126.5 (Ar*C*) 126.4 (Ar*C*H), 124.3 (Ar*C*H), 122.2 (Ar*C*H), 119.4 (Ar*C*H), 118.1 (Ar*C*H), 112.0 (Ar*C*), 108.3 (Ar*C*H), 48.8 (NH-*C*H_2-ArC), 47.8 (NH-*C*H_2-CH_2), 21.7 (NH-CH_2-*C*H_2).

Melting Point: 107 – 109 °C.

This data is in accordance with literature precedent.[13]

5.6.4 – Synthesis of 3-((2-(1*H*-indol-3-yl)ethyl)amino)propanenitrile, 2d

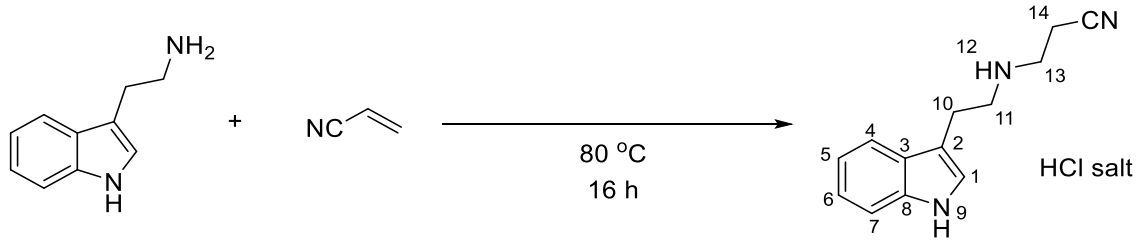

To an oven dried 50 mL round bottomed flask charged with magnetic stirrer was added: tryptamine (10 mmol, 1.60 g) and acrylonitrile (24 mL). A reflux condenser was then attached, and the reaction heated at 80 °C for 16 h. After this time the reaction mixture was concentrated under reduced pressure and the residue redissolved in Et_2O (50 mL) and then HCl in EtOH (50 mL) was added to precipitate the desired product. This precipitate was collected by vacuum filtration and watched with several portions of Et_2O (3 × 40 mL). The precipitate was then recrystallised from hot EtOH to yield the title compound as an off white crystalline solid, **2d**, 64% (1.37 g).

^{1}H NMR (500 MHz, D_2O): δ 7.57 (1H, d, J = 7.9 Hz, C(4)-*H*), 7.42 (1H, d, J = 8.2 Hz, C(7)-*H*), 7.21 (1H, s, C(1)-*H*), 7.17 (1H, ddd, J = 8.2, 7.0, 1.2 Hz, C(6)-*H*), 7.08 (1H, ddd, J = 8.2, 7.0, 1.2 Hz, C(5)-*H*), 3.33 (2H, t, J = 7.2 Hz, C(14)-*H*), 3.30 (2H, t, J = 6.8 Hz, C(11)-*H*), 3.11 (2H, t, J = 7.2 Hz, C(13)-*H*), 2.84 (2H, t, J = 6.8 Hz, C(10)-*H*).

^{13}C{^{1}H} NMR (126 MHz, $CDCl_3$): δ 136.3 (Ar-*C*), 126.2 (Ar-*C*), 124.2 (Ar-*C*), 122.2 (Ar-*C*), 119.4 (Ar-*C*), 118.1 (Ar-*C*), 117.4 (*C*≡N), 112.0 (Ar-*C*), 108.5 (Ar-*C*), 47.9 (NH-*C*H_2-CH_2-ArC), 42.5 (*C*H_2-CH_2-CN), 21.4 (NH-CH_2-*C*H_2-ArC), 14.6 (CH_2-*C*H_2-CN).

HR-MS (ESI) *m/z*: calculated for $C_{13}H_{15}N_3$ requires 214.1339 for $[M+H]^+$ found 214.1347.

FTIR (thin film): ν_{max} = 3418, 2954, 2737, 2462, 2258, 1620, 1589, 1457, 1429, 1405, 1338 cm^{-1}.

Melting Point: 193 – 195 °C.

5.6.5 – Synthesis of 9-(pyrimidin-2-yl)-9*H*-carbazole, **2e**

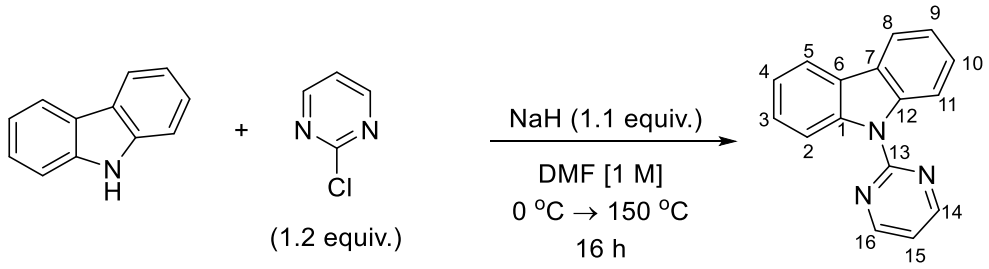

To a 50 mL oven dried round bottomed flask charged with magnetic stirrer was added 9*H*-carbazole (10 mmol, 1.670 g) and DMF (10 mL). The reaction was then cooled to 0 °C and NaH added to the suspension (60 *wt*.% in H_2O, 11 mmol, 430 mg) and the reaction stirred at this temperature for a further hour. After this time 2-chloropyrimidine (12 mmol, 1.380 g) was added in one portion to the flask. A reflux condenser was then fitted, and the reaction heated at 150 °C for 16 h. After allowing to cool back to room temperature after this time the reaction was poured into brine (150 mL) and the product then extracted with EtOAc (3 × 150 mL). The combined organic phases were then dried over $MgSO_4$, filtered and concentrated under reduced pressure to yield crude product. This was then purified by flash chromatography (1% EtOAc/hexanes → 10% EtOAc/hexanes), the product containing fractions were then concentrated under reduced pressure and the residue recrystallised from hot EtOH. This yielded the title compound as a white, needle like crystalline solid, **2e**, 36% (881 mg).

^{1}H NMR (500 MHz, $CDCl_3$): δ 8.86 (2H, d, J = 8.5 Hz, C(5)-*H*, C(8)-*H*), 8.84 (2H, d, J = 4.8 Hz, C(14)-*H*, C(16)-*H*), 8.09 (2H, dd, J = 7.8, 0.8 Hz, C(2)-*H*, C(11)-*H*), 7.52 (2H, ddd, J = 8.5, 7.2, 1.4 Hz, C(4)-*H*, C(9)-*H*), 7.40–7.36 (2H, m, C(3)-*H*, C(10)-*H*), 7.12 (1H, t, J = 4.8 Hz, C(15)-*H*).

^{13}C{^{1}H} NMR (126 MHz, $CDCl_3$): δ 159.2 (Ar*C*), 157.9 (2C, Ar*C*H), 139.2 (2C, Ar*C*), 126.6 (2C, Ar*C*H), 125.8 (2C, Ar*C*H), 122.3 (2C, Ar*C*), 119.5 (Ar*C*H), 116.2 (2C, Ar*C*), 116.0 (2C, Ar*C*H).

Melting Point: 157 – 159 °C.

This data is in accordance with literature precedent.[10]

5.6.6 – Synthesis of 9-(pyridin-2-yl)-9*H*-carbazole, **2f**

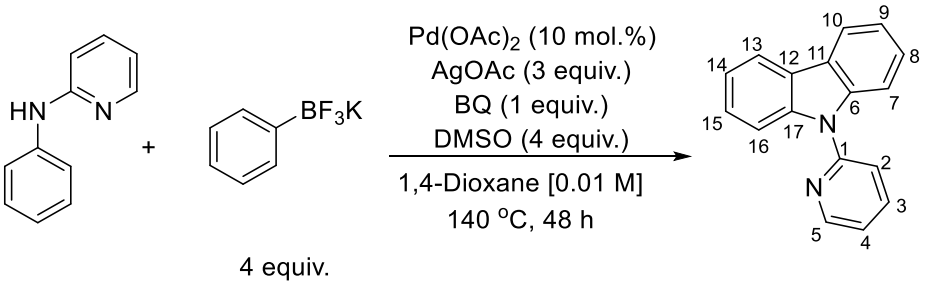

To a 100 mL round bottomed flask, charged with magnetic stirrer bar was added the following: *N*-phenylpyridin-2-amine (85 mg, 0.50 mmol), potassium phenyltrifluoroborate (368 mg, 2.0 mmol), palladium (ii) acetate (11 mg, 0.05 mmol), silver acetate (250 mg, 1.5 mmol), benzoquinone (54 mg, 0.5 mmol), DMSO (0.14 mL, 2.0 mmol) and 1,4-Dioxane (50 mL). A reflux condenser was then attached to the flask and the reaction heated at 140 °C for 2 days under air. After allowing to cool to room temperature, the reaction was filtered through a short pad of celite, eluting with DCM. The filtrate was then washed with water (3 × 30 mL) and the combined aqueous layers washed with DCM (3 × 30 mL). All the combined organic layers were then dried over $MgSO_4$, filtered and concentrated under reduced pressure to yield crude product. This was then purified by flash chromatography (hexanes → 0.5% EtOAc/hexanes →1% EtOAc/hexanes) to yield the title compound as a pale-yellow oil, **2f**, 54% (66 mg).

^{1}H NMR (500 MHz, $CDCl_3$): δ 8.74 (1H, dd, *J* = 4.9, 2.0, 0.8 Hz, C(5)-*H*), 8.13 (2H, d, *J* = 7.8 Hz, C(10)-*H*, C(13)-*H*), 7.93 (1H, td, *J* = 7.8, 2.0 Hz, C(3)-*H*), 7.85 (2H, dd, *J* = 8.2, 0.8 Hz, C(7)-*H*, C(16)-*H*), 7.65 (1H, d, *J* = 8.2 Hz, C(2)-*H*), 7.46–7.43 (2H, m, C(9)-*H*, C(14)-*H*), 7.35–7.29 (3H, m, C(4)-*H*, C(8)-*H*, C(15)-*H*).

^{13}C{^{1}H} NMR (126 MHz, $CDCl_3$): δ 151.9 (Ar*C*), 149.8 (Ar*C*H), 139.5 (Ar*C*H), 138.2 (2C, Ar*C*), 126.3 (2C, Ar*C*H), 124.3 (2C, Ar*C*H), 121.4 (2C, Ar*C*H), 120.9 (Ar*C*H), 120.1 (2C, Ar*C*H), 118.9 (2C, Ar*C*H), 111.0 (Ar*C*H).

This data is in accordance with literature precedent.[9]

5.7 – Optimisation for the C-4 alkylation of 9-(pyrimidin-2-yl)-9*H*-carabazoles

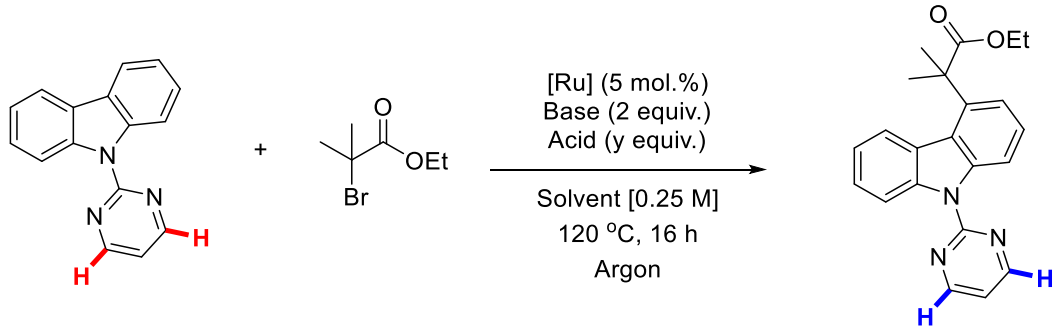

δ_H = 8.85

δ_H = 8.88

Proton NMR conversions were taken from the labelled diagnostic protons. No other observable by-products were formed during the reaction and no observed starting material decompositions led to ^{1}H NMR conversions being indicative of yield of alkylated product.

Entry	Ruthenium Catalyst	Base	Acid	Acid Eq.	Solvent	Conversion (%) (IY)
1	$[RuCl_2(p\text{-cymene})]_2$	KOAc	AcOH	2	1,4-Dioxane	**68 (48)**
2	$[RuCl_2(benzene)]_2$	KOAc	AcOH	2	1,4-Dioxane	**< 5**
3	$RuCl_3{\cdot}xH_2O$	KOAc	AcOH	2	1,4-Dioxane	**0**
4	$RuCl_2(PPh_3)_3$	KOAc	AcOH	2	1,4-Dioxane	**11**
5	$[Ru(1,10\text{-phen})_3]{\cdot}2Cl^-$	KOAc	AcOH	2	1,4-Dioxane	**0**
6	$[Ru(OAc)_2(p\text{-cymene})]$	KOAc	AcOH	2	1,4-Dioxane	**63 (36)**
7	$[Ru(O_2CAd)_2(p\text{-cymene})]$	KOAc	AcOH	2	1,4-Dioxane	**21**
8	$[RuCl(OAc)(p\text{-cymene})]$	KOAc	AcOH	2	1,4-Dioxane	**52 (30)**
9	$[RuCl_2(p\text{-cymene})]_2$	K_2CO_3	AcOH	2	1,4-Dioxane	**0**
10	$[RuCl_2(p\text{-cymene})]_2$	K_3Citrate	AcOH	2	1,4-Dioxane	**45**
11	$[RuCl_2(p\text{-cymene})]_2$	K_2Oxalate	AcOH	2	1,4-Dioxane	**0**
12	$[RuCl_2(p\text{-cymene})]_2$	K_2Tartrate	AcOH	2	1,4-Dioxane	**5**
13	$[RuCl_2(p\text{-cymene})]_2$	$KHCO_2$	AcOH	2	1,4-Dioxane	**25**
14	$[RuCl_2(p\text{-cymene})]_2$	Piv-Val-OH	AcOH	2	1,4-Dioxane	**< 5**
15	$[RuCl_2(p\text{-cymene})]_2$	$NaCO_2Ad$	AcOH	2	1,4-Dioxane	**58**
16	$[RuCl_2(p\text{-cymene})]_2$	KCO_2Mes	AcOH	2	1,4-Dioxane	**71 (54)**
17	$[RuCl_2(p\text{-cymene})]_2$	KCO_2Mes	$MesCO_2H$	2	1,4-Dioxane	**64 (51)**
18	$[RuCl_2(p\text{-cymene})]_2$	KCO_2Mes	$AdCO_2H$	2	1,4-Dioxane	**66 (50)**
19	$[RuCl_2(p\text{-cymene})]_2$	KCO_2Mes	HCl	2	1,4-Dioxane	**17**
20	$[RuCl_2(p\text{-cymene})]_2$	KCO_2Mes	TFA	2	1,4-Dioxane	**15**
21	$[RuCl_2(p\text{-cymene})]_2$	KCO_2Mes	HCO_2H	2	1,4-Dioxane	**34**
22	$[RuCl_2(p\text{-cymene})]_2$	KCO_2Mes	AcOH	2	2-MeTHF	**55**
23	$[RuCl_2(p\text{-cymene})]_2$	KCO_2Mes	AcOH	2	Toluene	**0**
24	$[RuCl_2(p\text{-cymene})]_2$	KCO_2Mes	AcOH	2	MeCN	**72(55)**
25	$[RuCl_2(p\text{-cymene})]_2$	KCO_2Mes	AcOH	2	Benzene	**39**
26	$[RuCl_2(p\text{-cymene})]_2$	KCO_2Mes	AcOH	2	AcOH	**31**
27	$[RuCl_2(p\text{-cymene})]_2$	KCO_2Mes	AcOH	2	2-Butanone	**55**
28	$[RuCl_2(p\text{-cymene})]_2$	KCO_2Mes	AcOH	2	DME	**49**
29	$[RuCl_2(p\text{-cymene})]_2$	KCO_2Mes	AcOH	2	DCE	**38**
30	$[RuCl_2(p\text{-cymene})]_2$	KCO_2Mes	AcOH	0.5	1,4-Dioxane	**80**
31	$[RuCl_2(p\text{-cymene})]_2$	KCO_2Mes	AcOH	1	1,4-Dioxane	**84 (68)**
32	$[RuCl_2(p\text{-cymene})]_2$	KCO_2Mes	AcOH	4	1,4-Dioxane	**68**

33	[$RuCl_2$(*p*-cymene)]$_2$	KCO_2Mes	AcOH	8	1,4-Dioxane	**< 5**
34	[$RuCl_2$(*p*-cymene)]$_2$	KCO_2Mes	–	–	1,4-Dioxane	**53**
35[1]	[$Ru(CO_2Mes)_2$(*p*-cymene)]	KCO_2Mes	AcOH	1	1,4-Dioxane	**91 (76)**
36[2]	[$RuCl_2$(*p*-cymene)]$_2$	KCO_2Mes	AcOH	1	1,4-Dioxane	**61**

[1] – 10 mol.% [Ru] [2] –100 °C

5.8 - Scope of Ruthenium Catalysed C-4 C-H Alkylation of Carbazole Substrates

5.8.1 – General Procedure **C** for the synthesis of methyl 2-methyl-2-(9-(pyrimidin-2-yl)-*9H*-carbazol-4-yl)alkylate substrates

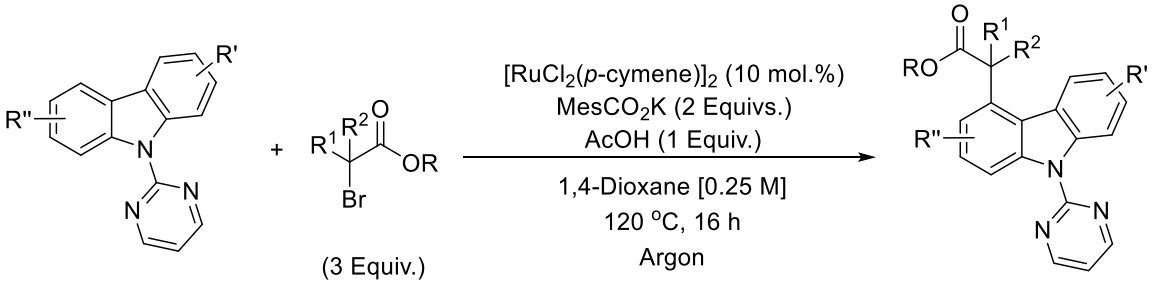

Or

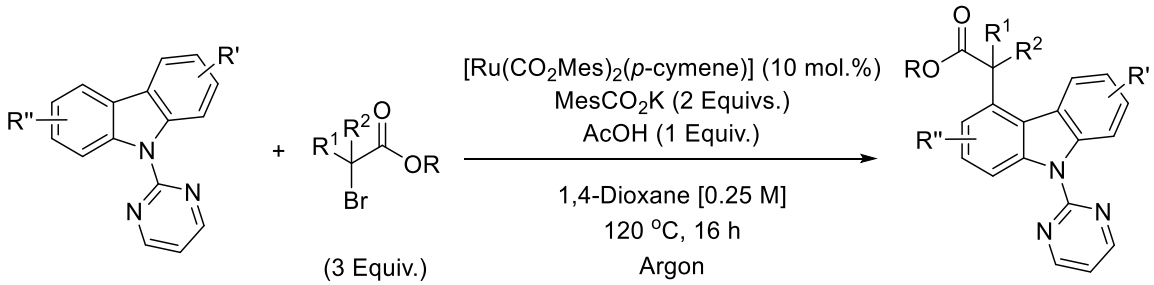

To an oven-dried carousel tube was charged with the relevant carbazole derivative (0.25 mmol), [$Ru(CO_2Mes)_2$(*p*-cymene)] (14 mg, 0.025 mmol) or [$RuCl_2$(*p*-cymene)]$_2$ (8 mg, 0.0125 mmol) and potassium 2,4,6-trimethylbenzoate (102 mg, 0.5 mmol). The reaction vessel was then sealed with a Teflon cap and 1,4-dioxane (1 mL), acetic acid (0.02 mL, 0.25 mmol), and the relevant coupling partner (0.75 mmol) were then added *via* syringe to the vessel. The reaction was then heated to 120 °C and refluxed for 16 h. After this time the reaction was allowed to cool to ambient temperature, before diluting with EtOAc (20 mL) and $NaHCO_3$ (sat) (aq.) (20 mL). The organic layer was then extracted and the aqueous layer then washed with further EtOAc (2 × 20 mL). The combined organic layers

were then dried over anhydrous $MgSO_4$, filtered and then concentrated *in vacuo*. The crude residue was then dry loaded onto silica and purified by flash chromatography (40-60 Petroleum ether/Ethyl acetate), to yield pure C4-alkylated structures.

5.8.2 – Synthesis of ethyl 2-methyl-2-(9-(pyrimidin-2-yl)-*9H*-carbazol-4-yl)propanoate, 2.1

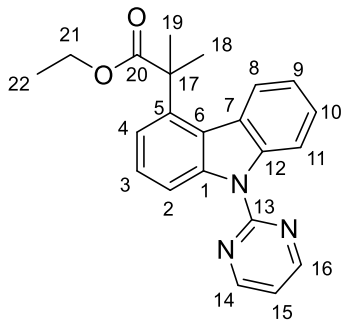

General procedure **C** was followed using the following compounds: 9-(pyrimidin-2-yl)-*9H*-carbazole (**2e**) (61 mg, 0.25 mmol), $[Ru(CO_2Mes)_2(p\text{-cymene})]$ (14 mg, 0.025 mmol) and ethyl 2-bromo-2-methylpropanoate (0.12 mL, 0.75 mmol). Column chromatography (1% EtOAc→10% EtOAc/hexanes) yielded the title compound as a white solid, **2.1**, 76% (68 mg).

*When $[RuCl_2(p\text{-cymene})]_2$ (8 mg, 0.0125 mmol) was used instead of $[Ru(CO_2Mes)_2(p\text{-cymene})]$, the title compound was obtained as a white solid, 68% (61 mg).

^{1}H NMR (500 MHz, $CDCl_3$): δ 8.87 (2H, d, J = 4.8 Hz, C(14)-*H*, C(16)-*H*), 8.69 (2H, d, J = 8.4 Hz, C(2)-*H*, C(11)-*H*), 8.02 (1H, d, J = 8.1 Hz, C(8)-*H*), 7.48–7.44 (3H, m, C(4)-*H*, C(9)-*H*, C(10)-*H*), 7.34–7.32 (1H, m, C(3)-*H*), 7.17 (1H, t, J = 4.8 Hz, C(15)-*H*), 4.04 (2H, q, J = 7.1 Hz, C(21)-*H*), 1.88 (6H, s, C(18)-*H*, C(19)-*H*), 0.95 (3H, t, J = 7.1 Hz, C(22)-*H*).

^{13}C{^{1}H} NMR (126 MHz, $CDCl_3$): δ 178.3 (*C*=O), 158.7 (Ar*C*), 158.0 (Ar*C*H), 140.0 (Ar*C*H), 139.5 (Ar*C*), 139.0 (Ar*C*), 126.0 (Ar*C*H), 125.7 (Ar*C*H), 124.5 (Ar*C*H), 123.5 (Ar*C*H), 123.2 (Ar*C*H), 121.8 (Ar*C*), 119.5 (Ar*C*), 116.7 (Ar*C*H), 114.4 (Ar*C*H), 113.7 (Ar*C*), 61.1 (O-*C*H_2-CH_3), 47.0 ((C=O)-*C*-(CH_3)$_2$), 27.0 (2C, ((C=O)-C-(*C*H_3)$_2$), 13.9 (O-CH_2-*C*H_3).

HR-MS (ESI) *m/z*: calculated for $C_{22}H_{21}N_3O_2$ requires 360.1707 for $[M+H]^+$ found 360.1715.

FTIR (thin film): ν_{max} = 3040, 2983, 2874, 2164, 1725, 1580, 1564, 1427 cm^{-1}.

Melting Point: 130 – 133 ˚C.

5.8.3 – Synthesis of methyl 2-methyl-2-(9-(pyrimidin-2-yl)-*9H*-carbozol-4-yl)propanoate, 2.2

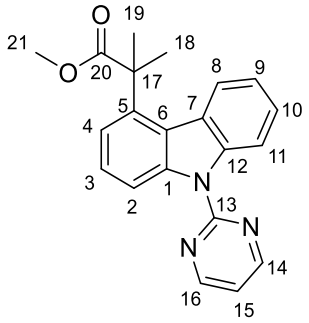

General procedure **C** was followed using the following compounds: 9-(pyrimidin-2-yl)-*9H*-carbazole (**2e**) (61 mg, 0.25 mmol), $[RuCl_2(p\text{-cymene})]_2$ (8 mg, 0.0125 mmol) and methyl 2-bromo-2-methylpropanoate (0.10 mL, 0.75 mmol). Column chromatography (1% EtOAc→10% EtOAc/hexanes) yielded the title compound as a white solid, **2.2**, 70% (60 mg).

*When $[Ru(CO_2Mes)_2(p\text{-cymene})]$ (14 mg, 0.025 mmol) was used instead of $[RuCl_2(p\text{-cymene})]_2$, the title compound was obtained as a white solid, 65% (56 mg).

^{1}H NMR (500 MHz, $CDCl_3$): δ 8.85 (2H, d, *J* = 4.8 Hz, C(14)-*H*, C(16)-*H*), 8.74–8.66 (2H, m, C(2)-*H*, C(11)-*H*), 7.54–7.45 (1H, m, C(8)-*H*), 7.45–7.41 (2H, m, C(3)-*H*, C(10)-*H*), 7.38–7.32 (1H, m, C(4)-*H*), 7.23 (1H, ddd, J = 7.9, 6.5, 1.9 Hz, C(9)-H), 7.14 (1H, t, *J* = 4.8 Hz, C(15)-*H*), 3.53 (3H, s, C(21)-*H*), 1.91 (6H, s, C(18)-*H*, C(19)-*H*).

^{13}C{^{1}H} NMR (126 MHz, $CDCl_3$): δ 179.1 (*C*=O), 158.8 (Ar*C*), 158.2 (Ar*C*H), 140.1 (Ar*C*H), 139.5 (Ar*C*), 139.1 (Ar*C*), 126.1 (Ar*C*H), 125.9 (Ar*C*H), 124.6 (Ar*C*H), 123.3 (Ar*C*H), 123.2 (Ar*C*H), 122.1 (Ar*C*), 119.5 (Ar*C*), 116.9 (Ar*C*H), 114.6 (Ar*C*H), 114.0 (Ar*C*), 52.7 (O-*C*H_3), 47.1 ((C=O)-*C*-(CH_3)$_2$), 27.2 ((C=O)-C-(*C*H_3)$_2$).

HR-MS (ESI) *m/z*: calculated for $C_{21}H_{19}N_3O_2$ requires 346.1550 for $[M+H]^+$ found 346.1583.

FTIR (thin film): ν_{max} = 2981, 1726, 1561 cm^{-1}.

Melting Point: 162 – 165 ˚C.

5.8.4 – Synthesis of *tert*-butyl 2-methyl-2-(9-(pyrimidin-2-yl)-*9H*-carbazol-4-yl)propanoate, 2.3

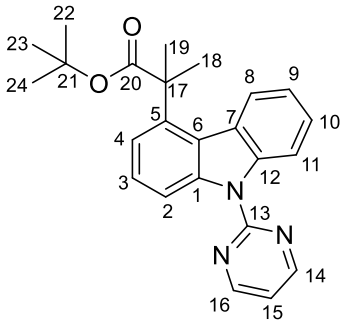

General procedure **C** was followed using the following compounds: 9-(pyrimidin-2-yl)-*9H*-carbazole (**2e**) (61 mg, 0.25 mmol), $[Ru(CO_2Mes)_2(p\text{-cymene})]$ (14 mg, 0.025 mmol) and *tert*-butyl 2-bromo-2-methylpropanoate (0.14 mL, 0.75 mmol). Column chromatography (1% EtOAc→10% EtOAc/hexanes) yielded the title compound as a white solid, **2.3**, 92% (89 mg).

*When $[RuCl_2(p\text{-cymene})]_2$ (8 mg, 0.0125 mmol) was used instead of $[Ru(CO_2Mes)_2(p\text{-cymene})]$, the title compound was obtained as a white solid, 72% (70 mg).

^{1}H NMR (500 MHz, $CDCl_3$): δ 8.84 (2H, d, J = 4.8 Hz, C(14)-*H*, C(16)-*H*), 8.72–8.63 (2H, m, C(2)-*H*, C(11)-*H*), 8.18–8.15 (1H, m, C(8)-*H*), 7.50–7.43 (2H, m, C(3)-*H*, C(10)-*H*), 7.40 (1H, dd, J = 7.7, 1.0 Hz, C(9)-*H*), 7.36–7.31 (1H, m, C(4)-*H*), 7.13 (1H, t, J = 4.8 Hz, C(15)-*H*), 1.89 (6H, s, C(18)-*H*, C(19)-*H*), 1.27 (9H, s, C(22)-*H*, C(23)-*H*, C(24)-*H*).

^{13}C{^{1}H} NMR (126 MHz, $CDCl_3$): δ 177.2 (*C*=O), 158.8 (Ar*C*), 158.1 (Ar*C*H), 140.1 (2C, Ar*C*H), 139.1 (Ar*C*), 126.0 (Ar*C*), 125.8 (Ar*C*H), 124.6 (Ar*C*H), 124.5 (Ar*C*H),

123.3 (Ar*C*H), 121.7 (Ar*C*), 119.7 (Ar*C*), 116.7 (Ar*C*H), 114.4 (Ar*C*H), 113.6 (Ar*C*), 80.9 (O-*C*(CH_3)$_3$), 47.8 ((C=O)-*C*(CH_3)$_2$-), 27.8 (-*C*H_3), 26.9 (-*C*H_3).

HR-MS (ESI) *m/z*: calculated for $C_{24}H_{25}N_3O_2$ requires 388.1947 for $[M+H]^+$ found 388.2069.

FTIR (thin film): ν_{max} = 2981, 1717, 1561 cm^{-1}.

Melting Point: 180 – 183 °C.

5.8.5 – Synthesis of benzyl 2-methyl-2-(9-pyrimidin-2-yl)-*9H*-carbazol-4-yl)propanoate, 2.4

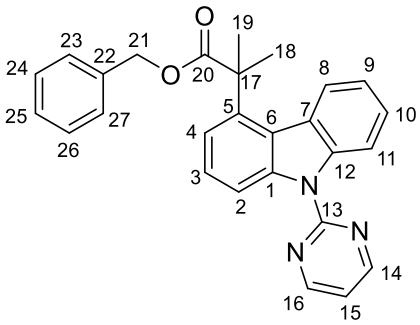

General procedure **C** was followed using the following compounds: 9-(pyrimidin-2-yl)-*9H*-carbazole (**2e**) (61 mg, 0.25 mmol), [Ru(CO_2Mes)$_2$(*p*-cymene)] (14 mg, 0.025 mmol) and benzyl 2-bromo-2-methylpropanoate (0.13 mL, 0.75 mmol). Column chromatography (1% EtOAc→10% EtOAc/hexanes) yielded the title compound as a white solid, **2.4**, 74% (78 mg).

*When [$RuCl_2$(*p*-cymene)]$_2$ (8 mg, 0.0125 mmol) was used instead of [Ru(CO_2Mes)$_2$(*p*-cymene)], the title compound was obtained as a white solid, 51% (54 mg).

^{1}H NMR (500 MHz, $CDCl_3$): δ 8.88 (2H, d, *J* = 4.8 Hz, C(14)-*H*, C(16)-*H*), 8.69 (2H, dd, *J* =8.3, 1.1 Hz, C(2)-*H*, C(11)-*H*), 7.96 (1H, ddd, *J* = 8.3, 1.1, 0.6 Hz, C(8)-*H*), 7.48 (1H, dd, *J* = 8.3, 7.6 Hz, C(3)-*H*), 7.43–7.40 (1H, m, C(10)-*H*), 7.22–7.15 (5H, m, C(23-27)-*H*), 7.02–6.99 (2H, m, C(4)-*H*, C(9)-*H*), 5.02 (2H, s, C(21)-*H*), 1.90 (6H, s, C(18)-*H*, C(19)-*H*).

$^{13}C\{^{1}H\}$ NMR (126 MHz, $CDCl_3$): δ 178.4 (*C*=O), 163.5 (Ar*C*), 158.4 (Ar*C*H), 139.6 (Ar*C*), 139.1 (Ar*C*), 128.6 (Ar*C*H), 128.2 (Ar*C*H), 126.4 (Ar*C*H), 126.0 (Ar*C*), 125.9 (Ar*C*), 124.8 (Ar*C*H), 123.6 (Ar*C*H), 123.5 (Ar*C*H), 122.3 (Ar*C*), 119.9 (Ar*C*H), 117.1 (Ar*C*H), 114.8 (Ar*C*H), 114.2 (Ar*C*), 67.2 (O-*C*H_2-Ar), 47.4 ((C=O)-*C*$(CH_3)_2$), 27.4 ((C=O)-C(*C*$H_3)_2$).

HR-MS (ESI) *m/z*: calculated for $C_{27}H_{23}N_3O_2$ requires 422.1870 for $[M+H]^+$ found 422.1943.

FTIR (thin film): ν_{max} = 2968, 1718, 1583, 1563 cm^{-1}.

Melting Point: 112 – 116 °C.

5.8.6 – Synthesis of cyclohexyl 2-methyl-2-(9-(pyrimidin-2-yl)-*9H*-carbazol-4-yl)propanoate, 2.5

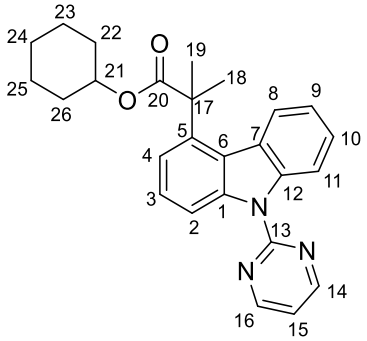

General procedure **C** was followed using the following compounds: 9-(pyrimidin-2-yl)-*9H*-carbazole (**2e**) (61 mg, 0.25 mmol), $[Ru(CO_2Mes)_2(p\text{-cymene})]$ (14 mg, 0.025 mmol) and cyclohexyl 2-bromo-2-methylpropanoate (147 mg, 0.75 mmol). Column chromatography (1% EtOAc→10% EtOAc/hexanes) yielded the title compound as a colourless solid, **2.5**, 74% (76 mg).

*When $[RuCl_2(p\text{-cymene})]_2$ (8 mg, 0.0125 mmol) was used instead of $[Ru(CO_2Mes)_2(p\text{-cymene})]$, the title compound was obtained as a colourless solid, 54% (55 mg).

^{1}H NMR (500 MHz, $CDCl_3$): δ 8.88 (2H, d, *J* = 4.8 Hz, C(14)-*H*, C(16)-*H*), 8.68 (2H, ddd, *J* = 8.2, 3.4, 1.1 Hz, C(2)-*H*, C(11)-*H*), 8.05 (1H, dd, *J* = 8.2, 1.1 Hz, C(8)-*H*), 7.49–7.44 (1H, m, C(10)-*H*), 7.43–7.39 (1H, m, C(3)-*H*), 7.30 (1H, ddd, *J* = 8.2, 7.2, 1.1 Hz,

C(9)-*H*), 7.14 (1H, s, C(4)-*H*), 4.81–4.73 (1H, m, C(21)-*H*), 1.87 (6H, s, C(18)-*H*, C(19)-*H*), 1.56 (3H, broad, -CH_2-), 1.45–1.32 (3H, m, -CH_2-), 1.22–1.00 (4H, m, -CH_2-).

^{13}C{^{1}H} NMR (126 MHz, $CDCl_3$): δ 178.2 (*C*=O), 163.3 (Ar*C*), 158.2 (Ar*C*H), 139.4 (Ar*C*), 135.9 (Ar*C*), 128.4 (Ar*C*), 128.0 (Ar*C*H), 126.2 (Ar*C*H), 125.8 (Ar*C*H), 124.6 (Ar*C*H), 123.4 (Ar*C*H), 122.1 (Ar*C*H), 119.7 (Ar*C*H), 116.9 (Ar*C*H), 114.6 (Ar*C*H), 114.0 (Ar*C*), 67.0 (O-*C*H-CH_2), 47.2((C=O)-*C*-(CH_3)$_2$), 27.2 ((C=O)-C-(*C*H_3)$_2$), 27.1 (*C*H_2), 25.3 (*C*H_2), 24.6 (*C*H_2).

HR-MS (ESI) *m/z*: calculated for $C_{26}H_{27}N_3O_2$ requires 436.1995 for $[M+Na]^+$ found 436.2027.

FTIR (thin film): ν_{max} = 2929, 2855, 1718, 1570 cm^{-1}.

5.8.7 – Synthesis of methyl 1-(9-(pyrimidin-2-yl)-*9H*-carbazol-4-yl)cyclohexane-1-carboxylate, 2.6

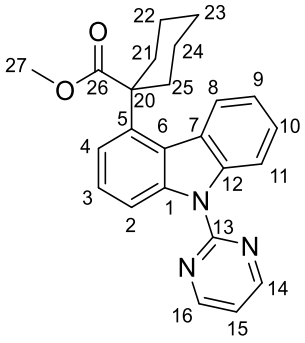

General procedure **C** was followed using the following compounds: 9-(pyrimidin-2-yl)-*9H*-carbazole (**2e**) (61 mg, 0.25 mmol), [Ru(CO_2Mes)$_2$(*p*-cymene)] (14 mg, 0.025 mmol) and methyl 1-bromocyclohexane-1-carboxylate (0.75 mmol, 0.12 mL). Column chromatography (1% EtOAc→10% EtOAc/hexanes) yielded the title compound as a white solid, **2.6**, 42% (40 mg).

*When [$RuCl_2$(*p*-cymene)]$_2$ (8 mg, 0.0125 mmol) was used instead of [Ru(CO_2Mes)$_2$(*p*-cymene)], the title compound was obtained as a white solid, 35% (33 mg).

^{1}H NMR (500 MHz, $CDCl_3$): δ 8.89 (2H, d, *J* = 4.8 Hz, C(14)-*H*, C(16)-*H*), 8.66–8.61 (2H, m, C(2)-*H*, C(11)-*H*), 8.10–8.06 (1H, m, C(8)-*H*), 7.52–7.46 (2H, m, C(3)-*H*, C(10)-

H), 7.45 (1H, ddd, *J* = 8.4, 7.1, 1.2 Hz, C(9)-*H*), 7.43–7.41 (1H, m, C(4)-*H*), 7.20 (1H, t, *J* = 4.8 Hz, C(15)-*H*), 3.49 (3H, s, C(27)-*H*), 2.48 (5H, s, C(20)-*H*, C(21)-*H*, C(25)-*H*), 1.81 (4H, s, C(22)-*H*, C(24)-*H*), 1.26 (2H, s, C(23)-*H*).

$^{13}C\{^{1}H\}$ NMR (126 MHz, $CDCl_3$): δ 178.6 (*C*=O), 158.3 (Ar*C*), 140.5 (Ar*C*H), 139.1 (Ar*C*), 138.5 (Ar*C*), 125.9 (Ar*C*), 125.8 (Ar*C*), 124.7 (Ar*C*H), 124.2 (Ar*C*H), 123.4 (Ar*C*H), 122.0 (Ar*C*H), 121.9 (Ar*C*H), 117.0 (Ar*C*H), 114.3 (Ar*C*H), 113.5 (Ar*C*), 52.5 (O-*C*H_3), 50.9 ((C=O)-*C*H-), 34.0 (-*C*H_2-), 25.9 (-*C*H_2-), 22.8 (-*C*H_2-).

HR-MS (ESI) *m/z*: calculated for $C_{24}H_{23}N_3O_2$ requires 386.1870 for $[M+H]^+$ found 386.1922.

FTIR (thin film): ν_{max} = 2955, 2932, 2362, 2165, 2034, 1718, 1560 cm^{-1}.

Melting Point: 182 – 185 °C.

5.8.8 – Synthesis of (perfluorophenyl) methyl 2-methyl-2-(9-(pyrimidin-2-yl)-*9H*-carbazol-4-yl) propanoate, **2.9**

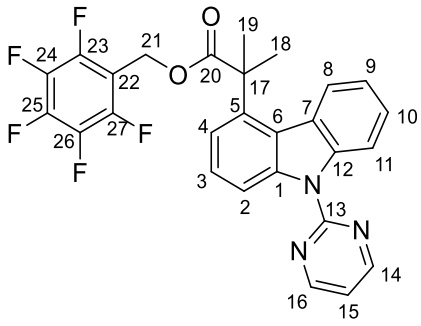

General procedure **C** was followed using the following compounds: 9-(pyrimidin-2-yl)-*9H*-carbazole (**2e**) (61 mg, 0.25 mmol), $[RuCl_2(p\text{-cymene})]_2$ (8 mg, 0.0125 mmol) and (perfluorophenyl) methyl 2-bromo-2-methyl propanoate (260 mg, 0.75 mmol). Column chromatography (1% EtOAc→10% EtOAc/hexanes) yielded the title compound as a white solid, **2.7**, 41% (52 mg).

*When $[Ru(CO_2Mes)_2(p\text{-cymene})]$ (14 mg, 0.025 mmol) was used instead of $[RuCl_2(p\text{-cymene})]_2$, the title compound was obtained as a white solid, 39% (50 mg).

^{1}H NMR (500 MHz, $CDCl_3$): δ 8.88 (2H, d, *J* = 4.8 Hz, C(14)-*H*, C(16)-*H*), 8.69 (2H, dd, *J* = 10.8, 8.4 Hz, C(2)-*H*, C(11)-*H*), 7.78 (1H, d, *J* = 8.1 Hz, C(8)-*H*), 7.49 (1H, t, *J* = 8.0 Hz, C(10)-*H*), 7.43–7.38 (1H, m, C(3)-*H*), 7.18 (1H, t, *J* = 4.8 Hz, C(15)-*H*), 7.12 (1H, t, *J* = 8.4 Hz, C(4)-*H*), 5.06 (2H, s, C(21)-*H*), 1.89 (6H, s, C(18)-*H*, C(19)-*H*).

^{13}C{^{1}H} NMR (126 MHz, $CDCl_3$): δ 177.8 (*C*=O), 158.8 (Ar*C*), 158.2 (Ar*C*), 145.5 (ddd, *J* = 251.3, 11.3, 7.7, 4.0 Hz, *C*(24/26)), 143.0 – 140.2 (m, Ar_FC), 140.1 (Ar*C*), 139.0 (Ar*C*), 138.8 (Ar*C*), 138.4 – 135.7 (m, Ar_FC), 126.3 (Ar*C*), 125.6 (Ar*C*), 124.1 (Ar*C*), 123.0 (Ar*C*), 122.9 (Ar*C*), 121.5 (Ar*C*), 119.5 (Ar*C*), 116.9 (Ar*C*), 114.7 (Ar*C*), 114.2 (Ar*C*), 109.2 (td, *J* = 17.5, 3.7 Hz, *C*(22)), 53.9 (O-*C*H_2-Ar_F), 47.1 ((C=O)-*C*$(CH_3)_2$), 29.8 ((C=O)-C(*C*$H_3)_2$).

^{19}F NMR (470 MHz, $CDCl_3$): δ -141.85 (2F, dd, *J* = 22.4, 8.3 Hz, C(23)-*F*, C(27)-*F*), -153.06 (1F, s, C(25)-*F*), -161.99 (2F, m, C(24)-*F*, C(26)-*F*).

HR-MS (ESI) *m/z*: calculated for $C_{27}H_{18}F_5N_3O_2$ requires 512.1392 for $[M+H]^+$ found 512.1426.

FTIR (thin film): ν_{max} = 2959, 1742, 1661, 1570, 1509 cm^{-1}.

Melting Point: 165 – 168 ˚C.

5.8.9 – Synthesis of methyl 2-(6-bromo-9-(pyrimidin-2-yl)-9*H*-carbazol-4-yl)-2-methylpropanoate, 2.10

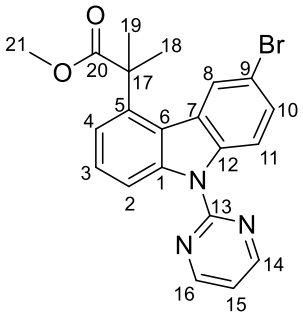

General procedure **C** was followed using the following compounds: 3-bromo-9-(pyrimidin-2-yl)-9*H*-carbazole (81 mg, 0.25 mmol), $[RuCl_2(p\text{-cymene})]_2$ (8 mg, 0.0125 mmol) and methyl 2-bromo-2-methylpropanoate (0.10 mL, 0.75 mmol). Column

chromatography (1% EtOAc→10% EtOAc/hexanes) yielded the title compound as a white solid, **2.7**, 54% (57 mg).

*When [Ru(CO_2Mes)$_2$(*p*-cymene)] (14 mg, 0.025 mmol) was used instead of [$RuCl_2$(*p*-cymene)]$_2$, the title compound was obtained as a white solid, 49% (52 mg).

^{1}H NMR (500 MHz, $CDCl_3$): δ 8.81 (2H, d, *J* = 4.8 Hz, C(14)-*H*, C(16)-*H*), 8.71 (1H, dd, *J* = 8.4, 1.0 Hz, C(2)-*H*), 8.62 (1H, d, *J* = 8.9 Hz, C(11)-*H*), 8.09 (1H, d, *J* = 1.9 Hz, C(8)-*H*), 7.55 (1H, dd, *J* = 8.9, 1.9 Hz, C(10)-*H*), 7.52 (1H, dd, *J* = 8.4, 7.6 Hz, C(3)-*H*), 7.43 (1H, dd, *J* = 7.6, 1.0 Hz, C(4)-*H*), 7.14 (1H, t, *J* = 4.8 Hz, C(15)-*H*), 3.68 (3H, s, C(21)-*H*), 1.89 (6H, s, C(18)-*H*, C(19)-*H*).

^{13}C{^{1}H} NMR (126 MHz, $CDCl_3$): δ 178.3 (*C*=O), 158.5 (Ar*C*), 158.2 (Ar*C*H), 140.5 (Ar*C*), 139.8 (Ar*C*), 137.8 (Ar*C*H), 128.4 (Ar*C*H), 126.9 (Ar*C*), 126.4 (Ar*C*H), 125.7 (Ar*C*H), 122.1 (Ar*C*), 119.8 (Ar*C*H), 117.0 (Ar*C*H), 116.4 (Ar*C*H), 115.0 (Ar*C*), 114.4 (Ar*C*), 52.6 (O-*C*H_3), 47.1 ((C=O)-*C*(CH_3)$_2$), 27.1 ((C=O)-C(*C*H_3)$_2$).

HR-MS (ESI) *m/z*: calculated for $C_{21}H_{18}N_3O_2Br$ requires 423.0482 for $[M+Na]^+$ found 423.0554.

FTIR (thin film): ν_{max} = 2981, 1728, 1567 cm^{-1}.

Melting Point: 183 – 185 °C.

5.8.10 – Synthesis of methyl 2-(6-chloro-9-(pyrimidin-2-yl)-9*H*-carbazol-4-yl)-2-methylpropanoate, 2.11

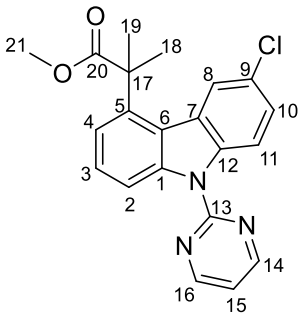

General procedure **C** was followed using the following compounds: 3-bromo-9-(pyrimidin-2-yl)-9*H*-carbazole (81 mg, 0.25 mmol), [$RuCl_2$(*p*-cymene)]$_2$ (8 mg, 0.0125

mmol) and methyl 2-bromo-2-methylpropanoate (0.10 mL, 0.75 mmol). Column chromatography (1% EtOAc→10% EtOAc/hexanes) yielded the title compound as a white solid, **2.7**, 60% (57 mg).

*When [Ru(CO_2Mes)$_2$(*p*-cymene)] (14 mg, 0.025 mmol) was used instead of [$RuCl_2$(*p*-cymene)]$_2$, the title compound was obtained as a white solid, 71% (67 mg).

^{1}H NMR (500 MHz, $CDCl_3$): δ 8.82 (2H, d, J = 4.8 Hz, C(14)-*H*, C(16)-*H*), 8.69 (2H, dd, J = 8.4, 1.0 Hz, C(2)-*H*, C(11)-*H*), 7.95 (1H, s, C(8)-*H*), 7.51 (1H, d, J = 8.4 Hz, C(10)-*H*), 7.47–7.37 (2H, m, C(3)-*H*, C(10)-*H*), 7.14 (1H, d, J = 4.9 Hz, C(15)-*H*), 3.66 (3H, s, C(21)-*H*), 1.89 (6H, s, C(18)-*H*, C(19)-*H*).

^{13}C{^{1}H} NMR (126 MHz, $CDCl_3$): δ 178.3 (*C*=O), 158.5 (Ar*C*), 158.2 (Ar*C*H), 140.6 (Ar*C*), 139.7 (Ar*C*), 137.5 (Ar*C*H), 127.4 (Ar*C*H), 126.9 (Ar*C*), 125.8 (Ar*C*H), 125.7 (Ar*C*H), 122.7 (Ar*C*), 122.3 (Ar*C*H), 119.8 (Ar*C*H), 117.0 (Ar*C*H), 116.0 (Ar*C*), 114.4 (Ar*C*), 52.6 (O-*C*H$_3$), 47.1 ((C=O)-*C*(CH$_3$)$_2$), 27.1 ((C=O)-C(*C*H$_3$)$_2$).

HR-MS (ESI) *m/z*: calculated for $C_{21}H_{18}N_3O_2Cl$ requires 402.0988 for $[M+Na]^+$ found 402.0918.

FTIR (thin film): ν_{max} = 2981, 1728, 1567 cm^{-1}.

Melting Point: 200 – 203 °C.

5.8.11 – Synthesis of methyl 2-methyl-2-(3,6,8-trichloro-9-(pyrimidin-2-yl)-9*H*-carbazol-4-yl) propanoate, 2.12

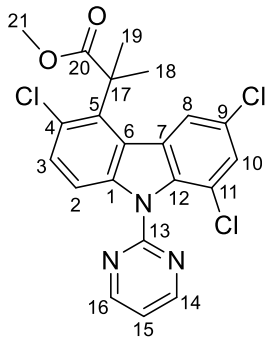

General procedure **C** was followed using the following compounds: 1, 3, 6-trichloro-9-(pyrimidin-2-yl)-9*H*-carbazole (87 mg, 0.25 mmol), $[RuCl_2(p\text{-cymene})]_2$ (8 mg, 0.0125 mmol) and methyl 2-bromo-2-methylpropanoate (0.10 mL, 0.75 mmol). Column chromatography (1% EtOAc→10% EtOAc/hexanes) yielded the title compound as a white solid, **2.7**, 10% (11 mg).

*When $[Ru(CO_2Mes)_2(p\text{-cymene})]$ (14 mg, 0.025 mmol) was used instead of $[RuCl_2(p\text{-cymene})]_2$, the title compound was obtained as a white solid, 7% (8 mg).

^{1}H NMR (500 MHz, $CDCl_3$): δ 8.92 (2H, d, J = 4.9 Hz, C(14)-*H*, C(16)-*H*), 8.03 (1H, d, J = 1.8 Hz, C(8)-*H*), 7.59 (1H, d, J = 8.9 Hz, C(2)-*H*), 7.45–7.41 (2H, m, C(3)-*H*, C(10)-*H*), 7.38 (1H, t, J = 4.9 Hz, C(15)-*H*), 3.63 (3H, s, C(21)-*H*), 2.08 (6H, s, C(18)-*H*, C(19)-*H*).

^{13}C{^{1}H} NMR (126 MHz, $CDCl_3$): δ 178.2 (*C*=O), 158.9 (Ar*C*), 158.0 (Ar*C*H), 137.0 (Ar*C*H), 131.7 (2C, Ar*C*), 127.7 (2C, Ar*C*), 127.4 (Ar*C*), 126.8 (2C, Ar*C*), 123.9 (Ar*C*H), 122.8 (Ar*C*H), 119.8 (Ar*C*H), 119.2 (Ar*C*H), 111.8 (Ar*C*), 52.7 (O-*C*H_3), 50.0 ((C=O)-*C*$(CH_3)_2$), 27.8 ((C=O)-C(*C*$H_3)_2$).

HR-MS (ESI) *m/z*: calculated for $C_{21}H_{18}N_3O_2Cl_3$ requires 470.0200 for $[M+Na]^+$ found 470.0162.

FTIR (thin film): ν_{max} = 2951, 1731, 1567 cm^{-1}.

5.9 - Mechanistic experiments for the C-4 alkylation of 9-(pyrimidin-2-yl)-9*H*-carabazoles

5.9.1 – Deuterium Labelling Experiment

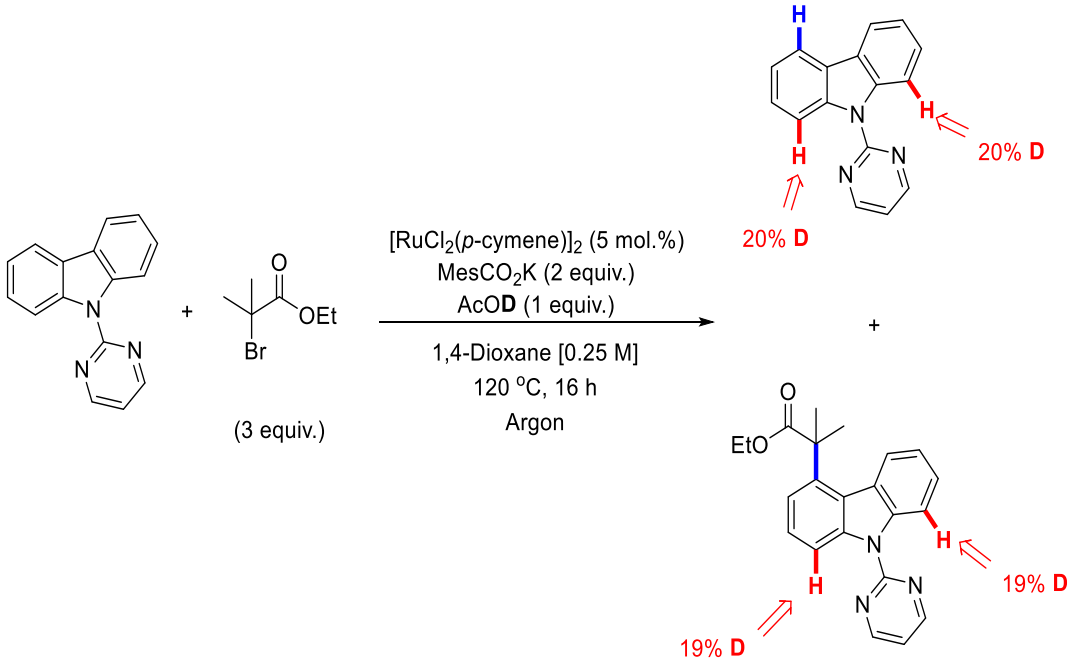

5.9.2 – TEMPO Experiments

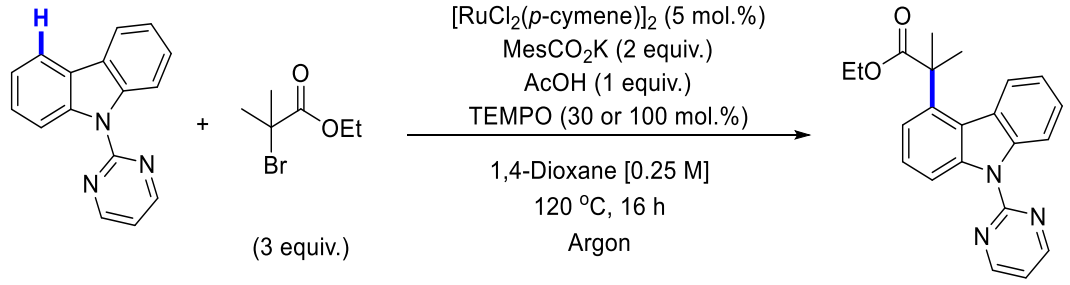

General procedure **C** was followed using the following compounds: 9-(pyrimidin-2-yl)-*9H*-carbazole (**2e**) (61 mg, 0.25 mmol), $[RuCl_2(p\text{-cymene})]_2$ (8 mg, 0.0125 mmol) and ethyl 2-bromo-2-methylpropanoate (0.12 mL, 0.75 mmol). To each reaction was then added TEMPO: 30 mol.% (0.075 mmol, 12 mg) and 100 mol.% (0.25 mmol, 39 mg).

Aliquots were then taken from each reaction and the conversion analysed *via* ^{1}H NMR. Addition of 30 mol.% TEMPO gave a conversion of 66%, and the addition of 100 mol.% TEMPO gave a conversion of 15% to the C4 alkylated product.

5.9.3 – Mercury Drop Test

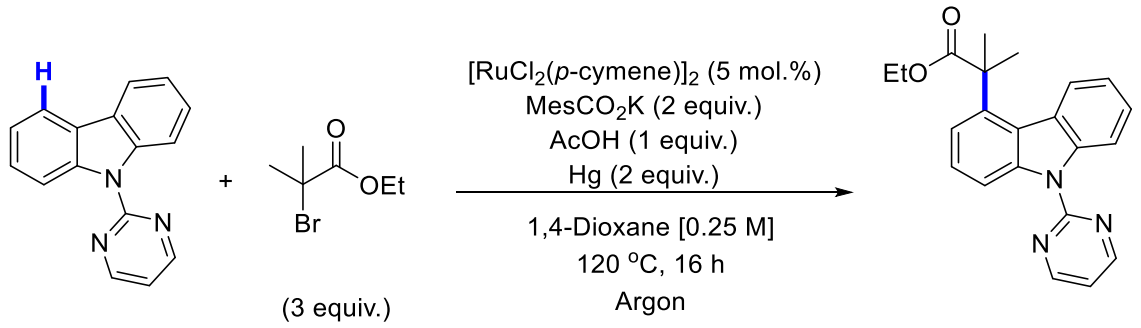

General procedure **C** was followed using the following compounds: 9-(pyrimidin-2-yl)-*9H*-carbazole (**2e**) (61 mg, 0.25 mmol), $[RuCl_2(p\text{-cymene})]_2$ (8 mg, 0.0125 mmol), ethyl 2-bromo-2-methylpropanoate (0.12 mL, 0.75 mmol) and mercury (0.50 mmol, 100 mg).

After reaction an aliquot was taken from the reaction vessel and analysed *via* ^{1}H NMR which showed a conversion of 85% to the C4 alkylated product.

5.10 – *para*-Functionalisation of Aniline Derivatives

5.10.1 – Optimisation for the *para* carboxylation of 5-chloro-*N*-phenylpyrimidin-2-amine

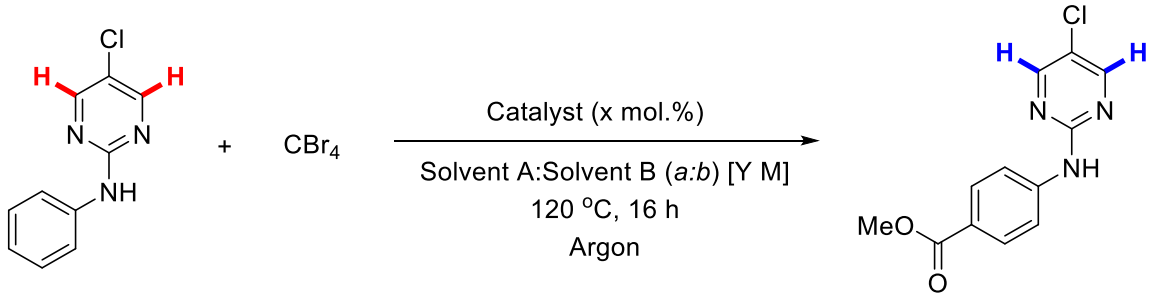

$\delta_H = 8.36$ $\delta_H = 8.42$

Proton NMR conversions were taken from the labelled diagnostic protons. No other observable by-products were observed during the reaction and no observed starting material decompositions lead to ^{1}H NMR conversions being indicative of yield of alkylated product.

Entry	Catalyst loading (mol.%)	Solvent A	Solvent B	Solvent Ratio (a:b)	Concentration (M)	Conversion (%) (IY)
1	$RuCl_3 \cdot xH_2O$ **(10)**	1,4-Dioxane	MeOH	1:1	0.17	**34(20)**
2	$[RuCl_2(p\text{-cymene})]_2$ **(5)**	1,4-Dioxane	MeOH	1:1	0.17	**20**
3	$[Ru(CO_2Mes)_2(p\text{-cymene})]$ **(10)**	1,4-Dioxane	MeOH	1:1	0.17	**0**
4	$[Ru(CO_2Ad)_2(p\text{-cymene})]$ **(10)**	1,4-Dioxane	MeOH	1:1	0.17	**13**
5	$[Ru(OAc)_2(p\text{-cymene})]$ **(10)**	1,4-Dioxane	MeOH	1:1	0.17	**12**
6	$[Fe(acac)_3]$ **(10)**	1,4-Dioxane	MeOH	1:1	0.17	**19**
7	$[Fe(NO_3)_3] \cdot 9H_2O$ **(10)**	1,4-Dioxane	MeOH	1:1	0.17	**9**
8	$[Fe(oxalate)_3]$ **(10)**	1,4-Dioxane	MeOH	1:1	0.17	**16**
9	Fe_2O_3 **(10)**	1,4-Dioxane	MeOH	1:1	0.17	**29 (15)**
10	$FeF_3 \cdot 3H_2O$ **(10)**	1,4-Dioxane	MeOH	1:1	0.17	**<5**
11	$FeBr_3$ **(10)**	1,4-Dioxane	MeOH	1:1	0.17	**<5**
12	$FeCl_3$ **(10)**	1,4-Dioxane	MeOH	1:1	0.17	**33(23)**
13	$FeCl_3$ **(5)**	1,4-Dioxane	MeOH	1:1	0.17	**37(18)**
14	$FeCl_3$ **(15)**	1,4-Dioxane	MeOH	1:1	0.17	**26**
15	$FeCl_3$ **(20)**	1,4-Dioxane	MeOH	1:1	0.17	**21**
16	$FeCl_3$ **(25)**	1,4-Dioxane	MeOH	1:1	0.17	**18**
17	$FeCl_3$ **(30)**	1,4-Dioxane	MeOH	1:1	0.17	**15**
18	$FeCl_3$ **(10)**	MeCN	MeOH	1:1	0.17	**0**
19	$FeCl_3$ **(10)**	DCE	MeOH	1:1	0.17	**<5**
20	$FeCl_3$ **(10)**	HFIP	MeOH	1:1	0.17	**17**
21	$FeCl_3$ **(10)**	2-butanone	MeOH	1:1	0.17	**17**
22	$FeCl_3$ **(10)**	Ph-Me	MeOH	1:1	0.17	**17**
23	$FeCl_3$ **(10)**	TBME	MeOH	1:1	0.17	**0**
24	$FeCl_3$ **(10)**	2-MeTHF	MeOH	1:1	0.17	**27(20)**
25	$FeCl_3$ **(10)**	H_2O	MeOH	1:1	0.17	**0**
26	$FeCl_3$ **(10)**	DMA	MeOH	1:1	0.17	**0**
27	$FeCl_3$ **(10)**	1,4-Dioxane	MeOH	2:1	0.17	**0**
28	$FeCl_3$ **(10)**	1,4-Dioxane	MeOH	4:1	0.17	**0**

29	$FeCl_3$ (**10**)	1,4-Dioxane	MeOH	5:1	0.17	**0**
30	$FeCl_3$ (**10**)	1,4-Dioxane	MeOH	10:1	0.17	**0**
31	$FeCl_3$ (**10**)	1,4-Dioxane	MeOH	1:2	0.17	**25**
32	$FeCl_3$ (**10**)	1,4-Dioxane	MeOH	1:4	0.17	**48(20)**
33	$FeCl_3$ (**10**)	1,4-Dioxane	MeOH	1:5	0.17	**39(18)**
34	$FeCl_3$ (**10**)	1,4-Dioxane	MeOH	1:10	0.17	**0**
35	$FeCl_3$ (**10**)	1,4-Dioxane	MeOH	1:1	1.0	**<5**
36	$FeCl_3$ (**10**)	1,4-Dioxane	MeOH	1:1	0.50	**44(23)**
37	$FeCl_3$ (**10**)	1,4-Dioxane	MeOH	1:1	0.25	**10**
38	$FeCl_3$ (**10**)	1,4-Dioxane	MeOH	1:1	0.10	**11**
39	$FeCl_3$ (**10**)	1,4-Dioxane	MeOH	1:1	0.01	**<5**
40	$ZnCl_2$ (**10**)	1,4-Dioxane	MeOH	1:1	0.17	**0**
41	$AlCl_3$ (**10**)	1,4-Dioxane	MeOH	1:1	0.17	**0**
42	AgCl (**10**)	1,4-Dioxane	MeOH	1:1	0.17	**0**
43	$Yb(OTf)(SO_4)$ (**10**)	1,4-Dioxane	MeOH	1:1	0.17	**0**
44[a]	$FeCl_3$ (**10**)	1,4-Dioxane	MeOH	1:1	0.17	**<5**
45[b]	$FeCl_3$ (**10**)	1,4-Dioxane	MeOH	1:1	0.17	**14**
46[c]	$FeCl_3$ (**10**)	1,4-Dioxane	MeOH	1:1	0.17	**14**
47	-	1,4-Dioxane	MeOH	1:1	0.50	**<5**

[a]-90 °C, [b]-Reaction done under air, [c]-Reaction done under O_2 atm.

5.10.2 – Synthesis of 5-chloro-*N*-phenylpyrimidin-2-amine, **3a**

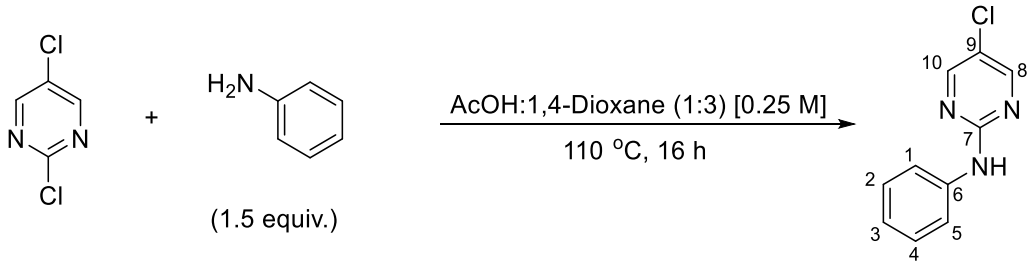

To a 1 L round-bottomed flask charged with magnetic stirrer bar was added the following: 2,5-dichloropyrimidine (40 mmol, 5.96 g), aniline (60 mmol, 5.47 mL), AcOH (40 mL) and 1,4-dioxane (120 mL). A reflux condenser was then attached, and the reaction refluxed at 110 °C for 16 hours. After cooling to room temperature, the reaction mixture was concentrated under reduced pressure and the remaining residue redissolved in EtOAc (450 mL) and the solution washed with $NaHCO_3$ (sat.) (aq.) (3 × 500 mL). The organic layer was then washed with brine (400 mL), dried over $MgSO_4$, filtered and concentrated under reduced pressure to yield crude product. This was then purified by flash chromatography (1% EtOAc/hexanes → 5% EtOAc/hexanes → 10% EtOAc/hexanes). The product containing fractions were then recrystallised from hot EtOH to yield the title compound as a white crystalline solid, **3a**, 36% (2.97 g).

^{1}H NMR (500 MHz, $CDCl_3$): δ 8.36 (2H, s, C(8)-*H*, C(10)-*H*), 7.58 (2H, dd, *J* = 8.6, 1.1 Hz, C(1)-*H*, C(5)-*H*), 7.53 (2H, dd, *J* = 8.6, 7.4 Hz, C(2)-*H*, C(4)-*H*), 7.08 (1H, tt, *J* = 7.4, 1.1 Hz, C(3)-*H*).

^{13}C{^{1}H} NMR (126 MHz, $CDCl_3$): δ 156.2 (Ar*C*H), 129.0 (Ar*C*H), 123.1 (Ar*C*), 119.5 (Ar*C*H).

Melting Point: 130 – 131 °C.

These are in accordance with literature data..[14]

5.10.3 – Synthesis of methyl 4-((5-chloropyrimidin-2-yl)amino)benzoate, 3.1

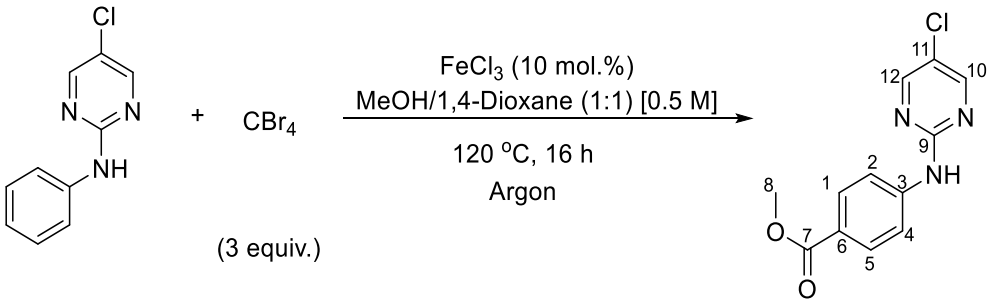

To an oven-dried carousel tube charged with magnetic stirrer bar was added the following: 5-chloro-*N*-phenylpyrimidin-2-amine (0.2 mmol, 41 mg), CBr_4 (0.6 mmol, 199 mg), $FeCl_3$ (0.02 mmol, 3 mg), MeOH (0.2 mL) and 1,4-dioxane (0.2 mL). The tube was then sealed with a Teflon capped and then evacuated and backfilled with argon three times. The reaction was then heated at 120 °C for 16 hours. After this time the reaction was quenched by addition of $NaHCO_3$ (sat.) (aq.) (10 mL) and the product extracted with EtOAc (3 × 15 mL). The combined organic phases were then dried over $MgSO_4$, filtered and concentrated under reduced pressure. The remaining residue was then purified by flash chromatography (10% EtOAc/hexanes) this yielded the title compound as a pale yellow solid, **3.1**, 23% (12 mg).

^{1}H NMR (500 MHz, $CDCl_3$): δ 8.41 (2H, s, C(10)-*H*, C(12)-*H*), 8.02 (2H, d, *J* = 8.4 Hz, C(1)-*H*, C(5)-*H*), 7.68 (2H, d, *J* = 8.4 Hz, C(2)-*H*, C(4)-*H*), 7.42 (1H, broad s, N-*H*), 3.90 (3H, s, C(8)-*H*).

$^{13}C\{^{1}H\}$ NMR (126 MHz, $CDCl_3$): δ 166.7 (*C*=O), 157.5 (Ar*C*), 156.2 (Ar*C*H), 143.2 (Ar*C*), 131.1 (Ar*C*H), 130.9 (Ar*C*H), 124.0 (Ar*C*), 117.8 (Ar*C*), 51.9 (O-*C*H_3).

HR-MS (ESI) *m/z*: calculated for $C_{12}H_{10}N_3O_2Cl$ requires 264.0534 for $[M+H]^+$ found 264.0499.

FTIR (thin film): ν_{max} = 3320, 3020, 1697, 1595, 1575, 1520, 1421 cm^{-1}.

Melting Point: 169 – 171 °C.

5.11 – Synthesis of Ruthenium Complexes

5.11.1 – Synthesis of [Ru(CO_2Mes)$_2$ η^6-(*p*-cymene)] (Mes = 2,4,6-trimethylbenzene)

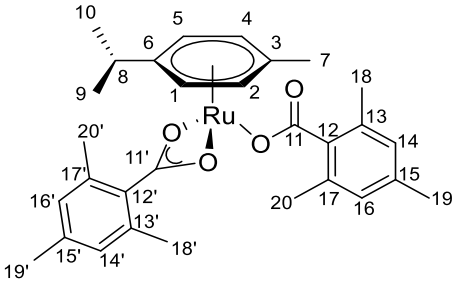

To an oven dried round-bottomed flask charged with stirrer bar was added [$RuCl_2$(*p*-cymene)]$_2$ (1.000g, 1.63 mmol), potassium 2, 4, 6-trimethylbenzoate (1.605 g, 7.82 mmol). The flask was then sealed and evacuated and back-filled with argon three times. After this time dried and deoxygenated dichloromethane (20 mL) was added to the flask *via* a rubber septum. The reaction was then stirred until the presence of Ru starting material was no longer observable by ^{1}H NMR. The reaction was then filtered through a celite pad. The filtrate was then collected and concentrated under reduced pressure to yield a red/orange solid as crude product. This was then recrystallised from dichloromethane/*n*-hexane to yield the desired product as an orange crystalline solid, 88% (1.606 g).

^{1}H NMR (500 MHz, $CDCl_3$): δ 6.68 (2H, s, C(7/19)-*H*, C(9/21)-*H*), 6.01 (2H, d, *J* = 5.7 Hz, C(1)-*H*, C(5)-*H*), 5.80 (2H, d, *J* = 5.7 Hz, C(2)-*H*, C(4)-*H*), 2.97 (1H, sept, *J* = 7.0 Hz, C(8)-*H*), 2.36 (3H, s, C(7)-*H*), 2.19 (6H, s, C(13)-*H*, C(25)-*H*), 2.16 (12H, s, C(11/23)-*H*, C(12/24)-*H*), 1.43 (6H, d, *J* = 7.0 Hz, C(9)-*H*, C(10)-*H*).

^{13}C{^{1}H} NMR (126 MHz, $CDCl_3$): δ 182.9 (*C*=O), 137.3 (Ar*C*), 135.1 (Ar*C*), 134.4 (Ar*C*H), 127.8 (Ar*C*H), 98.0 (ArC-*C*H(CH_3)$_2$), 92.1 (ArC-*C*H_3), 78.9 (ArC-*C*H_3), 78.1 (ArC-*C*H_3), 31.7 (ArC-*C*H_3), 22.8 (ArC-*C*H_3), 21.2 (ArC-*C*H_3), 20.0 (ArC-*C*H_3), 19.0 (ArC-*C*H_3).

HR-MS (ESI) *m/z*: calculated for $C_{32}H_{43}O_4Ru$ requires 594.2284 for $[M+H]^+$ found 594.2265.

FTIR (thin film): ν_{max} = 3322, 3063, 2964, 2916, 2167, 2033, 1623, 1611, 1574, 1479, 1436, 1403, 1326 cm^{-1}.

Melting Point: 146 – 148 ˚C (Decomp.).

These are in accordance with literature data.[15]

5.11.2 – Synthesis of [Ru(CO_2Me)Cl η^6-(*p*-cymene)]

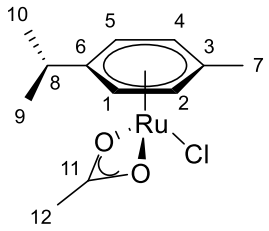

To an oven dried round-bottomed flask charged with stirrer bar was added [$RuCl_2$(*p*-cymene)]$_2$ (612 mg, 1.0 mmol) and a condenser with rubber septum attached fitted to the flask. The flask was then evacuated and back-filled with argon three times. Acetic anhydride (20 mL, 212 mmol) and acetic acid (80 mL) were then added to the flask *via* the rubber septum and the reaction then heated under reflux at 120 ºC for 4 h. After this time the reaction was allowed to cool, and the reaction mixture concentrated under reduced pressure and the remaining residue was recrystallised from *n*-hexane:acetone (5:1) at -20 ˚C. This yielded product as a bright red crystalline solid, 68% (120 mg).

^{1}H NMR (500 MHz, $CDCl_3$): δ 5.48 (2H, d, *J* = 5.9 Hz, C(1)-*H*, C(5)-*H*), 5.34 (2H, d, *J* = 5.9 Hz, C(2)-*H*, C(4)-*H*), 2.93 (1H, hept, *J* = 6.9 Hz, C(8)-*H*), 2.17 (3H, s, C(7)-*H*), 1.55 (3H, s, C(12)-*H*), 1.29 (6H, d, *J* = 6.9 Hz, C(9)-*H*, C(10)-*H*).

^{13}C{^{1}H} NMR (126 MHz, $CDCl_3$): δ 167.2 (C=O), 101.2 (Ar*C*), 96.7 (Ar*C*), 81.3 (Ar*C*H), 80.5 (Ar*C*H), 30.6 (ArC-*C*H(CH_3)$_2$), 22.1 (ArC-CH(*C*H_3)$_2$), 18.9 (ArC-*C*H_3).

HR-MS (ESI) *m/z*: calculated for $C_{12}H_{17}ClO_2Ru$ requires 331.0039 for $[M+H]^+$ found 331.0047.

FTIR (thin film): ν_{max} = 3055, 3031, 2960, 2927, 2867, 1739, 1496, 1448, 1389, 1379, 1363 cm^{-1}.

Melting Point: 135 – 137 °C.

5.11.3 – Synthesis of [Ru(CO_2Me)$_2$ η^6-(*p*-cymene)]

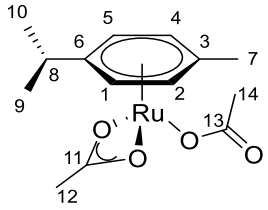

To an oven dried round-bottomed flask charged with magnetic stirrer bar was added [$RuCl_2$(*p*-cymene)]$_2$ (153 mg, 0.25 mmol) and KOAc (196 mg, 2.00 mmol). The flask was then sealed and evacuated and back-filled with argon three times. Toluene (20 mL) was then added *via* the rubber septum. The reaction was then stirred for 16 h after which time the reaction was filtered through a short pad of celite using DCM as eluent, until the washings were no longer coloured. The filtrate was then concentrated under reduced pressure to yield a red solid, which was then recrystallised from *n*-hexane:acetone (5:1) at -20 °C. This yielded product as an orange crystalline solid, 56% (100 mg).

^{1}H NMR (500 MHz, $CDCl_3$): δ 5.78 (2H, d, *J* = 5.7 Hz, C(1)-*H*, C(5)-*H*), 5.56 (2H, d, *J* = 5.7 Hz, C(2)-*H*, C(4)-*H*), 2.85 (1H, hept, *J* = 7.0 Hz, C(8)-*H*), 2.25 (3H, s, C(7)-*H*), 1.93 (6H, s, C(12)-*H*, C(14)-*H*), 1.35 (6H, d, *J* = 6.9 Hz, C(9)-*H*, C(10)-*H*).

^{13}C{^{1}H} NMR (126 MHz, $CDCl_3$): δ 184.4 (*C*=O), 114.4 (Ar*C*H), 114.3 (Ar*C*H), 110.0 (Ar*C*), 77.7 (O-*C*H_3), 31.4 (ArC-*C*H(CH_3)$_2$), 23.8 (ArC-CH(*C*H_3)$_2$), 22.5 (ArC-CH(*C*H_3)$_2$), 18.5 (ArC-*C*H_3).

Melting Point: 137 – 138 °C.

These are in accordance with literature data.[16]

5.11.2 – Synthesis of $[Ru(CO_2Ad)_2\ \eta^6\text{-}(p\text{-cymene})]$ (Ad = Adamantane)

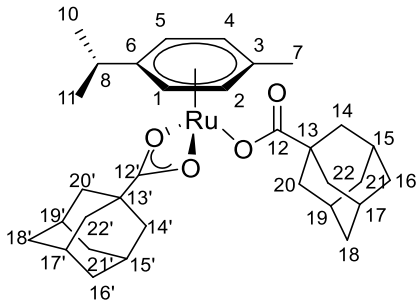

To an oven dried round-bottomed flask charged with magnetic stirrer was added $[RuCl_2(p\text{-cymene})]_2$ (1.00 g, 1.63 mmol) and sodium adamantanecarboxylate (1.45 g, 7.2 mmol). The flask was then sealed with a rubber septum and the flask evacuated and back-filled with argon three times. Toluene (35 mL) was then added *via* syringe into the flask through the rubber septum. The reaction was then stirred for 18 hours at ambient temperature, after which the mixture was filtered through a pad of celite with dichloromethane, until the washings were no longer coloured. The filtrate was then concentrated under reduced pressure to give a yellow solid and recrystallised from *n*-hexane:acetone (5:1) at -20 °C. This yielded product as an orange solid, 60%, (1.17 g).

^{1}H NMR (500 MHz, $CDCl_3$): δ 5.70 (2H, d, J = 5.8 Hz, C(1)-*H*, C(5)-*H*), 5.49 (2H, d, J = 5.8 Hz, C(2)-*H*, C(4)-*H*), 2.88 (1H, hept, J = 7.0 Hz, C(8)-*H*), 2.24 (3H, s, C(7)-*H*), 1.92 (6H, d, J = 7.0 Hz, C(10)-*H*, C(11)-*H*), 1.74 (12H, d, J = 2.7 Hz, C(14/14')-*H*, C(20/20')-*H*, C(22/22')-*H*), 1.63 (12H, s, C(16/16')-*H*, C(18/18')-*H*, C(21/21')-*H*), 1.34 (6H, d, J = 6.9 Hz, C(15/15')-*H*, C(17/17')-*H*, C(19/19')-*H*).

^{13}C{^{1}H} NMR (126 MHz, $CDCl_3$): δ 190.9 (*C*=O), 98.6 (Ar*C*), 93.8 (Ar*C*), 77.8 (2C, Ar*C*H), 42.0 (-*C*H_2-), 39.3 (-*C*H_2-), 36.4 (-*C*H_2-), 31.6 (ArC-*C*H(CH_3)$_2$), 28.2 (-*C*H-), 22.6 (ArC-CH(*C*H_3)$_2$), 18.6 (ArC-*C*H_3).

Melting Point: 226 – 227 °C.

These are in accordance with literature data.[16]

5.11.5 – Synthesis of (rac)-[RuCl(*p*-cymene)(C_6H_4-2-C_5H_4N-κ-C,N)]

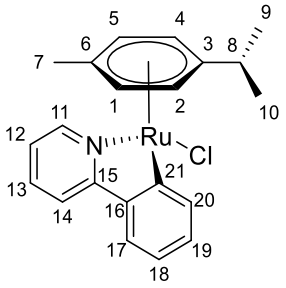

To an oven dried round bottomed flask charged with magnetic stirrer bar was added: $[RuCl_2(p\text{-cymene})]_2$ (1.00 g, 1.63 mmol), 2-phenylpyridine (0.52 mL, 3.59 mmol) and NaOAc (335 mg, 4.08 mmol). The flask was then sealed with a rubber septum and evacuated and back-filled with argon three times before then adding dry dichloromethane (10 mL). The reaction was then stirred for 4 hours at ambient temperature, before then filtering the reaction mixture through a short plug of celite with dichloromethane until the washings were no longer coloured. The filtrate was then concentrated under reduced pressure to yield a red/brown gummy solid, this was then recrystallised from *n*-hexane/dichloromethane. This yielded product as brown prism-like crystals, 81% (1.12 g).

^{1}H NMR (500 MHz, $CDCl_3$): δ 9.23 (1H, ddd, *J* =5.7, 1.2, 0.8 Hz, C(11)-*H*), 8.15 (1H, ddd, *J* = 7.6, 1.2, 0.5 Hz, C(17)-*H*), 7.73 – 7.70 (1H, m, C(14)-*H*), 7.66 (1H, ddd, *J* = 8.1, 7.6, 1.5 Hz, C(19)-*H*), 7.61 (1H, dd, *J* = 7.6, 1.5 Hz, C(18)-*H*), 7.17 (1H, td, *J* = 7.6, 1.5 Hz, C(20)-*H*), 7.07 – 7.01 (2H, m, C(12)-*H*, C(13)-*H*), 5.57 (1H, dd, *J* = 5.7, 1.2 Hz, C(2/4)-*H*), 5.56 (1H, dd, *J* = 5.9, 1.2 Hz, C(2/4)-*H*), 5.17 (1H, dd, *J* = 5.9, 1.2 Hz, C(1/5)-*H*), 4.98 (1H, dd, *J* = 5.9, 1.2 Hz, C(1/5)-*H*), 2.44 (1H, hept, *J* = 7.0 Hz, C(8)-*H*), 2.05 (3H, s, C(7)-*H*), 0.98 (3H, d, *J* = 7.0 Hz, C(9/10)-*H*), 0.88 (3H, d, *J* = 7.0 Hz, C(9/10)-*H*).

^{13}C{^{1}H} NMR (126 MHz, $CDCl_3$): δ 181.4 (Ar*C*-Ru), 165.4 (Ar*C*), 154.6 (Ar*C*H), 143.3 (Ar*C*), 139.6 (Ar*C*H), 136.6 (Ar*C*H), 129.4 (Ar*C*H), 123.8 (Ar*C*H), 122.5 (Ar*C*H), 121.3 (Ar*C*H), 118.8 (Ar*C*H), 100.6 (Ar*C*), 90.7 (Ar*C*), 89.6 (Ar*C*H), 84.1 (2C, Ar*C*H), 82.2 (Ar*C*H), 30.8 (ArC-*C*H(CH_3)$_2$), 22.5 (ArC-CH(*C*H$_3$)$_2$), 21.7 (ArC-CH(*C*H$_3$)$_2$), 18.8 (ArC-*C*H$_3$).

HR-MS (ESI) *m/z*: calculated for $C_{21}H_{22}NClRu$ requires 426.0562 for $[M+H]^+$ found 426.0580.

FTIR (thin film): ν_{max} = 3039, 2959, 2920, 2862, 1600, 1578, 1546, 1478, 1386 cm^{-1}.

Melting Point: 174 – 176 ˚C (Decomp.).

5.12 – Synthesis of Other Reagents

5.12.1 – Synthesis of (2-ethoxy-2-oxoethyl)triphenylphosphonium bromide

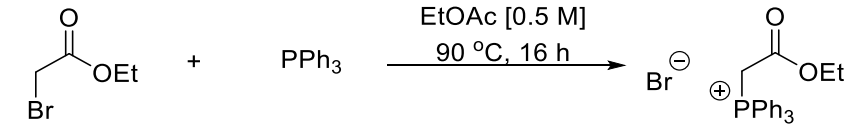

(1.06 equiv.)

To a 100 mL round bottom flask charged with magnetic stirrer was added the following: ethyl bromoacetate (20.20 mmol, 2.23 mL), PPh_3 (19.06 mmol, 5.00 g) and EtOAc (40 mL). The flask was then equipped with a condenser and the reaction refluxed at 90 °C for 16 h. After this time the reaction was filtered, and the precipitate washed with EtOAc and then dried using a Büchner funnel. The title compound was a collected as a white amorphous solid 96% (7.84 g).

^{1}H NMR (500 MHz, $CDCl_3$): δ 7.92 (6H, ddd, J = 13.4, 8.5, 1.3 Hz, Ph-*H*), 7.81 – 7.76 (3H, m, Ph-*H*), 7.68 (6H, td, J = 7.8, 3.6 Hz, Ph-*H*), 5.65 (2H, d, J = 13.7 Hz, P-CH_2-C=O), 4.05 (2H, q, J = 7.1 Hz, O-CH_2-CH_3), 1.08 (3H, t, J = 7.1 Hz, O-CH_2-CH_3).

^{13}C{^{1}H} NMR (126 MHz, $CDCl_3$): δ 172.5 (*C*=O), 138.0 (Ar*C*), 135.0 (Ar*C*H), 134.1 (Ar*C*H), 134.0 (Ar*C*H), 130.2 (Ar*C*H), 130.1 (Ar*C*H), 110.0 (PPh_3-*C*H_2-), 62.5 (O-*C*H_2-CH_3), 33.1 (O-CH_2-*C*H_3).

^{31}P NMR (202 MHz, $CDCl_3$): δ 20.97 (1P, s).

Melting Point: 152 – 154 °C.

These are in accordance with literature data.[17]

5.12.2 – Synthesis of potassium phenyltrifluoroborate

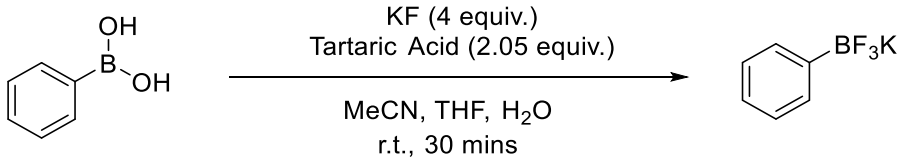

To a 100 mL round bottomed flask, charged with magnetic stirrer bar was added: phenyl boronic acid (10 mmol, 1.22 g) and MeCN (40 mL). A solution of KF (40 mmol, 2.32 g) was then dissolved in H_2O (4 mL) and this solution added in one portion. Once complete dissolution of the boronic acid was observed, another solution of L-(+)-tartaric acid (20.5 mmol, 3.08 g) in THF (15 mL) was added dropwise to the reaction over a 10 min period. The reaction was then left for another 30 mins, after which time MeCN (10 mL) was added to dilute the reaction and the reaction then filtered. The precipitate collected was then washed with further MeCN (3 × 50 mL). The combined filtrate washings were then concentrated under reduced pressure to yield the title compound as a white crystalline solid, 95% (1.75 g).

^{1}H NMR (500 MHz, CD_3CN): δ 7.41 (2H, d, J = 7.1 Hz, *o*-Ph-*H*), 7.16 – 7.12 (2H, m, *m*-Ph-*H*), 7.10 – 7.05 (1H, m, *p*-Ph-*H*).

^{13}C{^{1}H} NMR (126 MHz, CD_3CN): δ 131.3 (Ar*C*H), 126.5 (Ar*C*H), 125.3 (Ar*C*H). The *C*-B signal was not observed due to quadrupolar relaxation.

^{19}F NMR (470 MHz, CD_3CN): δ -142.36 (3F, 1:1:1:1 q, J = 52.8 Hz, -B*F*$_3$)

^{11}B NMR (160 MHz, CD_3CN): δ 3.34 (q, J = 55.1 Hz, -*B*F$_3$).

Melting Point: 297 – 298 ˚C.

These are in accordance with literature data.[18]

Note, this method renders the glassware used, operable after reaction. This is in comparison to other synthetic methods which render the glassware heavily etched.

5.12.3 – Synthesis of *N*-phenylpyridin-2-amine, 3b

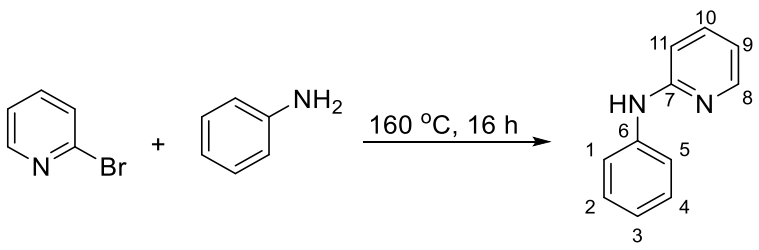

To an oven dried 50 mL round bottomed flask charged with magnetic stirrer bar was added: 2-bromopyridine (20 mmol, 1.91 mL) and aniline (20 mmol, 1.83 mL). A condenser was then attached, and the reaction heated at 160 ˚C for 16 h. After allowing to cool to room temperature $NaHCO_3$ (sat.) (aq.) (200 mL) was added and the product extracted with EtOAc (3 × 200 mL). The combined organic layers were then washed with brine (150 mL), dried over $MgSO_4$, filtered and concentrated under reduced pressure. This yielded a red solid which was purified by flash chromatography (40% EtOAc/hexanes) to yield pure the title compound as a pale red crystalline solid, 72% (2.46 g).

^{1}H NMR (500 MHz, $CDCl_3$): δ 8.21 (1H, d, J = 3.9 Hz, C(8)-*H*), 7.48 (1H, ddd, J = 8.4, 7.2, 1.9 Hz, C(10)-*H*), 7.34 (2H, d, J = 0.9 Hz, C(1)-*H*, C(5)-*H*), 7.33 (2H, s, C(2)*H*, C(4)-*H*), 7.09 – 7.03 (2H, m , N-*H*, C(3)-*H*), 6.89 (1H, d, J = 8.4 Hz, C(11)-*H*), 6.73 (1H, ddd, J = 7.1, 5.0, 1.0 Hz, C(9)-*H*).

^{13}C{^{1}H} NMR (126 MHz, $CDCl_3$): δ 156.2 (Ar*C*), 148.4 (Ar*C*H), 140.6 (Ar*C*), 137.7 (Ar*C*H), 129.3 (Ar*C*H), 122.8 (Ar*C*H), 120.4 (Ar*C*H), 114.9 (Ar*C*H), 108.2 (Ar*C*H).

Melting Point: 108 – 110 ˚C.

These are in accordance with literature data.[20]

5.12.4 – Synthesis of potassium 2,4,6-trimethylbenzoate ($MesCO_2K$)

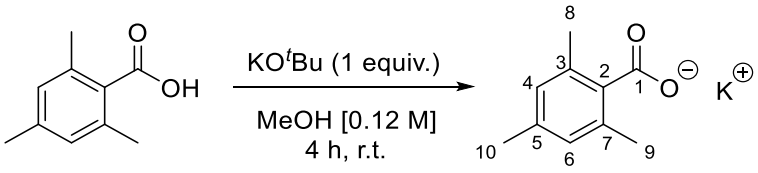

To a 100 mL round bottomed flask, charged with magnetic stirrer was added: 2, 4, 6-trimethylbenzoic acid (6.7 mmol, 1.10 g) and KO^{t}Bu (6.70 mmol, 752 mg) and MeOH (55 mL). The reaction was then stirred at room temperature for 4 hours. After this time the solvent was removed under reduced pressure to yield a sticky, white solid. This was then recrystallised from hot toluene to yield product as a white crystalline solid, 98% (1.33 g).

^{1}H NMR (500 MHz, D_2O): δ 6.92 (2H, s, C(4)-*H*, C(6)-*H*), 2.26 (3H, s, C(10)-*H*), 2.23 (6H, s, C(8)-*H*, C(9)-*H*).

^{13}C{^{1}H} NMR (126 MHz, D_2O): δ 185.3 (*C*=O), 137.2 (Ar*C*), 132.3 (Ar*C*), 127.4 (Ar*C*H), 20.0 (ArC-*C*H_3), 18.4 (ArC-*C*H_3).

Melting Point: 308 – 309 °C.

5.12.5 – Synthesis of pivaloyl-*L*-valine (Piv-Val-OH)

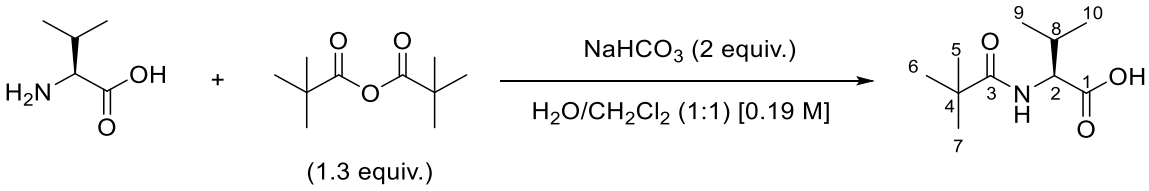

To an oven dried 250 mL round bottomed flask was added *L*-valine (2.69 g, 23 mmol), $NaHCO_3$ (3.86 g, 46 mmol), H_2O (60 mL) and CH_2Cl_2 (60 mL). The reaction was then cooled in an ice bath and allowed to stir for 10 mins. After this time the pivalic anhydride (6.09 mL, 30 mmol) was added dropwise using a syringe. After complete addition the reaction was allowed to head to room temperature and stirred for a further 4 hours. After completion the reaction was washed with Et_2O (3 × 100 mL), after which the remaining aqueous layer was acidified to pH 2, and then washed with further Et_2O (3 × 100 mL). The combined organic layers were then dried over $MgSO_4$, filtered and then concentrated under reduced pressure, to yield crude product. This was then recrystallised from Et_2O to yield the title compound as a white crystalline solid, 16% (721 mg).

^{1}H NMR (500 MHz, $CDCl_3$): δ 6.17 (1H, d, J = 9.2 Hz, N-*H*), 4.55 (1H, dd, J = 8.4, 4.9 Hz, C(2)-*H*), 2.25 (1H, sept, J = 6.9 Hz, C(8)-*H*), 1.23 (9H, d, J = 0.9 Hz, C(5)-*H*, C(6)-*H*, C(7)-*H*), 0.97 (6H, dd, J = 6.9, 1.6 Hz, C(9)-*H*, C(10)-*H*).

^{13}C{^{1}H} NMR (126 MHz, $CDCl_3$): δ 179.1 (*C*=O), 175.6 (O=*C*-OH), 57.0 (NH-*C*H-CO_2H), 38.9 (*C*-(CH_3)$_3$), 31.0 (*C*H-(CH_3)$_2$), 19.0 (3C,C-(*C*H_3)$_3$), 17.7 (2C, CH-(*C*H_3)$_2$).

Melting Point: 146 – 147 °C.

These are in accordance with literature data.[21]

Bibliography

1 S. Goggins, E. Rosevere, C. Bellini, J. C. Allen, B. J. Marsh, M. F. Mahon and C. G. Frost, *Org. Biomol. Chem.*, 2014, **12**, 47–52.

2 K. Wu, Z. Huang, C. Liu, H. Zhang and A. Lei, *Chem. Commun.*, 2015, **2**, 2286–2289.

3 K. Chen, J. W. Bats and M. Schmittel, *Inorg. Chem.*, 2013, **52**, 12863–12865.

4 L. Y. Xi, R. Y. Zhang, S. Liang, S. Y. Chen and X. Q. Yu, *Org. Lett.*, 2014, **16**, 5269–5271.

5 A. K. Pal, D. B. Cordes, A. M. Z. Slawin, C. Momblona, E. Ortĺ, I. D. W. Samuel, H. J. Bolink and E. Zysman-Colman, *Inorg. Chem.*, 2016, **55**, 10361–10376.

6 H. Woo, S. Cho, Y. Han, W. S. Chae, D. R. Ahn, Y. You and W. Nam, *J. Am. Chem. Soc.*, 2013, **135**, 4771–4787.

7 S. Bhadra, C. Matheis, D. Katayev and L. J. Gooßen, *Angew. Chemie - Int. Ed.*, 2013, **52**, 9279–9283.

8 C. Stathakis, P. Knochel, S. Bernhardt, J. R. Colombe and S. L. Buchwald, *Org. Lett.*, 2013, **15**, 5754–5757.

9 J. H. Chu, P. S. Lin, Y. M. Lee, W. T. Shen and M. J. Wu, *Chem. - A Eur. J.*, 2011, **17**, 13613–13620.

10 R. Qiu, V. P. Reddy, T. Iwasaki and N. Kambe, *J. Org. Chem.*, 2015, **80**, 367–374.

11 R. Singudas, S. R. Adusumalli, P. N. Joshi and V. Rai, *Chem. Commun.*, 2015, **51**, 473–476.

12 K. Walsh, H. F. Sneddon and C. J. Moody, *ChemSusChem*, 2013, **6**, 1455–1460.

13 T. Yajima, M. Okajima, A. Odani and O. Yamauchi, *Inorganica Chim. Acta*, 2002, **339**, 445–454.

14 J. A. Leitch, C. L. McMullin, A. J. Paterson, M. F. Mahon, Y. Bhonoah and C. G. Frost, *Angew. Chemie - Int. Ed.*, 2017, **56**, 15131–15135.

15 L. Ackermann, R. Vicente, H. K. Potukuchi and V. Pirovano, *Org. Lett.*, 2010, **12**, 5032–5035.

16 L. Ackermann, P. Novμk, R. Vicente and N. Hofmann, *Angew. Chemie - Int. Ed.*, 2009, **48**, 6045–6048.

17 Y. Xiao and P. Liu, *Angew. Chemie - Int. Ed.*, 2008, **47**, 9722–9725.

18 A. J. J. Lennox and G. C. Lloyd-Jones, *Angew. Chemie - Int. Ed.*, 2012, **51**, 9385–9388.

19 Patent no. US2006/58343, 2006, A1, 7.

20 T. Sugahara, K. Murakami, H. Yorimitsu and A. Osuka, *Angew. Chemie - Int. Ed.*, 2014, **53**, 9329–9333.

21 K. M. Engle, D. H. Wang and J. Q. Yu, *J. Am. Chem. Soc.*, 2010, **132**, 14137–14151.